Porous metal-organic frameworks for sorption of volatile organic compounds

Christophe Adrien Ndamyabera

Thesis presented for the degree of

DOCTOR OF PHILOSOPHY

in the Department of Chemistry

University of Cape Town

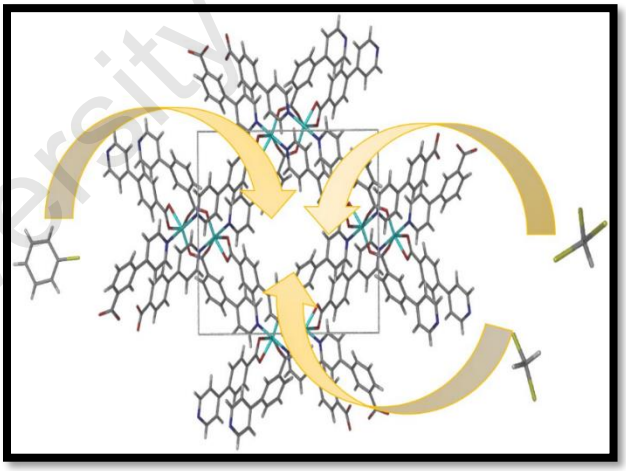

November 2020

University of Cape Town

The copyright of this thesis vests in the author. No quotation from it or information derived from it is to be published without full acknowledgement of the source. The thesis is to be used for private study or non-commercial research purposes only.

Published by the University of Cape Town (UCT) in terms of the non-exclusive license granted to UCT by the author.

University of Cape Town

DECLARATION

I, Christophe Adrien Ndamyabera, declare that the contents of this thesis represent my own work and that the thesis has not previously been submitted for academic examination towards any qualification.

Signed by candidate

Signature: Date: 24/11/2020

DEDICATION

This thesis is dedicated to my mother Thacienne Nyirabarundi and my wife Jeanne Umunyurwa.

ACKNOWLEDGEMENT

Special thanks to my main supervisor, Professor Susan Bourne for providing part of the funding for this program. She is also highly acknowledged for providing guidance with strong leadership from the beginning to the end of this PhD journey. Thank you for accepting me into your research group, I learnt a lot. I also acknowledge the help and guidance from my co-supervisor Dr. Clive Olive. His training on using software as well as instruments are highly appreciated.

I highly acknowledge Science Faculty fellowship, refugee and international scholarship, and National research foundation (NRF) at UCT for funding this research.

Thanks to Dr. Hong Su for her assistance on the single crystal X-ray diffractometers.

Professors Luigi R. Nassimbeni and Mino R. Caira provided suggestions and help whenever I needed it. I appreciate their assistance. I appreciate the help from supramolecular members at UCT such as F.M Amombo Noa, N. Sykes, and J. S. Bouanga Boudiombo. All supramolecular members at UCT contributed a lot to smooth the progression through my PhD studies.

Dr. Dalielah Jappie and Ms. Claire Lawrence-Naidoo, your kindness on offering access to FTIR instruments is acknowledged.

My flatmates, Mr. Christian Zenim, Mr. Dayo Sunday, and Dr. Kumar Malkeet, you created a conducive environment for me; your advice and support helped me a lot. I would also like to thank my friend Mahoro Antoine for his support. I highly appreciate Dr. Moira Niehauss who did her best to support me in different ways. I gratefully appreciate the support from Mr. Sylver Nahimana's family.

The inspiration and encouragement from Dr. Juvenal Biraguma are as well not to be forgotten. He stood as a brother in this journey. This acknowledgement also extends to my friend Mr. Janvier Ukwizagira, your part is appreciated.

The fundament of this achievement roots from Augustin Kamoso's family through Soeur Gorette. Your love, commitment, and advice to me are endless and considered as light to the society. You are my role model.

Finally, my wife Jeanne Umunyurwa Murara and my mother Thacienne Nyirabarundi as well as my family in general, you have been on my side. You were there to encourage and support me. You played a fundamental role in the completion of this PhD.

PUBLICATION AND CONFERENCES OR SYMPOSIA

Parts of this work have been published in a journal article, conferences, and symposia.

Publications

1. Ndamyabera, C. A.; Zacharias, S. C.; Oliver, C. L.; Bourne, S.A, *Chemistry*, 2019, **1**, 111−125.

   Title: Solvatochromism and Selective Sorption of Volatile Organic Solvents in Pyridylbenzoate Metal-Organic Frameworks.

Conference and symposia

1. International conference of the *Structural Chemistry Indaba*, held in the Kruger Park, South Africa in September 2018. Poster presentation.
   - Title: Accommodating volatile compounds in a *Cis*-$[Co(en)_2Cl_2]Cl{\cdot}H_2O$ ionic crystal.
2. Science postgrad symposium: Science Through an African Lens at Unversity of Cape Town in September 2017. Oral presentation.
   - Title: Porous metal-organic frameworks for sorption of volatile organics.
3. PhD seminar in Chemistry Department at UCT: Major part of this work was presented as “Porous metal-organic frameworks for sorption of volatile organics” September 2019.

ABSTRACT

Metal-organic frameworks (MOFs) present potential for various applications such as gas sorption, gas storage, sensing, drug delivery, and catalysis. This attracts researchers to design and synthesize MOFs that can respond to a specific application. In this thesis, mixed ligands 34pba and 44pba ligands (34pba = 3-(4-pyridyl)benzoate, and 44pba = 4-(4-pyridyl)benzoate) and Co^{2+} metal salts were used to synthesize porous MOFs $\{[Co(34pba)(44pba)]\cdot DMF\}_n$ (**1**) and $\{[Co(34pba)(44pba)]\cdot(C_3H_6O)\}_n$ (**2**), with DMF = N,N'-dimethylformamide and C_3H_6O = acetone through solvothermal reaction. These two relate to each other through hinge-like expansion or contraction of the guest-accessible void. The use of Zn^{2+} as a metal ion led to an isostructural MOFs $[Zn(34pba)(44pba)]\cdot DMF\}_n$ (**3**) of **1**. Using 34pba as a single ligand and Cu^{2+} as the metal ion led to the formation of a 2D $[(Cu(34pba)_2]\cdot DMF)$ (**4**) while a little variation of solvent mixture resulted in a 3D $\{[CuCl_2(34pba)_2]\cdot solvent\}_n$ (**7**) structures. The functionalized ligands 44paba and 34paba (34paba = 3-(pyridyn-4-ylmethyl)aminobenzoate, 44paba = 4-(pyridyn-4-ylmethyl)aminobenzoate) were used with Cu^{2+} centre to prepare $[Cu(44paba)\cdot(H_2O)\cdot(DMF)]_n$ (**5**) and $\{[Cu_3(34paba)_5(H_2O)_2]\cdot(DMF)_2\}_n$ (**6**), both of which are 1D structures. The activated MOFs **1d** and **3d** from (**1** and **2**) were used for the adsorption of volatile organic compounds (VOCs) and gases. In all tested guest molecules, there was higher sorption capacity in **1d** which could be attributed to some gate opening process occurring which does not occur in **3d**. Some effects responding to the sorption such as the change of colour in **1d** were characterized. This colour change may be associated with the d-d, metal to ligand charge transfer, or π to π^* transitions in coordination complex. Crystal structures and their stability, sorption properties and selectivity were characterized by single crystal X-ray diffraction, thermogravimetric analysis, differential scanning, hot stage microscopy, powder X-ray diffraction, infrared spectroscopy, and proton

nuclear magnetic resonance (^{1}H NMR) analysis. This thesis also reports the effect of methanol on discrete complexes of *cis*-dichloro-bis(ethylenediamine)cobalt(III) chloride (**Coen**) that led to the formation of a new crystal structure upon the removal of the water of hydration. The lattice energies calculated prove that **Coen** is more stable to allow a quick reversible sorption.

ABBREVIATIONS

Acac: Acetylacetonate

AC: Activated carbon

BDC: Benzenedicarboxylate

BET: Brunauer–Emmett–Teller

BPY: 4,4′-bipyridine

btc: Benzenetricarboxylic acid

BTRI: 1,3,5-benzenetricarboxylate

C_3H_6O: Acetone

CP: Coordination polymer

CSSD: Cambridge Structural Structure Database

DMA: Dimethylacetamide

DMF: *N*,*N*'-dimethylformamide

DSC: Differential scanning calorimetry

Ea: Activation energy

en: Ethyelenediamine

EtOH: Ethanol

FTIR: Fourier-Transform Infrared

H_2: Hydrogen

H_2ca: Chloranilic acid

HCl: Hydrochloric acid

H34pba: 3-(4-pyridyl)benzoic acid

H44pba: 4-(4-pyridyl)benzoic acid

H34paba: 3-(pyridyn-4-ylmethyl)aminobenzoic acid

H44paba: 4-(pyridyn-4-ylmethyl)aminobenzoic acid

HSM: Hot Stage microscopy

IRMOFs: Isoreticular metal-organic frameworks

MeOH: Methanol

MIL: Materials Institute Lavoisier

MOFs: Metal-organic frameworks

NH_3: Ammonia

NMR: Nuclear magnetic resonance spectrometry

PXRD: Powder X-ray diffraction

Qst: Heat of adsorption

R: The universal gas constant

TGA: Thermogravimetric analysis

SBU: Secondary building unit

SCXRD: Single crystal X-ray diffraction

UV-Vis: Ultraviolet-visible spectrophotometry

VOCs: Volatile organic compounds

TABLE OF CONTENTS

CHAPTER 1. INTRODUCTION AND LITERATURE REVIEW

1.1. INTRODUCTION

This chapter describes the properties and applications of solid adsorbents such as metal-organic frameworks (MOFs), activated carbon, zeolites, and mesoporous silica. MOFs are discussed in detail as they are considered to be more advantageous among other solid adsorbents while activated carbon, zeolites, and mesoporous silica are discussed briefly. MOFs have become more attractive as their porous structures, higher stability, higher surface area, tunability, and functionalization allow various application. On the other hand, the presence of volatile organic compounds (VOCs) in the environment, as well as their effects are also discussed. The negative effects among the reported VOCs suggest that their removal from the environment is important. Therefore, this work aimed to synthesize MOFs for sorption of VOCs and gases.

1.2. VOLATILE ORGANIC COMPOUNDS

1.2.1. Origin of volatile organic compounds

VOCs are organic compounds with an appreciable vapour pressure at ambient temperature. They include naturally-occurring and synthetic compounds and range in effect from harmless to toxic. Some naturally-occurring VOCs emanate from plants, especially fruits,[1] and others from the ocean.[2] The aroma in fruits is made up of molecules such as aldehydes, esters, and ketones,[1] while the contribution from the ocean is mainly halogenated VOCs.[2] In addition, in certain food products during storage and processing, some amine VOCs can be produced via biogenic processes.[3,4] Furthermore, VOCs are manufactured on a large scale for industrial and commercial use.[5]

1.2.2. Use and environmental effect of VOCs

VOCs show poor solubility, however, they are important in different applications. They are used as ingredients to produce aromas,[1] and medically apply VOCs such as iodoform as an antiseptic. Some industrial manufacturing uses VOCs as solvents, as reagents, or raw materials to produce the final products.[5] In addition, they are used in degreasing and cleaning metals, as pesticides, and as refrigerants. Thus, they are produced on a large scale as commercial products.[5] However, they constitute a large part of the contaminants present in the environment.[2,5] Some VOCs have been shown to have malodorous, mutagenic or carcinogenic properties[3,6–8] and some have been implicated in causing air pollution, particularly in developing countries[9] and are partly responsible for the generation of photochemical ozone and smog precursors. They are released into the environment during manufacturing, improper storage, and disposal methods. They contaminate water, soil and air[2,5] and they are strongly resistant to biodegradation.[5] It follows that human exposure is via inhalation, water drinking, and swimming.[5] They are thus considered as harmful pollutants.[6,7] Some governments have banned the use of some chlorinated VOCs to prevent the impact on human or environment.[5]

As a consequence, the development of effective technologies to mitigate the emission of VOCs has received increasing attention.[10] Some reports have shown promising removal and recovery methods of VOCs from air and water through adsorption processes.[11–13] Solid adsorbents are superior compared to other techniques of decontamination of air or water, owing to their relatively low cost, a wide range of applications, simplicity of design, easy operation, low harmful secondary products and the feasible regeneration of these solid adsorbents.[14]

1.3. SOLID SORBENTS

1.3.1. Activated carbon

Activated carbons (AC) are made from raw materials such as wood, coal, peat, lignite, coconut shells pyrolized with steam, carbon dioxide, and acids at high temperature in a process known as carbonisation.[15,16] These compounds have been used for different applications including removal of toxic substances such as carbon dioxide,[17] toxic metal ions,[18] and volatile organic compounds (VOCs).[16,18,19] Srivastava *et al.* explained the ability of AC being influenced by their mesoporous pores structures.[18] The effects of variation of porosities and the content of oxygen in AC were investigated for the adsorption of both benzene and toluene VOCs.[19] The AC adsorbents activated by hydroxide while lowering oxygen content in surface had improved adsorption capacity. Besides, their high microporous volume contributed to high adsorption of VOCs.[19] The documented adsorbents showed a good regeneration ready for reuse.[20] However, many factors negatively impact VOC adsorption by AC such as the presence of moisture in the system, compounds with a large number of π electrons,[21,22] and the pH value.[18] Their preparations also require high temperature[15] like 700 ^{o}C which is not usually readily available in most research laboratories.

1.3.2. Zeolites

Zeolites are usually synthesized from silica, alumina and organic bases.[23] In 2011, Chen *et al.*[23] reported synthetic methods to achieve the micro and mesoporosity of zeolites for the application of interest. They are used in different applications[23–25] such as catalytic activities,[23] adsorption and separation.[23,24,26] However, some disadvantages have been observed. For example, the use of zeolite 13X in the presence of moisture resulted in the hindrance of VOCs adsorption.[27] To

improve the effectiveness of zeolite, surfactants were used to produce surfactant-modified zeolite (SMZ) and investigated the adsorption of VOCs from water. Findings showed that water did not affect their adsorption but there was particle attrition, limiting the lifetime of the zeolites and the surfactants also deteriorated.[22,28]

1.3.3. Mesoporous silica

Mesoporous silica are solid adsorbents made from silicate or aluminium silicate often with structure directing agents to achieve the required porosity. Calcination at high temperature is involved in their synthesis.[29,30] They are used in applications such as adsorption of volatile organic compounds,[31] CO_2 and heavy metal adsorption.[29,30] Some mesoporous silica are not stable in hydrothermal conditions. In addition, their synthesis requires high temperature (more than 500 °C) during calcination.[29] Moreover, mesoporous silicas show low surface areas ranging between 300 and 1200 $m^2 g^{-1}$.[29] These characteristics including their low adsorption capacity[32] make them less suitable for application compared to ones identified from MOFs solid adsorbents as detailed in section below.

1.3.4. Metal-organic frameworks

1.3.4.1. Introduction

The coordination of metal nodes or clusters and organic ligands forms extended networks of crystalline porous materials. These porous materials are referred to as metal-organic frameworks (MOFs).[33,34] A number of these structures with defined networks have been achieved through a variety of reaction conditions between metal ions and organic linkers in solution.[34–36] Some solid reactions were used as alternative where grinding reactions may produce the same compounds as

from solution. This method can also produce compounds not-achievable by solvothermal synthesis.[37,38] The syntheses of MOFs attract much attention due to their versatility in synthesis,[39] low density,[40,41] robustness, high porosity, high surface area[41] and crystallinity,[33,40,42,43] as well as their high thermal and chemical stability.[44] These features are achieved due to the controlled synthetic conditions and can then contribute to a number of diverse applications.[45–48] Yaghi *et al*[49,50] were among the first researchers that reported the potential applications of these porous materials. Among many different applications, MOFs showed potential for gas separation[32,43,51] and storage,[52] catalysis,[53] drug delivery,[54] as sensors,[55–58] luminescence,[59] and photocatalytic activity.[60]

1.3.4.2. MOF nomenclature

There are many porous coordination polymer materials made by metal ions and organic linkers which form different classes. Terms used for these polymers include coordination polymers, metal-organic polymers, hybrid organic-inorganic materials, organic zeolite analogues, and metal-organic frameworks.[61] They are named according to their specific polymer structure and their connectivity. The term coordination polymer (CP) is globally referred as the polymers made from the extended connection of metal and ligand linker coordinated via bonds without considering their final structure and or morphology.[62] Cheetham *et al*[63] classified hybrid organic-inorganic materials as CPs that present different structural dimensions according to the sum of connectivity between metal-organic-metal and inorganic connectivity. The structural dimension is taken as the total dimensionality from the metal-ligand-metal and inorganic connectivity. Table 1.1 summarizes the effect of both the metal-ligand-metal and inorganic connectivity on the resulting hybrid. The system of I^mO^n was established where I^m and O^n stand for inorganic and organic connectivity while the overall summation of m and n is the dimensionality.

Table 1.1: *Proposed dimensional structures formed from both inorganic (I^m) and organic (O^n) connectivity*[63]

Metal-organic-metal connectivity, O^n (n =0-3	Dimensionality of inorganic connectivity I^m (n = 0-3)				
		0	1	2	3
	0	Molecular complexes I^0O^0	Hybrid inorganic chain I^1O^0	Hybrid inorganic layers I^2O^0	3D inorganic hybrids I^3O^0
	1	Chain coordination polymer I^0O^1	Mixed inorganic-organic layer I^1O^1	Mixed inorganic-organic 3D framework I^2O^1	
	2	Layered coordination polymers I^0O^2	Mixed inorganic-organic 3D framework I^1O^2		
	3	3D coordination polymers I^0O^3			

Inorganic hybrids may have connectivity to form dimensions from 1D up to 3D. MOF-5 is an example of 3D hybrids that results from a system of I^0O^3.[63] A system structure of I^1O^2 was classified from $[Cr^{III}(OH)(OOC–C_6H_4–COO)]$ (MIL-53) where octahedral corner-sharing of CrO_6 make a parallel 1D chains (I^1) that are crosslinked by the benzene-1,4-dicarboxylate groups to form 3D structure.[63,64] Another system of I^2O^1 can be schematically represented in Figure 1.1(a) and (b) corresponding to dimensional structures 1D and 2D CPs, respectively. Then Figure 1.1(c) is 3D where two-dimensional inorganic connectivities are in turn connected in third dimension by organic linkers.[63]

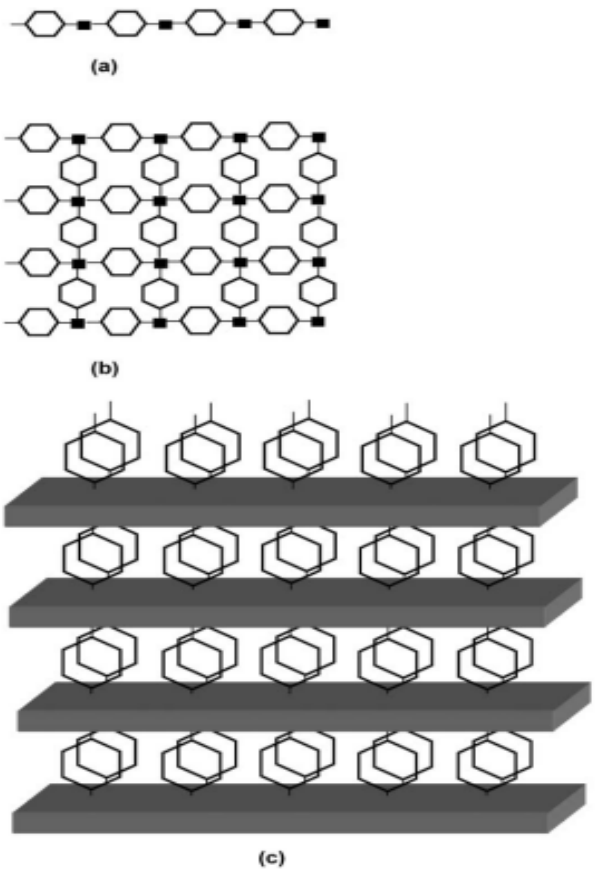

Figure 1.1: *Representation of (a) and (b) show 1-D and 2-D coordination polymers, respectively, and (c) extended inorganic connectivity in two dimension connected in three dimension by organic linker.*[63]

Figure 1.1 has $Fe^{III}(H_2O)(HO_3P(CH_2)_2PO_3)$[65] as an example where inorganic layers perpendicular to the *c*-axis of $FeO_6P_2(H_2O)$ are linked by the alkyl part of the diphosphonate group resulting in a 3D structure. Organic zeolite analogues MOFs or zeolitic imidazolate frameworks show the topology of zeolites.[62] In their crystal structures, the metal ions such as Co (II), Cu(II), In(II), Zn(II), etc are coordinated by imidazolate linkers similar to tetrahedral Si(Al) bridged by O in zeolites.[66]

Porous MOFs make a sub class of CPs characterized by strong coordination bonding which offers robustness. The organic linkers bridge the metal units providing the open porous structures that allow a geometrically well-defined structure and the exchange of guest molecules.[67,68] As per

Cheetham classification,[63] these compounds are commonly known in I^0O^3 and I^1O^2 system structures.[44,63,64] The system of I^1O^1 have also been synthesized.[43,69,70] The versatility in these compounds allows the replacement of linking units in the synthesis keeping the same topology of the framework.[62] This property also allows the variation of the functionality in pores through designed structures.[68] As a result, these extended MOFs can be termed as isoreticular metal-organic frameworks (IRMOFs). A series of sixteen IRMOFs (IRMOF-1 to IRMOF-16) from a prototype MOF-5 was synthesized with increased pore size for gas adsorption.[68] MOFs can also be named according to their place of discovery, Table 1.2. For example, MOFs based on zirconium metal and 1,4-benzenedicarboxylate (BDC) ligands termed as UiO-n were synthesized at the Universitetet i Oslo.[44] MIL-n were synthesized at the Materials Institute Lavoisier.[71] HKUST-1 was synthesized at the Hong Kong University of Science and Technology.[72]

Table 1.2: *Name of MOFs associated with their place of synthesis*

Name of MOF	Reason for name	Reference
IRMOF-n	Synthesized through isoreticular synthesis	68
UiO-n	Synthesized at the University of i Oslo	44
MIL-n	Synthesized based on Materials Institute Lavoisier	71
CAU-1	Synthesized at Christian-Albrechts-University	73
HKUST-1	Synthesized at Hong Kong University of Science and Technology	72
MOF-LIC-1	Synthesized at Leiden Institute of Chemistry	74
DUT	Synthesized at Dresden University of Technology	40
MTAF	Named for the TriAzolate used to synthesize the framework	75
UTSA-n	Synthesized at the University of Texas at San Antonio	76

n: number from 1 to 16.

MOFs are commonly known as CPs with structural dimensions of 2D or 3D[43,44,69,70,77–79] as one of their characteristics. However, Stock and Biswas proposed a restricted classification for MOFs as a class of 3D structures.[35]

1.3.4.3. Structural dimension in MOFs

The structural frameworks formation of MOFs depends on both the functionality of the ligand and metal ion.[50,62] The interesting key factor in these materials is their versatility offered by the coordination mode.[50,80] The coordination mode made by metal nodes or clusters and ligands gives the direction to the dimensional structure for these compounds. The functional unit or the donor group of ligand has bonding sites (dentate) to link to the metal cluster in order to form one, two, or three structural dimensions (1D, 2D, or 3D)[36,50,67] as illustrated in Fig 1.2. In this regard, metal-ligand connectivity known in metal-BPY (4,4′-bipyridine),[81] can lead to a linear or one dimensional structure (1D)[59,63,82,83] where the donor atom offers only one terminal coordination.[67] Different linear forms such as helix, zigzag chain, and molecular ladder can be expected.[84] This 1D formation can be a result of the incomplete deprotonation of the ligand and or the influence of low temperature.[83,85] In addition, the metal ion can offer limited coordination sites.[86] The formation of 2D structures can give different forms such as brick wall, bilayer, herringbone, long-and-short brick, basket weave,[59,84] honeycomb[83] or sheets.[87] The final structural dimension in metal coordination is the 3D in which the forms such as octahedral, cubic diamondoid, and hexagonal diamondoid can be formed.[59,84,88] In this latter structure, the ligands bridge the metal clusters to form layers or sheets as 2D. In turn, the layers can be pillared by the ligand leading to the formation of 3D structure in which the cubic or octahedral frameworks can be formed.[36,67,76]

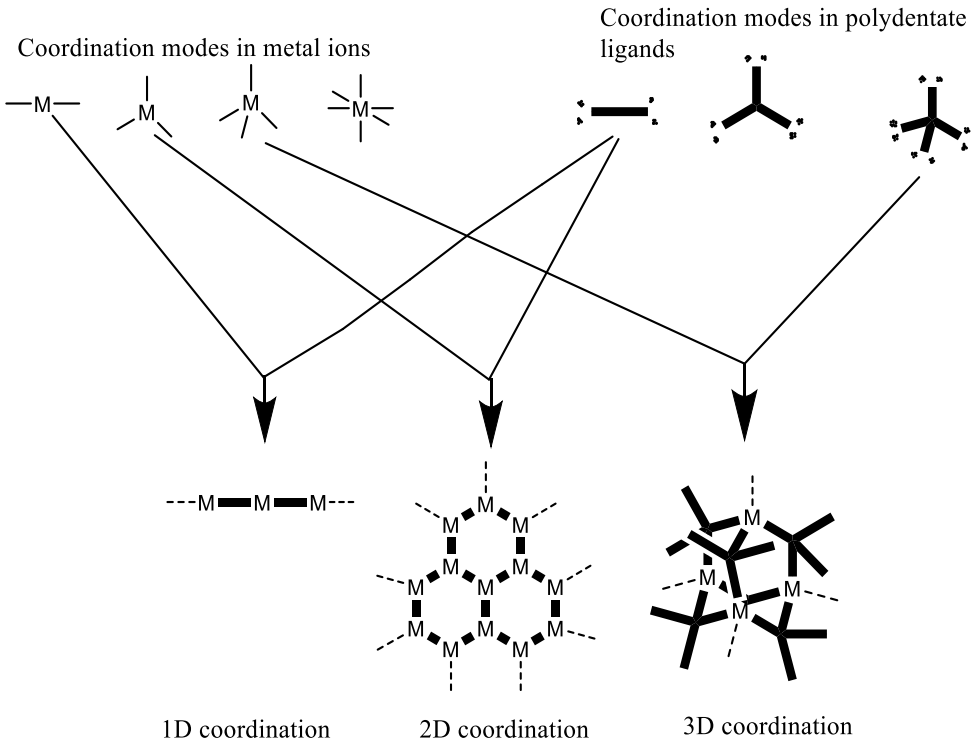

Figure 1.2:*Coordination modes and formation of dimensional structures.*[50]

Papaefstathiou *et al*. reported that the formation of 1D, 2D, or 3D structures depend on the coordination preference of the metal.[86] In most cases, this works together with the coordination modes of ligand to offer various coordination direction to form 1D, 2D, or 3D structures[50,67] as noted above. The ability to deprotonate the ligand can also play a role as reported by Li *et al.*,[85] where incomplete deprotonated multidentate ligand 1,3,5-tri(2-benzimidazolyl)benzene led to 1D while complete deprotonation led to 3D structures. On the other hand, other findings showed that the temperature can also influence the coordination mode in the framework.[83,87] One example is in the synthesis of Co(II)-succinate MOFs. The heating of the reaction mixture up to 100 ^{o}C generated 1D, at 150 ^{o}C 2D, and above 150 ^{o}C 3D structures were formed.[87]

The 3D structure of the frameworks allows the availability of features such as high surface area, pores, and channels.[36,76,79] On the other hand, the surface and pores structures can also be found from 2D frameworks.[89] The synthesis of MOFs with features that allow the potential applications are of primary importance. For that reason, the control of parameters to achieve 3D structure is important.[90]

1.3.4.4. Structural features of MOFs

The nature of metal ion and linker (ligand) are major factors which play a role in self-assembly of metal-organic complexes.[62] Ligands with nitrogen donors such as (BPY) have been used to produce different structures such as square[81] and ladder-like (2D) MOFs,[91] as well as diamondoid[86] three-dimensional frameworks.[92,93] The frameworks from metal and BPY are typically charged, and thus require the presence of counter ions in channels, which may be a shortcoming. In addition, interpenetration and low thermal stability after the removal of the guest molecules are also disadvantages of these MOFs.[62] Attempts have been made to increase the thermal stability in these compounds, such as using 1,4,5,8,9,12-hexaazatriphenylene as linker. These MOFs showed variable adsorption and desorption of guest molecules, however, the modifications in crystal symmetry and cell volume were observed.[94,95]

As the choice of ligand contributes to the formation of robust porous MOFs, the use of anionic and polydentate linkers offered the promise of reticular synthesis.[62] Multicarboxylates such as benzene-1,3,5-tricarboxylate[96,97] and benzene-1,4-dicarboxylate[98,99] could yield neutral, non-interpenetrated frameworks with retention or regain of crystallinity during adsorption and desorption of guest molecules. The results from TGA showed that many of these frameworks decompose between 300-500 ^{o}C.[62] Rowsell and Yaghi[62] reported strong coordination in metal-

carboxylate MOFs. Metal centres also possess high affinity for electrostatic attraction. In addition, the size and functionality of carboxylate offer the binding and/or chelation on metal/metal cluster leading to a rigid and well defined supramolecular architecture.[62] The reticular synthesis allowed the use of long linkers such as naphthalene-2,6-dicarboxylate, biphenyl-4,4'-dicarboxylate, pyrene-2,7-dicarboxylate, and terphenyl-4,4''-dicarboxylate instead of benzene-1,4-dicarboxylate to afford larger pore sizes, ranging from 3.8 to 28.8 Å. Concurrently, the free open space increased up to 91.1% of the crystal volume.[68] The result is that these frameworks have low densities.

The use of ligands containing both pyridinyl/triazolyl and carboxylates moieties have also been investigated. MOFs containing 4-(4-pyridyl)benzoate (44pba) have been reported with stability up to 400 ºC.[100–102] For example, $\{[Co(44pba)_2]_4 \cdot (DMF)_3 \cdot (EtOH)_{0.25} \cdot (H_2O)_4\}_n$ has channels which occupy 46.5% of the unit cell volume and can accommodate different solvents with flexible exchange in the channels.[100] Triazolyl isophthalate linkers with Cu or Zn were also used to synthesize frameworks with porosities of 31−53% with high thermal stability.[79] Larger open space and pore size have been developed as potential features for a number of different applications.[40,62,68,103,104] This has prompted work to design and synthesize isoreticular MOFs with increased surface and pore sizes to enhance their applications such as storage of hydrogen,[52,68] CO_2 adsorption,[105] sensing,[106] and catalysis.[104]

The most potent features are the availability of the surface and pores or channels accessible by the guest molecules.[98,99,107] In addition, a stable framework with permanent porosity and guest-dependent dynamic behaviour[99] with a flexible breathing properties have been reported.[78,80,95] Hence, the control of pore and channel size suitable for the specific application are desirable. The

pore size could be adjusted by the reaction conditions,[108] the length of ligand as mentioned above,[68,98] the nature of the solvent,[109,110] and through anchoring the pores by functionalization.[111]

1.3.4.5. Porous structural dimensionality

Kitagawa *et al*.[112] classified four types of porous structures based on their spatial dimensionality as follows. The first is characterized by isolated cavities or zero dimension. They are identified as porous structures inside the solid without windows. In some cases, there may be windows; however, these are smaller than the guest molecules. In both cases the guest molecules cannot pass out and the cavities do not communicate with each other. The system cavities in Figure 1.3 were characterized from $[Zn(CN)(NO_3)\text{-}(tpt)_{2/3}.3/4C_2H_2Cl_4.3/4CH_3OH]_n$ (tpt=2,4,6-tri(4-pyridyl)-1,3,5-triazine).[113] They are impenetrable by small molecules with the exception of H_2. The chambers in this framework are sealed off. The distance between a Zn_4 square to the opposite and parallel Zn_4 square from the inner shell presented a unit cell length of 23.448 Å. This structure leaves a chamber which is able to host nine1,1,2,2-tetrachloroethane molecules, and nine molecules of methanol.

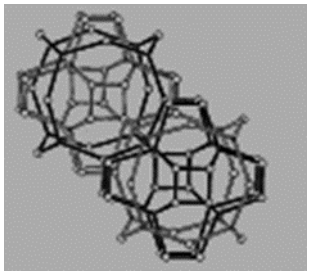

Figure 1.3: *Two independent cavities of* $\{[Zn(CN)(NO_3)(tpt)_{2/3}] \cdot \frac{3}{4}C_2H_2Cl_4 \cdot \frac{3}{4}CH_3OH\}_n$.

The second type of porous structure systems are 1D channels with several sizes and shapes. For example, $[Ni(acac)_2(L1)]\cdot 3CH_3CN\cdot 6H_2O$ (where acac represents acetylacetonate, and L1

represents 1,1-binaphthyl-6,6′-bipyridine) has a chiral channel (Figure 1.4.a) of 1.7 × 1.7 nm in dimension which is filled with acetonitrile and water guest molecules.[114] These homochiral nanotubes are based on helical chains that are built from C2-symmetric bipyridyl ligands and linear metal-connecting points.[114] Another example, $[Zr_6O_4(OH)_8(HCOO)_2(CPTTA)_2]$ is synthesized from Zirconium and 5′-(4-carboxyphenyl)-[1,1′:3′,1″-terphenyl]-3,4″,5-tricarboxylate (CPTTA) ions and has uniform 1D hexagonal channels of 24 Å diameter, Figure 1.4.b.[115]

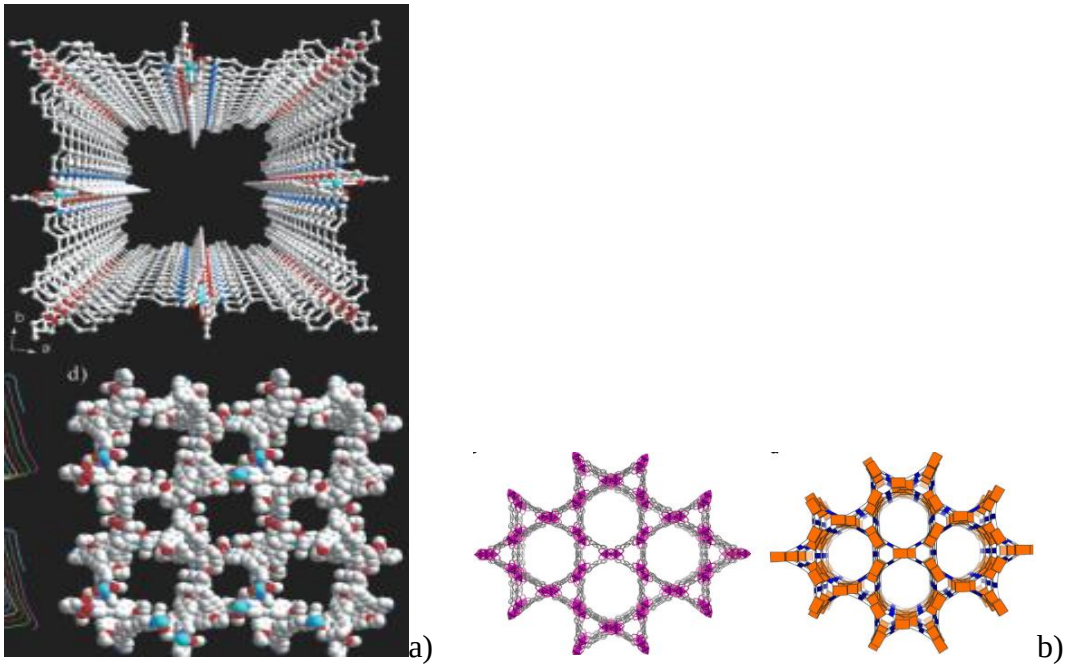

Figure 1.4: *a) Chiral 1D channels in $[Ni(acac)_2(L1)]\cdot 3CH_3CN\cdot 6H_2O$, b) interpretation network of Zr-MOF with pore in uniform 1D hexagonal channels.*

The third type of porous structures are layered-2D CPs, in which guests can be incorporated to link the layers.[112] Figure 1.5 shows the layers of dynamically unstable $[Cu(ca)(H_2O)_2]$ (H_2ca: chloranilic acid) in which phenazine (phz) and 2,5-dimethylpyrazine (dmpyz) can be incorporated having the effect on properties such as flexibility and stability.[112,116] The layers of $[Cu(ca)(H_2O)_2]_n$ showed the distance of 8.45 Å between copper atoms in different sheets. Once phz is intercalated

into layers to make $\{[Cu(ca)(H_2O)_2]\cdot phz\}_n$, the framework gains stability. The layers became tightly linked resulting in 9.25 Å distance between Cu ··· Cu (interlayers).[116] When dmpyz is incorporated, it forms columnar stacks between the sheets with two phases in the formed $\{[Cu(ca)(H_2O)_2]\cdot dmpyz\}_n$. The layers are flexible in lengthening the distance of $\{[Cu(ca)(H_2O)_2]_n\}_m$ ranging from 8.45 to 11.0 Å. In addition, the stability of these 2-D sheet structures was noticed. The intercalation of guests depends on a π-electron structure with which it forms a stacked column and hydrogen-bonding sites in opposing directions making bridges for the layers.[112,116]

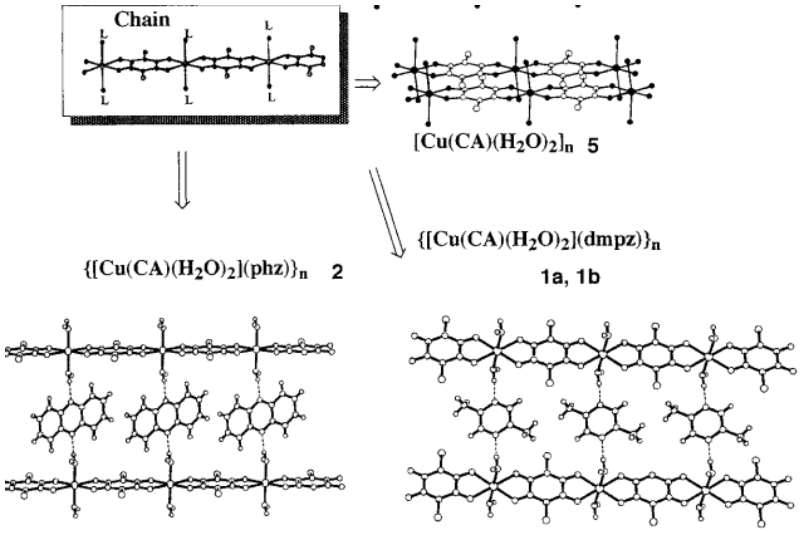

Figure 1.5: *2D space porous made by layers of Cu(ca)(H₂O)₂.*[116]

The fourth type of porous systems involve interconnecting 1D channels which run in different directions, such as those that frequently occur in zeolites [112] as shown in Figure 1.6. CPs containing 3D channels are not frequent and possess high porosity which contribute to the framework instability.[112] The framework of $[Ni_6(btc)_4(bipy)_6(CH_3OH)_3(H_2O)_9\cdot(guest)]$ (btc: benzenetricarboxilic acid) contains 3D porous networks built from 2D $Ni_3(btc)_2$ layers where the latter are in turn pillared by 4,4′-bpy ligands.[117] It forms hexagonal-shaped channels which run

parallel to the stacking direction. Furthermore, there are other 1D channels (8 x 4.4 $Å^2$) running both within and between the layers. As a result, these channels run a combination of parallel and perpendicular to the (6, 3) layer stacking directions forming the overall 3D channels.

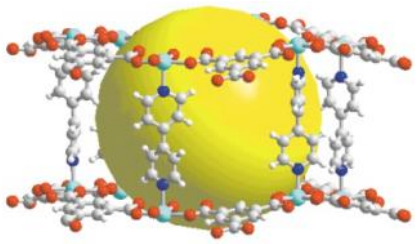

***Figure 1.6**: Channels parallel and perpendicular to the layers intersect to form a 3D large cavity of 15.6 Å centred on the 1c position in [$Ni_6(btc)_4(bipy)_6(CH_3OH)_3(H_2O)_9$·(guest)].*[117]

Another reported 3D channel structure is $[Cu_2(BTR)_2]·2NO_3$ (BTR: 4,4'-bis(1,2,4-triazole))[118] resulting from the connection between copper ions and the BTR linkers to form a 3D framework. The 3D channels showed triangle apertures and run along the [1 1 1], [-1 1 1], [1 -1 1], and [1 1 -1] directions.

On the other hand, porous structures can be classified into non-porous, microporous, and mesoporous structure based on their pore sizes. These porous structures can be identified from CPs including MOFs. Jiang *et al.*[108] characterized non-porous Cd(L)(bpy), microporous $Cd(L)(bpy)·4H_2O·2.5DMF$, and mesoporous $Cd(L)(bpy)·4.5H_2O·3DMF$ frameworks where L is 2-amino-1,4-benzene-dicarboxylic acid and bpy is bipyridine. The first framework is characterized by channels that are filled by interpenetration. The second structure is characterized by the coordination of Cd by L and bpy allowing the formation of microporous channels with size of 1.1 × 1.9 nm^2. The third framework of $Cd(L)(bpy)·4.5H_2O·3DMF$ is characterized by larger triangular and hexagonal open-channel with mesoporous size of 1.8 × 2.3 nm^2. Both microporous

and mesoporous spaces were also identified in $[(Zn_4O)_9(NH_2BDC)_6(BTB)_5]$ with dimension of 14 × 17 $Å^2$ and 27 × 32 $Å^2$ respectively.[119] The dimensions of mesoporous structures are estimated to be between 2 and 50 nm (20 and 500 Å respectively) while microporous structures contain pores of less than 2 nm (20 Å).[120,121] The pore sizes play important role for the adsorption capacity, kinetic sorption, and selectivity in sorbents.[62,122,123] Millward and Yaghi showed that larger pore sizes may have higher adsorption capacity.[123] This property was reported in MIL-101 known as $Cr_3O(F/OH)(H_2O)_2[C_6H_4(CO_2)_2]$ with pore size between 1.6 and 2.1 nm and Cr(OH)-$[C_6H_4(CO_2)_2]\cdot nH_2O$ known as MIL-53 with pore size less than 1 nm.[122] Their adsorption capacities for methyl orange were 114 and 57.9 mg g^{-1} respectively.

On the other hand, this trend does not apply for micro and meso-CuBTC.[121,124] It was noticed that meso-CuBTC has a lower adsorption capacity for CO_2/CH_4 than micro-CuBTC.[121] The same observation was reported from $Cu_3(BTC)_2$ where microporous (or small pores) adsorbed 12.01 mmol g^{-1} of hydrogen while mesoporous (higher pore size) adsorbed 8.79 mmol g^{-1}.[124] However, larger pore sizes can allow higher adsorption selectivity in the same compounds. In this regard, meso-CuBTC showed a higher CO_2/CH_4 selectivity over micro-CuBTC.[121] The pore size plays an important role in MOFs applications such as adsorption-desorption processes where structural transformations and colour changes may occur.[58,79,125,126] Even though large pores may present low adsorption in some cases, functionalization of the surface can overcome this drawback.[68,107,111,127] It also worth noting that the variation of concentration and reaction time can assist to control pore size.[108]

1.3.4.6. Sorption studies in MOFs

MOFs are used in different applications including sorption of small molecules.[21,43,79] The physico-chemical properties of MOFs play an important role in the sorption process[119] The pore diameter, orientation of substituents in pores,[79,111] the functional groups in the framework,[111,127,128] and the available metal sites affect the adsorption process for the guest molecules.[128] Thus, pore surface allows controlling functionality for the targeted application.[111] An and Rosi [129] showed that tuning pore sizes and functionalities in MOFs results in suitable adsorption capacity and selectivity. For example, a series of MOF-177 were synthesized utilizing the ligands with mixed functionalities to result in enhanced adsorption capacity for hydrogen gas compared to unfunctionalized analogs.[130] Figure 1.7 shows the advantage of a MOFs (MIL-101) for its higher adsorption capacity compared to other solid adsorbents, due to its high porosity, surface area, and functional groups.[32,130] MIL-101 (estimated surface area of S_{BET} = 3900 m^2 g^{-1}, $S_{Langmuir}$~5900 m^2 g^{-1} showed higher adsorption capacity compared to solid adsorbents such as mesoporous silica (SBA-15, S_{BET} = 805 m^2 g^{-1}), zeolite (HZSM-5, Zeolyst PQ, S_{BET} = 550 m^2 g^{-1}), and a commercial activated carbon (AC) (Darco, S_{BET} =1600 m^2 g^{-1}). The measured sorption capacities for the sorption of benzene at P/P_0 = 0.5 in MIL-101 was 16.7 mmol g^{-1} while in SBA-15, HZSM-5 , and AC these were 3.0, 1.9, and 8.0 mmol g^{-1}, respectively.[32]

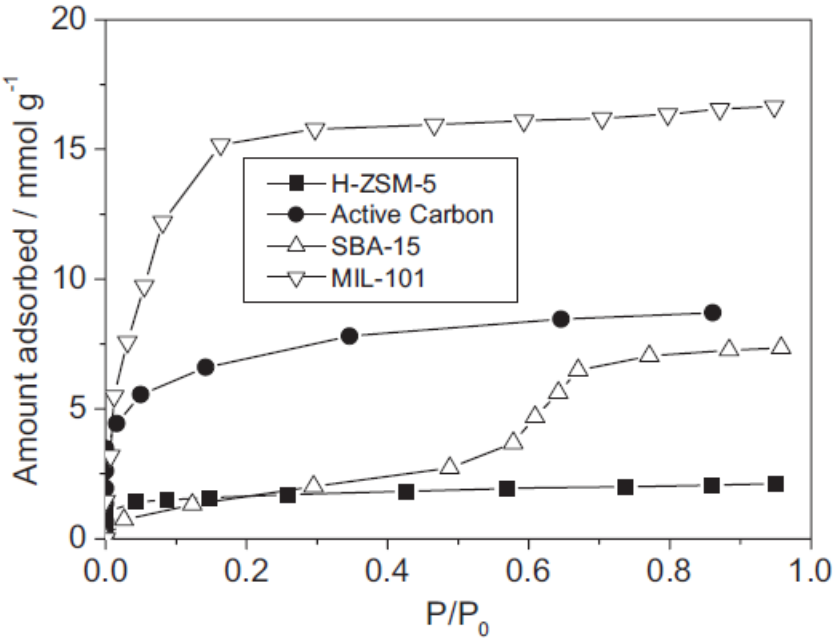

Figure 1.7: *Sorption isotherm of benzene at 30 °C on MIL-101 is higher than that of commercial actived carbon, HZSM-5 zeolite, and mesoporous silica SBA-15.*[32]

Sorption of guest molecules in MOFs can be characterized by different behaviours. The reversible, irreversible, or absence of changes occur depending on the nature of the framework. These changes allow the classification of MOFs such as flexible (breathing) and rigid frameworks.[99]

1.3.4.6.1. Flexibility and breathing phenomena in MOFs

The sorption process in MOFs is sometimes accompanied by the reversible or flexible changes in unit cell parameters so that the host can accommodate and release the guest molecules; this is sometimes called the "breathing phenomenon".[13,64,79] Figure 1.8 displays the reversible changes known as breathing effects observed in the vanadium-based MOF; VO(BPDC) (BPDC = biphenyl-4,4′-dicarboxylate).[79] They are stimulated by external stimuli such as the pressure and temperature during the sorption process.[80]

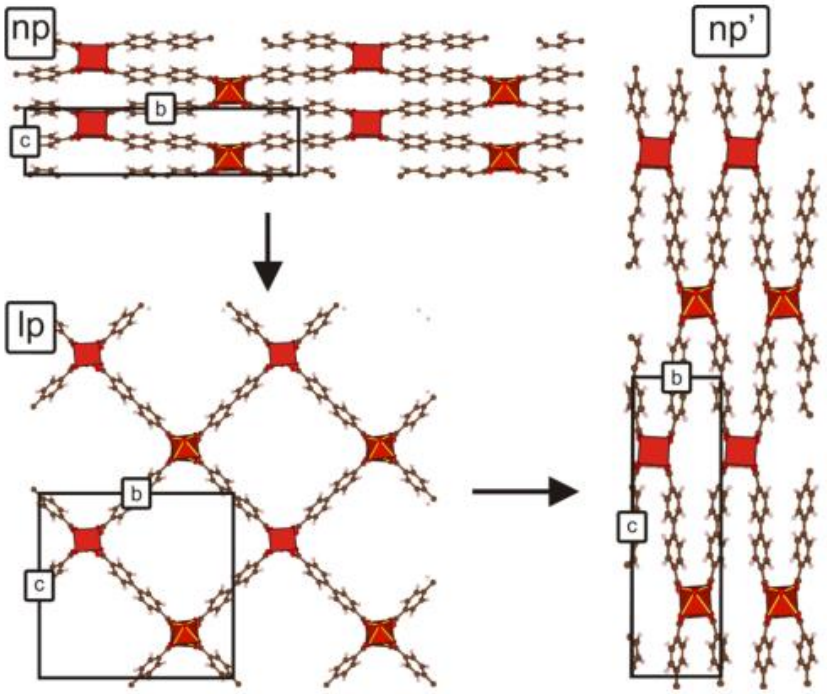

Figure 1.8: *Breathing effect due to the adsorption process from VO(BPDC) showing the changes from narrow to large and then back to narrow pores.*[80]

Once narrow pores (np) are accommodating guest molecules, the framework undergoes enlargement of the pore and forms large pores (lp). When the guest molecules are released, lp returns to np pores (np'). The phenomenon of breathing effect was also observed in $[Zn(34pba)_2]_n$ (34pba: 3-(4-pyridyl)benzoic acid).[43] In this framework, the unit cell volume was observed to increase during absorption of guests. It was also noted that, when using alcohols as guest molecules, the unit cell volume expands linearly due to the increase in number of carbon atoms of the guest molecules. The cell volume changed from 4681.0 $Å^3$ (empty) to 5005.0 $Å^3$ for the absorption of 1-propanol and 5086 $Å^3$ for the absorption of 1-butanol. This breathing effect was also observed for MIL-53 $[Cr^{III}(OH)(OOC–C_6H_4–COO)]$ during the sorption of CO_2.[64]

1.3.4.6.2. Rigid MOFs

Rigid frameworks are characterized by their stable structures without any transformation or change in dimension once inclusion occurs during isotherm sorption process.[118,131,132] The sorption and solvent exchange within DUT-4 (ndc = 2,6-naphthalene dicarboxylate), left intact framework confirming the rigidity of DUT-4.[132] Some thermal stimuli may cause dynamic responses as was observed within $[Cu_2(BTR)_2]\cdot 2NO_3$.[118] The documented rigid or flexible MOFs were found to result from the kind of ligand or solvent used during synthesis.[132]

1.4. KINETICS OF ADSORPTION/DESORPTION IN THE SOLID STATE

Kinetic studies in solid state reactions give informative results where the behaviour of a sample can be studied over a wide range of experimental conditions.[133,134] The similarities and differences between samples can be characterized to elicit the factors that influence the reaction. Therefore, it may provide information on the reaction rate and the relation with time and temperature during the process of occurring reaction.[134,135] These factors are determined using different techniques such as thermogravimetric analysis (TGA), differential scanning microscope (DSC), and ultraviolet-visible (UV-Vis) spectrophotometry. The kinetics of single step reactions can be expressed in term of mass conversion by equation (1)

$$\frac{d\alpha}{dt} = Ae^{-E_a/RT}f(\alpha) \qquad (1)$$

where α is the converted fraction at time t, A the Arrhenius pre-exponential factor, E_a the activation energy, R the universal gas constant, T is the absolute temperature, and $f(\alpha)$ a function depending on the reaction mechanism.[134]

The mass change that results from heating the sample at selected temperature provides information on kinetic parameters related to the desorption of the guest. This is an isothermal technique to determine the kinetic parameters for absorption or desorption of guest. In isothermal process, the sample is heated to a temperature where the complete desorption of guest molecules can be measured isothermally. Several temperatures close to one another are used to obtain isothermal desorption curves. These curves are then tested using simulated model desorption mechanisms to find the best fit between model and experimental data. This allows one to determine the mechanism associated with the removal of the guest molecules in solid state.[134] Various kinetic models have been proposed to characterize the progress of reactions (Table 1.3 lists some of the more common models).[134] In this regard, a model will suggest whether a reaction corresponds to reaction type such as nucleation, geometrical contraction, diffusion, and reaction order. From equation (1), the reaction of linear heating program allows the determination of α during the experiment by equation (2).

$$\alpha = \frac{m_o - m}{m_o - m_f} \qquad (2)$$

where α is the conversion level, m_o, m, and m_f are initial mass, mass at temperature t, and residual mass respectively.

In some cases, isothermal techniques do not work well, for example if the process is not a single step. In this case, non-isothermal kinetic techniques may be applied. The sample is heated at different heating rates to follow the desorption of the guest molecules. The relationship between heating rates and temperature allows the determination of the activation energy (Ea) associated with the desorption. Following Ozawa's model,[133] the equation (3) can be integrated to determine the activation energy.

$$\frac{d\alpha}{dt} = lnA - \frac{E_a}{R}T + \ln[f(\alpha)] \quad (3)$$

After plotting $\frac{d\alpha}{dt}$ against $\frac{1}{T}$, E_a can be obtained by equating the slope to $\frac{E_a}{R}$ [133,134] This method does not require a kinetic model to be fitted to the experimental data.

Table 1.3: *Some commonly used functions f(α) for solid thermal conversion reactions*

Model	**f(x)**	**g(x)**
Reaction order	$(1-\alpha)^n$	
0		α
1		$-\ln(1-\alpha)$
≥2		$[1/(n-1)](1-\alpha)^{n-1}$
Phase boundary reaction		
Cylindrical symmetry	$2(1-\alpha)^{0.5}$	$1-(1-\alpha)^{0.5}$
Spherical symmetry	$3(1-\alpha)^{2/3}$	$1-(1-\alpha)^{1/3}$
Diffusional		
One-dimension	1/2α	α^2
Two-dimension	$[-ln(1-\alpha)]^{-1}$	$(1-\alpha)[\ln(1-\alpha)]+\alpha$
Three-dimension spherical symmetry, Jander equation	$1.5(1-\alpha)^{\frac{2}{3}}[(1-\alpha)^{1/3}]^{-1}$	$[1-(1-\alpha)^{1/3}]^2$
Three-dimension spherical, Ginstling–Brounshtein	$1.5[(1-\alpha)^{\frac{1}{3}}-1]^{-1}$	$\left(1-\frac{2\alpha}{3}\right)-(1-\alpha)^{2/3}$

1.5. GAS SORPTION STUDIES

Gas sorption is used as an important tool to characterize the structural features associated with sorption in solids adsorbents and fine powders.[136] Features such as surface area, pore size, and volume are analysed through the sorption process.[136,137] The sorption process is the penetration of molecules through the external surface of the material and subsequent attachment on its internal surfaces.[136] The term sorption or adsorption is branched in both physisorption and chemisorption depending on the strength of interactions between the adsorbate and adsorbent. Chemisorption is

characterized by the adsorbate-adsorbent interaction leading to the formation of chemical bond while physisorption is characterized by the contact of the adsorbate gas with the surface of the solid adsorbents.[136] Adsorbate and adsorbent present particular geometric and electronic properties which generate molecular interactions as polarisation, field-dipole, or field gradient quadrupole. Brunauer–Emmett–Teller (BET) theory utilizes the physisorption for gases such as nitrogen, argon, and krypton to access the specific surface area of an adsorbent as they are less reactive. Thus, the surface area can be determined. The sorption of gases also allows studying the effect of free coordination sites using gases such as CO_2 which can interact with the Lewis-acidic metal centres.[138] In this regard, it was noted that a highly accurate manometric adsorption equipment is required for reliability.[136]

The physisorption process can be analysed by plotting curves of adsorbed amount against relative pressure. These allow classifying physisorption isotherm into six types.[136] The characteristic types of isotherms are related to particular pore structures and are illustrated in Figure 1.9. (i) Reversible type I isotherm characterizes microporous structures of width ≤ 1nm. The curve is concave to the p/p_0 axis and the amount adsorbed reached the equilibrium quickly. When the materials have pore size distribution over a broad range including microporous and possibly narrow mesopores (≤2.5 nm), this is referred to as type I(b) isotherms. (ii) Reversible type II isotherm characterizes the physisorption of nonporous or mesoporous materials. Those materials can be composed of multilayers. (iii) Type III isotherm is characterized by relatively weak adsorbate-adsorbent interactions. Nonporous or macroporous solid adsorb molecules which are clustered around the most favourable sites on the surface area. (iv) Type IV isotherms curves are only observed in mesoporous adsorbents. They are characterized by the adsorption on the mesopore walls of monolayer-multilayer which is followed by the condensation to liquid-like phase by adsorbate in

pores. Type IVa isotherm is characterized by the presence of hysteresis in capillary condensation and the pore width surpasses a certain critical width. Type IVb is observed in adsorbents possessing mesopores with smaller width. (v) Type V is observed in the adsorption of water on hydrophobic microporous and mesoporous adsorbents. In this case, weak adsorbate-adsorbent interaction and pore-filling at high p/p_0 low p/p_0 range are observed. (vi) Reversible stepwise Type VI isotherm is characteristic of layer-by-layer adsorption in the uniform nonporous surface.

If the adsorption and desorption curves do not coincide, this is known as hysteresis. Hysteresis is caused by the delayed desorption due to stronger adsorbate-adsorbent interactions.[136,137]

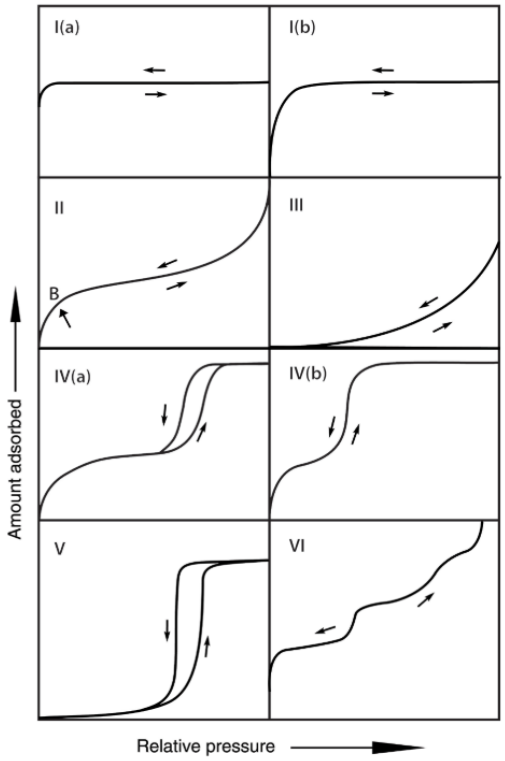

Figure 1.9: *Sorption isotherm types.*

1.5.1.1. Topology

In crystallography, topology is used to explain the periodic spacial occupation of nodes or vertices bridged by edges which does not change under continuous deformation.[88,139,140] This explains how two different structures can show the same inorganic or organic secondary building units.[95] In this regards, the topology of MOFs and other coordination polymers (CPs) are described based on the application of periodic nets and tilings. MOFs and CPs can be constructed from the atomic nets that include all atoms as nodes and all interatomic bonds as edges. On the other hand, in most cases nodes are considered as central vertices while the linkers represent the edges.[58,140]

Nodes in MOFs can be a result of well-defined molecular clusters (containing metal or organic atoms) rather than single atoms, thus forming a simple geometrical shape referred to as a secondary building unit (SBU).[141] The node in MOFs contains points of extension (to allow the attachment of the edge) that allow them to have a particular shape that is periodically repeated in the network. Figure 1.10 displays examples of SBUs: triangular, square, and octahedral. A triangular SBU (a) possesses three double points of extension (shown in green) to present three binding sites for the edges.[141] A square SBU (b) is characterized by the presence of two red double points of extension and two separate gray points of extension while the octahedral (c in blue) has six points of extension.[43]

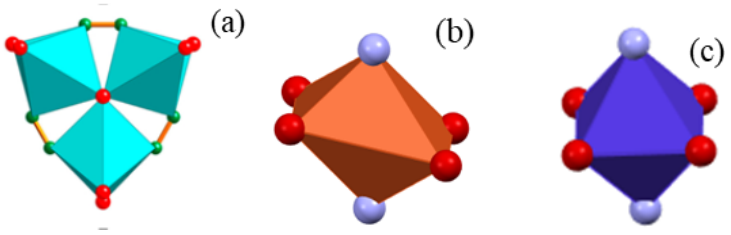

Figure 1.10: *(a)Triangular secondary building unit with three double points of extension,[141] and (b) four extension (double red = one point of extention) points for square SBU[43] and (c in blue) six extension points four octahedral SBU.[141]*

1.5.1.1.1. Simplification and coordination features in metals and ligands

The MOFs or CP-3D chemical composition influences the underlying net topology indirectly, predetermining coordination features of the nodes. Some nodes are the results of SBUs from more than one metal atoms which are simply considered as one node.[140,141] Figure 1.11 in (a) shows a cluster of a SBU from two metals (including oxygen and carbon atoms) that may give rise to either tetrahedron or square geometry while in (b) a SBU from four metal ions (including oxygen and carbon atoms) may also give rise to either an octahedron or trigonal prism.

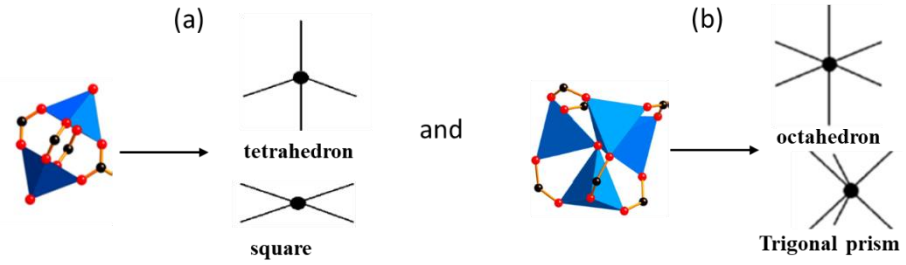

Figure 1.11: *Secondary building units (SBUs) in their possible corresponding arranged vertices*

Similarly, ligands undergo the simplification where a number of atoms represents an edge.[58] On the other hand, there are multitopic ligands that make both edge and centre as node.[141] Figure 1.12 (a) shows a tetratopic ligand that was simplified into edges and either two or one nodes in the middle. There is also the possibility that a ligand can be omitted from the underlying net while a metal atom can be simplified to an edge.[140]

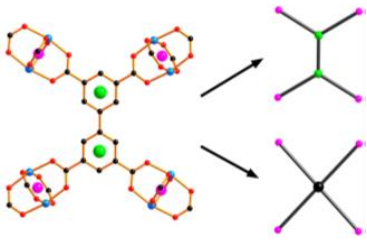

Figure 1.12: *Simplification of a tetratopic linker that contains edges and nodes in the centre. Edges are in black while metal centres are shown as violet.*[141]

The deconstruction and construction of an underlying net of a MOFs requires this simplification. The right attribution of some atoms to nodes and others to edge is most important to achieve a corresponding net.[58,140] An example is the Co^{2+} centre coordinated to four pyridylbenzoate (pba) ligands which are ended by another Co^{2+} ion. Figure 1.13a indicates the structure and simplification process outlined in green line. Once the nodes and edges are chosen, all Co^{2+} ions and pba ligands become nodes and edges respectively to form an underlying net (Figure 1.13b).

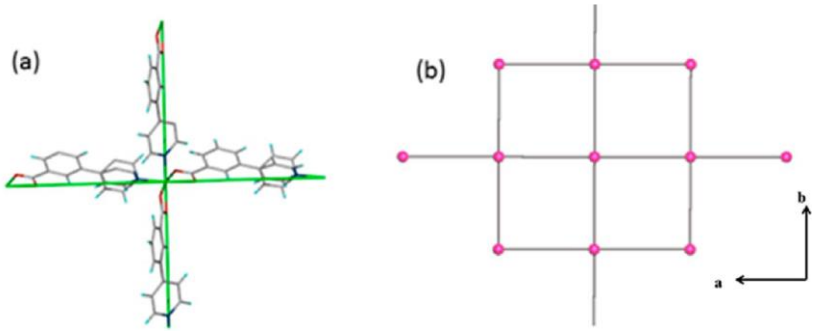

Figure 1.13: *Simplification of ligand and formation of underlying nets.*[58]

As explained above, metal or metal cluster in MOFs constitutes a node. The latter plays a key role in orienting or influencing the topology of a network (Figure 1.14).[58,140] For example, Co^{2+} was tetrahedrally coordinated to form a square planar (**sql**) topological network.[137,142] However, this can also be achieved by considering a number of edges through the extension points.[101] Similarly,

an octahedral SBU leads to **pcu** underlying net.[88] In general, the coordination fashion of triangle, square, tetrahedron, octahedron, and cube give rise to **srs**, **nbo**, **dia**, **pcu,** and **bcu** respectively which are the most frequent nets.[140]

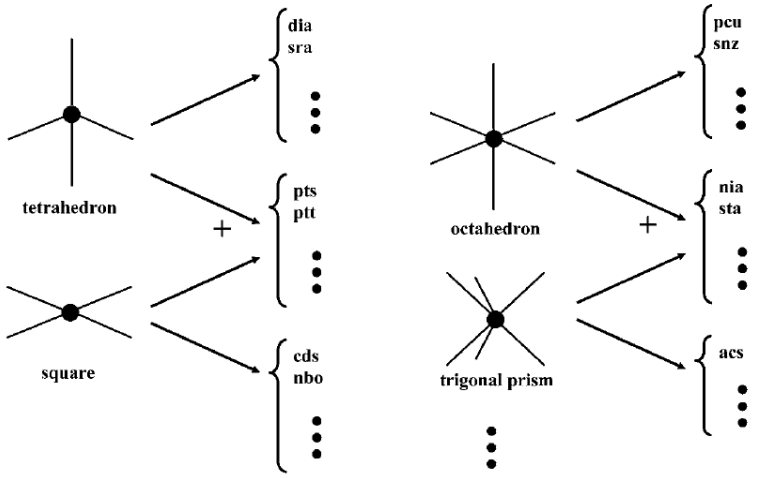

Figure 1.14: *Formation of underlying net from coordination figures (or nodes).*[140]

1.5.1.1.2. Network topology

Figure 1.15 in (a) presents a simple 2D net with one type of vertix throughout the whole underlying net; such a net is therefore referred to as a uninodal net.[88,100] The net can contain types of node such as unimodal net, binodal net, and other complicated ones.[55,78,100,141] Figure 1.15 (b) and (c) shows a binodal net with different types of vertices. The sequence of these shape of the rings around a node form point symbol.[142,143] The net in (b) shows a vertex (surrounded by a green solid line) that is surrounded by a sequence of three triangular and two square rings, thus giving rise to $3^3.4^2$ point symbol. The net in (c) also has a vertex surrounded by a sequence of two triangular, one square, one triangular, and one square rings, thus, having $3^2.4.3.4$ as point symbol.[144]

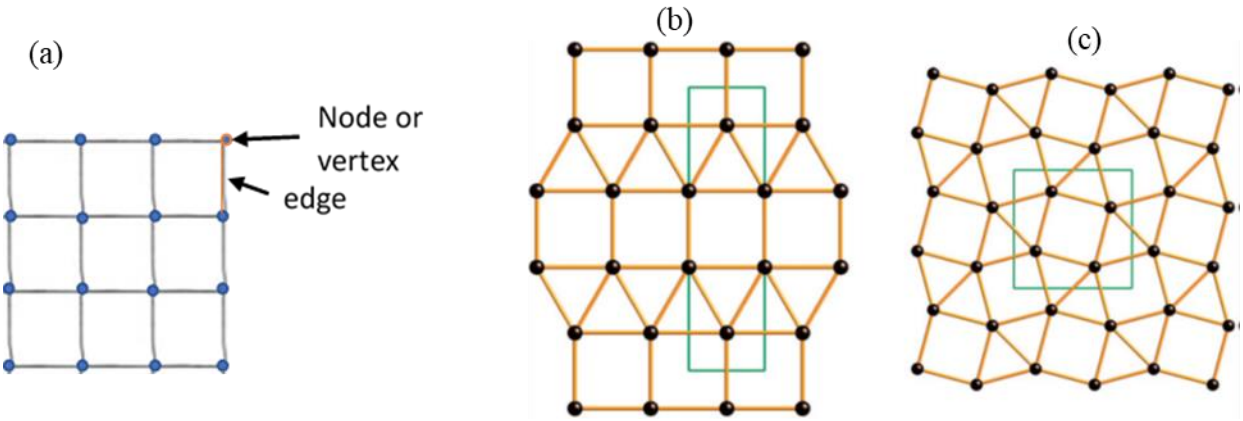

Figure 1.15: *(a) Uninodal net showing vertex and edge, (b) two 2-periodic binodal nets of tilings by triangles and squares $3^3.4^2$ (**cem**), and (c) $3^2.4.3.4$ (**tts**).*[144]

Common terminology and software can be used to examine the architecture of networks with correct topology.[144] The assignment of a MOF to a particular underlying net and topology is not an easy task. Care must be taken during simplification for a correct node or edge. However, common regulation to achieve networks with correct topology have been established. The computer program, TOPOSPRO, is equipped with an algorithm developed to solve this challenge.[140,144]

1.5.1.2. Synthesis of MOFs

The synthesis of porous compounds depends on specific conditions such as temperature, pressure, time, concentration, pH, and solvents.[44,145,146] These conditions form different synthetic methods of MOFs. Among them, traditional syntheses known as solvothermal and non-solvothermal methods involve the use of solvent other than water at high temperature.[61] Solvothermal synthesis is preferable as it produces higher yields and better crystallinity of the product. In this case, the mixtures of starting materials are loaded in closed steel autoclaves and heated at high temperature to generate the pressure.[102,147] This allows the solubility of the reagents which promotes the

crystallization. Both solvent and temperature have been reported to influence the diversity of MOFs synthesis.[102,148] For example, the synthesis of UiO-66 from $ZrCl_4$ and 2-amino-1,4-benzenedicarboxylic acid (H_2N-H_2BDC) in DMF at 120 ^oC for 24 h resulted in an amorphous phase. However, when the same starting materials were first heated at 80 ^oC for 12 h and then at 100 ^oC for 24 h the targeted crystalline compound was successfully produced.[44] The nature of the solvent was also found to influence the preparation of MIL-96(Cr) and MIL-100(Cr) which differ only in the use of a solvent mixture of water/methanol and water/acetone respectively.[109] When water and DMF were used as an alternative solvent mixture, no solid phase was produced from the same ligand and metal centre.[109] In non-solvothermal synthesis, the reagents should reach a certain concentration to start nucleation for crystal formation. This can be achieved through the slow evaporation of the solution, solvent layering or slow diffusion of one of the reactants. The reactions are performed in open reactors at atmospheric pressure.

Mechanochemical synthesis is an emerging approach to synthesize MOFs.[61,149] This method uses mechanical force for chemical transformation such as breaking and formation of new bonds, amorphization, and charge separation effects.[150] Milling or grinding is the form of mechanochemistry most commonly known. The reaction is fast with a high yield and is usually solvent-free.[149] Sometimes very small amount of solvent may be needed to achieve a better crystallinity. Mechanochemical synthesis method is environmentally friendly and can produce materials not readily accessible in solution or solvothermally.[149]

1.5.1.3. Ligands and metal centres in MOFs

A number of structural frameworks of porous MOFs containing carboxylates have been studied and investigated for their applications.[39,52,73,119] Figure 1.16 shows SBUs of Zn_4O which are extended by terephthalates[68] in which carboxylate oxygen atoms coordinate to the metal centres to construct a secondary building units (SBU) of the MOFs.

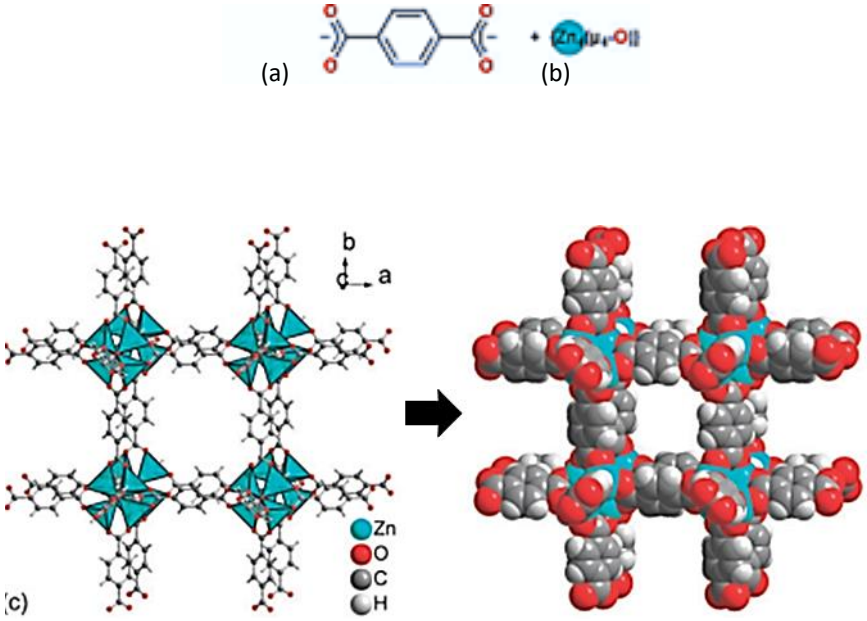

Figure 1.16: *(a) Carboxylate ligand with oxygen donor atoms, (b) Secondary Building Unit (SBU) Zn_4O, and (c) Window formed by SBU (green: Zinc, red: oxygen) and ligand extension (grey: carbon with).*[6868]

The coordination of MOFs involving nitrogen donor atoms such as $\{[Cu(4,4'\text{-bpy})_2](BF_4)\}_\infty$, $[\{Ni(4,4'\text{-bpy})_2(H_2O)_2\}_2Mo_8O_{26}]n$, $\{[Ag(2,4'\text{-bpy})]\cdot ClO_4\}n$, and $[Cd(4,4'\text{-bpy})_2]$,[112] have also been reported. Studies on MOFs which are built using ligands containing both oxygen and nitrogen donor atoms are increasing.[85,88,126,139] The ligands 3-(4-pyridyl)benzoate (34pba) and 4-(4-pyridyl)benzoate (44pba) in Figure 1.10 (a) and (b) were used to synthesize different MOFs.[43,58,101,139] Functionalized ligands, 34paba and 44paba (34paba = 3-(pyridyn-4-

ylmethyl)aminobenzoate, 44paba = 4-(pyridyn-4-ylmethyl)aminobenzoate) which are derivatives of 34pba and 44pba (Figure c and d) can also be used in synthsis. They showed free rotational movement between the pyridyl and benzene rings along the ligand backbone which can facilitate the inclusion of the guest molecules.[43] Figure 1.16 (e) shows the coordination of cobalt ions by 34pba ligand resulting in the framework with channels.[43] The latter showed the breathing mechanism as proved by a linear increase of unit cell volume with an increase in the number of carbon atoms of the alcohol molecule that was adsorbed. This is an important property where the channel of the framework can adapt its size depending on the size of incoming guest molecules. However, the threshold conformation was noted.[43]

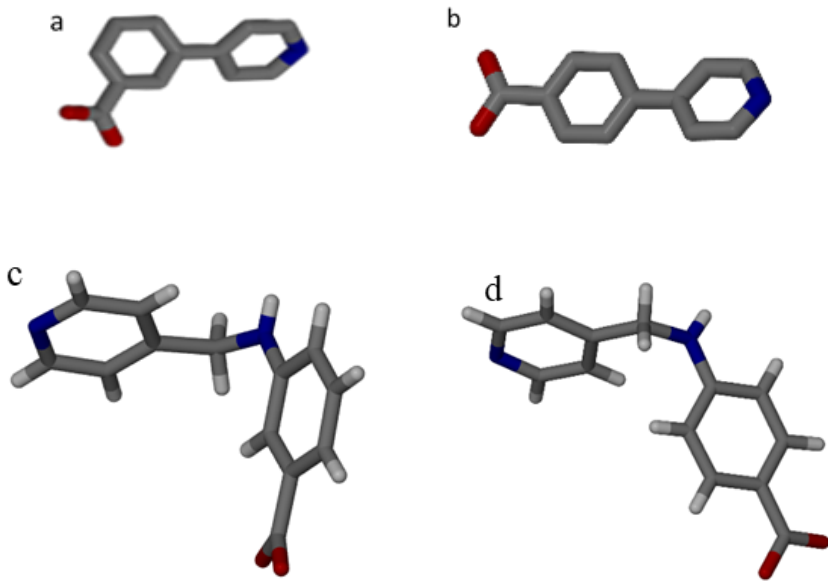

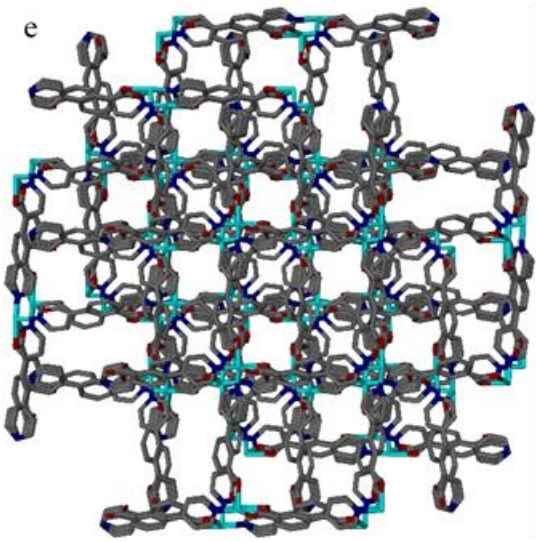

Figure 1.17: *(a and b) Two single ligands 3-(4-pyridyl)benzoate and 4-(4-pyridyl)benzoate, (c) Framework* $[Zn(34pba)_2]_n$ *showing channels made by Zn (green) coordinated by both oxygen (red sticks) and nitrogen atom (blue sticks). The grey sticks are carbon atoms and hydrogen are omitted for clarity.*[43]

Utilizing pyridylbenzoate as linkers, MOFs without interpenetration could be synthesized.[101] In these frameworks, high uptake for hydrogen, methane, and carbon dioxide gases, and solvatochromic and luminescent sensing properties were reported.[55,151] The ability of MOFs to change colour in response to the sorption of small guest molecules also make them candidates for sensors.[58,152]

Concerning metal centres, cobalt (II) ion acts as a Lewis acid in MOFs coordination.[103] Cobalt(II) is widely used, in MOFs such as $\{[Co(34pba)_2]\cdot DMF\}_n$ (where 34pba = 3-(4-pyridyl) benzoate and DMF = dimethylformamide). Cobalt-containing MOFs have been reported to form three dimensional structural frameworks with interesting channels[62] and have been used for sorption applications.[58] This metal has also been used in the synthesis of Co-MOF-74 using 2,5-dihydroxy benzenedicarboxylic acid (H_4DHBDC) as ligand for CO_2 adsorption and catalytic activity.[103] Another interesting property of some MOFs formed from this metal centre is the colour change

(solvatochromic) associated with recognition of new guest molecules (solvents), which can be applied for sensing.[58]

Copper(II) has been used in different MOFs.[33,76] Its coordination into $[Cu_3(\mu_3\text{-}OH)_2(H_2O)_2\{(SO_3)C_6H_3(COO)_2\}(CH_3COO)]$ showed a reversible removal of water molecules forming $Cu_6(\mu_3\text{-}OH)_4\{(SO_3)C_6H_3(COO)_2\}_2\text{-}(CH_3COO)_2$.[77] The synthesis of Cu(BDC-OH)(4,4'-bipy) H_2BDC-OH = 2-hydroxy-benzenedicarboxylic acid, 4,4'-bipy = 4, 4'-bipyridine resulted in a framework with a higher affinity for ethylene and carbon dioxide than methane showing high selectivity for separation.[76] In this regard, copper centres in the synthesis of MOFs may contribute to different applications.

Zinc(II) is a metal centre widely known in MOFs such as $(Zn_4O[(OOC)_2{\cdot}C_6H_4]_3)$ and $[Zn(\mu_2\text{-}ia)(\mu_2\text{-}bpe)]_n{\cdot}nDMF$ (ia = isophthalate, bpe = 1,2-bis(4-pyridyl)ethane)[72,90] Another zinc compound, $[Zn_2(\mu_2\text{-}OH_2)(HBTRI)(BTRI)\text{-}(H_2O)_2]{\cdot}DMA{\cdot}3H_2O$, (BTRI = 1,3,5-benzenetricarboxylate, DMA = dimethylacetamide) showed breathing phenomenon where it loses and restores its crystallinity during water sorption.[82] $[Zn(34pba)_2]_n$ where 34pba is 3-(4-pyridyl)benzoate linker was characterized by a breathing effect and could accommodate selectively the alcohols in channels.[43] Therefore, zinc can also be seen as an important metal centre in the synthesis of MOFs for potential applications.[43,97]

1.6. MOTIVATION AND OBJECTIVES

1.6.1. Motivation

MOFs have become attractive targets for their potential application in sorption properties.[43,59,153] They often present permanent porosities and can withstand high temperatures. They can be flexible

and able to retain their crystallinity after the sorption or removal of guest molecules.[139] Many MOFs have superior efficiency in their sorption capacity over other traditional solid adsorbents as discussed above. Ligands containing both carboxylate and pyridyl linkers are attracting attention to construct MOFs for their interesting sorption properties. On the other hand, the synthesis of MOFs, such as $\{[Ni_4(44pba)_8]\cdot sol\}_n$ were reported to have interpenetration of their frameworks.[152] Even though there was interpenetration, solvents could be adsorbed and accompanied by colour change. In addition, a system of the mixed ligands of 44pba and 34pba was used to synthesize Cd(34pba)(44pba) MOF without interpenetration.[139] This MOF was characterized by an interesting property of breathing mode responding to the respective size of the guest molecules. Therefore, these compounds are attractive for various applications. However, there are limited reports on the synthesis of MOFs based on the ligands containing both oxygen and nitrogen donor atoms.

This work intends to extend the synthesis of MOF based on divalent metal centres using mixed 34pba and 44pba ligands. The functionalized ligands 34paba and 44paba, which are longer than 34pba and 44pba and incorporate a non-coordinating amine moiety, (34paba = 3-(pyridyn-4-ylmethyl)aminobenzoic acid, and 44paba = 4-(pyridyn-4-ylmethyl)aminobenzoic acid) were also used to generate larger pores with inherent functionality. Considering the stability and robustness, synthesized MOFs were tested for their capacity and selectivity for the removal of chlorinated and amine VOCs. In an unrelated study, a discrete complex, *cis*-dichloro-bis(**en**)cobalt(III) chloride (en: ethylediamine) showed the interactions of water guest molecules with chloride as counter ion in their channels. A study of sorption property for different vapour solvents was carried out using this complex.

1.6.2. Objectives

The overall objectives of this study were to:

- Synthesize of MOFs based on single and mixed 34pba and 44pba ligands with divalent metal ions
- Synthesize of MOFs based on 4-(pyridyn-4-ylmethyl)aminobenzoic acid (44paba), 3-(pyridyn-4-ylmethyl)aminobenzoic acid (34paba) as functionalized pyridylbenzoate ligands
- Study the structural networks using single crystal X-ray diffraction and characterization using powder X-ray diffraction, Fourier-Transform infrared spectroscopy, thermogravimetric analysis, differential scanning calorimetry, and nuclear magnetic resonance spectrometry
- Investigate the adsorption properties of the synthesized MOFs for a series of chlorinated and amine VOCs
- Investigate the regeneration of the activated MOFs to check their recyclability
- Consider as a separate study in this thesis, the sorption properties of *cis*-dichloro-bis(en)cobalt(III) chloride for a range of organic solvents.

1.7. REFERENCES

1. El Hadi, M. A. M., Zhang, F. J., Wu, F. F., Zhou, C. H. & Tao, J. Advances in fruit aroma volatile research. *Molecules* **18**, 8200–8229 (2013).

2. Ziska, F. *et al.* Global sea-to-air flux climatology for bromoform , dibromomethane and methyl iodide. *Atmos. Chem. Phys.* **13**, 8915–8934 (2013).

3. Erim, F. B. Trends in Analytical Chemistry Recent analytical approaches to the analysis of biogenic amines in food samples. *Trends Anal. Chem.* **52**, 239–247 (2013).

4. Tabanelli, G. Biogenic Amines and Food Quality: Emerging Challenges and Public Health Concerns. *Foods* **9**, 7–10 (2020).

5. Huang, B., Lei, C., Wei, C. & Zeng, G. Chlorinated volatile organic compounds (Cl-VOCs) in environment - sources, potential human health impacts, and current remediation technologies. *Environ. Int.* **71**, 118–138 (2014).

6. Martin, L., Ognier, S., Gasthauer, E., Cavadias, S., Dresvin, S., Amouroux, J. Destruction of highly diluted Volatile Organic Components (VOCs) in air by dielectric barrier discharge and mineral bed adsorption. *Energy and Fuels* **22**, 576–582 (2008).

7. Hinojosa-Reyes, M., Arriaga, S., Diaz-Torres, L. A. & Rodríguez-González, V. Gas-phase photocatalytic decomposition of ethylbenzene over perlite granules coated with indium doped TiO2. *Chem. Eng. J.* **224**, 106–113 (2013).

8. Odiba, S., Olea, M., Sasaki, T., Iro, E., Hodgson, S., Adgar, A., Russell, P. Volatile Organic Compounds. *catalysts* **846**, 1–23 (2020).

9. Vallack, H. W., Olawoyin, O. O., Hicks, W. K., Kuylenstierna, J. C. I. & Emberson, L. D. The Global Atmospheric Pollution Forum (GAPF) emission inventory preparation tool and its application to Côte d'Ivoire. *Atmos. Pollut. Res.* **11**, 1500–1512 (2020).

10. Zou, W., Gao, B., Ok, Y. S. & Dong, L. Integrated adsorption and photocatalytic degradation of volatile organic compounds (VOCs) using carbon-based nanocomposites: A critical review. *Chemosphere* **218**, 845–859 (2019).

11. Yang, K., Sun, Q., Xue, F. & Lin, D. Adsorption of volatile organic compounds by metal–organic frameworks MIL-101: Influence of molecular size and shape. *J. Hazard. Mater.* **195**, 124–131 (2011).

12. Long, C., Li, Q., Li, Y., Liu, Y., Li, A., Zhang, Q. Adsorption characteristics of benzene-chlorobenzene vapor on hypercrosslinked polystyrene adsorbent and a pilot-scale application study. *Chem. Eng. J.* **160**, 723–728 (2010).

13. Bacchi, A., Bourne, S., Cantoni, G., Cavallone, S. A.M., Mazza, S., Mehlana, G., Pelagatti, P., Righi, L. Reversible guest removal and selective guest exchange with a covalent dinuclear wheel-and-axle metallorganic host constituted by half-sandwich Ru(II) wheels connected by a linear diphosphine axle. *Cryst. Growth Des.* **15**, 1876–1888 (2015).

14. Khan, N. A., Hasan, Z. & Jhung, S. H. Adsorptive removal of hazardous materials using metal-organic frameworks (MOFs): A review. *J. Hazard. Mater.* 444–456 (2012).

15. Lozano-Castelló, D., Lillo-Ródenas, M, A., Cazorla-Amorós, D. & Linares-Solano, A. Preparation of activated carbons from Spanish anthracite I . Activation by KOH. *Carbon N. Y.* **39**, 741–749 (2001).

16. Bansode, R. R., Losso, J. N., Marshall, W. E., Rao, R. M. & Portier, R. J. Adsorption of volatile organic compounds by pecan shell- and almond shell-based granular activated carbons. *Bioresour. Technol.* **90**, 175–184 (2003).

17. Heidari, A., Younesi, H., Rashidi, A. & Ghoreyshi, A. A. Evaluation of CO2adsorption with eucalyptus

wood based activated carbon modified by ammonia solution through heat treatment. *Chem. Eng. J.* **254**, 503–513 (2014).

18. Srivastava, V. C., Mall, I. D. & Mishra, I. M. Adsorption of toxic metal ions onto activated carbon Study of sorption behaviour through characterization and kinetics. *Chem. Eng. Process. Process Intensif.* **47**, 1269–1280 (2008).

19. Lillo-Ródenas, M, A., Cazorla-Amorós, D. & Linares-Solano, A. Behaviour of activated carbons with different pore size distributions and surface oxygen groups for benzene and toluene adsorption at low concentrations. *Carbon N. Y.* **43**, 1758–1767 (2005).

20. Dwivedi, P., Gaur, V., Sharma, A. & Verma, N. Comparative study of removal of volatile organic compounds by cryogenic condensation and adsorption by activated carbon fiber. *Sep. Purif. Technol.* **39**, 23–37 (2004).

21. Xiao, J., Song, C., Ma, X. & Li, Z. Effects of Aromatics , Diesel Additives , Nitrogen Compounds , and Moisture on Adsorptive Desulfurization of Diesel Fuel over Activated Carbon. *Ind. Eng. Chem. Res.* **51**, 3436–3443 (2012).

22. Meng, F., Song, M., Wei, Y. & Wang, Y. The contribution of oxygen-containing functional groups to the gas-phase adsorption of volatile organic compounds with different polarities onto lignin-derived activated carbon fibers. *Environ. Sci. Pollut. Res.* **26**, 7195–7204 (2019).

23. Chen, H., Wydra, J., Zhang, X., Lee, P., Wang, Z., Fan, W., Tsapatsis, M. Hydrothermal Synthesis of Zeolites with Three-Dimensionally Ordered Mesoporous-Imprinted Structure. *J. Am. Chem. Soc.* **133**, 12390–12393 (2011).

24. Meininghaus, C. K. W. & Prins, R. Sorption of volatile organic compounds on hydrophobic zeolites. *Microporous Mesoporous Mater.* **35**–**36**, 349–365 (2000).

25. Mazur, M., Wheatley, P., Navarro, M., Roth, W. J., Mayoral, A., Eliášová, P., Nachtigall, P., Čejka, J. Synthesis of ‘ unfeasible ’ zeolites. *Nat. Chem.* **8**, 1–14 (2016).

26. Li, R., Chong, S., Altaf, N., Gao, Y., Louis, B., Wang, Q. Synthesis of ZSM-5/Siliceous Zeolite Composites for Improvement of Hydrophobic Adsorption of Volatile Organic Compounds. *Front. Chem.* **7**, 1–10 (2019).

27. Tao, W., Yang, T. C., Chang, Y., Chang, L. & Chung, T. Effect of Moisture on the Adsorption of Volatile Organic Compounds by Zeolite 13 Ã. *J. Environ. Eng.* **130**, 1210–1216 (2005).

28. Altare, C. R., Bowman, R. S., Katz, L. E., Kinney, K. A. & Sullivan, E. J. Regeneration and long-term stability of surfactant-modified zeolite for removal of volatile organic compounds from produced water. *Microporous Mesoporous Mater.* **105**, 305–316 (2007).

29. Chew, T. L., Ahmad, A. L. & Bhatia, S. Ordered mesoporous silica (OMS) as an adsorbent and membrane for separation of carbon dioxide (CO2). *Adv. Colloid Interface Sci.* **153**, 43–57 (2010).

30. Yan, X., Meng, J., Hu, X., Feng, R. & Zhou, M. Synthesis of thiol-functionalized mesoporous silica nanoparticles for adsorption of Hg 2+ from aqueous solution. *J. Sol-Gel Sci. Technol.* **89**, 617–622 (2019).

31. Hamdi, K., Hébrant, M., Martin, P., Galland, B. & Etienne, M. Mesoporous silica nanoparticle film as sorbent for in situ and real-time monitoring of volatile BTX (benzene, toluene and xylenes). *Sensors Actuators, B Chem.* **223**, 904–913 (2016).

32. Jhung, S. H., Lee, J. H., Yoon, J. W., Serre, C., Férey, G., Chang, J. S., Microwave synthesis of chromium terephthalate MIL-101 and its benzene sorption ability. *Adv. Mater.* **19**, 121–124 (2007).

33. Lincke, J., Lässig, D., Kobalz, M., Bergmann, J., Handke, M., Möllmer, J., Lange, M., Roth, C., Möller, A., Staudt, R., Krautscheid, H. An isomorphous series of cubic, copper-based triazolyl isophthalate MOFs: Linker substitution and adsorption properties. *Inorg. Chem.* **51**, 7579–7586 (2012).

34. Yaghi, O. M. Metal–organic frameworks: A tale of two entanglements. *Nat. Mater.* **6**, 92–93 (2007).

35. Stock, N. & Biswas, S. Synthesis of Metal-Organic Frameworks (MOFs): Routes to Various MOF Topologies, Morphologies, and Composites. *Am. Chem. Soc.* **112**, 933–969 (2012).

36. Amombo Noa, F. M., Svensson G. E., Brülls, S. M., Cheung, O., Malmberg, P., Inge, A. K., Mckenzie, C. J., Mårtensson, J., Öhrström, L. Metal-Organic Frameworks with Hexakis(4-carboxyphenyl)benzene: Extensions to Reticular Chemistry and Introducing Foldable Nets. *J. Am. Chem. Soc.* **142**, 9471–9481 (2020).

37. Friščić, T. Halasz, I., Beldon, P. J., Belenguer, A. M., Adams, F., Kimber, S. A. J., Honkimäki, V., Dinnebier, R. E. Real-time and in situ monitoring of mechanochemical milling reactions. *Nat. Chem.* **5**, 66–73 (2013).

38. DeSantis, D., Mason, J. A., James, B. D., Houchins, C., Long, J. R., Veenstra, M. Techno-economic Analysis of Metal–Organic Frameworks for Hydrogen and Natural Gas Storage. *Energy & Fuels* **31**, 2024–2032 (2017).

39. Eddaoudi, M., Moler, D. B., Li, H., Chen, B., Reineke, T. M., O'Keeffe, M., Yaghi, O. M. Modular Chemistry : Secondary Building Units as a Basis for the Design of Highly Porous and Robust Metal − Organic Carboxylate Frameworks. **34**, 319–330 (2001).

40. Gedrich, K. Senkovska, I., Klein, N., Stoeck, U., Henschel, A., Lohe, M. R., Baburin, I. A., Mueller, U., Kaskel, S. A highly porous metal-organic framework with open nickel sites. *Angew. Chemie - Int. Ed.* **49**, 8489–8492 (2010).

41. Furukawa, H., Cordova, K. E., O'Keeffe, M. & Yaghi, O. M. The Chemistry and Applications of Metal-Organic Frameworks. *Sci. (Washington, DC, U. S.)* **341**, 974 (2013).

42. Sánchez-Sánchez, M. Getachew, N., Díaz-García, M., Díaz, K., Díaz-García, M., Chebude, Y., Díaz, I. Synthesis of metal–organic frameworks in water at room temperature: salts as linker sources. *Green Chem.* **17**, 1500–1509 (2015).

43. Mehlana, G., Bourne, S. A. & Ramon, G. The role of C–H···π interactions in modulating the breathing amplitude of a 2D square lattice net: alcohol sorption studies. *CrystEngComm* **16**, 8160 (2014).

44. Kandiah, M. Nilsen, M. H., Usseglio, S., Jakobsen, S., Olsbye, U., Tilset, M., Larabi, C., Quadrelli, E. A., Bonino, F., Lillerud, K. P. Synthesis and stability of tagged UiO-66 Zr-MOFs. *Chem. Mater.* **22**, 6632–6640 (2010).

45. Zaarour, M., Dong, B., Naydenova, I., Retoux, R. & Mintova, S. Progress in zeolite synthesis promotes advanced applications. *Microporous Mesoporous Mater.* **189**, 11–21 (2014).

46. Zhou, L., Chen, Y., Zhang, X., Tian, F. & Zu, Z. Zeolites developed from mixed alkali modified coal fly ash for adsorption of volatile organic compounds. *Mater. Lett.* **119**, 140–142 (2014).

47. Siriwardane, R. V., Shen, M. S., Fisher, E. P. & Losch, J. Adsorption of CO2 on zeolites at moderate temperatures. *Energy and Fuels* **19**, 1153–1159 (2005).

48. Liang, Z., Marshall, M. & Chaffee, A. L. CO2 adsorption-based separation by metal organic framework (Cu-BTC) versus zeolite (13X). *Energy and Fuels* **23**, 2785–2789 (2009).

49. Yaghi, O. M., Li, G. & Li, H. Selective binding and removal of guests in a microporous metal-organic framework. *Nature* **378**, 703–706 (1995).

50. James, S. L. Metal-organic frameworks. *Chem. Soc. Rev.* **32**, 276–288 (2003).

51. Choi, E., Park, K., Yang, C., Kim, H., Son, J., Lee, S. W., Lee, Y. H., Min, D., Kwon, Y. Benzene-templated hydrothermal synthesis of metal-organic frameworks with selective sorption properties. *Chem. - A Eur. J.* **10**, 5535–5540 (2004).

52. Getzschmann, J., Senkovska, I., Wallacher, D., Tovar, M., Fairen-Jimenez, D., Düren, T., van Baten, J., Krishna, R., Kaskel, S. Methane storage mechanism in the metal-organic framework Cu3(btc)2: An in situ

neutron diffraction study. *Microporous Mesoporous Mater.* **136**, 50–58 (2010).

53. Lee, J. S., Halligudi, S., Jang, N. H., Hwang, D. W., Chang, J. S., Hwang, Y. K. Microwave synthesis of a porous metal-organic framework, nickel(II) dihydroxyterephthalate and its catalytic properties in oxidation of cyclohexene. *Bull. Korean Chem. Soc.* **31**, 1489–1495 (2010).

54. He, C., Lu, K., Liu, D. & Lin, W. Nanoscale metal-organic frameworks for the co-delivery of cisplatin and pooled siRNAs to enhance therapeutic efficacy in drug-resistant ovarian cancer cells. *J. Am. Chem. Soc.* **136**, 5181–5184 (2014).

55. Liu, B., Wu, W.-P., Hou, L. & Wang, Y.-Y. Four uncommon nanocage-based Ln-MOFs: highly selective luminescent sensing for Cu2+ ions and selective CO2 capture. *Chem. Commun. (Camb).* **50**, 8731–8734 (2014).

56. Chen, B. Yang, Y., Zapata, F., Lin, G., Qian, G., Lobkovsky, E. B. Luminescent open metal sites within a metal-organic framework for sensing small molecules. *Adv. Mater.* **19**, 1693–1696 (2007).

57. Mahata, P., Mondal, S. K., Singha, D. K. & Majee, P. Luminescent rare-earth-based MOFs as optical sensors. *Dalt. Trans.* **46**, 301–328 (2017).

58. Mehlana, G., Bourne, S. A., Ramon, G. & Öhrström, L. Concomitant metal organic frameworks of cobalt(II) and 3-(4-pyridyl) benzoate: Optimized synthetic conditions of solvatochromic and thermochromic systems. *Cryst. Growth Des.* **13**, 633–644 (2013).

59. Janiak, C. & Vieth, J. K. MOFs, MILs and more: concepts, properties and applications for porous coordination networks (PCNs). *New J. Chem.* **34**, 2366–2388 (2010).

60. Qiu, Y. Yuan, S., Li, X., Du, D., Wang, C., Qin, J., Drake, H. F., Lan, Y., Jiang, L., Zhou, H. Face-Sharing Archimedean Solids Stacking for the Construction of Mixed-Ligand Metal − Organic Frameworks. (2019).

61. Butova, V. V, Soldatov, M. A., Guda, A. A., Lomachenko, K. A. & Lamberti, C. Metal-organic frameworks : structure , properties , methods of synthesis and characterization. *Russ. Chem. Rev.* **85**, 280–307 (2016).

62. Rowsell, J. L. C. & Yaghi, O. M. Metal-organic frameworks: A new class of porous materials. *Microporous Mesoporous Mater.* **73**, 3–14 (2004).

63. Cheetham, A. K., Rao, C. N. R. & Feller, R. K. Structural diversity and chemical trends in hybrid inorganic-organic framework materials. *Chem. Commun.* 4780 (2006).

64. Serre, C., Bourrelly, S., Vimont, A., Ramsahye, N. A., Maurin, G., Llewellyn, P. L., Daturi, M., Filinchuk, Y., Leynaud, O., Barnes, P., Férey, G. An explanation for the very large breathing effect of a metal-organic framework during CO2 adsorption. *Adv. Mater.* **19**, 2246–2251 (2007).

65. Merrill, C. A. & Cheetham, A. K. Pillared layered structures based upon M(III) ethylene diphosphonates: The synthesis and crystal structures of MIII(H2O)(HO3P(CH2)2PO3) (M = Fe, Al, Ga). *Inorg. Chem.* **44**, 5273–5277 (2005).

66. Park, K. S., Ni, Z., Coˆte´, A. P., Choi, J. W., Huang, R., Uribe-romo, F.J., Chae, H.K., O'Keeffe, M., Yaghi, O.M. Exceptional chemical and thermal stability of zeolitic imidazolate frameworks. *Proc. Natl. Acad. Sci. USA* **103**, 10186 (2006).

67. Biemmi, E., Bein, T. & Stock, N. Synthesis and characterization of a new metal organic framework structure with a 2D porous system: (H2NEt2)2[Zn3(BDC)4]·3DEF. *Solid State Sci.* **8**, 363–370 (2006).

68. Eddaoudi, M. Kim, J., Rosi, N., Vodak, D., Wachter, J., O'Keeffe, M., Yaghi, O.M. Systematic design of pore size and functionality in isoreticular MOFs and their application in methane storage. *Science* **295**, 469–472 (2002).

69. Clough, A. J. Skelton, J.M., Downes, C. A., De La Rosa. A. A., Yoo, J. W., Walsh, A., Melot, B. C., Marinescu, S. C. Metallic Conductivity in a Two-Dimensional Cobalt Dithiolene Metal-Organic

Framework. *J. Am. Chem. Soc.* **139**, 10863–10867 (2017).

70. Guan, C., Zhao, W., Hu, Y., Lai, Z., Li, X., Sun, S., Zhang, H., Cheetham, A. K., Wang, J. Cobalt oxide and N-doped carbon nanosheets derived from a single two-dimensional metal–organic framework precursor and their application in flexible asymmetric supercapacitors. *Nanoscale Horiz.* **2**, 99–105 (2017).

71. Livage, C., Egger, C. & Férey, G. Hybrid Open Networks (MIL-16): Synthesis, Crystal Structure, and Ferrimagnetism of Co4(OH)2(H2O)2(C4H4O4)3 ·2H2O, a New Layered Co(II) Carboxylate with 14-Membered Ring Channels. *Chem. Mater.* **11**, 1546–1550 (1999).

72. Chui, S. S.-Y., Lo, S. M., Charmant, J. P. H., Orpen, A. G. & Williams, I. D. A Chemically Functionalizable Nanoporous Material [Cu3(TMA)2(H2O)3]n. *Science (80-.).* **283**, 1148–1150 (1999).

73. Ahnfeldt, T., Guillou, N., Gunzelmann, D., Margiolaki, I., Loiseau, T., Férey, G., Senker, J., Stock, N. [Al4(OH)2(OCH3)4(H2N-bdc) 3]·xH2O: A 12-Connected Porous Metal-Organic Framework with an Unprecedented Aluminum-Containing Brick. *Angew. Chemie* **121**, 5265–5268 (2009).

74. Costa, J. S., Gamez, P., Black, C. A., Roubeau, *O.*, Teat, *S.J* Reedijk, J. Chemical Modification of a Bridging Ligand Inside a Metal – Organic Framework while Maintaining the 3D Structure. *Eur. J. Inorg. Chem.* 1551–1554 (2008).

75. Gao, W., Yan, W., Cai, R., Williams, K., Salas, A., Wojtas, L., Shi, X., Ma, S. A pillared metal – organic framework incorporated with 1 , 2 , 3-triazole moieties exhibiting remarkable enhancement of CO2 uptake. **2**, 8898–8900 (2012).

76. Chen, Z., Xiang, S., Arman, H. D., Mondal, J. U., Li, P., Zhao, D., Chen, B. Three-Dimensional Pillar-Layered Copper(II) Metal-Organic Framework with Immobilized Functional OH Groups on Pore Surfaces for Highly Selective CO2/CH4 and C2H2/CH4 Gas Sorption at Room Temperature. *Inorg. Chem.* **50**, 3442–3446 (2011).

77. Sarma, D. & Natarajan, S. Usefulness of in situ single crystal to single crystal transformation (SCSC) studies in understanding the temperature-dependent dimensionality cross-over and structural reorganization in copper-containing metal-organic frameworks (MOFs). *Cryst. Growth Des.* **11**, 5415–5423 (2011).

78. Davies, K., Bourne, S. A., Öhrström, L. & Oliver, C. L. Anionic zinc-trimesic acid MOFs with unusual topologies: Reversible hydration studies. *Dalt. Trans.* **39**, 2869–2874 (2010).

79. Kobalz, M., Lincke, J., Kobalz, K., Erhart, O., Bergmann, J., Lässig, D., Lange, M., Möllmer, J., Gläser, R., Staudt, R., Krautscheid, H. Paddle Wheel Based Triazolyl Isophthalate MOFs: Impact of Linker Modification on Crystal Structure and Gas Sorption Properties. *Inorg. Chem.* **55**, 3030–3039 (2016).

80. Liu, Y., Couck, S., Vandichel, M., Grzywa, M., Leus, K., Biswas, S., Volkmer, D., Gascon, J., Kapteijn, F., Denayer, J. F. M., Waroquier, M., Speybroeck, V. V., Voort, P. V. New VIV-Based Metal − Organic Framework Having Framework Flexibility and High CO 2 Adsorption Capacity. *Inorg. Chem.* **52**, 113–120 (2013).

81. Gable, R. W., Hoskins, B. F. & Robson, R. A New Type of Interpenetration Involving Enmeshed Independent Square Grid Sheets. The Structure of Diaquabis-(4,4'-bipyridine)zinc Hexafluorosilicate. *ournal Am. Chem. Soc.* **118**, 1677–1678 (1996).

82. Davies, K., Bourne, S. A. & Oliver, C. L. Solvent- and Vapor-Mediated Solid-State Transformations in 1,3,5- Benzenetricarboxylate Metal−Organic Frameworks. *Cryst. Growth Des.* **12**, 1999–2003 (2012).

83. Sun, Y.-X. & Sun, W.-Y. Influence of temperature on metal-organic frameworks. *Chinese Chem. Lett.* **25**, 823–828 (2014).

84. Zaworotko, M. J. Superstructural diversity in two dimensions: crystal engineering of laminated solids. *Chem. Commun.* 1–9 (2001).

85. Li, X. P., Zhang, J. Y., Pan, M., Zheng, S. R., Liu, Y., Su, C. Zero to three dimensional increase of silver(I) coordination assemblies controlled by deprotonation of 1,3,5-Tri(2-benzimidazolyl)benzene and aggregation

of multinuclear building units. *Inorg. Chem.* **46**, 4617–4625 (2007).

86. Papaefstathiou, G. S. & MacGillivray, L. R. Inverted metal-organic frameworks: solid-state hosts with modular functionality. *Coord. Chem. Rev.* **246**, 169–184 (2003).

87. Forster, P. M., Burbank, A. R., Livage, C., Férey, G. & Cheetham, A. K. The role of temperature in the synthesis of hybrid inorganic-organic materials: the example of cobalt succinates. *Chem. Commun. (Camb).* **5**, 368–369 (2004).

88. Vasylevskyy, S. I., Senchyk, G. A., Lysenko, A. B., Rusanov, E. B., Chernega, A. N., Jezierska, J., Krautscheid, H., Domasevitch, K. V., Ozarowski, A. 1,2,4-triazolyl-carboxylate-based MOFs incorporating triangular Cu(II)-hydroxo clusters: Topological metamorphosis and magnetism. *Inorg. Chem.* **53**, 3642–3654 (2014).

89. Yan, Q., Zhang, J. Y., Pan, M., Zheng, S. R., Liu, Y., Su, C. Y. Designed synthesis of functionalized two-dimensional metal-organic frameworks with preferential CO2 capture. *Chempluschem* **78**, 86–91 (2013).

90. Biemmi, E., Christian, S., Stock, N. & Bein, T. High-throughput screening of synthesis parameters in the formation of the metal-organic frameworks MOF-5 and HKUST-1. *Microporous Mesoporous Mater.* **117**, 111–117 (2009).

91. Fujita, M., Kwon, Yoon, J., Sasaki, O., Yamaguchi, K. & Ogura, K. Interpenetrating Molecular Ladders and Bricks Makoto. *J. Am. Chem. Soc.* **117**, 7287–7288 (1995).

92. Yaghi, O. M. & Li, H. T-Shaped Molecular Building Units in the Porous Structure of Ag (4, 4′ -bpy) , NO 3. *J. Am. Chem. Soc* **118**, 295–296 (1996).

93. Subramanian, S. & Zaworotko, M. J. Porous Solids by Design :[Zn(4,4'-bpy)2(SiF,)1,*x DMF, a Single Framework Octahedral Coordination Polymer with Large Square Channels. *Angew. Chemie Int. Ed. English* **34**, 2127–2129 (1995).

94. Abrahams, B. F., Jackson, P. A. & Robson, R. A Robust (10, 3) -a Network Containing Chiral Micropores in the Ag I Coordination Polymer of a Bridging Ligand that Provides Three Bidentate Metal-Binding Sites. *Angew. Chemie Int. Ed.* **37**, 2656–2659 (1998).

95. Alhamami, M., Doan, H. & Cheng, C.-H. A Review on Breathing Behaviors of Metal-Organic-Frameworks (MOFs) for Gas Adsorption. *Materials (Basel).* **7**, 3198–3250 (2014).

96. Hou, L., Zhang, J.-P., Chen, X.-M. & Ng, S. W. Two highly-connected, chiral, porous coordination polymers featuring novel heptanuclear metal carboxylate clusters. *Chem. Commun. (Camb).* 4019–4021 (2008).

97. Yaghi, O. M., Davis, C. E., Li, G. & Li, H. Selective guest binding by tailored channels in a 3-D porous zinc(II)-benzenetricarboxylate network. *J. Am. Chem. Soc.* **119**, 2861–2868 (1997).

98. Li, H., Eddaoudi, M., Groy, T. L. & Yaghi, O. M. Establishing microporosity in open metal-organic frameworks: Gas sorption isotherms for Zn (BDC)(BDC= 1, 4-benzenedicarboxylate). *J. Am. Chem. Soc.* **7863**, 8571–8572 (1998).

99. Dybtsev, D. N., Chun, H. & Kim, K. Rigid and flexible: A highly porous metal-organic framework with unusual guest-dependent dynamic behavior. *Angew. Chem. Int. Ed.* **43**, 5033–5036 (2004).

100. Mehlana, G., Ramon, G. & Bourne, S. A. Methanol mediated crystal transformations in a solvatochromic metal organic framework constructed from Co(ii) and 4-(4-pyridyl) benzoate. *CrystEngComm* **15**, 9521–9529 (2013).

101. Dzesse T, C. N., Nfor, E. N. & Bourne, S. A. Vapor Sorption and Solvatochromism in a Metal-Organic Framework of an Asymmetric Pyridylcarboxylate. *Cryst. Growth Des.* **18**, 416–423 (2018).

102. Xiong, G., Wang, Y., Zhao, B., You, L., Ren, B., He, Y., Wang, S., Sun, Y. Temperature-tuned topologies and interpenetrations of two 3D porous copper(II)-organic frameworks and gas adsorption behaviors.

Inorganica Chim. Acta **471**, 180–185 (2018).

103. Cho, H.-Y., Yang, D.-A., Kim, J., Jeong, S.-Y. & Ahn, W.-S. CO2 adsorption and catalytic application of Co-MOF-74 synthesized by microwave heating. *Catal. Today* **185**, 35–40 (2012).

104. Ji, P., Feng, X., Oliveres, P., Li, Z., Murakami, A., Wang, C., Lin, W. Strongly Lewis Acidic Metal-Organic Frameworks for Continuous Flow Catalysis. *J. Am. Chem. Soc.* **141**, 14878–14888 (2019).

105. Sabouni, R., Kazemian, H. & Rohani, S. Microwave Synthesis of the CPM-5 Metal Organic Framework. *Chem. Eng. Technol.* **35**, 1085–1092 (2012).

106. Tang, Y.-Y., Wang, C.-J., Chen, S. & Dai, H.-Y. A terbium(III) organic framework as a fluorescent probe for selectively sensing of organic small molecules and metal ions especially nitrobenzene and Fe3+. *J. Coord. Chem.* **70**, 3996–4007 (2017).

107. Arstad, B., Fjellvåg, H., Kongshaug, K. O., Swang, O. & Blom, R. Amine functionalised metal organic frameworks (MOFs) as adsorbents for carbon dioxide. *Adsorption* **14**, 755–762 (2008).

108. Jiang, H. L., Tatsu, Y., Lu, Z. H. & Xu, Q. Non-, micro-, and mesoporous metal-organic framework isomers: Reversible transformation, fluorescence sensing, and large molecule separation. *J. Am. Chem. Soc.* **132**, 5586–5587 (2010).

109. Long, P., Wu, H., Zhao, Q., Wang, Y., Dong, J., Li, J. Solvent effect on the synthesis of MIL-96(Cr) and MIL-100(Cr). *Microporous Mesoporous Mater.* **142**, 489–493 (2011).

110. Yang, G.-S., Lan, Y.-Q., Zang, H.-Y., Shao, K.-Z., Wang, X.-L., Su, Z.-M., Jiang, C.-J. Two eight-connected self-penetrating porous metal-organic frameworks: Configurational isomers caused by different linking modes between terephthalate and binuclear nickel building units. *CrystEngComm* **11**, 274–277 (2009).

111. Jiang, H. L., Feng, D., Liu, T. F., Li, J. R. & Zhou, H. C. Pore surface engineering with controlled loadings of functional groups via click chemistry in highly stable metal-organic frameworks. *J. Am. Chem. Soc.* **134**, 14690–14693 (2012).

112. Kitagawa, S., Kitaura, R. & Noro, S. I. Functional porous coordination polymers. *Angew. Chemie - Int. Ed.* **43**, 2334–2375 (2004).

113. Batten, S. R., Hoskins, B. F. & Robson, R. Two Interpenetrating 3D Networks Which Generate Spacious Sealed-Off Compartments Enclosing of the Order of 20 Solvent Molecules in the Structures of Zn(CN)(N03)(tpt)2/3.solv (tpt = ~2,4,6-tri(4-pyridyl)-1,3,5-triazine, solv = -3/4C2H2Cl4.3/4CH3OH or ~3/2C. *J. Am. Chem. Soc.* **117**, 5385–5386 (1995).

114. Cui, Y., Lee, S. J. & Lin, W. Interlocked Chiral Nanotubes Assembled from Quintuple Helices. 6014–6015 (2003).

115. Wang, B., Wang, P., Xie, L. H., Lin, R. B., Lv, J., Li, J. R., Chen, B. A stable zirconium based metal-organic framework for specific recognition of representative polychlorinated dibenzo-p-dioxin molecules. *Nat. Commun.* **10**, 1–8 (2019).

116. Kawata, S., Kitagawa, S., Kumagai, H., Kudo, C., Kamesaki, H., Ishiyama, T., Suzuki, R., Kondo, M., Katada, M., April, R. V. Rational Design of a Novel Intercalation System. Layer-Gap Control of Crystalline Coordination Polymers, {[Cu(CA)(H(2)O)(m)()](G)}(n)() (m = 2, G = 2,5-Dimethylpyrazine and Phenazine; m = 1, G = 1,2,3,4,6,7,8,9-Octahydrophenazine). *Inorg. Chem.* **35**, 4449–4461 (1996).

117. Prior, T. J., Bradshaw, D., Teat, S. J. & Rosseinsky, M. J. Designed layer assembly : a three-dimensional framework with 74 % extra-framework volume by connection of infinite two-dimensional sheets †. *Chem. Commun.* 500–501 (2003).

118. Gao, Q., Xu, J., Cao, D., Chang, Z. & Bu, X. A Rigid Nested Metal – Organic Framework Featuring a Thermoresponsive Gating Effect Dominated by Counterions Angewandte. **100029**, 15027–15030 (2016).

119. Babu, R., Kathalikkattil, A. C., Roshan, R., Tharun, J., Kim, D., Park, D. Dual-porous metal organic framework for room temperature CO2 fixation via cyclic carbonate synthesis. *Green Chem.* **18**, 232–242 (2015).

120. Koh, K., Wong-foy, A. G. & Matzger, A. J. A Crystalline Mesoporous Coordination Copolymer with High Microporosity. *Angew. Chemie Int. Ed.* **47**, 677–680 (2008).

121. Yoon, H. C., Rallapalli, P. B. S., Han, S. S., Beum, H. T., Jung, T. S., Cho, D. W., Ko, M., Kim, J. N. Micro- and mesoporous CuBTCs for CO2/CH4 separation. *Korean J. Chem. Eng.* **32**, 2501–2506 (2015).

122. Haque, E., Lee, J. E., Jang, I. T., Hwang, Y. K., Chang, J. S., Jegal, J., Jhung, S. H. Adsorptive removal of methyl orange from aqueous solution with metal-organic frameworks, porous chromium-benzenedicarboxylates. *J. Hazard. Mater.* **181**, 535–542 (2010).

123. Millward, A. R. & Yaghi, O. M. Metal Organic Frameworks with Exceptionally High Capacity for Storage of Carbon Dioxide at Room Temperature. *J. Am. Chem. Soc.* **127**, 17998–17999 (2005).

124. Xiang, Z., Cao, D., Shao, X., Wang, W., Zhang, J., Wu, W. Facile preparation of high-capacity hydrogen storage metal-organic frameworks: A combination of microwave-assisted solvothermal synthesis and supercritical activation. *Chem. Eng. Sci.* **65**, 3140–3146 (2010).

125. Mehlana, G., Bourne, S. A. & Ramon, G. A new class of thermo- and solvatochromic metal–organic frameworks based on 4-(pyridin-4-yl)benzoic acid. *Dalt. Trans.* **41**, 4224 (2012).

126. Lv, X., Shi, L., Li, K., Li, B. & Li, H. An unusual porous cationic metal – organic framework fast and highly efficient dichromate trapping through a single-crystal to single-crystal process. *Chem. Commun.* **53**, 1860–1863 (2017).

127. Toirris, A., Bell, R. G. & Mellot-Draznieks, C. Functionalized MOFs for enhanced CO2 capture. *Cryst. Growth Des.* **10**, 2839–2841 (2010).

128. López-Maya, E., Montoro, C., Colombo, V., Barea, E. & Navarro, J. A. R. Improved CO2 capture from flue gas by basic sites, charge gradients, and missing linker defects on nickel face cubic centered MOFs. *Adv. Funct. Mater.* **24**, 6130–6135 (2014).

129. An, J. & Rosi, N. L. Tuning MOF CO(2) Adsorption Properties via Cation Exchange. *J. Am. Chem. Soc.* **132**, 5578–5579 (2010).

130. Zhang, Y.-B., Furukawa, H., Ko, N., Nie, W., Park, H. J., Okajima, S., Cordova, K. E., Deng, H., Kim, J., Yaghi, O. M. Introduction of Functionality, Selection of Topology, and Enhancement of Gas Adsorption in Multivariate Metal–Organic Framework-177. *J. Am. Chem. Soc.* **147**, 2641–2650 (2015).

131. Leclerc, H., Devic, T., Devautour-Vinot, S., Bazin, P., Audebrand, N., Férey, G., Daturi, M., Vimont, A., Clet, G. Influence of the oxidation state of the metal center on the flexibility and adsorption properties of a porous metal organic framework: MIL-47(V). *J. Phys. Chem. C* **115**, 19828–19840 (2011).

132. Senkovska, I., Hoffmann, F., Fröba, M., Getzschmann, J., Böhlmann, W., Kaskel, S. New highly porous aluminium based metal-organic frameworks: Al(OH)(ndc) (ndc = 2,6-naphthalene dicarboxylate) and Al(OH)(bpdc) (bpdc = 4,4′-biphenyl dicarboxylate). *Microporous Mesoporous Mater.* **122**, 93–98 (2009).

133. Ozawa, T. A New Method of Analyzing Thermogravimetric Data. *Bull. Chem. Soc. Jpn.* **38**, 1881–1886 (1965).

134. Khawam, A. & Flanagan, D. R. Solid-state kinetic models: Basics and mathematical fundamentals. *J. Phys. Chem. B* **110**, 17315–17328 (2006).

135. Ragon, F., Horcajada, P., Chevreau, H., Hwang, Y. K., Lee, U. H., Miller, S. R., Devic, T., Chang, J. S., Serre, C. In situ energy-dispersive x-ray diffraction for the synthesis optimization and scale-up of the porous zirconium terephthalate UiO-66. *Inorg. Chem.* **53**, 2491–2500 (2014).

136. Thommes, M., Kaneko, K., Neimark, A. V., Olivier, J. P., Rodriguez-Reinoso, F., Rouquerol, J., Sing, K. S.

W. Physisorption of gases, with special reference to the evaluation of surface area and pore size distribution (IUPAC Technical Report). *Pure Appl. Chem.* **87**, 1051–1069 (2015).

137. Gcwensa, N., Chatterjee, N. & Oliver, C. L. Interchanged Hysteresis for Carbon Dioxide and Water Vapor Sorption in a Pair of Water-Stable, Breathing, Isoreticular, 2-Periodic, Zn(II)-Based Mixed-Ligand Metal-Organic Frameworks. *Inorg. Chem.* **58**, 2080–2088 (2019).

138. Yuan, Y., Li, J., Sun, X., Li, G., Liu, Y., Verma, G., Ma, S. Indium-Organic Frameworks Based on Dual Secondary Building Units Featuring Halogen-Decorated Channels for Highly Effective CO2 Fixation. *Chem. Mater.* **31**, 1084–1091 (2019).

139. Zhou, H. L., Zhang, Y. B., Zhang, J. P. & Chen, X. M. Supramolecular-jack-like guest in ultramicroporous crystal for exceptional thermal expansion behaviour. *Nat. Commun.* **6**, 1–7 (2015).

140. Alexandrov, E. V., Blatov, V. A., Kochetkov, A. V. & Proserpio, D. M. Underlying nets in three-periodic coordination polymers: Topology, taxonomy and prediction from a computer-aided analysis of the Cambridge Structural Database. *CrystEngComm* **13**, 3947–3958 (2011).

141. Li, M., Li, D., O'Keeffe, M. & Yaghi, O. M. Topological analysis of metal-organic frameworks with polytopic linkers and/or multiple building units and the minimal transitivity principle. *Chem. Rev.* **114**, 1343–1370 (2014).

142. Klein, Y. M., Constable, C. E., Housecroft, E. C. & Prescimone, A. A 3-dimensional {42·84} lvt net built from a ditopic bis(3,2′:6′,3″-terpyridine) tecton bearing long alkyl tails. *CrystEngComm* **17**, (2015).

143. Delgado-Friedrichs, O. & Okeeffe, M. Edge-transitive lattice nets. *Acta Crystallogr. Sect. A Found. Crystallogr.* **65**, 360–363 (2009).

144. Blatov, V. A., O'Keeffe, M. & Proserpio, D. M. Vertex-, face-, point-, Schläfli-, and Delaney-symbols in nets, polyhedra and tilings: Recommended terminology. *CrystEngComm* **12**, 44–48 (2010).

145. Bennett, T. D. & Cheetham, A. K. Amorphous Metal − Organic Frameworks. *Acc. Chem. Res.* **47**, 1555-1562. (2014).

146. Jobbágy, C., Molnár, M., Baranyai, P. & Deák, A. Mechanochemical synthesis of crystalline and amorphous digold(I) helicates exhibiting anion- and phase-switchable luminescence propertie. *Dalt. Trans.* **43**, 11807–11810 (2014).

147. Zhou, H., Zhang, J. & Chen, X. Controlling Thermal Expansion Behaviors of Fence-Like Metal-Organic Frameworks by Varying / Mixing Metal Ions. *Front. Chem.* **6**, 1–7 (2018).

148. Wu, Y., Yang, G., Zhao, Y., Wu, W., Liu, B., Wang, Y. Three new solvent-directed Cd(II)-based MOFs with unique luminescent properties and highly selective sensors for Cu(2+) cations and nitrobenzene. *Dalton Trans.* **44**, 3271–7 (2015).

149. Friščić, T., Mottillo, C. & Titi, H. M. Mechanochemistry for Synthesis. *Angew. Chemie - Int. Ed.* **59**, 1018–1029 (2020).

150. Mottillo, C. & Friš˘, T. Advances in Solid-State Transformations of Coordination Bonds : From the Ball Mill to the Aging Chamber. *Moleculess* **22**, 1–38 (2017).

151. Yan, Y., Suyetin, M., Bichoutskaia, E., Blake, A. J., Allan, D. R., Barnett, S. A., Schröder, M. Modulating the packing of [Cu24(isophthalate)24] cuboctahedra in a triazole-containing metal–organic polyhedral framework. *Chem. Sci.* **4**, 1731–1736 (2013).

152. Mehlana, G., Ramon, G. & Bourne, S. A. A 4-fold interpenetrated diamondoid metal-organic framework with large channels exhibiting solvent sorption properties and high iodine capture. *Microporous Mesoporous Mater.* **231**, 21–30 (2016).

153. Zhou, H.-C. "Joe" & Kitagawa, S. Metal–Organic Frameworks (MOFs). *Chem. Soc. Rev.* **43**, 5415–5418 (2014).

CHAPTER 2. MATERIALS AND EXPERIMENTAL METHODS

2.1. MATERIALS

All chemicals were obtained from commercial sources and were used without further purification. 4-(4-pyridyl)benzoic acid and 3-(4-pyridyl)benzoic acid (both with purity 95%) were purchased from CGeneTech while 4-(pyridyn-4-ylmethyl)aminobenzoic acid and 3-(pyridyn-4-ylmethyl)aminobenzoic acid of 95% purity were purchased from Matrix Scientific. Metal salts such as cobalt (II) chloride hexahydrate, copper (II) chloride trihydrate, and zinc (II) nitrate hexahydrate were 98-99% pure. A 70% solution of ethylene diamine was purchased from Sigma Aldrich. Solvents such as dimethylformamide, methanol, ethanol of purity 99, 99.5, 99.9% respectively, and deionised water were used as solvents for the synthesis of MOFs. All halogenated and amine VOCs were first dried using molecular sieves before sorption tests.

2.2. GENERAL SYNTHESIS

MOFs were synthesized using two different methods: solvothermal synthesis using autoclaves (Figure 2.1(a)), or slow evaporation at room temperature (r.t) in glass vials (Figure 2.1.(b)). A short description is given below and further details are provided in Chapter Three.

Solvothermal synthesis

Ligands and metal salts were dissolved in their respective solvent systems. After mixing the solutions in a Teflon beaker, they were sealed in an aluminium autoclave and heated in an oven for one to three days followed by slow cooling to allow crystallization. Figure 2.2 shows an example of some crystals obtained.

Slow evaporation

Ligands and metal salts were dissolved in their respective solvents which were mixed in a glass vial and left on the benchtop at room temperature. Slow evaporation of the solvent allowed MOF crystallization.

The synthesized MOFs were activated under vacuum to remove guest molecules before use in sorption experiments.

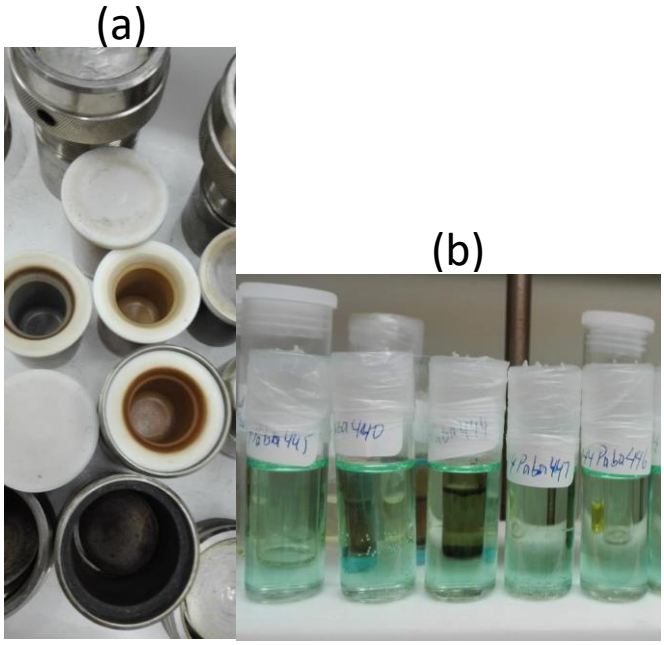

Figure 2.1: *(a) Autoclaves used for solvothermal synthesis to crystallise MOFs, (b) formation of crystalline MOFs from solution.*

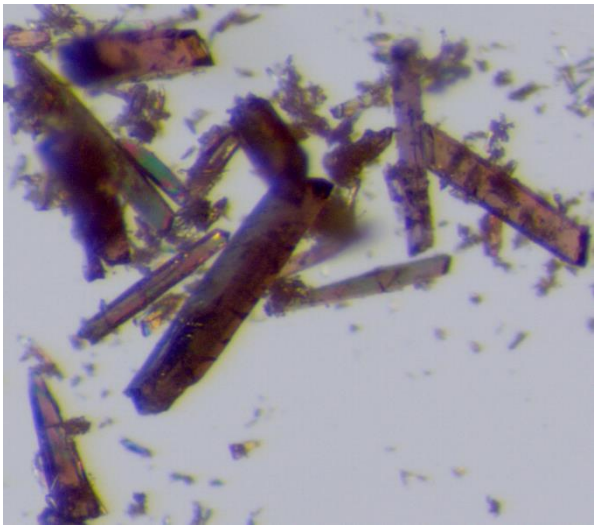

Figure 2.2: *Crystals obtained from* $[Co(34pba)(44pba)]_n$ MOF (**1**).

2.3. THERMOGRAVIMETRIC ANALYSIS (TGA) AND DIFFERENTIAL SCANNING CALORIMETRY (DSC)

Thermal stability concerning the temperature at which the guest molecules are removed from the channels of the MOFs was determined by thermogravimetric analysis (TGA) using a TA instrument TA-Q500. Samples of mass between 1–2 mg were loaded into an open platinum crucible and placed in TA instrument. The samples were then heated within the temperature range 25–500 ^{o}C at a heating rate of 10 ^{o}C min^{-1} under nitrogen gas flow (50 mL min^{-1}).

The onset temperature for a guest loss was determined using Differential Scanning Calorimetry (DSC). Samples of mass between mass 1–2 mg were placed in aluminium pans Aluminium lids were vented with two holes before covering the pans. After loading the pans in a TA Instrument DSC-Q200, the sample was heated at 10 ^{o}C min^{-1} under nitrogen gas flow (50 mL min^{-1}).

2.4. HOT STAGE MICROSCOPY (HSM)

Hot stage microscopy (HSM) was used to monitor the relative temperature at which the sample melts, releases guest gases, or decomposes. This can be observed through changes in colour and texture of the sample. It also allows to correlate and confirm the events observed during TGA and DSC analysis. The temperature corresponding to an event occurrence slightly differs from that in TGA and DSC. This is because there is no gas purge used in HSM.

Crystals were immersed in paratone oil on a slide glass on a Nikon SMZ-10 stereoscopic microscope fitted with a Sony Digital Hyper HAD colour video camera. The sample was heated by Linkam THMS600 hot stage and the temperature was controlled by a Linkam TP92 unit. The heating rate was 10 °C.min^{-1} and images were captured at every 25 ^{o}C increment.

2.5. FOURIER-TRANSFORM INFRARED SPECTROSCOPY (FTIR)

Fourier-Transform Infrared (FTIR) spectroscopy was used to characterize the functional groups of the guest molecules, functionalised ligands, and to give insight into the coordination mode, and possible interactions in the framework.[1] This method can assist to elucidate the interactions and the effect of inclusion in the host.[1] Dried and powdered samples were prepared and loaded on PerkinElmer Spectrum Two FTIR spectrometer equipped with an ATR Diamond accessory. Powders of the samples were then scanned over a range of 400–4000 cm^{-1}.

2.6. SOLVENT VOCs AND GAS SORPTION

Stable activated MOFs were used to investigate their sorption capacity for a series of halogenated and amine VOCs. Masses between 5-7 mg of the activated samples were loaded in narrow glass vials which were placed into larger vials containing the VOCs. The larger vials were then sealed

(Figure 2.2) to allow vapour sorption at room temperature (r.t., ca. 25 ^{o}C) for between one day and two weeks depending on their boiling point. The VOCs selected for study were dichloromethane (DCM), chloroform ($CHCl_3$), chlorobenzene (ClBenz), dibromomethane (CH_2Br_2), bromoform ($CHBr_3$), bromobenzene (BrBenz), diiodomethane (CH_2I_2), iodoform (CHI_3), iodobenzene (IBenz), water (H_2O), ammonia (NH_3), methylamine ($MeNH_2$), 1-propylamine ($PropNH_2$), 1-butylamine ($ButNH_2$), benzylamine ($BzNH_2$), and 1-phenylethylamine ($PhEtNH_2$). Table 2.1 provides code names for the corresponding phases form the activated [Co(34pba)(44pba)] and [Zn(34pba)(44pba)] MOFs named as **1d** and **3d** respectively. The MOFs adsorbent could be recovered on heating under vacuum, using conditions similar to the activation.

Figure 2.3: *Sorption of VOCs from big vials into MOF adsorbents in narrow vials.*

Table 2.1: *Code names of the phase changes from the adsorbents.*

VOC	Code name in 1d Adsorbent	Code name in 3d Adsorbent
CH_2Cl_2	1dCH_2Cl_2	3dCH_2Cl_2
$CHCl_3$	1d$CHCl_3$	3d$CHCl_3$
ClBenz	1dClBenz	3dClBenz
CH_2Br_2	1dCH_2Br_2	3dCH_2Br_2
$CHBr_3$	1d$CHBr_3$	3d$CHBr_3$
BrBenz	1dBrBenz	3dBrBenz
CH_2I_2	1dCH_2I_2	3dCH_2I_2
CHI_3	1dCHI_3	3dCHI_3
IBenz	1dIBenz	3dIBenz
H_2O	1dw	3dw
NH_3	1dNH_3	3dNH_3
$MeNH_2$	1d$MeNH_2$	3d$MeNH_2$
$PropNH_2$	1d$PropNH_2$	3d$PropNH_2$
$ButNH_2$	1d$ButNH_2$	3d$ButNH_2$
$BzNH_2$	1d$bzNH_2$	3d$BzNH_2$
$PhEtNH_2$	1d$PhEtNH_2$	3d$PhEtNH_2$

Gas sorption capacity of **1d** and **3d** adsorbents was also investigated for carbon dioxide (CO_2) and hydrogen (H_2) gases using a Micromeritics 3Flex Surface Area Analyzer. Each sample was ground to homogenise the surface area contacts and weighed between 130-140 mg. The sample preparation includes the removal of some guest molecules or moisture in excess using a Micromeritics Flowprep with the flow of nitrogen over the samples for 3 h with continuous heating at 60 °C. Thereafter, samples were degassed by heating at 140 °C under vacuum for 2 h prior to the analysis. The sorption for CO_2 was performed at various temperatures in order to determine the heat of adsorption (Qst)**.** The sorption capacity for H_2 was only carried out at 77K. Loading of gas into the samples was characterized by the pressure change from 0 mmHg to the maximum

equilibrium pressure and the latter varied between 600-1000 mmHg. The complete sorption corresponded to the equilibrium pressure which was followed by the desorption process.

The sorption for nitrogen to determine Brunauer−Emmett−Teller (BET) surface area was not successful due to the absence of interaction between these adsorbents and nitrogen. To this end, the sorption process has been used to provide information regarding pore size, pore volume, and interaction between the surface adsorbent and adsorbate.[2]

2.7. NUCLEAR MAGNETIC RESONANCE (NMR)

Nuclear magnetic resonance (NMR) analysis was performed to characterize the structures and functional groups of a compound. In this thesis, it was used to analyse the guest molecules adsorbed into the channels of MOFs. Solid MOFs containing the guest species were soaked into DMSO-d_6 and heated at 80 ^{o}C for 1h to release the guests into the solution for the NMR analysis. ^{1}H NMR spectra were recorded in DMSO-d_6 solution using a BRUKER 300 MHz spectrometer at 303 K. Appropriate signals were integrated to determine the ratio of the respective guests in the MOFs.

2.8. CRYSTAL STRUCTURE DETERMINATION

The determination of crystal structure provides information such as type of atoms, connectivity of atoms, interatomic distance and angles, and symmetry operations in crystal. This is obtained from a non-destructive single crystal X-ray diffraction (SCXRD) technique that requires a crystal with good diffraction. The crystal was selected using optical microscopy under plane-polarised light. It was then mounted on a nylon loop covered by paratone oil in case of cracking of crystal due to guest loss. Intensity data were recorded on a Bruker KAPPA APEX II DUO diffractometer using graphite monochromated Mo-Kα radiation (λ = 0.71073 Å) at 100 or 173 K. The intensity data

were collected by phi scan and omega scan techniques. Unit cell refinement and data reduction were performed using Program SAINT.[3] Data were corrected for Lorentz-polarization effects and absorption (SADABS).[4] The structures were solved by direct methods in SHELXS[5] and refined by full-matrix least-squares on F^2 using SHELXL[5] within the XSEED[6] interface. The non-hydrogen atoms were located in different electron density maps and were refined anisotropically while hydrogen atoms were placed in calculated positions and refined with isotropic temperature factors. The refinement could also require the use of Platon package[7] depending on the behaviour of guest solvent in the MOFs. Details of crystal structure refinements are provided in Chapter Four. **XPREP**:[7] XPREP software analyzes intensity data from the X-ray diffractometer to determine the space group of the crystal structure. It generates input files ready for refinement in the SHELX program. **Platon**:[8] Software which is a versatile crystallographic tool that calculates the structure molecular parameters such as bonds, angles, torsions, planes, rings, coordination, and tests for missing symmetry and voids in the lattice. In this work, it provided a SQUEEZE option for handling disordered solvents.

ConQuest:[9] Software for searching and retrieving information about compounds from Cambridge Structural Database (CSD). **Mercury**:[10] A program that assists to generate information from the existing crystal structure from Conquest or experimental structures refined from SHELX. Mercury generates calculated powder patterns and provides an option of overlaying structure for comparisons. It allows us to visualise bonding type (such as hydrogen bondings) and to calculate their interatomic distance and torsion angles. Mercury also provides a statistical option that allows the analysis using a histogram.

2.9. CALCULATION OF BONDING ENERGIES

The interaction force between two molecules was calculated using Density Function Theory (DFT) calculations. Energy interaction between water and the channels of cobalt ethylenediamine complex against energy interaction between H_2O and MeOH in the channels of the complex were optimized at the B3LYP/cc-pVDZ[11–14] level of theory and frequencies to determine a minimum energy conformation. Counterpoise corrected single point calculations were then performed at both the cc-pVDZ and 6-311++G(d,p)[15] levels of theory to calculate the intermolecular interaction energies between the H_2O and the channels of the complex. The same calculation was applied between H_2O and three MeOH molecules as H_2O has the ability to interact with three MeOH molecules. Note (6-311++G(d,p) basis set is slightly larger and provides more accurate results. This basis set was used to determine lattice energy in crystal structures.

2.10. POWDER X-RAY DIFFRACTION (PXRD)

For each single crystal structure, a SHELX RES or CIF file was treated by Mercury software[10] to generate calculated PXRD patterns. The same wavelength was used as in the experimental measurement, λ = 1.5406 Å. The patterns generated were compared with those from experiment to determine whether the single crystal is representative of the bulk material. Furthermore, PXRD was used to investigate the host-guest interaction after inclusion as characterized by the phase change observed. The experimental PXRDs were performed using two instruments: Bruker D8 Advance X-ray diffractometer and a Bruker D2 phaser benchtop instrument, details given below. Dried samples were powdered and placed on a zero-background sample holder in the path of an X-ray beam. Powder X-ray diffraction (PXRD) patterns were measured on a Bruker D8 Advance X-ray diffractometer equipped with a Lynxeye detector using CuKα-radiation (λ = 1.5406 Å).

X-rays were generated at 30 kV voltage and 40 mA current. Samples placed on a zero-background sample holder were scanned over a range of 4–40° in 2θ operating with 0.016° step size per second.

Some samples were analyzed by Bruker D2 phaser benchtop equipped with 1-dimensional Lynxeye detector using CuKα-radiation (λ = 1.54184 Å). The X-rays were generated at 30 kV/10 mA and samples were scanned as with D8 Advance X-ray diffractometer. The collected data were analyzed using Origin software.[16]

2.11. REFERENCES

1. Mehlana, G., Ramon, G. & Bourne, S. A. A 4-fold interpenetrated diamondoid metal-organic framework with large channels exhibiting solvent sorption properties and high iodine capture. *Microporous Mesoporous Mater.* **231**, 21–30 (2016).

2. Thommes, M. , Kaneko, K., Neimark, A. V., Olivier, J. P., Rodriguez-Reinoso, F., Rouquerol, J., Sing, K. S. W. Physisorption of gases, with special reference to the evaluation of surface area and pore size distribution (IUPAC Technical Report). *Pure Appl. Chem.* **87**, 1051–1069 (2015).

3. Program SAINT, version 7.12a; Bruker AXS Inc.: Madison, Wisconsin, USA. (2006).

4. Sheldrick. G. M. SADABS: Program for Area Detector Adsorption Correction; University of Göttingen: Germany,. 33–38 (1996).

5. Sheldrick, G, M. Crystal Structure Refinement with SHELXL. *Acta Cryst* 3–8 (2015).

6. Barbour, L. J. X-Seed 4: updates to a program for small-molecule supramolecular crystallography. *J. Appl. Cryst.* **1141**, (2020).

7. XPREP: Data Preparation & Reciprocal Space Group Exploration, version 5.1© Bruker Bruker Analytical X-ray System,. (1997).

8. Spek, A. L. A Multipurpose Crystallographic Tool, Version 10500: e,. 1980-2000.

9. ConQuest: A Program for the Search of the CSD, Version 5.41© March. (2020).

10. Macrae, C. F., Bruno, I. J., Chisholm, J. A., Edgington, P. R., Mccabe, P., Pidcock, E., Rodriguez-monge, L., Taylor, R., Streek, J. V., Wood, P. A. Mercury CSD 2.0 – new features for the visualization and investigation of crystal structures. *J. Appl. Crystallogr.* **41**, 466–470 (2008).

11. Lee, C., Yang, W. & Parr, G, R. Development of the Colic-Salvetti correlation-energy into a functional of the electron density. *Am. Phys. Soc.* **37**, 785–789 (1988).

12. Becke, A. D. Densityfunctional thermochemistry . III . The role of exact exchange Density-functional thermochemistry . III . The role of exact exchange. *J. Chem. Phys.* **98**, 5648–5652 (1993).

13. Dunning, T. H. & Dunning, T. H. Gaussian basis sets for use in correlated molecular calculations . I . The atoms boron through neon and hydrogen. *ameAmerican Inst. Phys.* **90**, 1007–1023 (1989).

14. Tsuzuki, S. & Lüthi, H. P. Interaction energies of van der Waals and hydrogen bonded systems calculated using density functional theory: Assessing the PW91 model. *J. Chem. Phys.* **114**, 3949–3957 (2001).

15. Frisch, M. J., Pople, J. A. & Binkley, J. S. Self-consistent molecular orbital methods 25. Supplementary functions for Gaussian basis sets. *J. Chem. Phys.* **80**, 3265–3269 (1984).

16. Origin 8. OriginLab Corporation, version 7.5. *One Roundhouse Plaza,Northampton, MA,U.S.A., 01060. 1-800-969-7720*

CHAPTER 3. STRUCTURAL CHARACTERIZATION OF THE SYNTHESIZED METAL-ORGANIC FRAMEWORKS

3.1. INTRODUCTION

This chapter presents the characterization of the synthesized metal-organic frameworks. The linkers used were either pyridylbenzoates or pyridin-4-ylmethyl aminobenzoates, which differ from one another in two respects: (i) the connectivity of the pyridine and carboxylate moieties can be linear or bent, and (ii) the pyridin-4-ylbenzoates include a methylamino group between the pyridyl and benzoic acid rings. Compounds $\{[Co(34pba)(44pba)]\cdot DMF\}_n$ (**1**), $\{[Co(34pba)(44pba)]\cdot(C_3H_6O)\}_n$ (**2**), and $\{[Zn(34pba)(44pba)]\cdot DMF\}_n$ (**3**) are **3D** frameworks prepared from Co^{2+} and Zn^{2+} with the mixed 44pba = 4-(4-pyridyl)benzoate and 34pba = 3-(4-pyridyl)benzoate ligands. The solvothermal synthesis using Cu^{2+} with 34pba led to a **2D** structure, $\{[Cu(34pba)_2]\cdot DMF\}_n$ named as **4**. By extending the synthesis using functionalized ligands longer than 34pba and 44pba, the coordination mode of 3-(pyridyn-4-ylmethyl)aminobenzoate (34paba) and 4-(pyridyn-4-ylmethyl)aminobenzoate (44paba) ligands to a Cu^{2+} centre was investigated. No **3D** structures were obtained with these ligands, rather, **1D** $\{[Cu(44paba)_2]\cdot 2H_2O\cdot 2DMF\}_n$ (**5**) and $\{[Cu(34paba)_2(H_2O)]_2\cdot[Cu(34paba)]\cdot 2DMF\}_n$ (**6**) structures were formed. Little change on the experimental conditions of **4** was performed to synthesize a **3D** structure, $\{[Cu_3Cl_8(34pba)_6]$.solvent$\}$ (**7**). The characterization focused on structural, thermal, and functional elucidation.

3.2. MIXED PYRIDYLBENZOATE METAL-ORGANIC FRAMEWORKS

3.2.1. Synthesis and Characterization of {[M(34pba)(44pba)]·guest}$_n$ (1, 2, and 3)

3.2.1.1. Synthesis

The summary of the synthesis of **1**, **2**, and **3** is presented in Table 3.1. The starting materials for compound **2** differ from the one in **1** by the use of acetonitrile/water instead of DMF/ethanol solvent system. Besides, the synthesis in **3** differs from **1** by the use of Zn^{2+} rather than Co^{2+} metal centres. Compounds **1**, **2**, and **3** were activated at 210 ^oC under vacuum for 6 hours which resulted in **1d**, **2d**, and **3d** respectively.

Table 3.1: *Synthetic conditions for **1**, **2**, and **3***

Compound	Metal salt	Ligands	Solvent system	Conditions
1	$CoCl_2 \cdot 6H_2O$ (6 mg, 0.03 mmol)	34pba/44pba (10 mg, 0.050 mmol each)	DMF(6 ml)/Ethanol (2 ml)	120 °C for 3 days
2	$CoCl_2 \cdot 6H_2O$ (6 mg, 0.03 mmol)	34pba/44pba (10 mg, 0.050 mmol each)	Acetonitrile (6 ml)/water (2 ml)	
3	$Zn(NO_3)_2 \cdot 6H_2O$ (30 mg, 0.13 mmol)	34pba/44pba (40 mg, 0.20 mmol each)	DMF(6 ml)/Ethanol (2 ml)	

3.2.1.2. Structural characterization

The frameworks in **1**, **2**, and **3** are identical in terms of connectivity and geometry, with the asymmetric unit consisting of a metal ion (Co^{2+} in **1** and **2**, Zn^{2+} in **3**) bound to one 34pba and one 44pba linker. A centre of inversion generates a dinuclear secondary building unit (SBU) in which the two metal ions are connected by two bridging 34pba linkers through carboxylate groups while each metal ion is also coordinated to one 34pba and one 44pba through the pyridyl-N and to a 44pba through a bidentate carboxylate. The metal M-O and M-N bond lengths are 2.013 - 2.230 Å and 2.136 - 2.146 Å, respectively and fall in the expected range.[1,2] The extension of this SBU through space gives rise to a double-walled network of **bcu** topology where each side of the square

channels consists of a 34pba and a 44pba linker (Figure 3.1 and Table 3.1). Hour-glass shaped channels running parallel to [100] contain DMF (**1** and **3**) or acetone (**2**) guest molecules. The presence of acetone in **2** was unexpected as a mixture of acetonitrile and water had been used to prepare this compound. Conversion of acetonitrile to acetone is likely to proceed via hydrolysis to acetic acid[3] followed by ketonization to form acetone.[4] There are weak hydrogen bonds between the guest oxygens and the aromatic walls of the MOF. While **1** and **3** are isostructural, the structure of **2** is subtly different. Torsion angles indicate that the rings of both linkers are twisted slightly more away from coplanar in **2** than in **1** or **3**, while the orientation of the carboxylate groups is closer to coplanar with the aromatic ring in **2** than in the other compounds (see Figure 3.2 and Table 3.3). The effect of these small changes is a lengthening of unit cell axes *a* and *c* while axis *b* shortens, but without changing the symmetry or space group. It is likely that the guest influences this change through the flexibility of the bent 34pba and linear 44pba linkers which allow a hinge-like expansion or contraction of the guest-accessible void.

Table 3.2: *Crystallographic information for compound **1**, **2**, and **3***

Compound	**1**	**2**	**3**
Formula	$C_{27}H_{23}CoN_3O_5$	$C_{27}H_{22}CoN_2O_5$	$C_{27}H_{23}N_3O_5Zn$
Mass (g.mol^{-1})	528.41	513.39	534.85
Crystal size (mm^3)	0.080x 0.10 x 0.11	0.030 x 0.060 x 0.090	0.030 x 0.030 x 0.090
Crystal system	Monoclinic	Monoclinic	Monoclinic
Space group	$P2_1/c$	$P2_1/c$	$P2_1/c$
a (Å)	9.203(3)	10.075(6)	9.339(1)
b (Å)	17.823(6)	15.69(12)	17.678(3)
c (Å)	14.718(8)	15.429(8)	14.735(2)
β (°)	92.75(3)	98.588(7)	93.189(5)
V (Å^3)	2411.(3)	2412.(4)	2428.84(7)
T (K)	100(2)	100(2)	173(2)
Z	4	4	4
D_c (g·cm^{-3})	1.456	1.423	1.463
μ(Mo−Kα) (mm^{-1})	0.756	0.757	1.055
F(000)	1092	1060	1104
Range scanned, θ (°)	1.80-28.34	1.87-25.09	1.80-27.58
No. reflections collected	22928	18219	22013
No. unique reflection	5981	4250	5584
No. reflections with I ≥ 2σ(I)	4089	2860	3713
Parameters/restraints	327/0	318/0	327/0
Goodness of fit, S	1.034	1.024	1.006
Final R indices (I ≥ 2σ(I))	R1 = 0.0482, wR2 = 0.1066,	R1 = 0.0493 wR2 = 0.1091	R1 = 0.0468 wR2 = 0.0972
Final R indices (all data)	R1 = 0.0859, wR2 = 0.1197	R1 = 0.0899 wR2 = 0.1239	R1 = 0.0867 wR2 = 0.1108
Min, max e$^-$ density (e Å^{-3})	0.414,-0.417	0.653,-0.455	0.421,-0.443

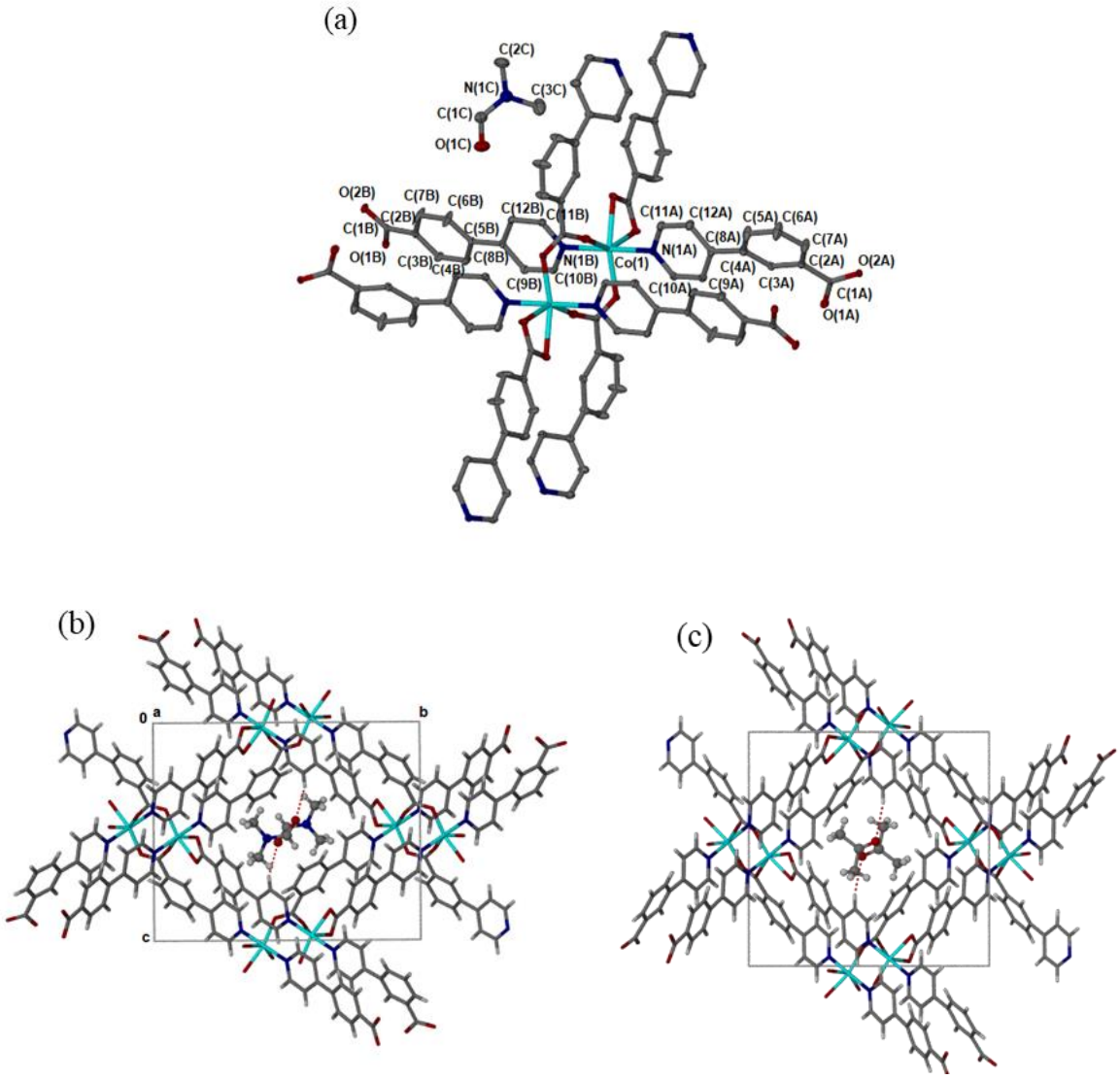

Figure 3.1: *(a) Coordination geometry and SBU in **1**. Only the asymmetric unit atoms are labelled, Packing diagrams of **1** (b) and **2** (c) showing the interactions between guest molecules and walls of the metal-organic frameworks (MOF).*

Table 3.3: *Selected torsion angles*

Compound	**1**	**2**	**3**
34pba:			
C3A-C4A-C8A-C12A	-146.0(3)	-139.1(4)	-145.6(3)
O1A-C1A-C2A-C7A	161.1(3)	-177.1(4)	163.0(3)
44pba:			
C4B-C5B-C8B-C12B	163.8(3)	158.0(4)	163.9(3)
O1B-C1B-C2B-C7B	174.3(3)	-179.7(4)	173.4(3)

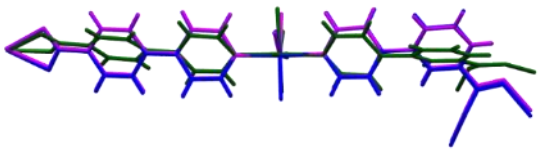

Figure 3.2: *Overlay of core of framework in **1** (blue), **2** (green), and **3** (purple).*

3.2.1.3. Phase characterization

The measured PXRD patterns in Figure 3.3 show the similarity of **1**, **2**, and **3** frameworks which matched well to the patterns calculated from single crystal structures. However, compound **2** had a small peak at 8.9^{o} instead of 9.4^{o} as for **1**. There are subtle differences in the pattern for **2** compared to those for **1** and **3**, for example, the shift in peaks at positions 12^{o} and 21^{o}. This dissimilarity could reflect the difference in the crystallographic data explained above. However, the activated forms of both **1d** and **2d** were the same after the removal of guest solvents. All activated forms **1d**, **2d**, and **3d** (**d**: activated) retained their crystallinities with a slight shift of peaks (except **3d**) to higher 2θ values which corresponds to a small decrease in interplanar spacing in the frameworks after guest removal. Hence, these compounds were stable after removal of guest molecules which is not observed in all MOFs.[4–6]

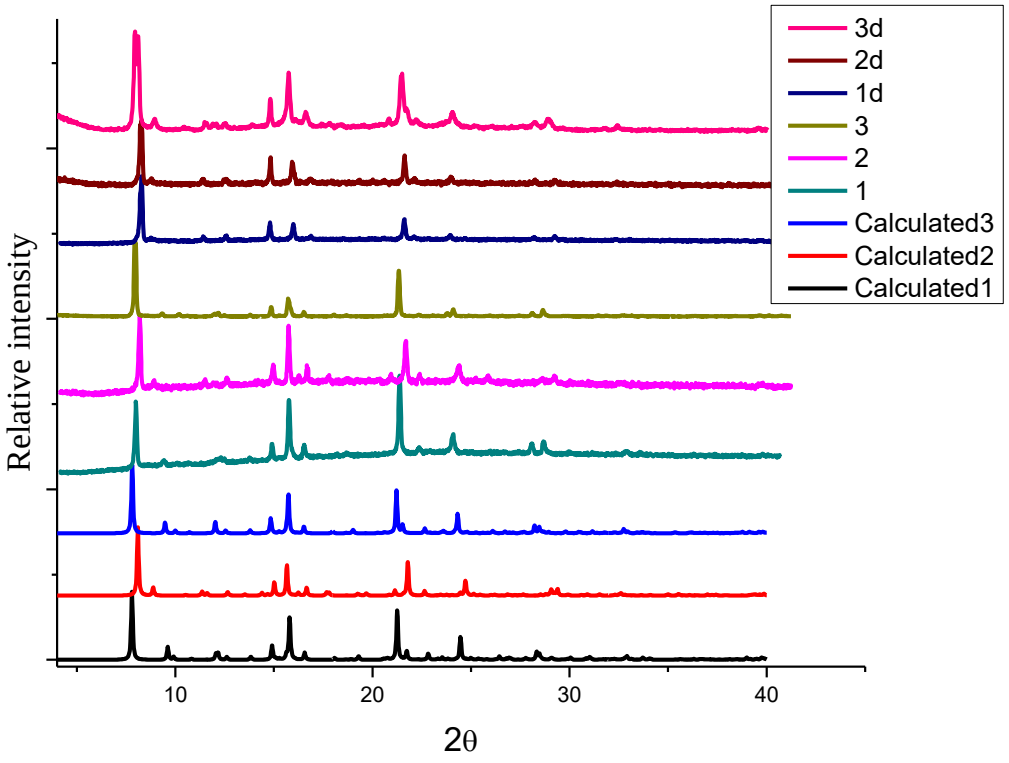

Figure 3.3: *PXRD patterns for **1**, **2**, **3**, **1d**, **2d,** and **3d** and their corresponding activated forms compared to their calculated patterns.*

Carbonyl stretches in the FTIR spectra (Figure 3.4) confirm the presence of DMF (in **1** and **3**) at 1678 cm^{-1} and acetone (in **2**) at 1713 cm^{-1}. The removal of these guest solvents was confirmed by the absence of these bands in the spectra of **1d** and **3d**. The spectra of the activated compounds are similar to one another as expected from the PXRD analysis.

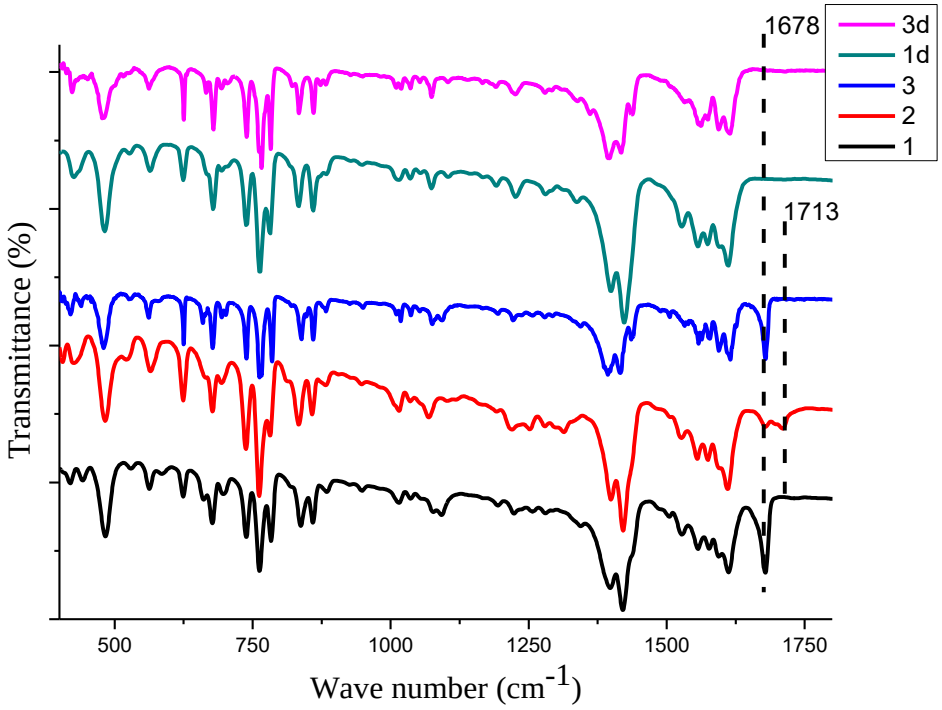

Figure 3.4: *Infrared spectra of **1**, **2**, **3**, **1d**, and **3d** showing functional groups of guest molecules and coordination modes.*

Thermogravimetric analysis (TGA) and DSC are shown in Figure 3.5. The weight loss of 14.1% between 120 and 216 ^{o}C in **1** was assigned to the removal of one DMF molecule (calculated 13.8%). This was characterized by a broad endothermic peak from 115–280 ^{o}C in the DSC. MOF **2** shows a weight loss of 24.5% (calculated 11.3%). The corresponding DSC trace shows an endothermic peak between 110 and 150 ^{o}C, followed by a small exothermic and a broad endothermic peak between 160 and 250 ^{o}C. It is possible that the removal of the acetone guest overlaps with the decomposition of the framework. This is contradictory to the PXRD evidence that the framework is robust. It is more likely therefore that the bulk sample selected for thermal analysis may contain a mixture of crystalline forms, only some of which correspond to the MOF characterized by crystal structure elucidation. An observed weight loss of 12.7% for **3** in the range of 120 and 216 ^{o}C was attributed to the removal of one DMF molecule (calculated 13.7%). The

corresponding DSC curve shows a broad endothermic process between 130 and 260 °C. The TGA traces for **1d**, **2d**, and **3d** show no mass loss before 300 °C, indicating the solvent has been removed from the framework.

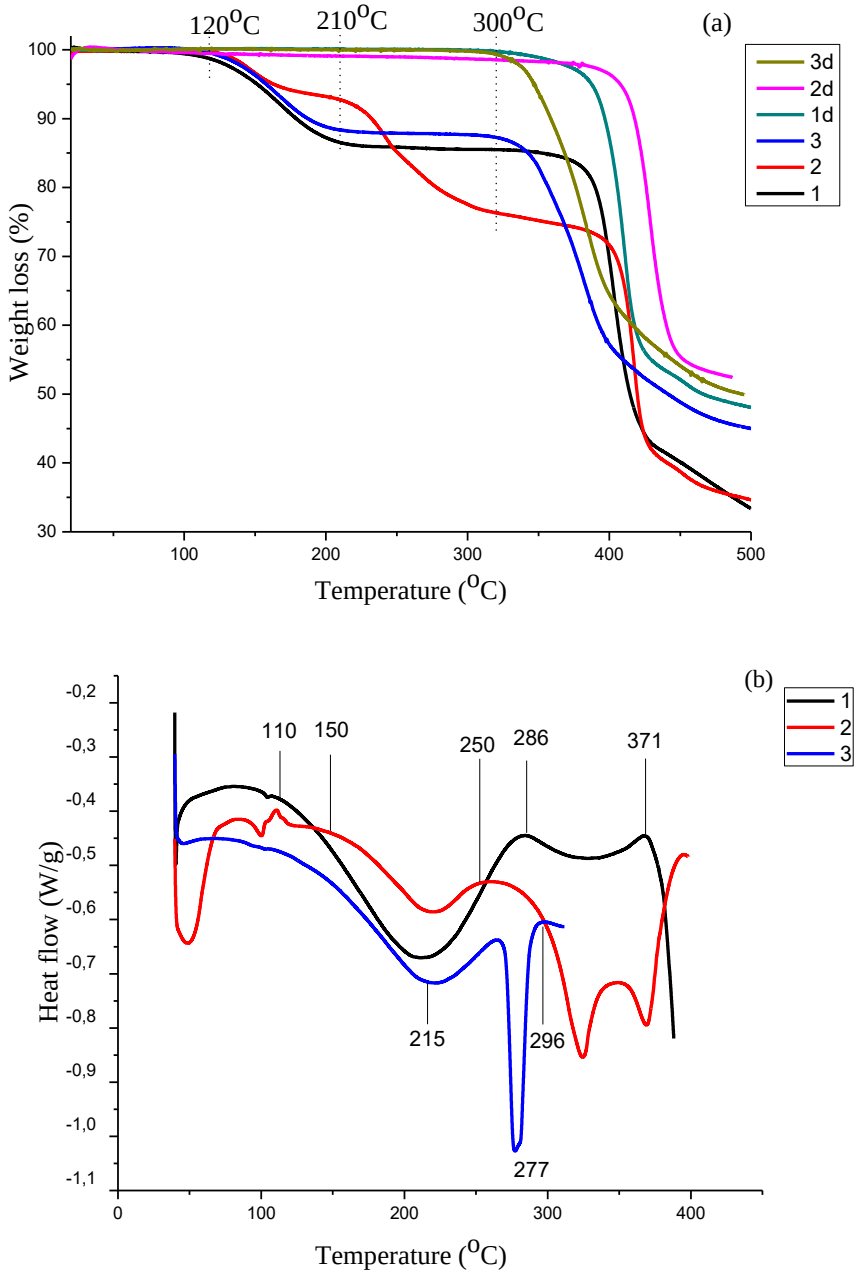

Figure 3.5: *(a) TGA curves for **1**, **2**, **3**, **1d**, **2d**, and **3d** (b) DSC curves showing the process of the removal of guest molecules and decomposition of the framework.*

3.3. COPPER-FRAMEWORKS BASED ON SINGLE AND FUNCTIONALIZED LIGANDS

3.3.1. Synthesis and Characterization of $\{[Cu(34pba)_2]\cdot DMF\}_n$ (4)

3.3.1.1. Synthesis

The synthesis of $\{[Cu(34pba)_2]\cdot DMF\}_n$ was a delicate balance (Table 3.4). Small variations in solvent mixture formed a new phase that did not crystallize well. Figure 3.6 (a) shows **4** as crystallized once $1.5\cdot10^{-1}$ ml of HCl measured using a syringe (without needle) were used in the solvent mixture. While the **4'** phase was predominantly formed when 0.5 ml measured using micropipette were used or when the quantity of HCl was not carefully controlled. The starting materials for both **4** and **4'** were heated at 140 °C for three days.

Table 3.4**: Experimental conditions for the synthesis of **4

Compound	Metal salt	Ligands	Solvent system	Conditions
4 (Crystal)	$CuCl_2\cdot2H_2O$ (14 mg, 0.08 mmol)	34pba (20 mg, 0.10 mmol)	H_2O/DMF/HCl ($1:3:1.5\cdot10^{-1}$ ml)	140 °C for 3 days
4' (Preciptitate)	$CuCl_2\cdot2H_2O$ (7 mg, 0.04 mmol)	34pba (10 mg, 0.050 mmol)	H_2O/DMF/HCl ($1:3:5\cdot10^{-1}$ ml)	

After cooling at room temperature (r.t), the samples were then filtered and kept in vial sealed with some holes. Purple thin rhombus-like crystals of **4** were formed within a week while green powder precipitated for **4'**. Figure 3.6 (b) shows PXRD patterns of the corresponding phases. This solvent system is comparable to the reported ones where acidified solutions containing HCl influence the topology, crystallization, crystallinity, and reproducibility of MOFs.[7–9] We were able to get a single crystal for **4** for structural characterization while no single crystal was obtained for **4'** despite many attempts.

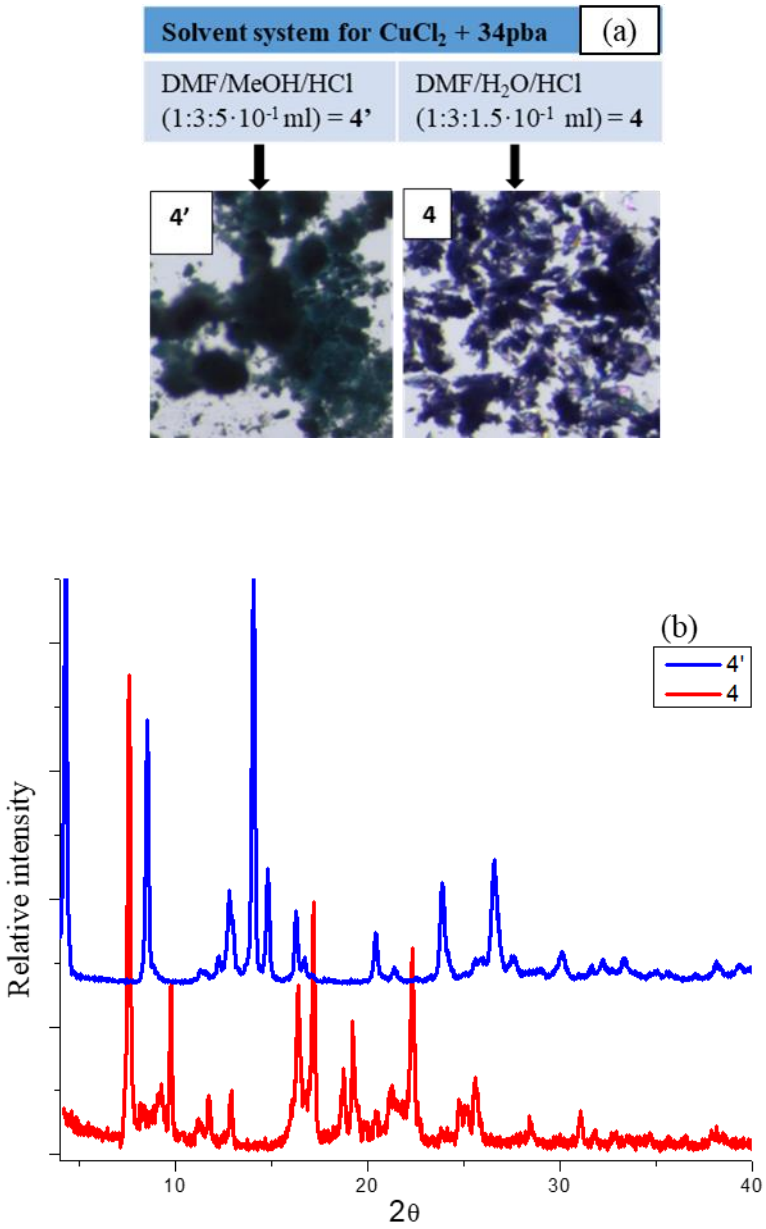

***Figure 3.6**: (a) Experimental conditions for **4** and **4'**, (b) corresponding PXRD patterns.*

3.3.1.2. Structural Characterization

The asymmetric unit of **4** shows that Cu^{2+} is coordinated to two pyridyl nitrogens and two carboxylate oxygens in a 4-coordinate square-planar fashion (Figure 3.7a). The Cu–O and Cu–N bond lengths are 1.9390(19) Å and 2.037(2) Å respectively, which are within the expected range. The compound crystallizes in monoclinic space group *C*2/*c* where the Cu^{2+} centre has a site occupancy of 0.5. The guest molecule, DMF is disordered over a centre of inversion with a site occupancy of 0.5. The remaining atoms were assigned with full site occupancy. The coordination gives rise to a **2D** layered structure with a square lattice (Figure 3.7b). These layers pack parallel to the *a* and *c* axes, and guest-DMF molecules are located between the parallel MOF layers with no observable host-guest interactions. The disordered DMF is positioned with its nitrogen atom on the centre of inversion at (0.25, 0.25, 0.50). The layered structure of alternating MOF and DMF molecules is evident in the packing diagram viewed along the *c* axis in Figure 3.7c. Also evident in this Figure is that **4** is an interwoven framework (one layer colour green). The coordination and space group are similar to these in QEYYIE with a formula of $[Cu(3,4\text{-pybz})_2]_n$ (3,4-pybz = 34pba).[5] However, the unit cell of **4** has a shorter *b* axis but with longer *a* and *c* axes (Table 3.5). The volume was slightly higher probably due to the presence of guest molecules which are absent in QEYYIE. Compound **4** was activated to remove DMF guest molecules using two different methods: heating under vacuum gave **4d1** (for which single crystals were not obtained) while soaking in methanol directly gave **4d2**. As a desolvated phase, **4d2** might be expected to be similar to QEYYIE, but more closely resembles the unit cell of **4**. The comparison with related compounds is detailed in the following sections.

Table 3.5**: Crystallographic information for **4

Compound	**4**	**4d2**	**QEYYIE**
Formula	$C_{27}H_{27}N_3O_5C_{l0}Cu$	$C_{24}H_{16}N_2O_4Cu$	$C_{24}H_{16}N_2O_4Cu$
Mass (g.mol^{-1})	537.05	459.93	459.93
Crystal size (mm^3)	0.030 x 0.170 x 0.210	0.020 x 0.140 x 0.160	N/A
Crystal system	Monoclinic	Monoclinic	monoclinic
Space group	*C2/c*	*C2/c*	*C*2/*c*
a (Å)	23.4432(3)	20.2073(12)	21.667(6)
b (Å)	5.5300(6)	5.5595(3)	6.7668(18)
c (Å)	18.4872(2)	18.4988(10)	16.745(4)
β (°)	96.425(2)	110.641(2)	127.264(3)
V (Å^3)	2381.64(2)	1944.80(19)	1953.8(9)
T (K)	293(2)	293(2)	
Z	4	4	
D_c (g·cm^{-3})	1.498	1.571	
μ(Mo−K*α*) (mm^{-1})	0.962	1.159	
F(000)	1116	940	
Range scanned, θ (°)	1.748-27.473	2.154-30.513	
No. reflections collected	27054	27869	
No. unique reflection	2720	2968	
No. reflections with I ≥ 2σ(I)	2169	2376	
Parameters/restraints	201/0	142/0	
Goodness of fit, S	1.120	1.149	
Final R indices (I ≥ 2σ(I))	R1 = 0.0420 wR2 = 0.0975	R1 = 0.0469 wR2 = 0.0934	
Final R indices (all data)	R1 = 0.0583 wR2 = 0.1031	R1 = 0.0647 wR2 = 0.1010	
Min, max e$^-$ density (e Å^{-3})	0.375, -0.529	0.712, -0.689	

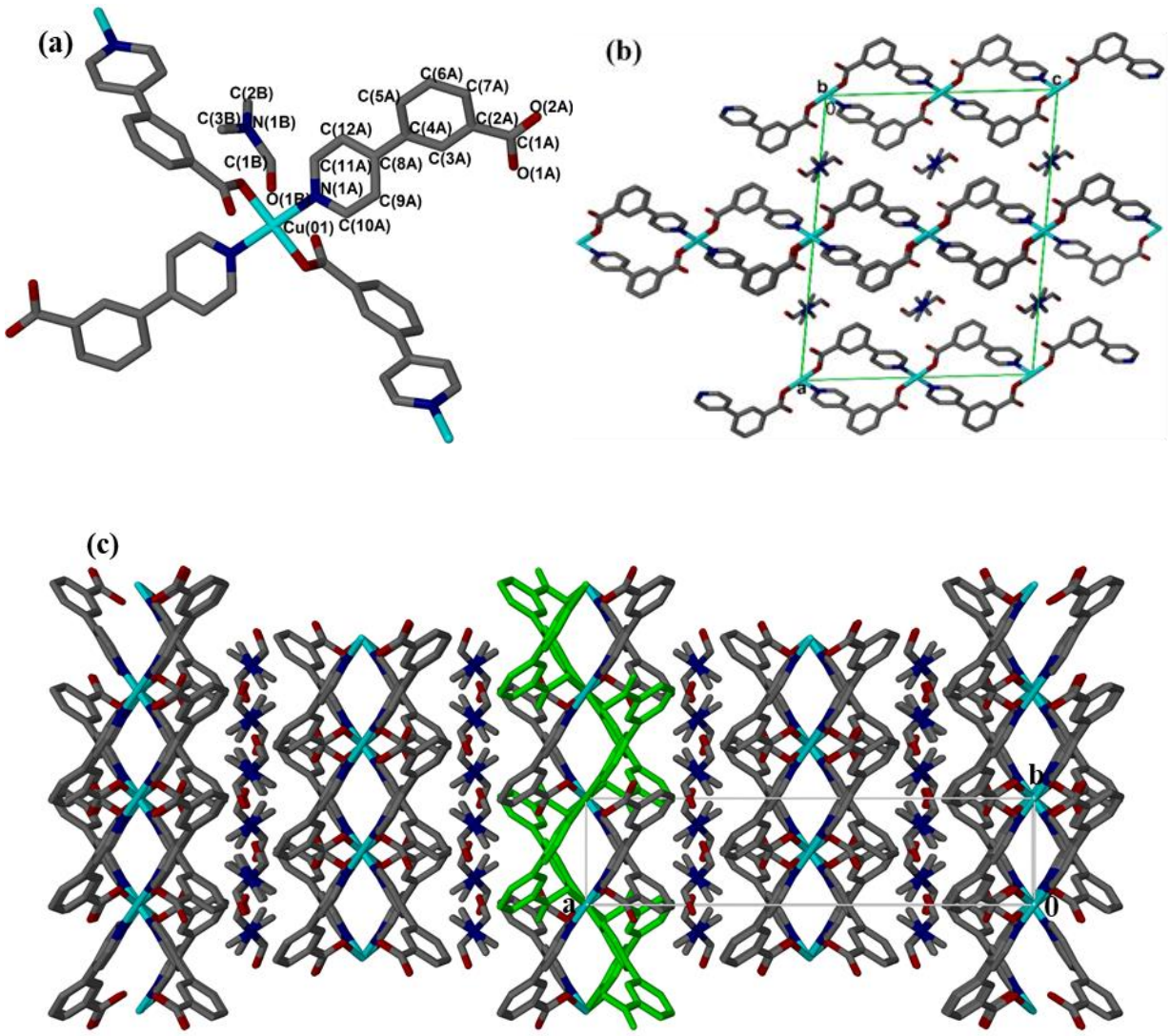

Figure 3.7: *(a) Coordination geometry about Cu^{2+} in **4**; the asymmetric unit is labeled, (b) disordered DMF between parallel MOF layers viewed along [010], (c) packing diagram viewed along [001] demonstrates the alternating layers (one in green) of MOF and solvent DMF.*

3.3.1.3. Comparison of 4 with structures of the related ligand

The literature contains a number of reports on the coordination of 34pba with other metals, notably Cu^{2+} and Co^{2+} which are interesting to compare with compound **4**. The resulting structures have dissimilarities in coordination around metal centres and conformation. These structures were extracted from the Cambridge Structure Database (CSD: version 5.41 March 2020).[6]

QEYYIE[5] with a formula of $[Cu(3,4\text{-pybz})_2]_n$ (3,4-pybz = 34pba) was synthesized using KOH solution rather than DMF, H_2O and HCl in the solvent mixture as in **4**. The similarity is explained by Cu^{2+} centres bridged by four 34pba linkers and extend in 2D layers which are interpenetrated. Furthermore, it crystallizes in monoclinic *C*2/*c* and the angle of O–Cu^{2+}–O or N–Cu^{2+}–N is also 180°. However, there are some distinctions observed in the coordination fashion. QEYYIE presents the coordination fashion that involves the chelating of Cu^{2+} centres by both carboxylates while **4** is in monodentate fashion as detailed in FTIR section. Moreover, the 2D layers form π–π stacking interactions originating from the pyridyl rings of the adjacent layers to result in 3D supramolecular structure. Furthermore, the framework does not contain any guest molecule.

WORXOS[7] is a copper based dinuclear coordination similar to **4** but the extension as a framework was closed by the coordination of 1,1-bis(diphenylphosphanyl)ferrocene ligand to Cu^{2+} and results in a discrete complex. It crystallizes in different crystal system and space group (*P*ī in triclinic system) with a square planar geometry. The use of 1,1-bis(diphenylphosphanyl)ferrocene ligand different from pba could influence the difference in conformation with **4**.

The carboxylate coordination to the Co^{2+} centre can also be used in comparison. It is usually bidentate, which is different from **4**. GEKJUE[1] crystallizes in the triclinic system with a space group of *P*ī. Carboxylate moiety coordinates to Co^{2+} in both chelating and monodentate fashion. Weak interactions such as O−H···O and C−H···O hydrogen bonds across the framework were reported. XEVXUT referred to as $\{[Co(34pba)_2]\cdot DMF\}_n$ formula[2] was synthesized at 75 °C and crystallizes in $P4_32_12$ space group with a tetragonal plane net of **sql** topology. A change in temperature as the reaction condition led to the formation of its structural isomer, XEVXON which crystallizes in orthorhombic crystal system and space group *Pbca*. The carboxylate of 34pba ligand coordinates to Co^{2+} in chelate fashion. FUMJAZ[8] is an interpenetrated framework of

$[Co(pbc)_2(H_2O)]_n$ formula with monoclinic system and space group *C*2/*c*. The carboxylates are coordinated in both monodentate and chelating mode. ZIRYOR[9] crystallizes as $\{[Cd(pba)_2]\cdot 2DMA\}_n$ in the orthogonal space group $P2_12_12_1$. GEKJOY[1] has the formula of $\{[Co(34pba)_2]\cdot 2DMA\}_n$ and crystallizes in the orthorhombic system, space group $C222_1$. The coordination in IDECOL[10] structure shows an angle of 180° and space group of *C*2/*c* similar to compound **4**. However, the Co^{2+} centre is coordinated to other four H_2O moieties as a discrete complex and forms a 3D supramolecular network due to the formation of multiple hydrogen bonding of the coordinated H_2O molecules and the uncoordinated carboxylate groups. Figure 3.8, indicates the atoms around Cu^{2+} in red and the corresponding angles measured for comparison. Apart from IDECOL, the considered angles around Cu^{2+} or Co^{2+} are with O–M–N sequence (M: metal centre) of atoms. Table 3.6 indicates that the angles of bonds around metal centres in these structures vary notably from 90 or 180°.

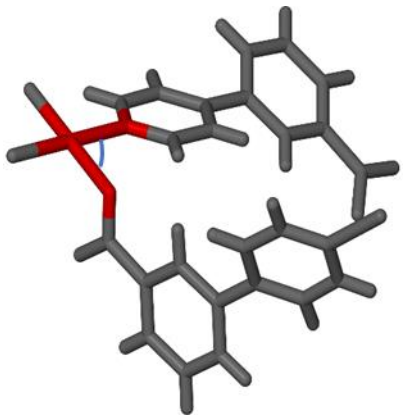

Figure 3.8: *Measured angles around Cu^{2+} as indicated in red colour.*

Table 3.6: *Angles around metal centres in the asymmetric units.*

Compound	M−O (Å)	M−N (Å)	Resulting Angle (°)	O-M-N or N-M- N
4	1.9390	2.037	180°	N-Cu-O
QEYYIE	1.92	2.43	90.4	N-Cu-O
WORXOS	2.02	2.10	91.50	N-Cu-O
GEKJUE	2.034	2.104	108	N-Co-O
XEVXUT	2.171 or 2.224	2.140	90.7 and 96.2	N-Co-O
XEVXON	2.109 or 2.076	2.103	94.3 and 96.3	N-Co-O
FUMJAZ	2.167 or 2.018	2.124	94.9 and 108.2	N-Co-O
ZIRYOR	2.080 or 2.217	2.091	89.70 and 100.5	N-Co-O
GEKJOY	2.23 or 2.08	2.09	100.7 and 90.0	N-Co-O
IDECOL	2.148	2.148	180	N-Co-N

The structures were overlaid against **4** in Figure 3.9 for comparison. The rings of some structures are remarkably twisted away from the coplanar rings in **4** while the others are slightly twisted. In addition, the angles between two ligands through O–M–N coordination are different in one another. The origin of the variations in these conformations might be due to the difference in the size of guest molecules,[11] metal ion radius,[9] and stimuli such as temperature and solvent system used during the synthesis.[9,11] These factors might also cause the single bond between pyridyl and benzoate rings to undergo a free rotation which affects the conformation, torsion angle, and O–M–N or N–M–N angles in the asymmetric unit. Hence, corresponding torsion angles between the two rings are presented in Table 3.7.

- ***Overlay of 4 with Cu^{2+} structures***

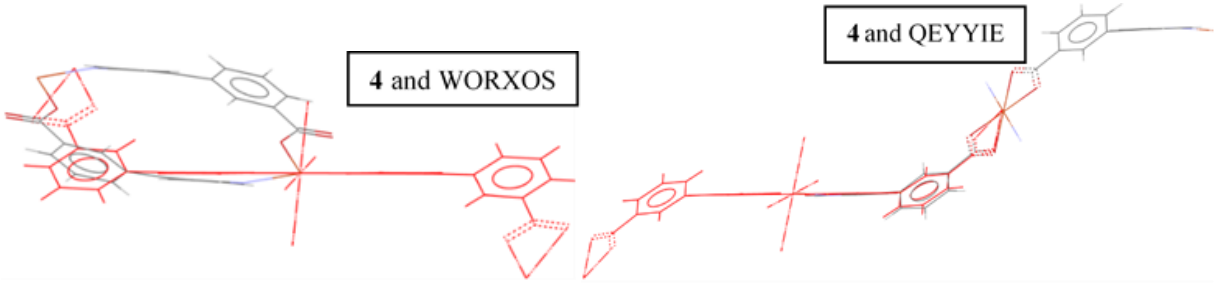

- ***Overlay of 4 with Co^{2+} structures***

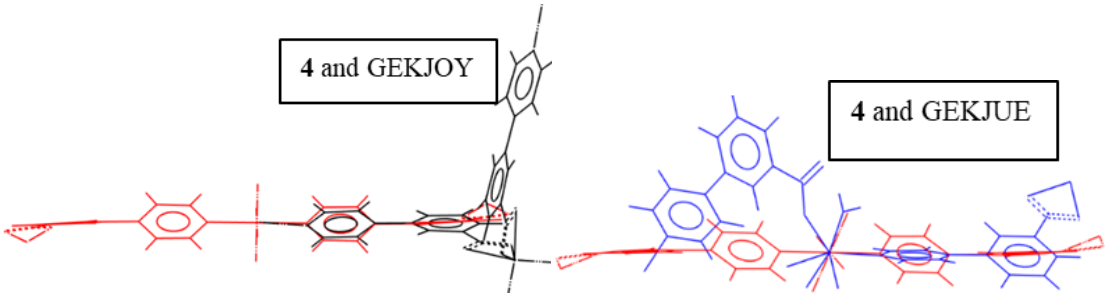

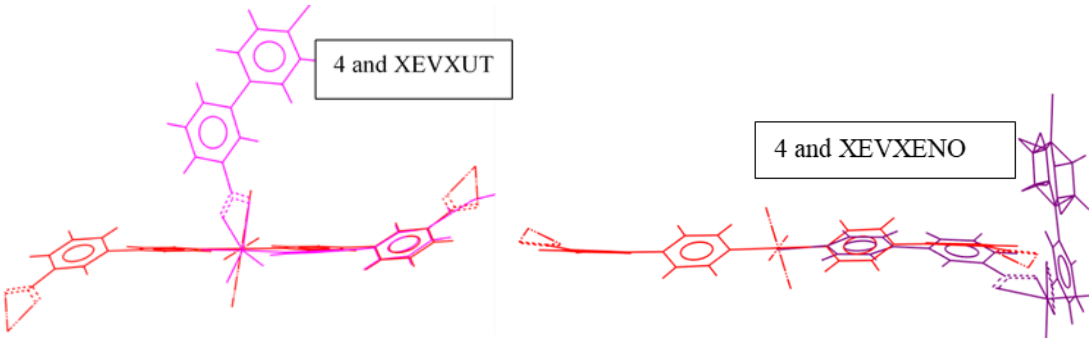

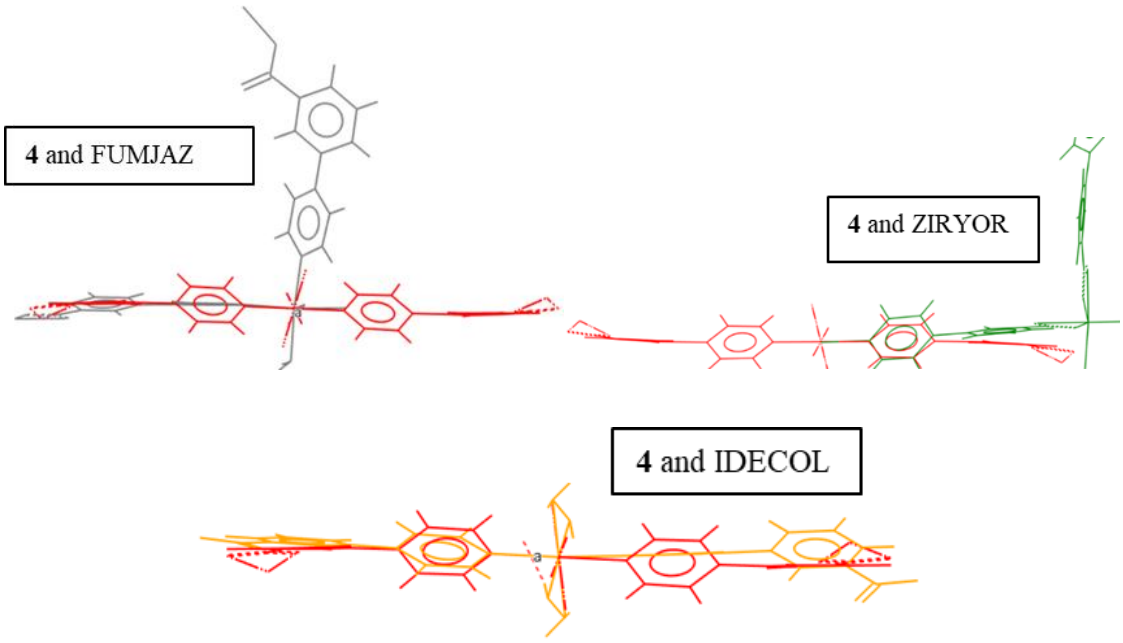

Figure 3.9: *Overlaid structures in comparison with compound* ***4*** *(****4*** *is coloured red in each overlay).*

Table 3.7: *Comparison of selected torsion angles*

Torsion angle Compounds	C3-C4-C8-C12	O1-C1-C2-C7
4	-144.25	-178.06
QEYYIE	140.2	175.2
WORXOS	150.6	171.7
GEKJUE	-150.92	-175.59
XEVXUT	151.26	-152.43
XEVXON	168.59	-174.08
FUMJAZ	167.59	-174.08
ZIRYOR	137.13	178.26
GEKJOY	-138.48	178.60
IDECOL	-153.54	-177.42

3.3.1.4. Activation of 4 and characterization

Compound **4** was activated by removing DMF guest molecules using two different techniques which led to two new phases. Heating **4** at 160 ^{o}C under vacuum formed **4d1** while soaking into methanol for five days formed **4d2**. Methanol was refreshed once after the first two days. Single crystals suitable for X-ray diffraction were only obtained from **4d2** and characterized. The unit cells of **4d2** are different from those in **4** and QEYYIE (Table 3.5). Cell volume of **4d2** and QEYYIE are close but hydrogen bonding is only found in the latter. The distance between layers viewed parallel to *c* in **4d2** is shorter and the layers become nested into one another compared to **4** (Figure 3.10a and b). The shortened unit cell *a* can also be explained by the layers having slid relative to one another and becoming nested and thus closer to one another as shown in Figure 3.10c and d view parallel to *b*. Hence, the removal of DMF caused the contraction of layers.

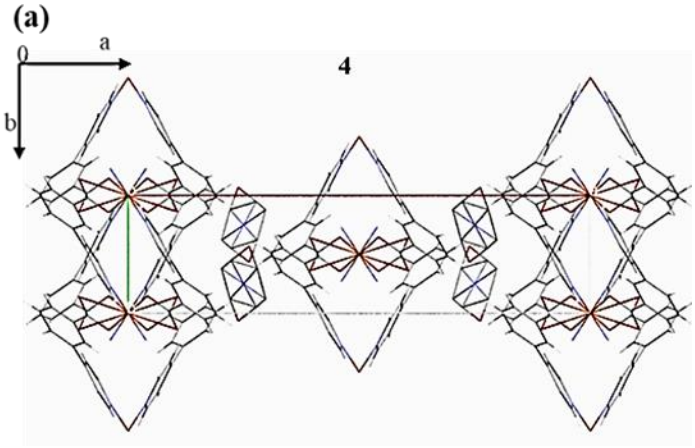

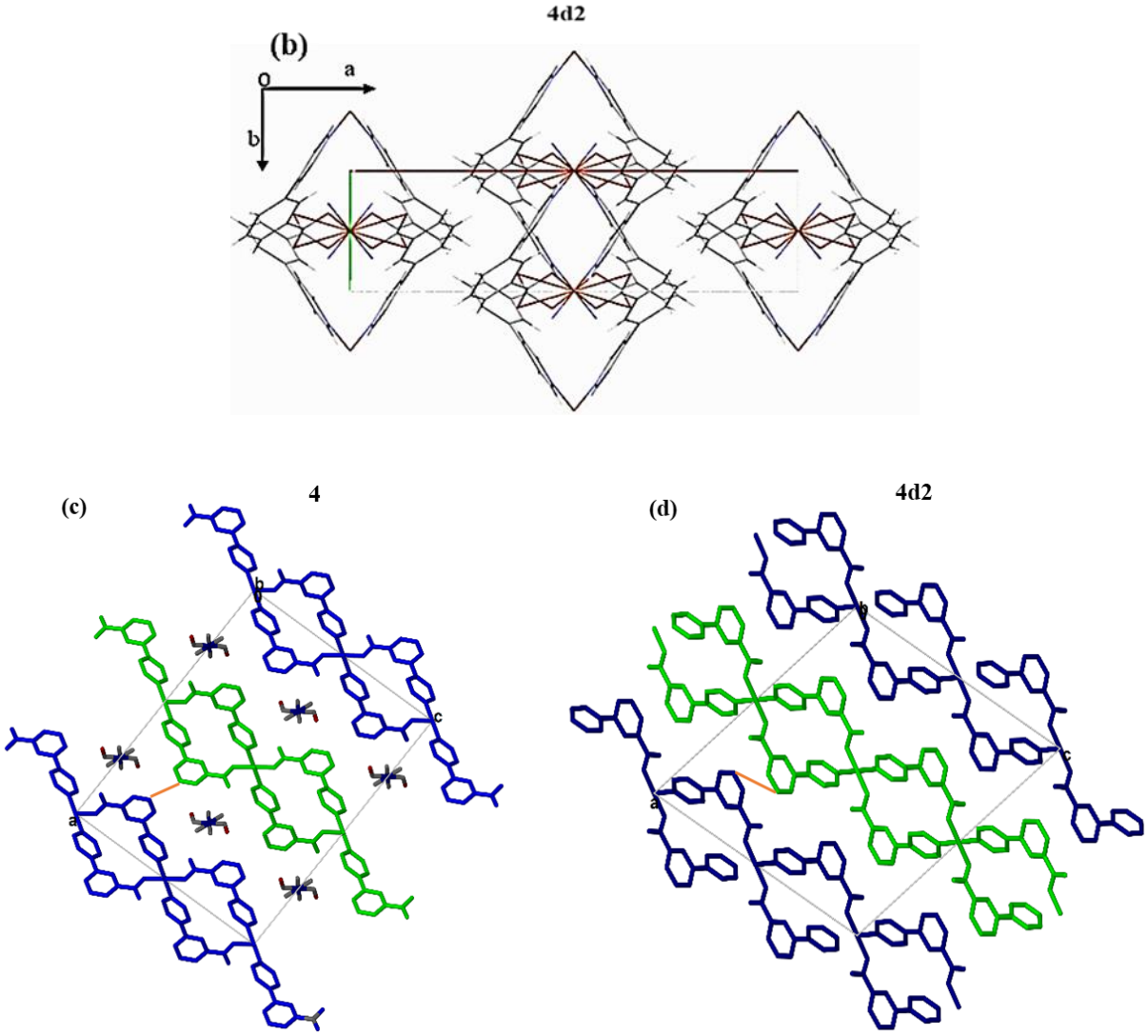

Figure 3.10: *Viewed parallel to c (a) Layers in **4** are far apart, (b) layers in **4d2** are closer to one another and viewed parallel to b (c) Layer in **4**, (d) slided and nested layers in **4d2**.*

Figure 3.11 presents the PXRD patterns of the synthesized **4** and corresponding phases after activation. The experimental PXRD measured for **4** matches the calculated pattern. On the other hand, the activated **4d1** shows a new pattern compared to that of **4**, this more closely resembles the PXRD of QEYYIE. The PXRD of **4d2** is different from those of both **4** and **4d1**. This shows that apart from the removal of DMF, the two activation techniques have different effects on frameworks **4**. The layers move to a different extent and result in the change of structures.

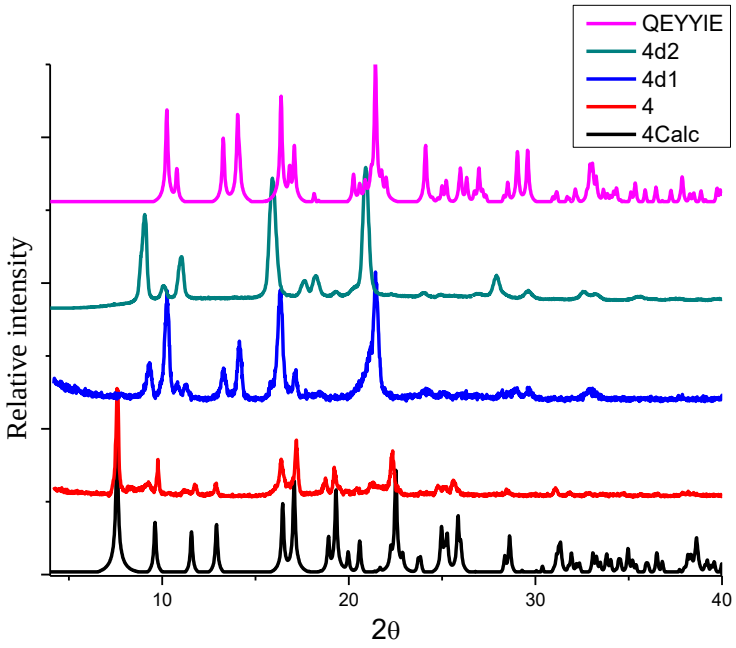

Figure 3.11: *PXRD patterns for **4** and the activated phases.*

Figure 3.12 illustrates the presence of some functional groups in **4** and the activated forms. The bands at 1614 cm^{-1} and 1366 correspond to the asymmetric and symmetric stretching respectively of the carboxylate group. The extent of separation between symmetric and asymmetric carboxylate stretches $\Delta = 245$ cm^{-1} corresponds to the coordination in the monodentate fashion.[2] This confirms the difference in coordination fashion between **4** and QEYYIE as the latter has $\Delta = 132$ cm^{-1} showing bidentate mode of coordination. The absorption of the bands at 1674 cm^{-1} indicated the presence of DMF as illustrated in SCXRD in **4** while the absence of band at 1674 confirms the complete removal of DMF in **4d1** and **4d2**.

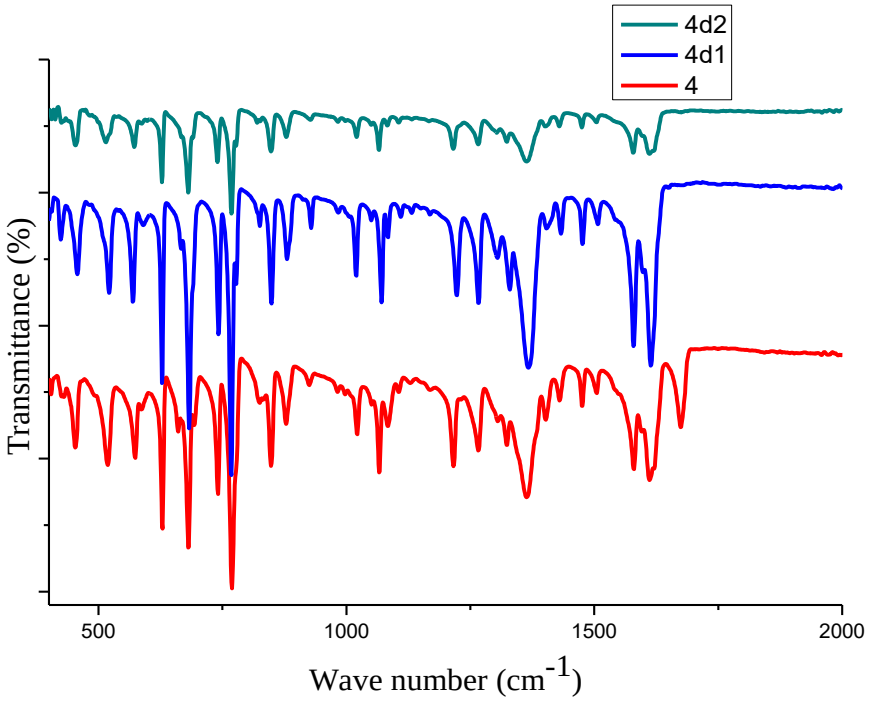

Figure 3.12: *FTIR spectra of* ***4*** *and its two activated forms.*

Figure 3.13 (a) shows the TGA traces of compound **4** with a weight loss of 11.1% at 225 ^{o}C corresponding to the removal of the 0.8 DMF molecule (calculated 13.7%). The removal of the guest solvent was confirmed by the absence of the weight loss of the TGA traces of the activated form (**4d1** and **4d2**). It can be seen that the temperature of the decomposition of **4d1** and **4d2** differs from 27 ^{o}C. This difference can explain the dissimilarities in the activated phases. DSC for **4** in Figure 3.13 (b) shows a narrow endothermic peak at 210 ^{o}C for the removal of DMF. The framework collapsed at 286 ^{o}C.

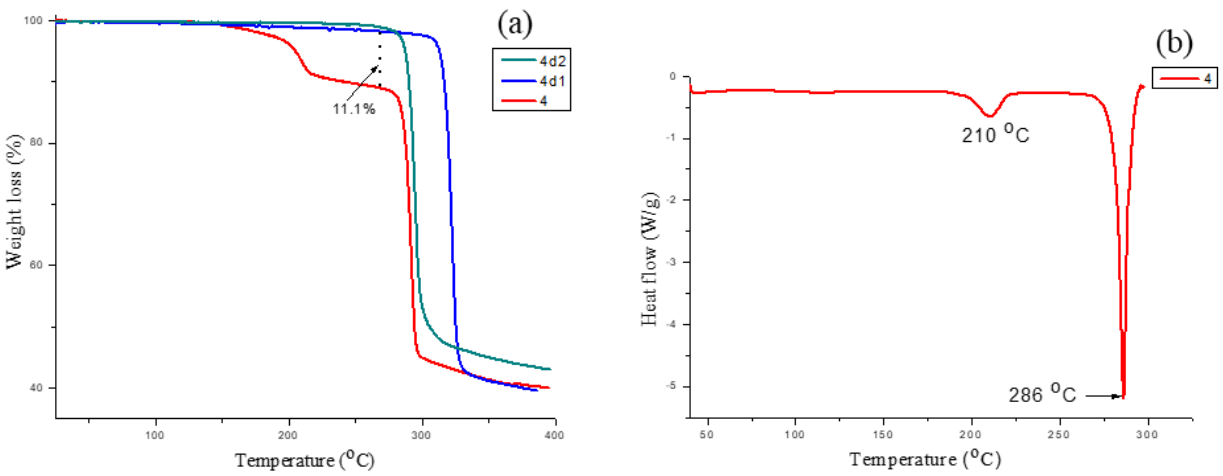

Figure 3.13: *(a) TGA for **4** and its activated forms (**4d1** and **4d2**), (b) DSC curves of **4**.*

3.3.2. Synthesis and Characterization of $\{[Cu(44paba)_2]\cdot 2H_2O\cdot 2DMF]_n$ (5) and $\{[Cu(34paba)_2(H_2O)]_2.[Cu(34paba)]\cdot 2DMF\}_n$ (6)

3.3.2.1. Synthesis

The synthesis using solutions of copper salt and 44paba, or 34paba ligands afforded compound **5** and **6** respectively after some days. Figures 3.14 (a) show the amount of $CuCl_2\cdot H_2O$ metal salt, ligand solvent system used to crystallize **5** and **6** at r.t (Table 3.8). On the other hand, using a different solvent system or higher concentrations resulted in the formation of **5'** rather than **5**. Figure 3.14 (b) shows the corresponding PXRD patterns of **5**, **5'**, and **6**.

Table 3. 8: *Experimental conditions for the synthesis of **5** and **6***

Compound	Metal salt	Ligands	Solvent system (ml)	Conditions
5	$CuCl_2\cdot 2H_2O$ (14 mg, 0.08 mmol)	44pba (24 mg, 0.10 mmol)	H_2O/DMF (2:5)	Room temperature
5'	$CuCl_2\cdot 2H_2O$ (28 mg, 0.16 mmol)	44pba (48 mg, 0.20 mmol)	H_2O/DMF or EtOH/DMF (2:5)	
6	$CuCl_2\cdot 2H_2O$ (14 mg, 0.08 mmol)	34pba (24 mg, 0.1 mmol)	H_2O/DMF (2:5)	

It can be seen that the PXRD patterns in **5** and **5'** do not match. Also, there are major peaks present in **5** but not present in **6** and vice-versa. In this regard, the two structures differ from their respective ligands and possibly the coordination geometry. It was possible to crystallize single crystals for both compound **5** and **6**, however, only a green powder precipitated for compound **5'**. The crystallographic data are presented in Table 3.9.

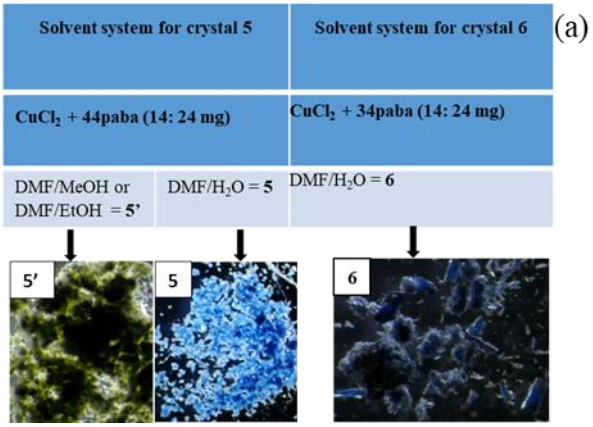

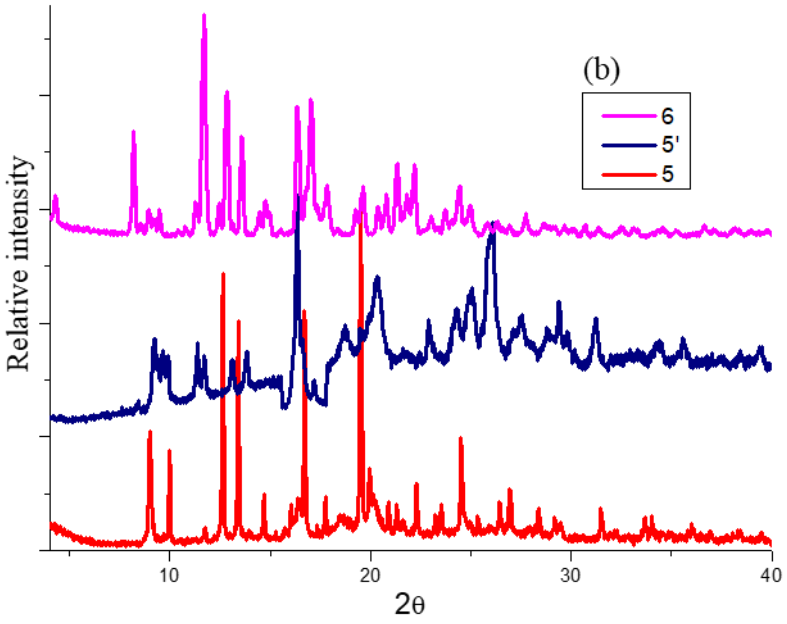

Figure 3.14: *Showing (a) the synthetic condition in* ***5*** *and* ***6****, (b) the corresponding PXRD patterns.*

Table 3.9: *Crystal data for compound **5** and **6**.*

Compound	**5**	**6**
Formula	$C_{16}H_{20}N_3O_4Cu_{0.5}$	$C_{71}H_{73}Cu_{2.50}N_{12}O_{14}$
Mass (g.mol^{-1})	350.13	1477.26
Crystal size (mm^3)	0.130 x 0.170 x 0.200	0.040 x 0.040 x 0.300
Crystal system	Monoclinic	Triclinic
Space group	$P2_1/n$	P-1
a (Å)	7.9667(8)	10.3559 (4)
b (Å)	11.9365(11)	16.5278(8)
c (Å)	17.9077(17)	21.9540(10)
β (°)	96.678(2)	78.4900(10)
V (Å^3)	1691.37(0)	3380.9(4)
T (K)	293(2)	293(2)
Z	4	2
D_c (g·cm^{-3})	1.373	1.451
μ(Mo−Kα) (mm^{-1})	0.703	0.858
F(000)	734	1535
Range scanned, θ (°)	2.055-28.406	2.182-28.301
No. reflections collected	27672	100761
No. unique reflection	4236	16767
No. reflections with I ≥ 2σ(I)	3241	14524
Parameters/restraints	294/0	957/0
Goodness of fit, S	1.034	1.082
Final R indices (I ≥ 2σ(I))	R1 = 0.0381 wR2 = 0.0865	R1 = 0.0521 wR2 = 0.1122
Final R indices (all data)	R1 = 0.0558 wR2 = 0.0953	R1 = 0.0620 wR2 = 0.1170
Min, max e$^-$ density (e Å^{-3})	0.351, -0.430	3.229, -1.608

3.3.2.2. Structure characterization

Compound **5** in Figure 3.15a displays the coordination of Cu^{2+} by 44paba in a 4-coordinate square-planar fashion. Two 44paba linkers are coordinated to the Cu^{2+} centre through two monodentate carboxylates and two nitrogen atoms from pyridyl rings. The bond lengths, Cu–O and Cu–N, were measured as 1.9768(13) Å and 2.0100(16) Å respectively. These values are within the range of the

published bond lengths. The system crystallizes in monoclinic system in the $P2_1/n$ space group. One H_2O and one DMF guest molecules are present in the asymmetric unit. Figure 3.15b shows that the frameworks form 1D chains where two 44paba linkers bridge adjacent Cu^{2+} ions. A view of the packing along [100] shows that these chains form 2D layers via hydrogen bonding between the unbonded carboxylate oxygen of one chain and the amino hydrogen from the next chain and vice-versa. The same carboxylate oxygen forms a hydrogen bond with H_2O and the latter is also hydrogen bonded to the guest DMF. The distance measured between H_2O and Cu^{2+} is 2.532 Å. The view along [010], (Figure 3.15c) shows the separated layers (highlighted in green) hosting H_2O and DMF guest molecules between them. Note that the two guest molecules do not interconnect the layers via hydrogen bonding.

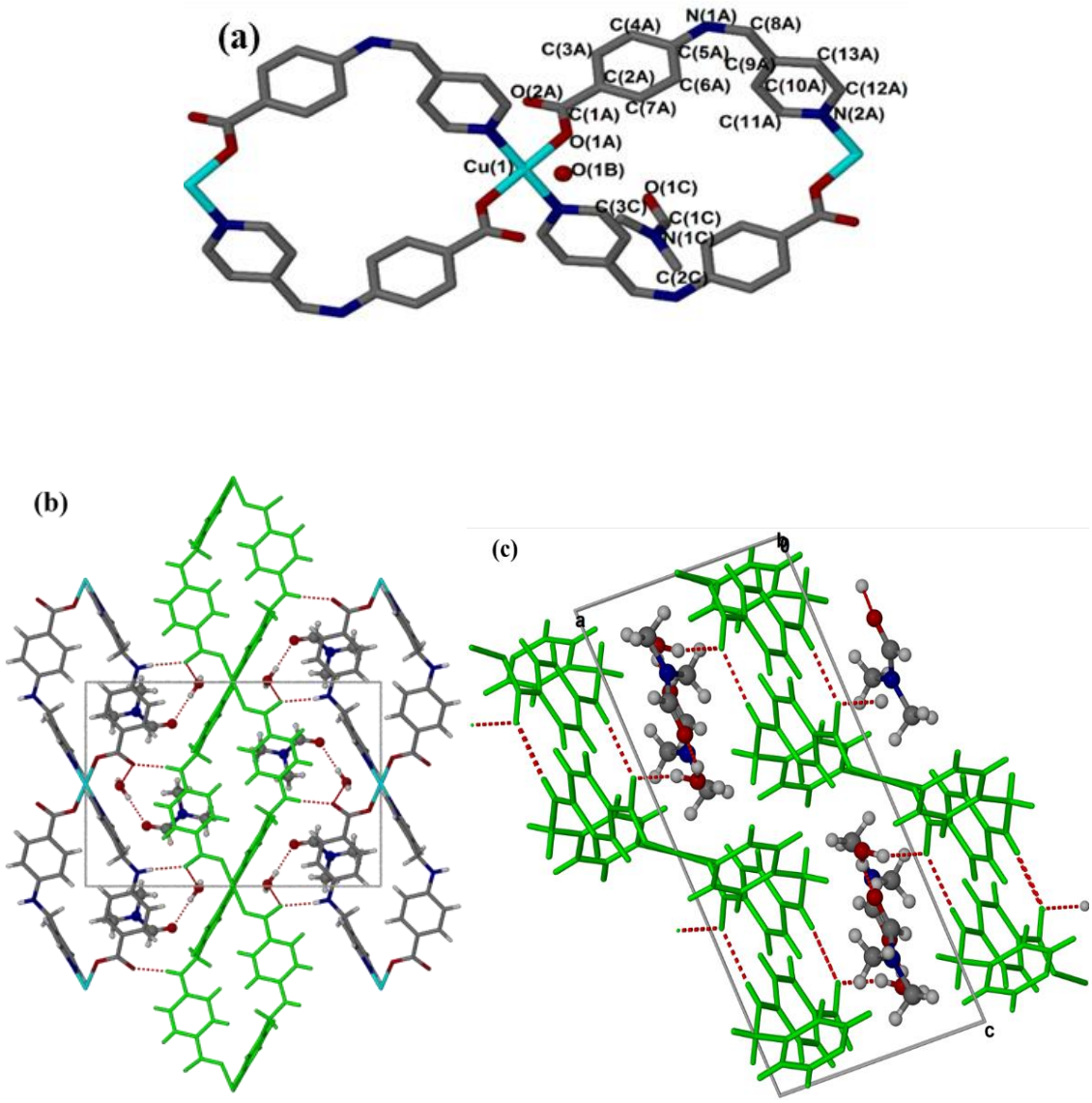

Figure 3.15: *(a) coordination environmental of copper in* ***5****, (b) hydrogen bond and layers in* ***5*** *(c), location of guest molecules between layers in* ***5****.*

Compound **6,** shown in Figure 3.16a crystallizes in the triclinic *P*-1 space group. The asymmetric unit contains three Cu^{2+} centres, featuring two different coordination geometries. Two Cu^{2+} ions have identical coordination, forming 1D chains in which the Cu^{2+} ion is coordinated in a monodentate fashion to two carboxylate groups, and two pyridyl nitrogens. Even though the second $Cu(2)^{2+}$ coordination does not show any difference from the first one $Cu(1)^{2+}$, they both

are included in the asymmetric unit. In addition, H_2O also coordinates the two metal centres to exhibit a square pyramidal coordination geometry in each Cu^{2+} centre. The third unique $Cu(3)^{2+}$ ion is only coordinated by one carboxylate in the asymmetric unit. It is coordinated by four 34paba as is in the first two. However, it does not have a coordinated H_2O and thus has a square planar coordination.

The bond lengths around the a metal centres such as Cu(1)–O(paba): 1.9458(17) Å, Cu(1)–N(paba): 2.023(2) Å, and Cu(1)–O(H_2O): 2.328(2) Å, Cu(2)–O(paba): 1.9677(19) Å, Cu(2)–N(paba): 2.005(2) Å, and Cu(2)–O(H_2O): 2.379(2) Å, Cu(3)–O(paba): 1.9901(17) Å, and Cu(3)–N(paba): 2.020(2) Å fall in the expected ranges. Two DMF guest molecules were each located along a direction close to H_2O molecule in the asymmetric unit. This allowed hydrogen bonding between the coordinated H_2O and DMF (Figure 3.16b). In addition, there is an intra-hydrogen bond between each coordinated H_2O and uncoordinated carboxylate oxygen atom in the same Cu^{2+} centre. The uncoordinated carboxylate oxygen atom of the $Cu(3)^{2+}$ chain shows hydrogen bonding with the amino group from $Cu(2)^{2+}$ chain, while, the chain formed by $Cu(1)^{2+}$ stands alone. Figure 3.16c displays the structure viewed along *a* where the layers of $Cu(1)^{2+}$ centres reside in between the two layers of $Cu(2)^{2+}$ and $Cu(3)^{2+}$ centres. The same view direction shows that $Cu(1)^{2+}$ chains interact through hydrogen bonding between their uncoordinated oxygen atoms and amino groups.

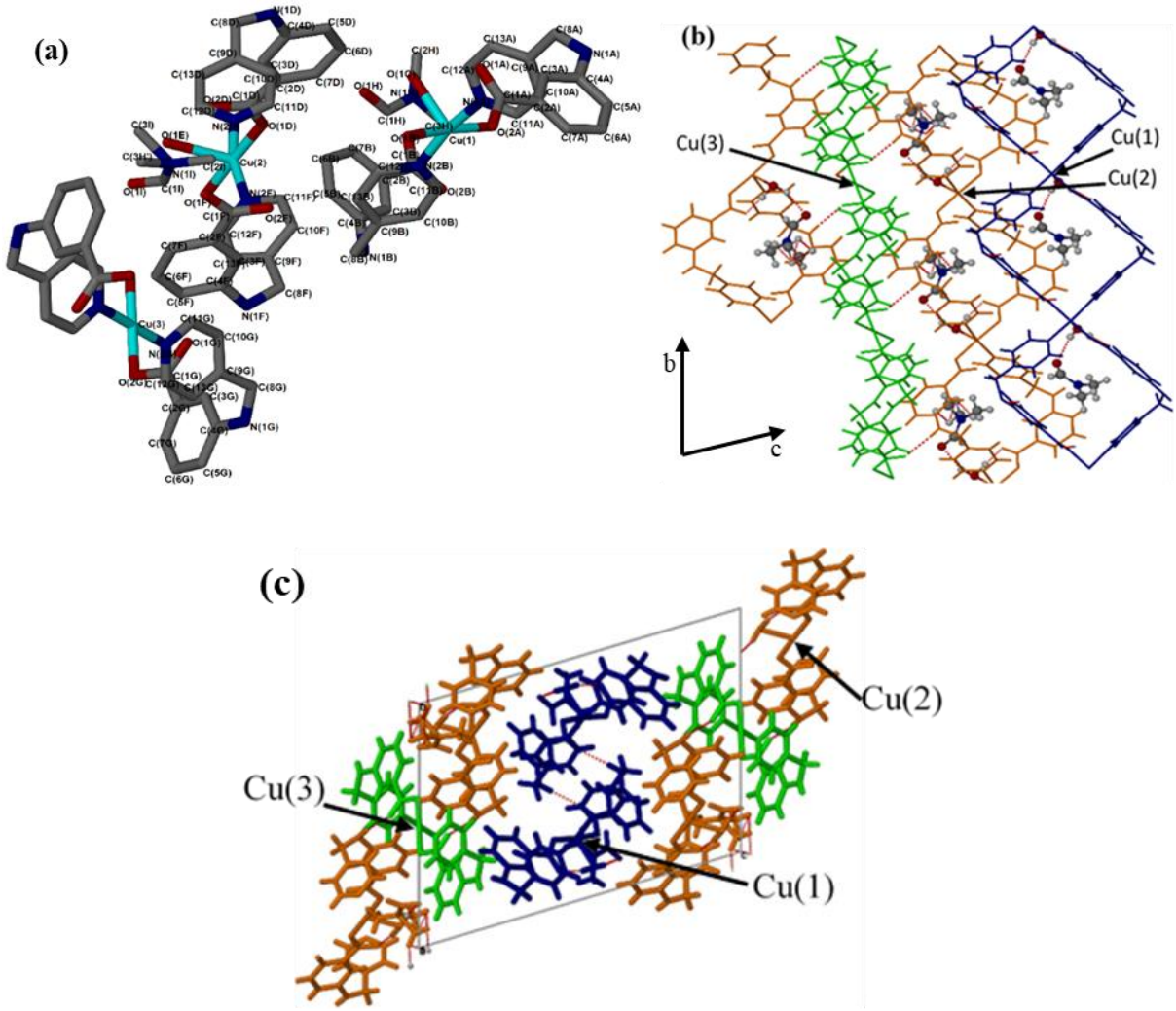

Figure 3.16: *(a) Coordination environment in **6**, (b) hydrogen bonding interactions between the chains containing* $Cu(2)^{2+}$ *and* $Cu(3)^{2+}$ *(c) packing of **6** showing layers formed by the three independent copper ions.*

The bond length between two elements in the synthesized compounds should be in acceptable and known range in coordination chemistry. Figure 3.17 corresponds to a histogram that shows the possible bond lengths of Cu–O that are possible in Cu bonded to 2N and 3O atoms. Many Cu–O coordination compounds have bonds length in the range of 1.850 - 2.050 Å. There are also some Cu–O coordination compounds in the range between 2.050 and 2.550 Å. Therefore, it could be reasonable to attribute the coordination of H_2O to Cu with a bond length of 2.379 Å in **6**. On the

other hand, the coordination of H_2O to Cu^{2+} in **5** where the contact distance is 2.532 Å seems less probable.

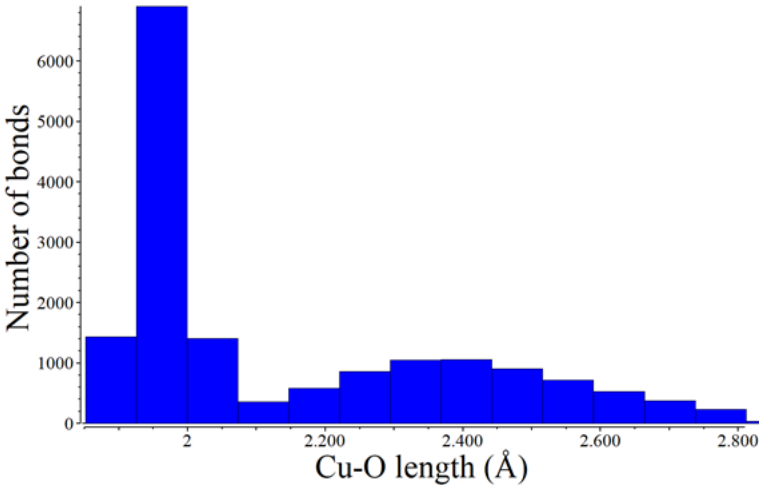

Figure 3.17: *Bond length in Cu-O coordination.*

3.3.2.3. Comparison of coordination in 5, 6, and structures of similar ligands

The length of the 44paba ligand in **5** is longer than that of 34paba ligand in **6** due to the position of the methylaminopyridinyl group relative to the benzoate ring. The distance between two bridged Cu^{2+} centres in **5** and **6** are 11.933 and 10.536 Å respectively. Hence, the charge-donating ability (polarity) of the 44paba ligand in **5** might be stronger to favour square planar coordination while 34paba in **6** maybe weaker to favour a square pyramidal coordination.[12]

The structures with ligands similar to those in **5** and **6** were extracted from CSD for comparison. The ligands in HEJCIL,[13] WOJZOK,[14] UVARUF,[15] UVAROZ,[15] and AMUXAI[16] contain a vinyl group rather than the methylamino present in 44paba and 34paba. 4-(2-(pyridin-4-yl)vinyl)benzoic acid ligand was used to coordinated Cu^{2+} in HEJCIL. The compound crystallizes in tetragonal crystal system space group $I4_1/a$. When the reaction temperature is reduced, a new structure of HEJCIL01 crystallizes in monoclinic crystal system with a *Cc* space group. The same ligand in

HEJCIL was used to coordinate Zn^{2+} in WOJZOK. This framework is constructed by dinuclear Zn^{2+} centres that crystallizes in chiral space group *C*2. The same ligand was used in isomorphous structures, UVARUF and UVAROZ coordinate to Zn^{2+} and crystallize in monoclinic space group *Cc*. AMUXAI is characterized by the coordination of Cu^{2+} by (E)-4-(2-(pyridin-4-yl)vinyl)benzoic acid ligand. However, the same metal centre is coordinated by pyridine-2,3,5,6-tetracarboxylic acid and H_2O ligand to crystallize in triclinic *P*$\bar{1}$ space group. In this regard, the crystal systems of these structures are not the same. The reaction conditions have influenced the diversity of the crystallization.

The structures of **5** (red) and **6** (green) were overlaid for comparison in Figure 3.17 (a). The right hand side shows the conformation of benzoate ring of 34paba relative to 44paba. The selected torsion angle O1-C1-C2-C7 in **6**, 173^o shows a noticeable difference from 165^o of **5**. In addition, the benzoate ring in 34paba is twisted away from the horizontal plane in 44paba. Other structures were overlaid against **5** or **6** (Figure 3.18b and c) for further comparison. The angles around the metal centre in Figure 3.18a marked in blue were recorded. Table 3.10 shows that the angle in HEJCIL is similar to that in **5** and **6**, while the angles in other structures vary. The observed conformation in the ligands in the asymmetric unit is facilitated by the single bonds between pyridyl and benzoate rings. The variation of conformation and building unit in these compounds could be influenced by a metal centre, ligands, solvent used, and temperature used in synthesis.[13,17,18]

Table 3.10: *Bond lengths in N-M-O or O-M-O and the resulting angle.*

Compounds	M−O (Å)	M−N or M−O (Å)	Considered angle	Angle (o)
5	1.9768	2.010	O-Cu-O	180
6	1.9458	2.023	O-Cu-O	180
HEJCIL	1.9522	2.020	O-Cu-O	180
WOJZOK	2.09	2.09	O-Zn-O	97.7 and 104
UVARUF	1.959	2.24	O-Zn-O	91.8 and 105
UVAROZ	1.970	2.11	N-Zn-O	99.8
AMUXAI	2.04	1.98	N-Cu-O	161

- ***(a) overlay of 5 (in red) and 6 structures in (green)***

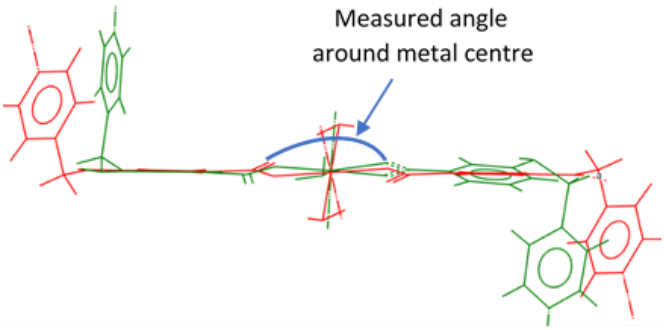

- ***(b) Overlay of structures in 5***

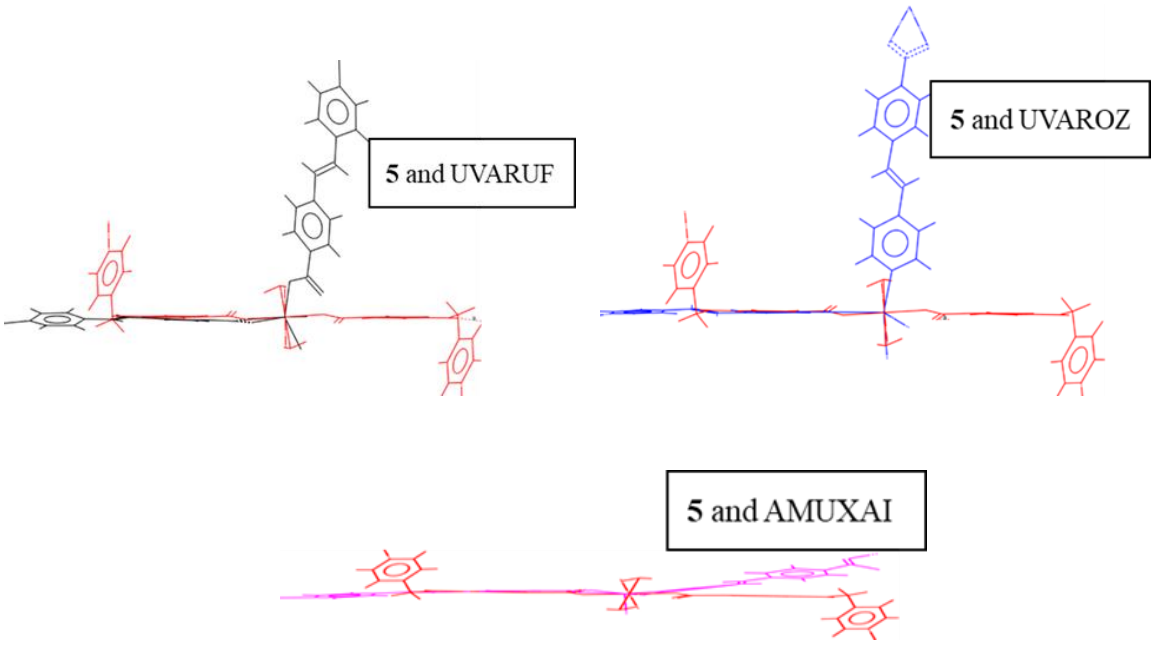

- ***(c) Overlay of structures in 6***

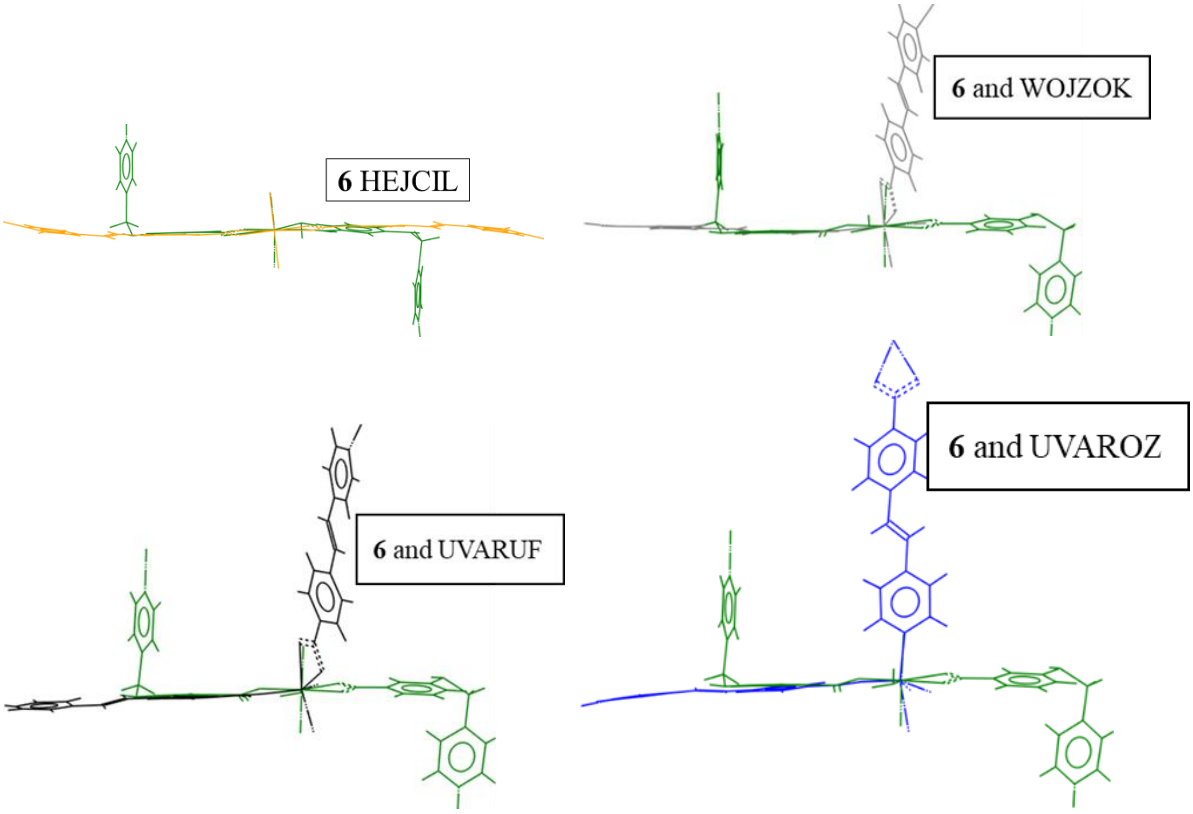

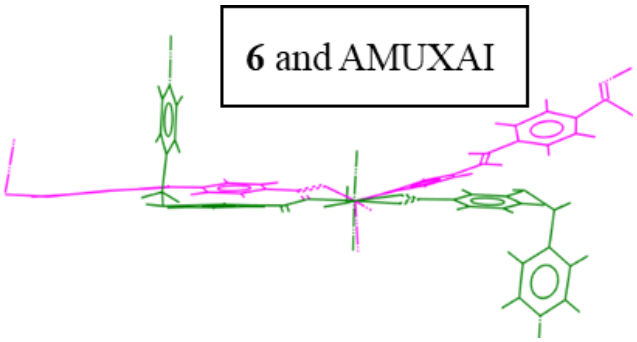

Figure 3.18: *Overlay of structures with* ***5*** *(red) and* ***6*** *(green).*

3.3.2.4. Activation and characterization

Figure 3.19(a) presents the PXRD patterns of **5** matching with its corresponding calculated patterns. The compound was activated by removing guest molecules on heating at 60 ^{o}C for two hours under vacuum and formed new phase **5d**. The synthesized **5** is highly unstable as once left in a new solvent or out of its mother solvent, it loses its guest molecules to form the activated form **5d** even at r.t. Single crystal suitable for X-ray diffraction could not be obtained from the activated forms. **5d** is characterized by the absence and shift of some peaks compared to the original compounds. The phase change is attributed to the loss of H_2O and DMF guest molecules. In addition, it could be the result of the collapse of the framework due to the breaking of hydrogen bondings after the activation. Therefore, guest molecules and hydrogen bonding play a role in maintaining this structure.

Figure 3.19(b) presents the PXRD pattern of **6** which matches its corresponding calculated pattern. The compounds were activated on heating at 165 ^{o}C under vacuum and the change to a new phase **6d** suggest the removal of guest molecules. This is also characterized by the disappearance, the shift, and appearance of new peaks. Unlike **5**, there was not a phase change of **6** at r.t. It can be

noted the PXRD patterns in **5d** and **6d** are close. It is possible that after the removal of both guest molecules the resulting coordination of the frameworks (**5d** and **6d**) become similar.

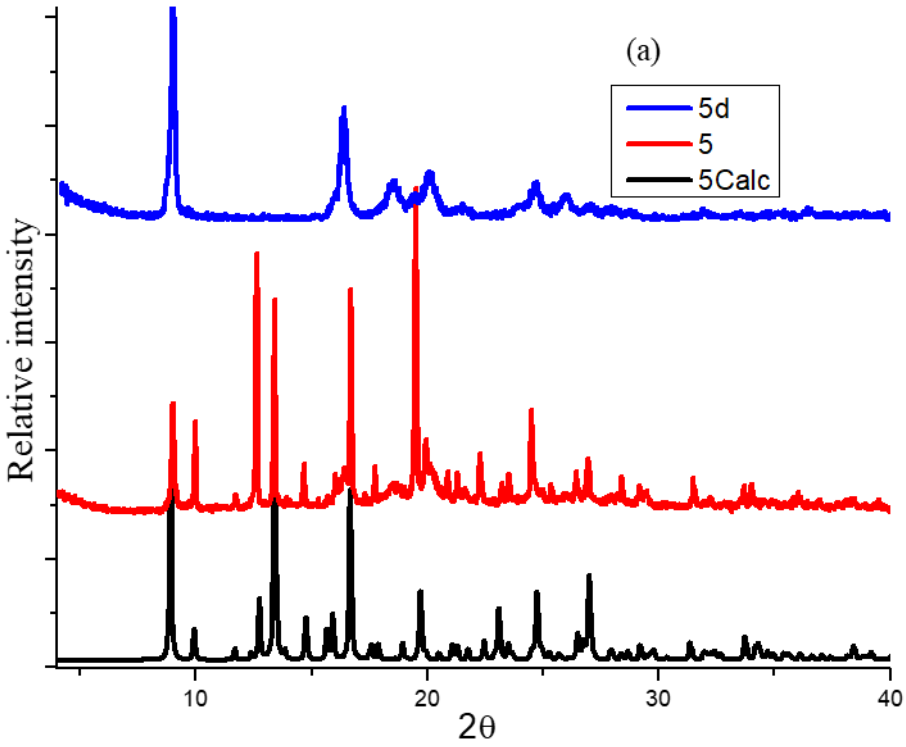

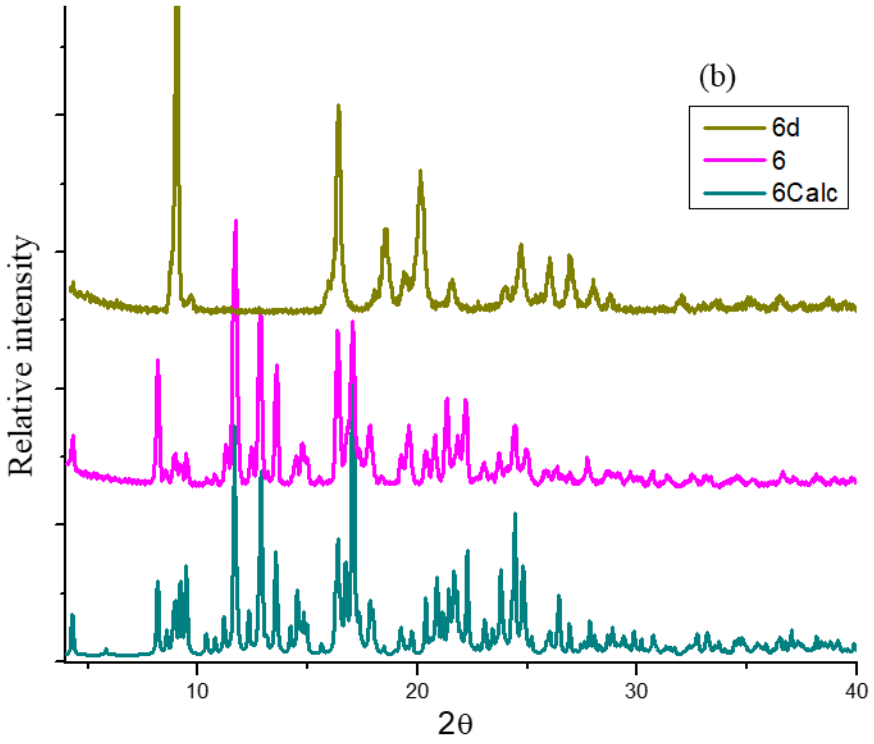

Figure 3.19: *PXRD patterns for **5** (a) and **6** (b) and related phases.*

FTIR spectra in Figure 3.20 shows the stretching band at 3295 cm^{-1} which indicates the presence of N-H bond of the amino group in the framework. The presence of guest molecules in **5** as well as in **6** were also confirmed by FTIR bands at 3446 and 1671 cm^{-1} of H_2O and DMF respectively. The extent of the difference between asymmetric and symmetric stretch Δ = 240 cm^{-1} is an indicator of monodentate coordination of the carboxylate in **5** and **6**. The absence of these bands in the activated form of **5d** confirms the removal of DMF and water guest molecules.

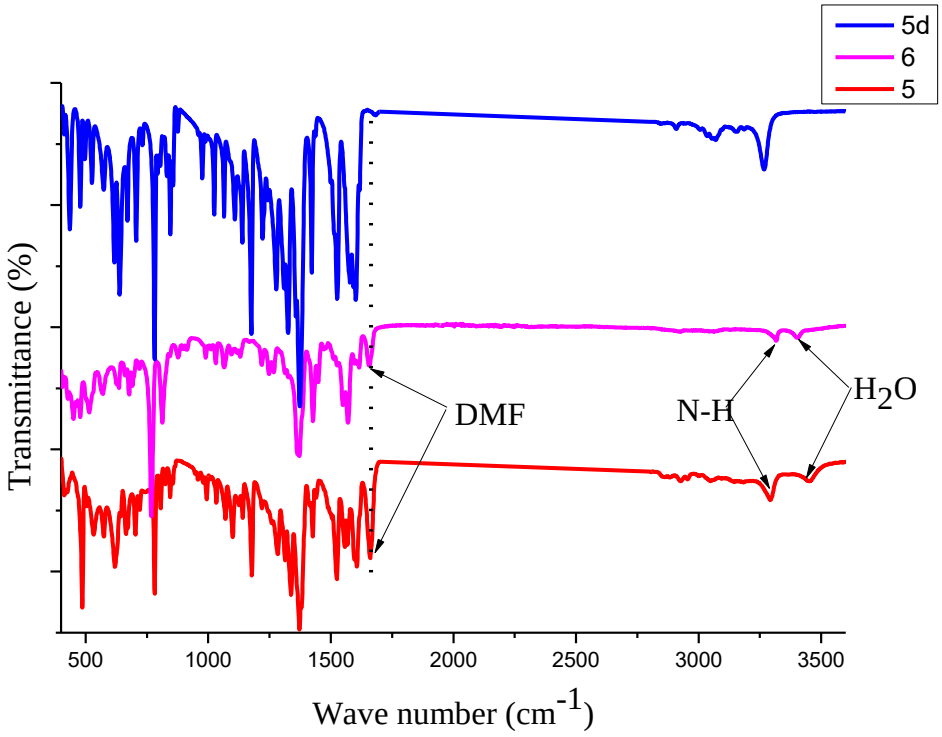

Figure 3.20: *FTIR showing functional groups in **5**, **5d**, and **6**.*

TGA and DSC analysis in Figure 3.21 shows the corresponding weight loss and thermal behaviour in **5** and **6**. Compound **5** showed 23.9% weight loss between 45 and 84 ^{o}C while the calculated total weight loss for both guest molecules corresponds to 25.9%. Therefore, there was overlap in the removal of both H_2O and DMF molecules. DSC analysis confirmed the presence of two endothermic peaks for H_2O and DMF at 92 ^{o}C and 110 ^{o}C respectively. At 230, ^{o}C **5** shows an endothermic peak which could be a structural rearrangement before the decomposition. TGA trace for **6** shows two steps for desorption. The temperature ranges between 75-162 ^{o}C corresponds to 3% (calc: 2.4%) weight loss and between 162-179 ^{o}C corresponds to 8% (calc: 9.9%) weight loss. The first desorption could be attributed to the removal of two coordinated H_2O molecules while the second could be attributed to two DMF molecules. This was further characterized by DSC (b) with a weak endothermic peak between 65 ^{o}C and 120 ^{o}C and a strong endothermic peak at 168 ^{o}C.

The removal of these guest solvents was confirmed by the absence of the weight loss TGA traces of these activated forms (**5d** and **6d**). All these phases collapsed around 250 °C.

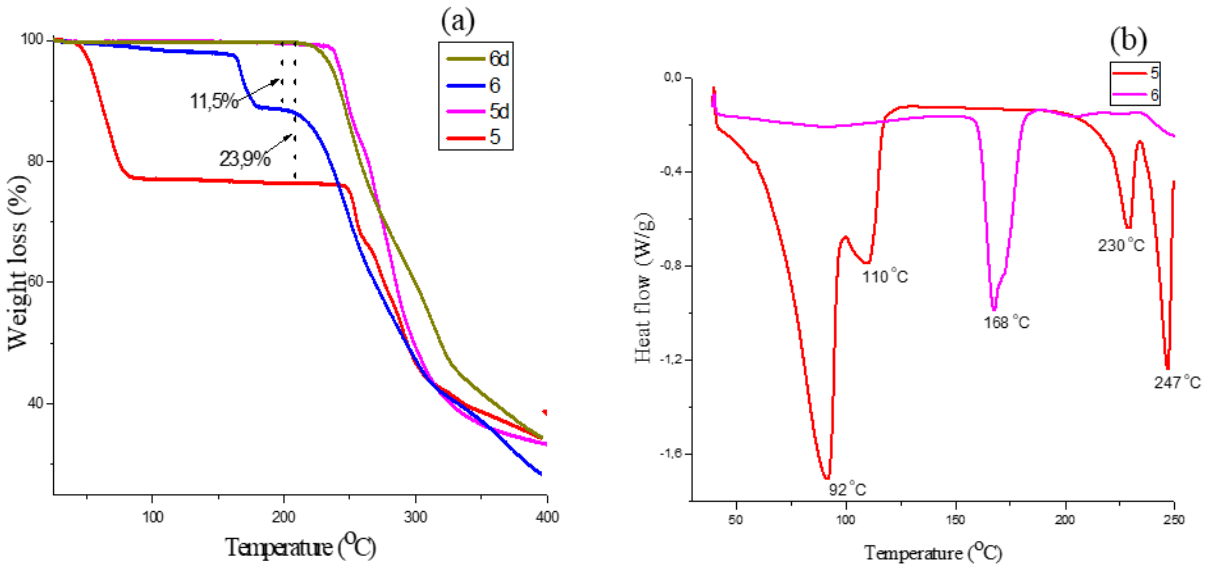

Figure 3.21: *(a) Weight loss in **5** and **6**, (b) DSC curves of corresponding **5** and **6** compounds.*

3.3.3. Synthesis and Characterization of $\{[CuCl_2(34pba)_2]\cdot solvent\}_n$ (7)

Compound **7** was synthesized in similar conditions to **4** except that more volume of HCl (0.05 ml compared to $1.5x10^{-1}$ ml in **4**) was used in the solvent mixture. **7** crystallizes in trigonal system *P*-31*c* space group (Table 3.11). The Cu^{2+} centre is coordinated to two carboxylate oxygens and two pyridyl nitrogens as well as a chloride ion, making it square pyramidal. A further chloride ion (required for charge balance) is located on a 3-fold rotoinversion rotation axis at (1/3, 2/3, 1/4). The bond lengths Cu–O and Cu–N are 2.0405(19) and 2.004(2) Å respectively. The bond length Cu–Cl 2.573(2) is a bit longer but still in the range of similar published values. Figure 3.22a displays the coordination environment of Cu^{2+} in the framework. This generates a 3D MOF containing a large void which is occupied by disordered solvent. The channels run in all directions to form a

3D structure (Figure 3.22b). The structure was refined using the SQUEEZE routine in PLATON,[19] and refined to an R1 value of 0.0468 (0.1058 before SQUEEZE). The squeezed void volume was 5102 A^3, equivalent to 46.9% of the unit cell. Unfortunately, we could not get enough material for further characterization. Thus, we were not able to estimate the solvent content, so we opted to the SQUEEZE routine in this case.

Table 3.11**: Crystallographic data for compound **7

Compound	**7**
Formula	$C_{24}H_{16}N_2O_4CuCl_2$
Mass (g.mol^{-1})	530.85
Crystal size (mm^3)	0.200 x 0.280 x 0.300
Crystal system	Monoclinic
Space group	*P*-31*c*
a (Å)	17.7559(10)
b (Å)	17.7559(10)
c (Å)	18.689(2)
β (°)	120
V (Å^3)	5102.8(8)
T (K)	293(2)
Z	6
D_c (g·cm^{-3})	1.036
μ(Mo−Kα) (mm^{-1})	0.822
F(000)	1614
Range scanned, θ (°)	1.715-26.367
No. reflections collected	28910
No. unique reflection	3495
No. reflections with I ≥ 2σ(I)	2500
Parameters/restraints	148/0
Goodness of fit, S	1.070
Final R indices (I ≥ 2σ(I))	R1 = 0.0468 wR2 = 0.1295
Final R indices (all data)	R1 = 0.0726 wR2 = 0.1418
Min, max e$^-$ density (e Å^{-3})	0.351, -0.430

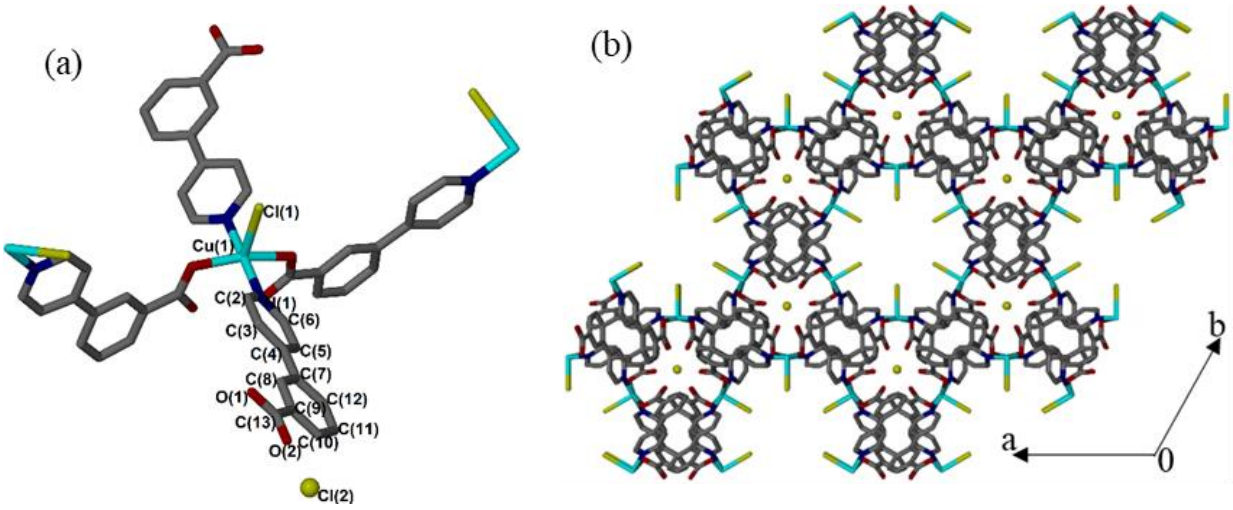

Figure 3.22: *Coordination environment of Cu^{2+} (a) and packing (b) showing the location of chloride in the smaller channel and the remaining larger solvent-filled in **7**.*

3.4. SUMMARY

Mixed ligands were used in solvothermal synthesis of isostructural {[Co(34pba)(44pba)]·DMF}n (**1**) and {[Zn(34pba)(44pba)]·DMF}n (**3**) compounds from cobalt(II) and zinc(II) metal centres respectively. Using an acetonitrile/water instead of a DMF/ethanol solvent system led to a framework isomorphous to **1**, {[Co(34pba)(44pba)]·(C_3H_6O)}n (**2**). The acetonitrile had undergone hydrolysis and ketonization to produce the guest acetone (C_3H_6O) in **2**. Comparing the unit cell of **1** and **2** shows that there is expansion and contraction due to the solvent stimulus during the reaction. Single crystal characterization showed that the compounds are 3D structures with a double-walled network of **bcu** topology. The activation of these frameworks at high temperature under vacuum showed stable and retained structures, **1d**, **2d**, and **3d**. They contain 1D channels which can be investigated for their sorption properties. This is described in Chapter 4.

A single ligand, 34pba was used to coordinate Cu^{2+} centre in a square planar fashion to form compound **4** where its extension results in a 2D structure. This framework transforms into new phases once activated by heating under vacuum (**4d1**) or soaking into methanol (**4d2**). The two activated forms are different. The single crystal structure analyzes of **4d2** and **4** indicate that the activation causes contraction of layers at different extent. This allows us to conclude that structures **4**, **4d1**, and **4d2** differ in the spacing of their respective layers. On the other hand, the PXRD patterns of **4d1** are similar to those of the reported structure, QIYYIE. In this case, the layers in both structures are similar but the latter forms a 3D structure via hydrogen bonding. Structure **4** was also compared to other compounds with similar ligand including QIYYIE. The ligands in these structures show conformations which differ because of stimuli such as solvent, temperature, and the dentition of the ligand bind to the metal centre. On the other hand, little change in the experimental conditions of **4** led to the crystallization of compound **7**. The Cu^{2+} centre is coordinated by 34pba and chloride ion favoring a 3D structure. This means that the coordinated 34pba ligands in **7** are oriented differently from **4** to accommodate a large void volume.

The linkers 44paba and 34paba are similar to 44pba and 34pba but have a methylamine linker between the pyridyl and benzoic acid rings. These functionalized linkers were combined with Cu^{2+} salts to form 1D structural chains in **5** and **6** respectively. However, hydrogen bonds serve as bridges between the chains to form layers. PXRD patterns show that their activated forms resulted in a new **5d** and **6d** phases. These collapsed on the removal of guest molecules due to the breaking of the hydrogen bonds.

The activated compounds **4d**, **5d**, and **6d** are not porous and do not adsorb new guest molecules. We have not yet managed to synthesize MOFs from mixed 34paba and 44paba linkers. Even though long linkers can be used to increase the size and allow the functionalization of pores or

channels in the stable framework,[11] the ligands such as 44paba and 34paba used in this work did not follow the same pattern. Thus, the structure of the ligand may play an important role to form a stable framework. However, different approaches of the synthesis of metal-organic frameworks using 34paba and 44paba are ongoing.

3.5. REFERENCES

1. Dzesse T, C. N., Nfor, E. N. & Bourne, S. A. Vapor Sorption and Solvatochromism in a Metal-Organic Framework of an Asymmetric Pyridylcarboxylate. *Cryst. Growth Des.* **18**, 416–423 (2018).

2. Mehlana, G., Bourne, S. A., Ramon, G. & Öhrström, L. Concomitant metal organic frameworks of cobalt(II) and 3-(4-pyridyl) benzoate: Optimized synthetic conditions of solvatochromic and thermochromic systems. *Cryst. Growth Des.* **13**, 633–644 (2013).

3. Wang, Z., Richter, S.M., Rozema, M.J., Schellinger, A., Smith, K., Napolitano, J.G. Potential Safety Hazards Associated with Using Acetonitrile and a Strong Aqueous Base. *Org. Process Res. Dev.* **21**, 1501–1508 (2017).

4. Bennett, J. A., Parlett, C.M.A., Isaacs, M.A., Durndell, L.J., Olivi, L., Lee, A.F., Wilson, K. Acetic Acid Ketonization over Fe3O4/SiO2 for Pyrolysis Bio-Oil Upgrading. *ChemCatChem* **9**, 1648–1654 (2017).

5. Tang, L., Fu, F., Gao, L., Wei, Q., Zhang, Z., Liu, Q. Synthesis , Crystal Structure , and Magnetic Properties of a New 2D Twofold Interpenetrated Coordination Polymer [Cu(3,4-pybz)2]n. *Anorg. Allg. Chem* **639**, 918–921 (2013).

6. C. R. Groom., I. J Bruno., M. P. L. and S. C. W. The Cambridge Structural Database. *Acta Cryst* 171–179 (2016).

7. Wu, X., Zhang, W., Zhang, X., Ding, N. & Hor, T. S. A. Pyrididine-carboxylate ligands as double-bridge spacers in CuI metallacycles. *Eur. J. Inorg. Chem.* **2015**, 876–881 (2015).

8. Guo, F. A new 4-connected Co(II) coordination framework with an uncommon two-fold interpenetrating net: Synthesis, structure and luminescence property. *J. Inorg. Organomet. Polym. Mater.* **19**, 406–409 (2009).

9. Zhou, H., Zhang, J. & Chen, X. Controlling Thermal Expansion Behaviors of Fence-Like Metal-Organic Frameworks by Varying / Mixing Metal Ions. *Front. Chem.* **6**, 1–7 (2018).

10. Wang, H. R. & Li, G. T. Tetraaquabis-[3-(pyridin-4-yl)benzoato-κN]cobalt(II). *Acta Crystallogr. Sect. E* **67**, 1–6 (2011).

11. Ndamyabera, C. A., Zacharias, S. C., Oliver, C. L. & Bourne, S. A. Solvatochromism and Selective Sorption of Volatile Organic Solvents in Pyridylbenzoate Metal-Organic Frameworks. *Chemistry (Easton).* **1**, 111–125 (2019).

12. Dudev, M., Wang, J., Dudev, T. & Lim, C. Factors governing the metal coordination number in metal complexes from cambridge structural database analyses. *J. Phys. Chem. B* **110**, 1889–1895 (2006).

13. Xiong, G., Wang, Y., Zhao, B., You, L., Ren, B., He, Y., Wang, S., Sun, Y. Temperature-tuned topologies and interpenetrations of two 3D porous copper(II)-organic frameworks and gas adsorption behaviors. *Inorganica Chim. Acta* **471**, 180–185 (2018).

14. Xiong, R. G., Zuo, J. L., You, X. Z., Abrahams, B. F., Bai, Z. P., Che, C. M., Fun, H. K. Opto-electronic multifunctional chiral diamondoid-network coordination polymer: Bis{4-[2-(4-yridyl)ethenyl]benzoato}zinc with high thermal stability. *Chem. Commun.* 2061–2062 (2000).

15. Sharma, M. K., Lama, P. & Bharadwaj, P. K. Reversible single-crystal to single-crystal exchange of guests in a seven-fold interpenetrated diamondoid coordination polymer. *Cryst. Growth Des.* **11**, 1411–1416 (2011).

16. Shi, L. X. & Wu, C. De. A nanoporous metal-organic framework with accessible Cu2+ sites for the catalytic Henry reaction. *Chem. Commun.* **47**, 2928–2930 (2011).

17. Mehlana, G., Ramon, G. & Bourne, S. A. Methanol mediated crystal transformations in a solvatochromic metal organic framework constructed from Co(ii) and 4-(4-pyridyl) benzoate. *CrystEngComm* **15**, 9521–

9529 (2013).

18. Mehlana, G., Bourne, S. A. & Ramon, G. The role of C–H···π interactions in modulating the breathing amplitude of a 2D square lattice net: alcohol sorption studies. *CrystEngComm* **16**, 8160 (2014).

19. Spek, A. L. PLATON SQUEEZE: a tool for the calculation of the disordered solvent contribution to the calculated structure factors. *Acta Cryst.* **C71**, 9–18 (2015).

CHAPTER 4. SORPTION OF VOLATILE ORGANIC COMPOUNDS, CARBON DIOXIDE, AND HYDROGEN

4.1. INTRODUCTION

This chapter reports the sorption behaviour of two activated MOFs, **1d** and **3d** with respect to several volatile organic compounds (VOCs) and gases. It presents the adsorption capacity of the MOFs for several gases, dried halogenated solvents, volatile amines, and iodine. Selective sorption experiments were used to elucidate the factors that govern the selectivity seen in the two activated MOFs. Some sorption processes performed here were characterized by the visible colour changes or solvatochromism. Kinetic activation energies associated with the removal some guest molecules were also determined. MOFs **4**, **5**, and **6** collapsed after activation and formed new phases that we were not able to characterize. Thus, no sorption testing was carried out on these.

4.2. SORPTION OF VOCs BY ACTIVATED MOFS 1d AND 3d

To test the potential of these MOFs to serve as sorbents for pollutants, we carried out vapour sorption experiments using a series of chlorinated volatile organic compounds (VOCs) and another series of volatile amines. Sorption of water and ammonia were also studied. Sorption experiments were carried out using activated samples. In this regard, the activated MOFs such as $[Co(34pba)(44pba)]_n$ (**1d**) and $[Zn(34pba)(44pba)]_n$ (**3d**) were used. Note that **2d** was not used as this was isostructural to **1d**.

4.2.1. Sorption of halogenated VOCs

Different halogenated VOCs such as dichloromethane (CH_2Cl_2), chloroform ($CHCl_3$), chlorobenzene (ClBenz), dibromomethane (CH_2Br_2), bromoform ($CHBr_3$), bromobenzene (BrBenz), diiodomethane (CH_2I_2), iodoform (CHI_3), and iodobenzene (IBenz) were investigated. They differ in their polarity, vapour pressure, and structural shape. Thus, these features can

influence a particular sorption property. The sorption of water (H_2O) was also carried out for comparison. Note that the new forms were named as **1dCH_2Cl_2** or **3dCH_2Cl_2**, **1dCH_2Br_2**, or **3dCH_2Br_2** and so on. This is described in detail in the experimental section.

Sorption of chlorinated VOCs (CH_2Cl_2, $CHCl_3$, and ClBenz) were achieved in a single crystal to single crystal manner, which allowed the elucidation of these crystal structures (Table 4.1 and Figure 4.1). The crystallographic data show few differences from the original activated framework. These compounds crystallize in the same crystal system and space group with very similar unit cells and little difference in their volumes. The whole molecule of CH_2Cl_2 (**1dCH_2Cl_2**) was disordered while one chlorine atom in $CHCl_3$ (**1d$CHCl_3$**) was disordered. The guests are stabilized in place by a number of weak interactions, including C−H···π interactions, in the case of chlorobenzene, through C−H···π, C−H···C−H, and π···C−H interactions with the walls of the MOF. Comparable interactions have been observed in similar systems.[1–3] The unit cells volume of **1dCH_2Cl_2** and **1d$CHCl_3$** were slightly lower than that of **1d**, while, the unit cell volume in **1dClBenz** was 2.9% higher than that in **1d**. Therefore, the presence of ClBenz in the channels could cause the framework to expand with the influence of C−H···C−H repulsion. A similar sorption process was applied on other halogenated solvents such as CH_2Br_2, $CHBr_3$, BrBenz, CH_2I_2, CHI_3, and IBenz on **1d** and **3d**. However, we could not obtain suitable single crystals for their structural elucidation. Their PXRD characterization showed some differences explained by their particular interactions. This has been thoroughly explained in the next paragraph.

Table 4.1: *Cell parameter of crystal from sorption of chlorinated solvents.*

Compound	**1d**	**1dCH_2Cl_2**	**1d$CHCl_3$**	**1dClBenz**
Formula	$C_{24}H_{16}N_2O_4Co_1$	$C_{25}H_{18}Cl_2CoN_2O_4$	$C_{25}H_{16.83}Cl_3CoN_2O_4$	$C_{30}H_{21}ClCoN_2O_4$
Mass (g.mol^{-1})	455.34	540.24	574.52	567.89
Crystal size (mm)	0.080 x 0.090 x 0.140	0.16 x 0.20 x 0.34	0.11 x 0.21 x 0.33	0.10 x 0.13 x 0.20
Crystal system	Monoclinic	Monoclinic	Monoclinic	Monoclinic
Space group	$P2_1/c$	$P2_1/c$	$P2_1/c$	$P2_1/c$
a/(Å)	10.3931(14)	10.5973(11)	10.0048(16)	10.2944(16)
b/(Å)	16.027(2)	15.3082(15)	16.371(3)	16.272(3)
c/(Å)	14.996(2)	14.8848(15)	15.036(3)	15.248(3)
β/(°)	98.243(2)	99.964(2)	97.402(3)	95.232(4)
V/(Å^3)	2472.2(6)	2378.3(4)	2442.3(7)	2543.6(7)
Z	4	4	4	4
T/(K)	100	100	173	173
D (g·cm^{-3})	1.223	1.509	1.562	1.483
μ(Mo−Kα) (mm^{-1})	0.722	0.981	1.066	0.820
F(000)	932	1100	1163	1164
range scanned, θ (deg)	1.870-27.963	1.923-28.14	1.847-28.31	1.834-28.26
no. reflections collected	22935	42669	42591	51772
no. unique reflection	5896	5821	6062	6296
no. reflections with I ≥ 2σ(I)	3900	4338	4504	4493
parameters/restraints	336/0	335/0	326/0	343/0
goodness of fit, S	1.079	1.015	1.019	1.038
final R indices (I ≥ 2σ(I))	R1 = 0.0638	R1 = 0.0454	R1 = 0.0479	R1 = 0.0550
	wR2 = 0.1506	wR2 = 0.0987	wR2 = 0.1155	wR2 = 0.1386
final wR2 (all data)	R1 = 0.1080	R1 = 0.0696	R1 = 0.0741	R1 = 0.0857
	wR2 = 0.1689	wR2 = 0.1092	wR2 = 0.1293	wR2 = 0.1571
Min, max e$^-$ density/(e Å^{-3})	0.821, -0.786	0.646, -0.699	0.674, -0.946	1.282, -1.117

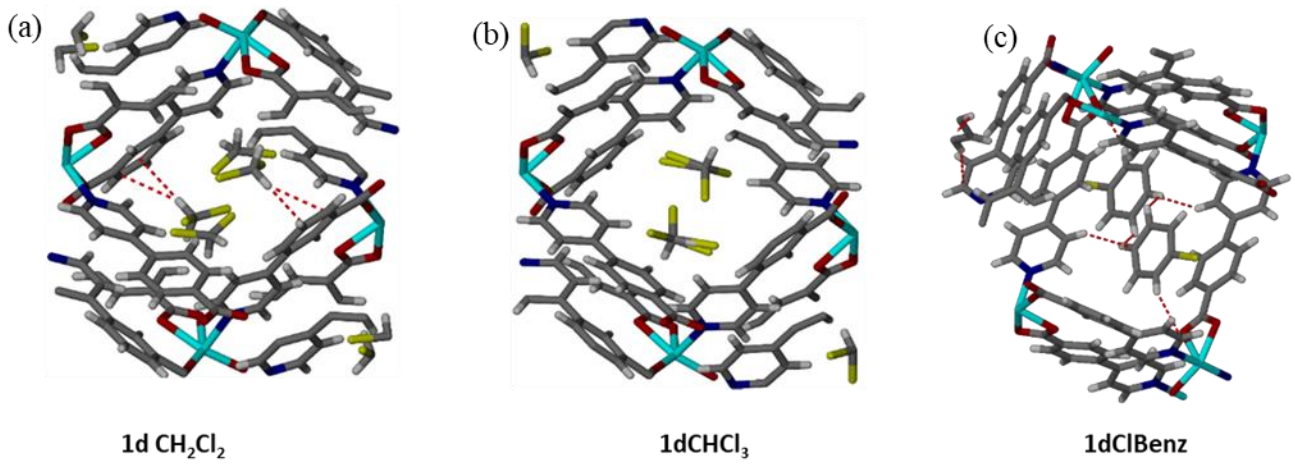

Figure 4.1: *Inclusion of dichloromethane (a), chloroform (c) and chlorobenzene (c) into MOF* ***1d****.*

PXRD patterns (Figure 4.2a and b) of the phases obtained by vapour sorption of all tested chlorinated VOCs into **1d** or **3d** are unchanged from the starting activated phases. Comparably, PXRD of the halogenated compound containing bromine or iodine atoms in only **3d** (Figure 4.2d) were slightly changed, thus confirming the robustness of the retained framework structure.[4] On the other hand, Figure 4.2c shows greater variation in the patterns obtained for **1d** with bromine and iodine derivatives. Iodinated compounds showed more changes than VOCs containing bromine. Halogenated compounds containing a benzene ring showed little change in patterns from the original ones. The phase change in **1d** is probably caused by the interactions of the guest solvents which is likely to be influenced by the presence of halogen substitute. Apart from the halogen interaction, the uptake of H_2O also formed new crystalline phases in both **1d** and **3d**. Thus, different effects in the phase change can be attributed to the difference in the polarity and steric structure.

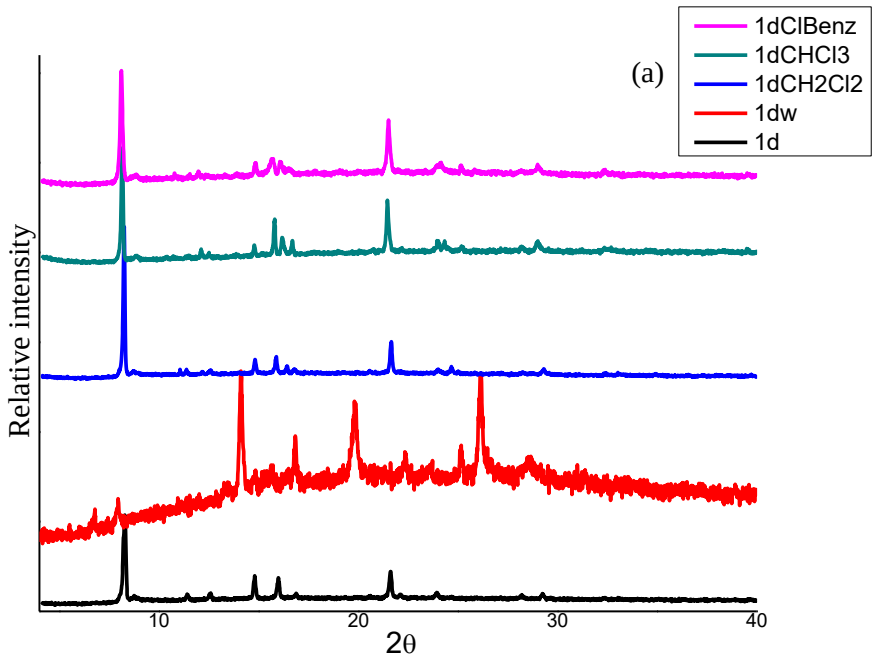
(a)
1dClBenz
1dCHCl3
1dCH2Cl2
1dw
1d
Relative intensity
10
20
30
40
2θ

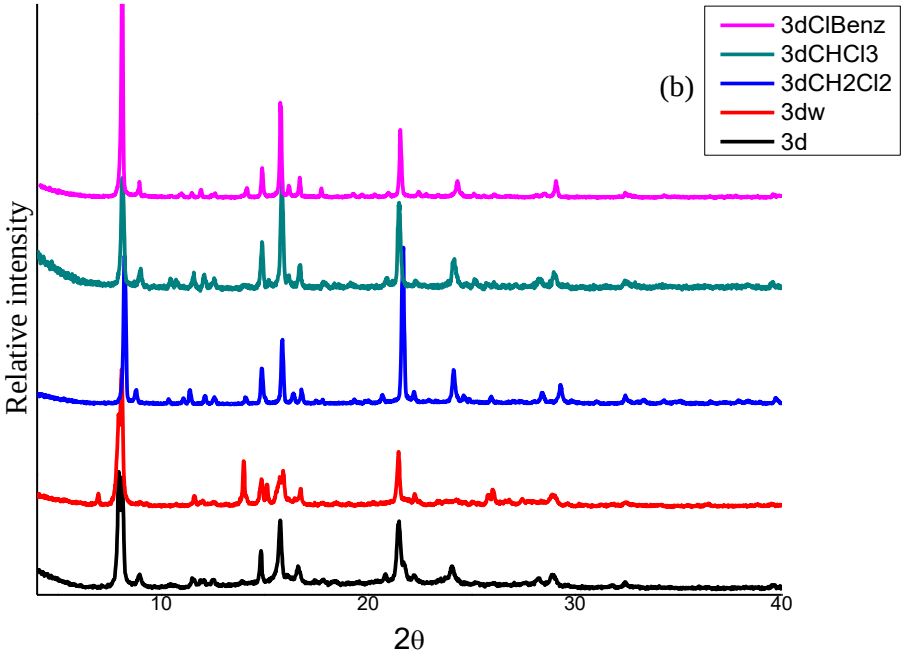
(b)
3dClBenz
3dCHCl3
3dCH2Cl2
3dw
3d
Relative intensity
10
20
30
40
2θ

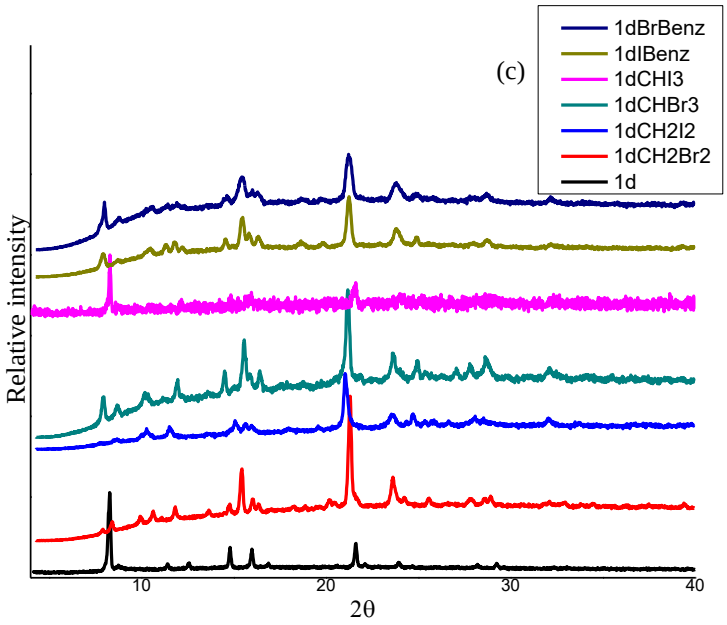

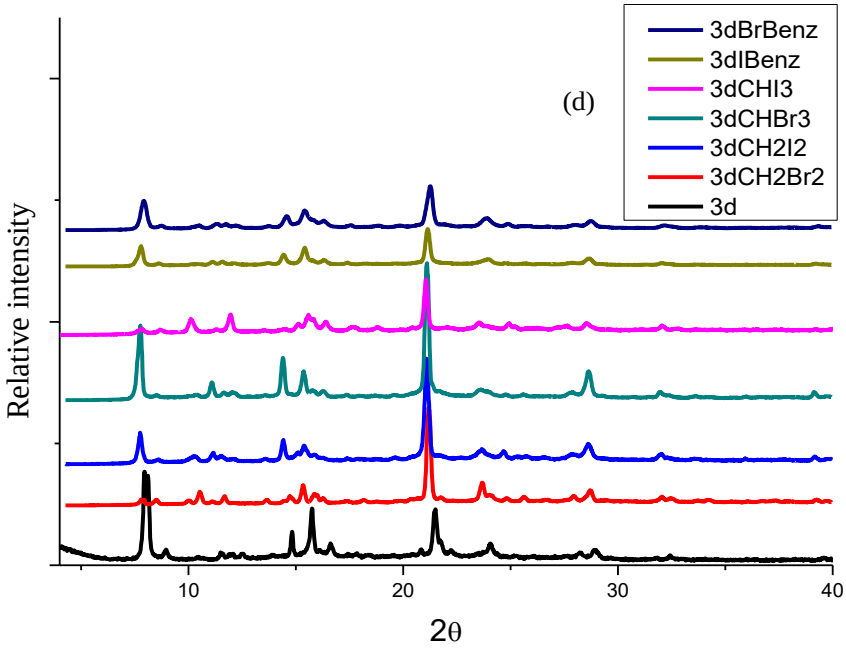

Figure 4.2: *PXRD of sorption of halogenated VOCs in* ***1d*** *(a and c) and* ***3d*** *(b and d).*

1d and **3d** show similar sorption trends for halogenated VOCs in terms of adsorption capacity and desorption temperature, (Figure 4.3). The loading values were calculated from TGA analysis and compared to the theoretical maximum loading capacities. The VOCs with a lower boiling point show a lower starting temperature of the desorption as displayed in Table 4.2. The desorption process took place over a broad range of temperatures which might be affected by the guest-host interactions or kinetic process taken by the guest molecules to vacate from the channels. It was noted that halogenated VOCs of aliphatic compounds resulted in a one-step TGA traces. On the other hand, halogenated VOCs containing aromatic ring showed a two-step desorption process. This was attributed to the fact that guest molecules containing aromatic rings can occupy the channels of MOFs by aromatic stacking between the guest and host to allow additional interaction with specific desorption and causes a large range of desorption.[5] Corresponding DSC traces in Figure S3 also show the broad endothermic processes for halogen VOCs desorption.

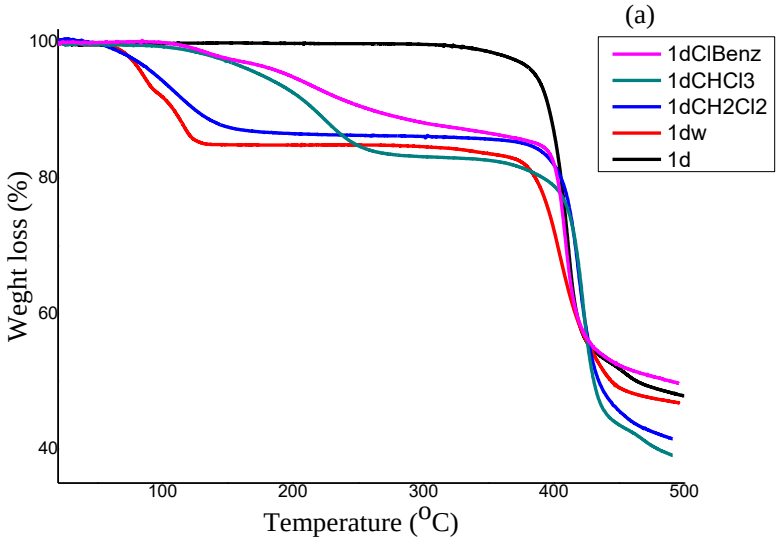

(b)

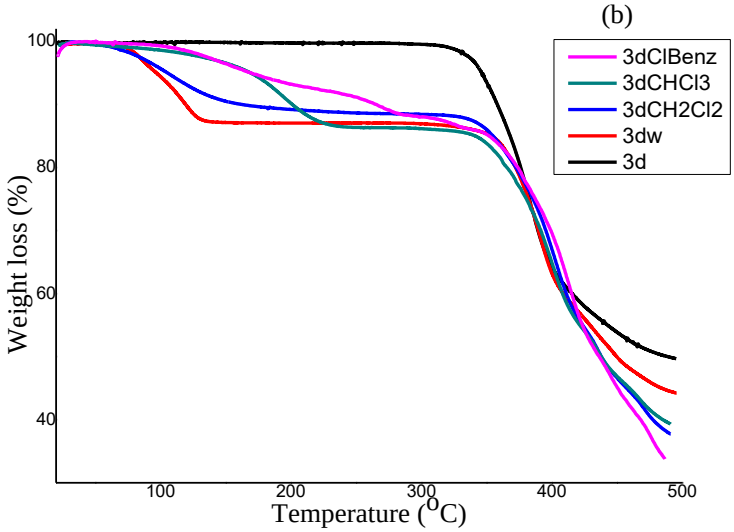
3dClBenz
3dCHCl3
3dCH2Cl2
3dw
3d
Weight loss (%)
Temperature (°C)
100
80
60
40
100
200
300
400
500

(c)

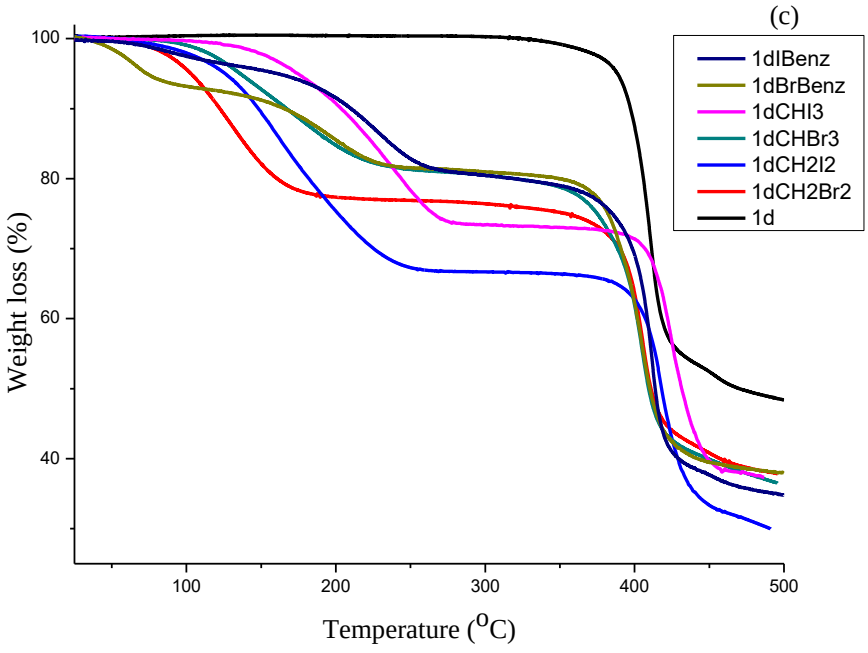
1dIBenz
1dBrBenz
1dCHI3
1dCHBr3
1dCH2I2
1dCH2Br2
1d
Weight loss (%)
Temperature (°C)
100
80
60
40
100
200
300
400
500

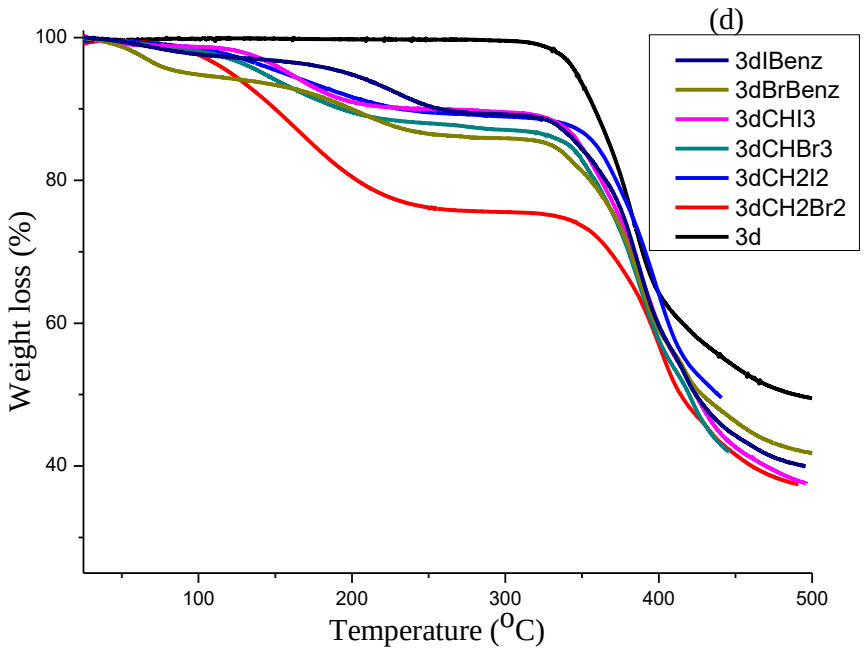

Figure 4.3: *TGA curves showing the desorption of corresponding halogenated VOCs from* ***1d*** *and* ***3d****.*

Table 4.2 lists the VOC sorption results for **1d** and **3d**. The loading capacity (Lc) is calculated from the crystallographically derived void volume and the liquid density of the respective solvents. The maximum loading capacity (MLc) for the empty networks was estimated from

$$\textbf{MLc = (solvent accessible void volume)/(Z × molecular volume)} \qquad \textbf{(1)}$$

To determine the solvent-accessible void volume, the coordinates of solvent guest molecules were deleted first from the host structures. Then, the void volumes in **1d** and **3d** were estimated using Mercury with a probe radius of 1.2 Å and a grid step of 0.2 Å and were found to be 549.0 $Å^3$ (22.8%) and 571.4 $Å^3$ (23.5%) per unit cell respectively.[6] The molecular volumes of solvents were calulcated depending on their respective liquid density as in formula (N_A: Avogadro number):

$$\textbf{Molecular volume of solvent} = \frac{\textbf{Molecular Weight}}{N_A \times \textbf{Density}} \qquad \textbf{(2)}$$

Table 4.2: *Uptake of selected solvents by the activated phases* ***1d*** *and* ***3d****.*

VOC	Experimental mass loss, TGA (%)	Temperature range of mass loss (°C)	Loading capacity, L_c (x in proposed formula): $\{[M(34pba)(44pba)]\cdot x\ solvent\}_n$	ML_c	% Loading capacity
1d					
CH_2Cl_2	14.0	60-154	0.9	1.3	69
CH_2Br_2	23.1	70-200	0.8	1.2	67
CH_2I_2	33.3	70-260	0.8	1.0	80
$CHCl_3$	17.1	118-285	0.8	1.0	80
$CHBr_3$	19.2	91-236	0.4	0.9	44
CHI_3	26.0	125-278	0.4	0.8	50
ClBenz	13.0	87-264	0.6	0.8	75
BrBenz	19.2	38-235	0.7	0.8	88
IBenz	19.1	40-277	0.5	0.8	63
H_2O	15.4	60-155	4.6	4.6	100
3d					
CH_2Cl_2	11.0	88-220	0.7	1.4	50
CH_2Br_2	23.0	78-266	0.8	1.2	67
CH_2I_2	10.0	87-290	0.2	1.0	20
$CHCl_3$	13.3	110-232	0.6	1.1	55
$CHBr_3$	12.7	109-233	0.3	1	30
CHI_3	10.0	105-248	0.1	0.9	11
ClBenz	11.0	61-252	0.5	0.8	63
BrBenz	14.0	58-278	0.5	0.8	63
IBenz	10.6	58-270	0.3	0.8	38
H_2O	12.9	60-134	3.8	4.8	79

For the halogenated solvents, the loading capacity (Lc) in the proposed formula $\{[M(34pba)(44pba)]\cdot x\ solvent\}_n$ for both systems is lower than the maximum loading capacity. The aliphatic VOCs containing two halogen atoms showed higher loading capacity than those containing three halogen atoms except chloroform. This can be associated with the higher vapour

pressure (Table S1) in VOCs. The aromatic halogenated VOCs have lower vapour pressure but their loading capacity was higher. It is assumed that the aromatic ring increased the interaction host-guest which favours the loading capacity.[5] Note that the iodobenzene made an exception possibly due to the size effect. For each individual solvent, the sorption is higher for **1d** than for **3d**. Water is taken up to near full capacity by both **1d** and **3d**, but results in the formation of new crystalline phases. Selective sorption was only investigated on chlorinated VOCs.

The extent of selectivity in **1d** and **3d** was investigated from binary mixtures of the chlorinated VOCs. Equal volumes (2 cm^3) of two different chlorinated solvents were mixed into a large vial. The activated solid adsorbents (20-25 mg) were loaded into a small vial. The small vial was then placed inside the large one which was then sealed for two days and kept at r.t. (ca. 22 °C). The ideal was the rise of the vapour of both VOCs out of the large vial to reach the adsorbent for the sorption to take place at r.t. The adsorbent was then poured into DMSO-d_6 (DMSO-d_6: deuterated dimethylsulfoxide) and heated at 80 °C for 1h to release the chlorinated VOCs into the $DMSO_d$ solvent. After filtering, the liquid sample was analyzed by ^{1}H NMR spectrometry. The ^{1}H NMR analysis provided the relative proportions of each of the solvents in the binary mixture. Table 4.3 presents the solvent ratios obtained from the integration of relevant NMR peaks (Figures S4 in appendix) from the competition studies. For **1d**, a mixture of CH_2Cl_2 and chloroform were taken up without selectivity, while **3d** exposed to the same mixture selectivity absorbed CH_2Cl_2 preferentially. Both MOFs selected CH_2Cl_2 and chloroform over chlorobenzene from these respective binary mixtures. On the other hand, CH_2Cl_2 was selectively sorbed 8.3 times over chlorobenzene in **1d**. It should be noted that no attempt was made to compensate for differences in vapour pressure and that the more volatile solvent was absorbed in each case, in contrast to a previous study carried out in our laboratory.[3]

Table 4.3: *Selectivity of **1d** and **3d** for chlorinated VOCs*

1d	**Mole ratio of VOCs in 1d[a]**	**Selectivity (major component)**
$CH_2Cl_2/CHCl_3$	1:1	none
CH_2Cl_2/ClBenz	8.3:1	CH_2Cl_2
$CHCl_3$/ClBenz	10:1	$CHCl_3$
3d	**Mole ratio of VOCs in 3d**	**Selectivity (major component)**
$CH_2Cl_2/CHCl_3$	1.3:1	CH_2Cl_2
CH_2Cl_2/ClBenz	1:0	CH_2Cl_2
$CHCl_3$/ClBenz	3:1	$CHCl_3$

[a] Determined by NMR (Figures S4 in Appendix)

4.2.2. Sorption of volatile amines

To test the potential of these compounds as sorbents for amines, the activated MOFs **1d** and **3d** were exposed to the vapours of a series of amines, viz. ammonia (NH_3), methylamine ($MeNH_2$), propylamine ($PropNH_2$), 1-butylamine ($ButNH_2$), benzylamine ($BzNH_2$), and phenylethylamine ($PhEtNH_2$). The crystal quality of the resultant compounds was too poor to allow full structural characterization. PXRD patterns show that the sorption of amines VOCs led to new phases. In this regard, the complexes in **1d** become amorphous, except for $PhEtNH_2$ and NH_3 (Figure 4.4a), while, those in **3d** formed new crystalline phases (Figure 4.4b). To further understand this, we exposed **1d** to benzylamine ($BzNH_2$) and found that the material remained crystalline (Figure 4.4c) until a mass loss of 40% was recorded in the TGA. This amount corresponds to 2.8 molecules of $BzNH_2$ per 549.0 $Å^3$ molecular void volume of the unit cell. Subsequent desorption of the $BzNH_2$ from amorphous **1dBzNH2** under vacuum recovered crystalline **1d** (Figure 4.5). This can be explained by the fact that amine groups likely exert strong hydrogen bonding on the carboxylates of the

framework in form of Co-O···HN. This may undergo partial breakage of Co-O as on the subsequent activation, the hydrogen bonding can be broken by restoring the framework to its initial crystalline phase. Therefore, there is a self-restoration of the crystalline **1d** which indicates a breathing phenomenon of the framework. A similar process of the reverse mechanism, however, had been observed in MOFs.[7]

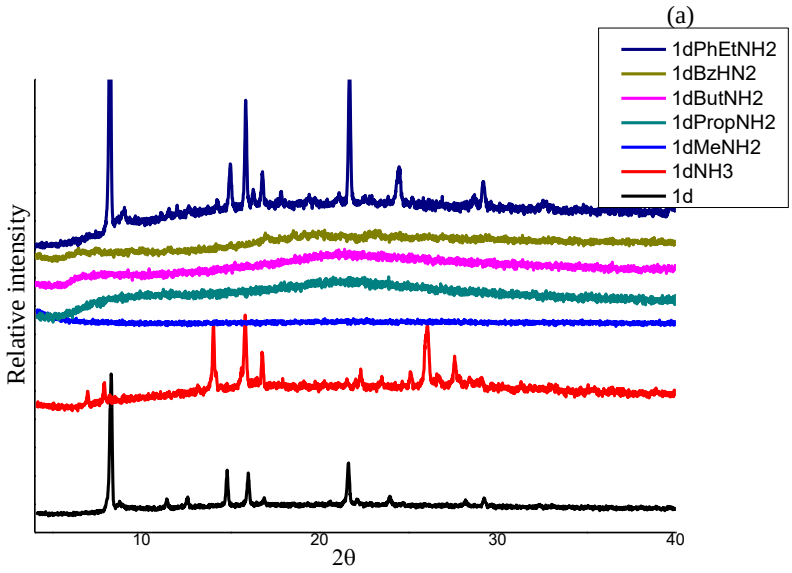

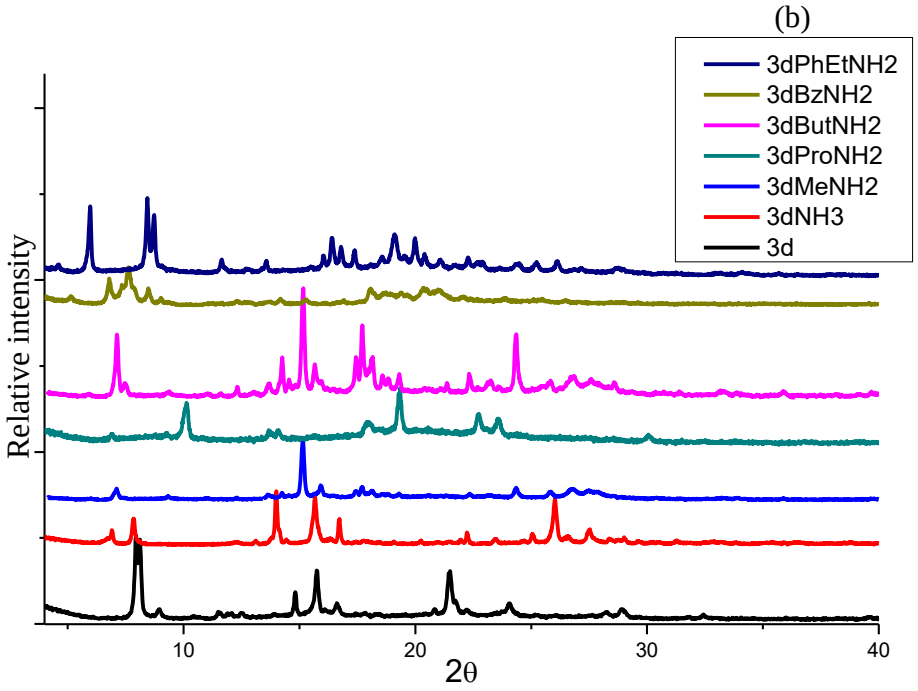

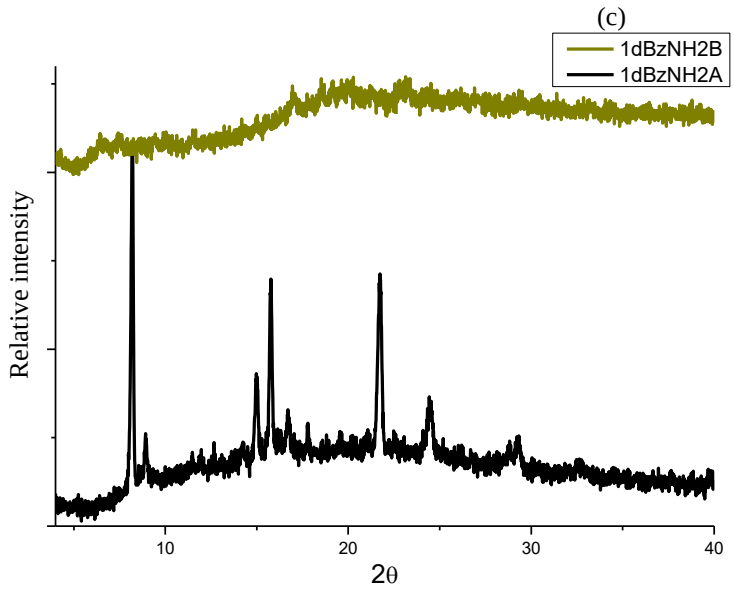

Figure 4.4: *PXRD showing sorption (a) of amine compounds in* ***1d*** *and* ***3d****, (c) XRD patterns for* ***1dBzNH₂A*** *with 40% weight loss of* $BzNH_2$ *and* ***1dBzNH₂B*** *with 52% weight loss of* $BzNH_2$*.*

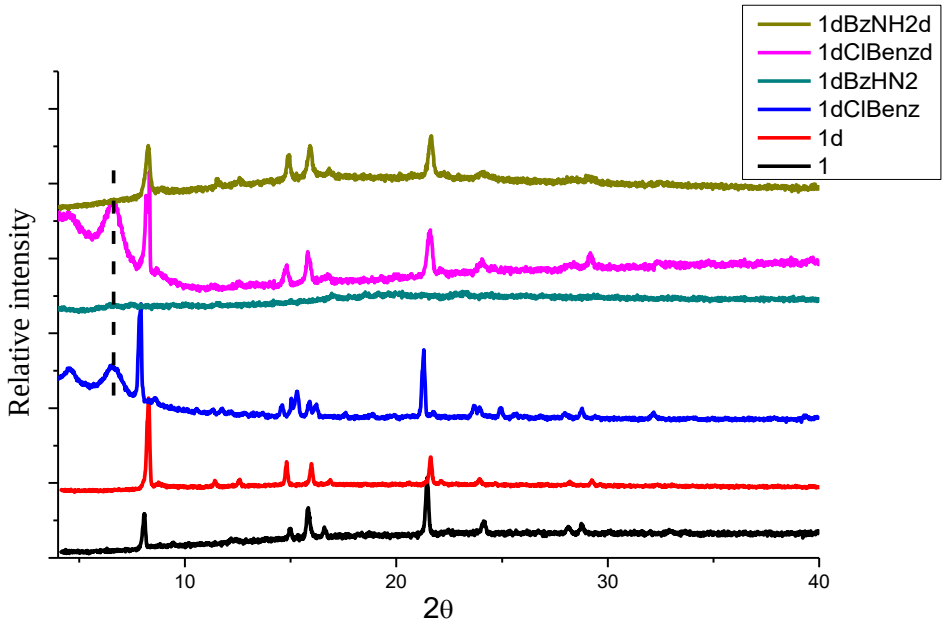

Figure 4.5: *PXRD showing the regeneration of solid* ***1d*** *from chlorinated and amine VOCs. Note that the peaks at 6.6 (2θ) are due to the sample holder used during for these experiments.*

The loading capacity for the amines VOCs was also determined from TGA traces, Figure 4.6 as with the chlorinated VOCs. Apart from NH_3, amines VOCs have more than one desorption step in both adsorbents. It was also noted that except phenylethylamine, the loading capacity of both **1d** and **3d** exceeds the calculated maximum from simple molecular volumes (Table 4.4). This can be explained by the fact that the framework expanded to accommodate guest amines VOCs more than the expected. Furthermore, some MOFs are reported for their exceptional properties to accommodate more guest molecules due to the high degree of hydrogen bonding.[7] Besides, studies on these frameworks in chapter three have shown that the guest molecules apply the force as a hinge-like expansion or contraction on the frameworks[8] which can allow accommodating the excess of loading capacity. In **3d** on the other hand, while the loading values obtained were again higher than the calculated maximum, the compounds retained their crystallinity but show some

differences in phase in their PXRD traces. As with the chlorinated solvents, the amount sorbed by **1d** is greater than that for **3d**.

Amines are capable of hydrogen bonding, hence stronger intermolecular interactions, than chlorinated VOCs, which may allow them to pack more compactly into the channels, and to interact strongly with the internal surfaces of the MOFs, leading to higher loading values[2,9] and phase changes.[10–12] For benzylamine in particular, the MOFs took up a large amount, which could be attributed to the aromatic stacking between $BzNH_2$ and the aromatic rings in the MOF walls.[13] The lower sorption capacity for $PhEtNH_2$ is the result of steric effects and lower polarity. No tests for selectivity among amine VOCs were performed. As there was no single crystal suitable for characterization, we were unable to definitively establish the intermolecular interactions involved.

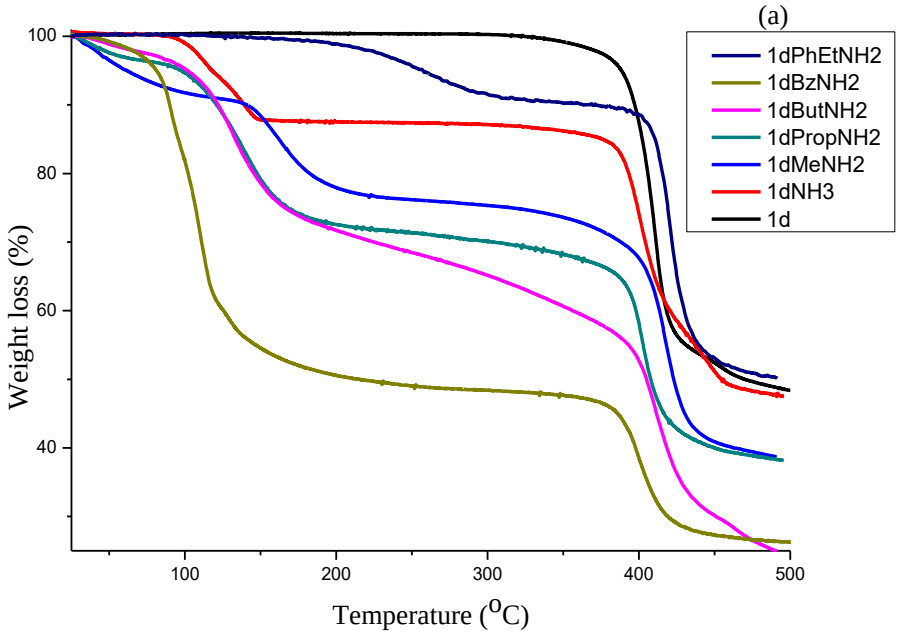

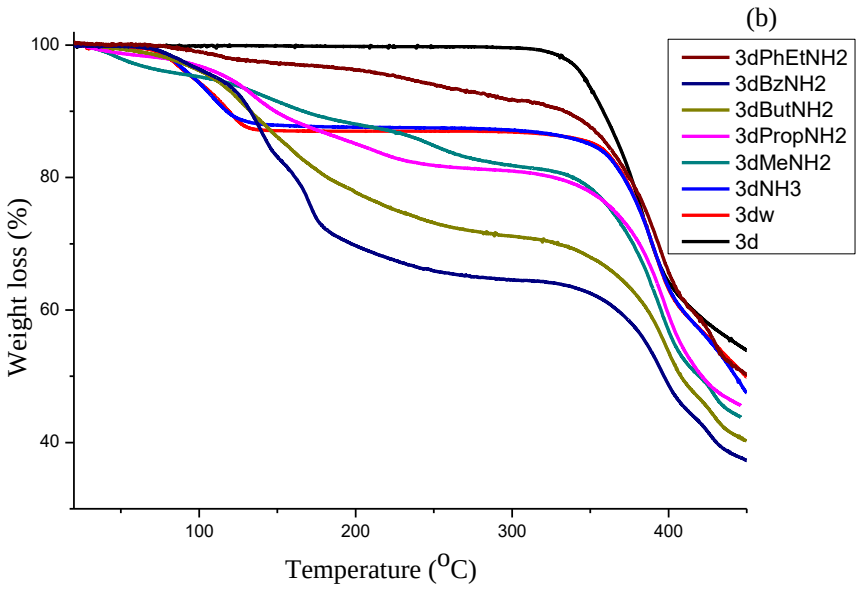

Figure 4.6: *TGA curves showing the desorption of corresponding amine VOCs from* ***1d*** *(a) and* ***3d*** *(b).*

Table 4.4: *Uptake of selected amine VOCs by the activated phases* ***1d*** *and* ***3d****.*

VOC	Experimental mass loss, TGA (%)	Temperature range of mass loss (°C)	Loading capacity, Lc (x in proposed formula: {[M(34pba)(44pba)]·x solvent}n	MLc	% Loading capacity
1d					
NH_3	12.9	59-127	4.0	3.5	114
$MeNH_2$	26.1	30-220	5.2	1.9	273
$PropNH_2$	33.4	30-220	3.9	1.0	390
$ButNH_2$	31.0	30-220	2.8	0.8	350
$BzNH_2$	52.0	65-260	4.6	0.8	575
$PhEtNH_2$	9.7	170-310	0.4	0.7	57
3d					
NH_3	12.5	60-127	3.9	3.6	108
$MeNH_2$	18.2	30-280	3.3	1.9	174
$PropNH_2$	18.4	30-263	1.8	1.0	180
$ButNH_2$	29.2	50-290	2.6	0.9	289
$BzNH_2$	36.0	88-290	2.4	0.8	300
$PhEtNH_2$	8.4	77-290	0.3	0.7	43

4.2.3. Sorption of carbon dioxide and hydrogen gases in 1d and 3d

Micromeritics 3Flex surface area analyzer was used to perfom gas sorption in **1d** and **3d**. The sample activation was carried out using a Micromeritics Flowprep with a flow of nitrogen over the sample which was heated at 60 ^{o}C for 2 hrs. The sample was then heated at 150 ^{o}C under a vacuum for a further 2 hrs before the start of the analysis.

The activated **1d** and **3d** from Co(34pba)(44pba)DMF and Zn(34pba)(44pba) respectively were used for the sorption of CO_2 and H_2 at different temperatures. The heat of adsorption of CO_2 was also determined. Figure 4.7 shows the adsorption traces for both **1d** and **3d**. At the temperatures studied, the sorption behaviour was a type-Ib isotherm. In light of this type of sorption, the adsorbent is characterized by small external surfaces having pore size with distributions over a broader range and the presence of wider micropores with possibility of narrow mesopores ($\leq$ 2.5 nm).[14] The steep uptake observed at very low p/p_0 is due to enhanced adsorbent-gas interactions in narrow micropores and some narrow mesopores, thus filling up the pores at very low p/p_0. Table 4.5 recorded the higher adsorption capacity at 195 K and 676 mmHg for both samples. **1d** showed more than a double 114 cm^3 (STP) g^{-1} (2.35 molecules per ASU) compared to that of **3d** with 52 cm^3 (STP) g^{-1} (1.11 molecules per ASU). Little hysteresis was observed in both isostructural frameworks except at the lower temperature (195 K) owing to the lower mobility of gas molecules. Stage **A** (Figure 4.8a) matches with the maximum adsorption in **3d** while corresponding to the half adsorption capacity in **1d**. This may indicate the flexible gate opening in **1d** which do not occur in **3d**. Similar flexibility upon sorption of CO_2 or CH_4 in networks were reported.[15] The lowest adsorption recorded at 298 K and 910 mmHg for **1d** and **3d** was 41.0 cm^3 (STP) g^{-1} (0.84 molecules per ASU) and 17.7 cm^3 (STP) g^{-1} (0.37 molecules per ASU) respectively. Sample **1d** showed higher adsorption capacity than **3d** at a similar temperature and pressure.

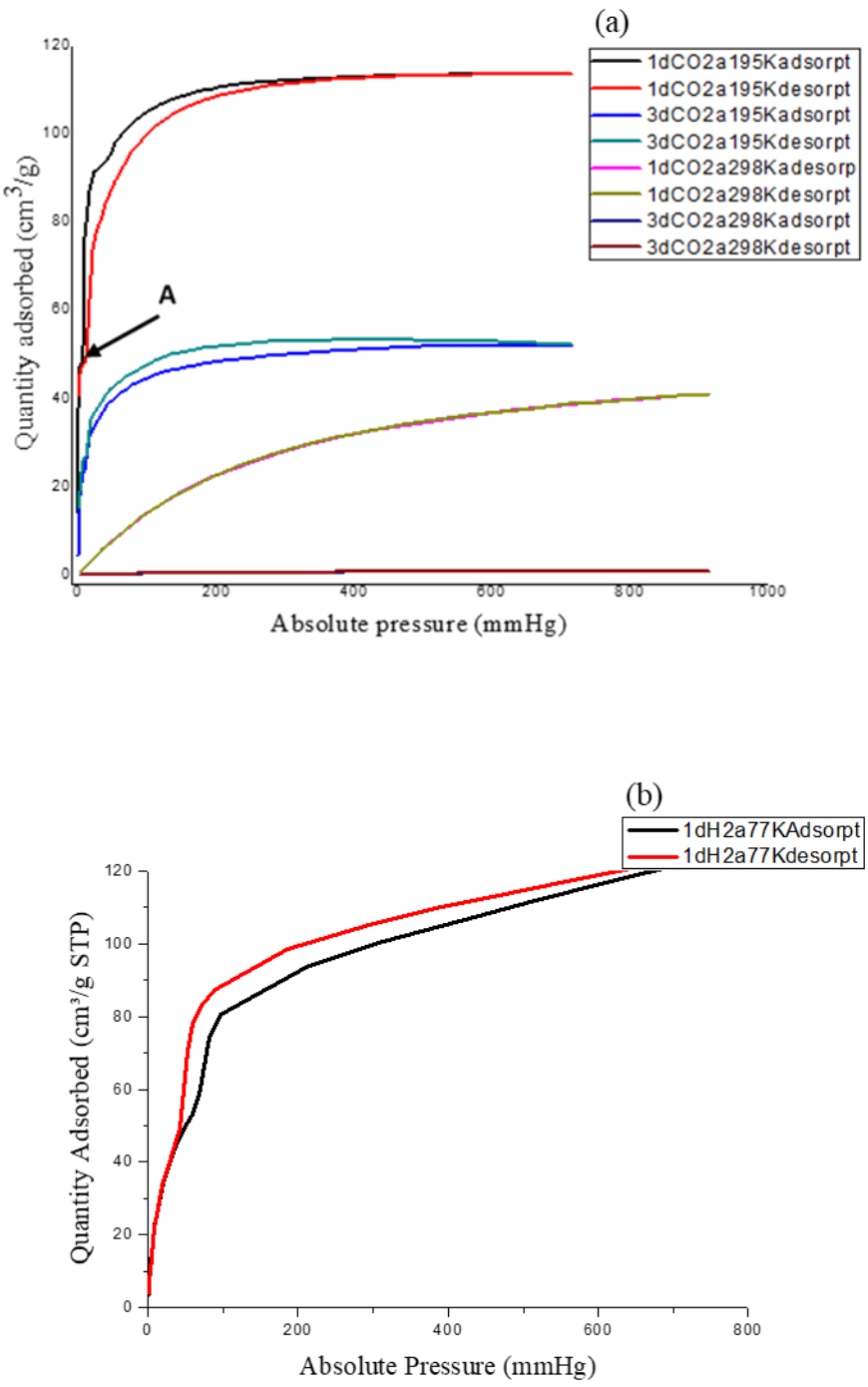

Figure 4.7: *Sorption of CO_2 (a) and H_2 (b).*

Table 4.5: *Sorption capacity for CO_2*

No	Sample	Volume adsorbed (cm^3/g)	Pressure (mmHg)	Temperature (K)	Corresponding to (mmol/g)
1	3d 1d	52.0 114	676	195	2.40 **5.06**
2	3d 1d	22.4 47.6	784	273	1.00 2.10
3	3d 1d	21.7 47.0	803	278	1.00 2.10
4	3d 1d	19.7 44.6	910	288	0.90 2.00
5	3d 1d	18.8 43.1	900	293	1.92 0.84
6	3d 1d	17.7 41.0	910	298	0.80 1.80

The trend of higher adsorption capacity in **1d** compared to **3d** could be related again to its higher sorption for chlorinated and amines volatile organic compounds (VOCs) as the result of smaller void space and flexible gate opening in in **1d** than **3d**.[5,16] However, this attribution of adsorption capacity related to the size of pores has been controversial in other reported structures.[17] Rather, the small size of void accessible volume causes stronger interactions between the guest and the framework. This can be attributed to their respective structures and functionalization. The determination of isosteric heat of adsorption (Q_{st}) of CO_2 showed that the sample **1d** adsorbed the quantity between 0.8 mmol and 1.38 mmol at a cost between (Q_{st}) 29.8 kJ and (Q_{st}) 30.3 kJ heat of adsorption, while sample **3d** adsorbed between 0.1 mmol and 0.4 mmol corresponding to the range between 28.5 kJ and 28.9 kJ heat of adsorption. It shows that there is a higher interaction in **1d** than in **3d**.[18] The uptake for hydrogen gas Figure 4.7b in **1d** was 120 cm^3 (STP) g^{-1} at 800 mmHg at 77K corresponding to 2.44 molecules of H_2 per ASU. In contrast, **3d** did not adsorb H_2. We tried to investigate the nitrogen adsorption but there was no interaction in both adsorbents.

4.2.4. Chromism behaviour of adsorbent 1d

While the exposure of **1d** to halogenated and amine VOCs did not show visible colour changes, the sorption of iodine, H_2O, and NH_3 were characterized by an easily observed colour change. Microscope photographs and PXRD was used to characterize the corresponding phase change.

4.2.4.1. Iodine sorption and colour change

Several groups have reported on the use of iodine as a template to achieve structurally stable Co-MOFs.[19] In most cases, the MOFs showed partial release of iodine in methanol medium which could be followed by observing the colour change. In this project, **1d** was exposed to iodine vapour. The solid adsorbent was loaded into a small vial and this was then placed in a larger vial containing solid iodine which was then closed and sealed at 22 ^oC. The characterization was performed on the sample after two hours, two days, and finally two weeks. Each sample taken was analyzed by TGA to determine the corresponding weight loss and by PXRD for the corresponding phases (**1dI$_2$**). The maximum weight loss was then used to determine the corresponding guest-host ratios. In addition, the desorption of iodine from **1dI$_2$** was performed by soaking crystals of **IdI$_2$** in methanol for three days, to recover the activated form from **1dI$_2$** (**1dI$_2$d** phase). Crystals of sufficient quality for diffraction (**1dI$_2$**) allowed us to locate an iodine dimer in the channels of the MOF (Figure 4.8). The modeled iodine atoms were disordered. As there was not a noticeable increase in the unit cell volume, the crystallographic data of **1dI$_2$** are similar to that of the empty form of **1d** as presented in Table 4.6. Examination of the structure shows host-guest interactions which stabilise the iodine molecules in the channels without contracting or expanding the channels significantly. These host-guest interactions in form of I···π and I···I are detailed in Table 4.7. After

the desorption, the crystal structure **1dI$_2$d** was analyzed and is similar to that of **1d** and **1dI$_2$** which shows that the iodine interactions in channels did not effect the structure.

Table 4.6: *(a) Crystallographic data for **1dI$_2$** against **1d** and **1dI$_2$d**.*

Compound	**1d**	**1dI$_2$**	**1dI$_2$d**
Formula	$C_{24}H_{16}N_2O_4Co_1$	$C_{24}H_{16}N_2O_4I_{1.6}Co_{15}$	$C_{24}H_{16}N_2O_4Co_1$
Mass (g.mol^{-1})	455.34	658.36	455.34
Crystal size (mm^3)	0.080 x 0.090 x 0.140	0.030 x 0.060 x 0.090	0.080 x 0.120 x 0.180
Crystal system	Monoclinic	Monoclinic	Monoclinic
Space group	$P2_1/c$	$P2_1/c$	$P2_1/c$
a (Å)	10.3931(14)	10.1143 (3)	10.4014(11)
b (Å)	16.027(2)	16.501(4)	16.1330(17)
c (Å)	14.996(2)	14.7002(4)	14.6878(15)
β (°)	98.243(2)	97.159(5)	98.482(2)
V (Å^3)	2472.2(6)	2434.28(18)	2437.7(4)
T (K)	100	100	293(2)
Z	4	4	4
T/(K)	100	293(2)	293(2)
D (g·cm^{-3})	1.223	1.796	2.019
μ(Mo−Kα) (mm^{-1})	0.722	2.766	3.277
F(000)	932	1271	1428
range scanned, θ (deg)	1.870-27.963	1.863-26.425	1.886-25.043
no. reflections collected	22935	18607	13629
no. unique reflection	5896	4970	4308
no. reflections with I ≥ 2σ(I)	3900	3691	3074
parameters/restraints	336/0	334/3	280/0
goodness of fit, S	1.079	1.089	1.055
final R indices (I ≥ 2σ(I))	R1 = 0.0681	R1 = 0.0685	R1 = 0.0616
	wR2 = 0.1887	wR2 = 0.1786	wR2 = 0.1532
final wR2 (all data)	R1 = 0.1112	R1 = 0.0932	R1 = 0.0942
	wR2 = 0.2084	wR2 = 0.1903	wR2 = 0.1701
Min, max e$^-$ density/(e Å^{-3})	0.821, -0.786	2.176, -0.626	1.370, -0.576

Table 4.7: *Interaction distance between iodine and other atoms.*

Atoms	Interaction distance (Å)
I2···C4A	3.566
I2···C5A	3.628
I3···C9A	3.604
I3···C10A	3.636
I4···C4A	3.533
I4···C5A	3.460
I4···C6A	3.662
I5···C5A	3.820
I5···C6A	3.625
I3···I5	3.875

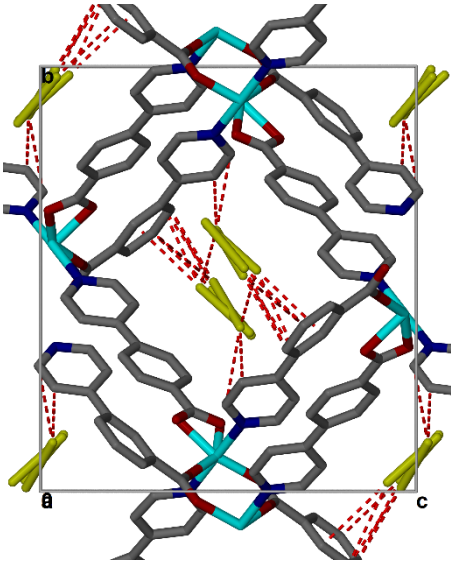

Figure 4.8: *Weak interaction of iodine guest molecule into* ***1d*** *channels.*

The void space in **1d** was 457.9 corresponding to 18.5% of the unit cell. The sorption process was characterized using PXRD where gradual changes of patterns up to eight days were observed, Figure 4.9 (a). Most notable is a gradual decrease in peak intensity around 8^{o} while there was a gradual increase in the peak around 22.5^{o}. The gradual disappearance of the peak around 14.8^{o} was also observed. The patterns of **1dI$_2$** after 8 days show the growth of peaks at 9^{o} and 21.5^{o} in addition to the shift of peak at ca. 10.5^{o}. There was also the absence of a peak at 14.8^{o} and a new peak at

25°. This can be attributed to the interaction of iodine molecule and the channels of the **1d** framework. PXRD (Figure 4.9b) also shows the robustness of **1d**, (**1dI$_2$d**) after the recovery of iodine into methanol.

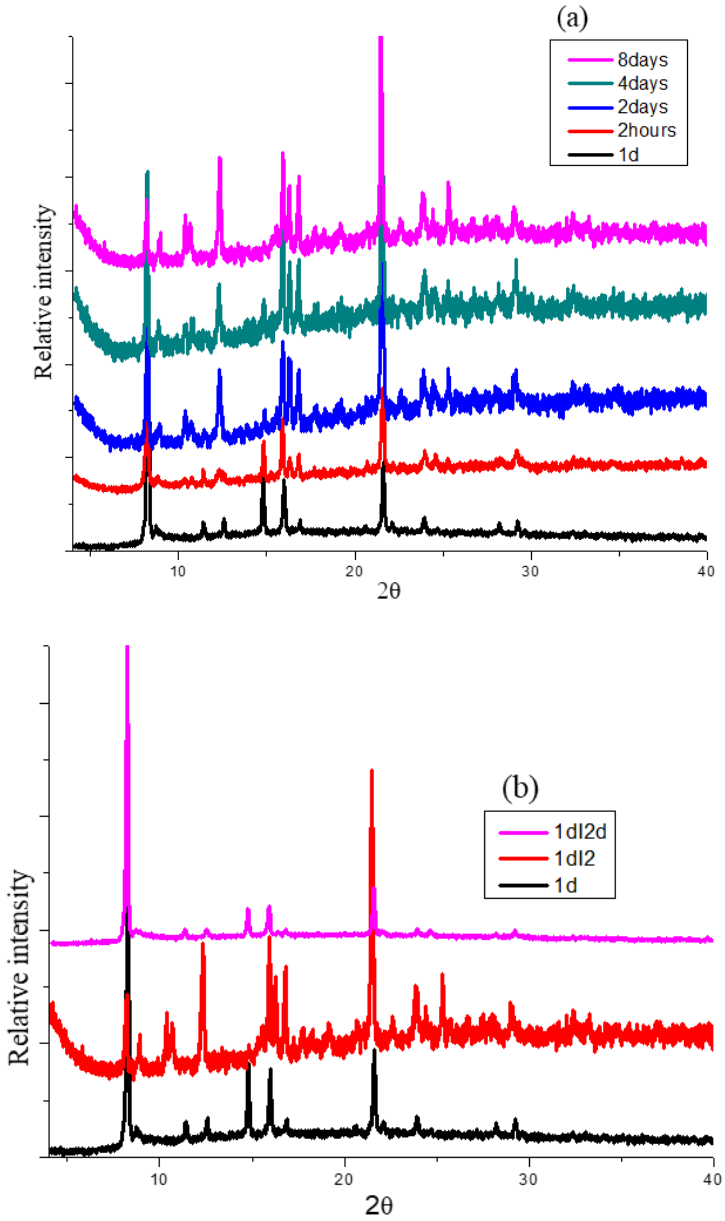

***Figure 4.9**: (a) Gradual phase changes related to the sorption of iodine in **1d** to form **1dI2** phase, (b) PXRD for iodine desorption from **1dI2** into methanol (**1dI2d**).*

The desorption of iodine from the channels into methanol medium was then monitored using hot stage microscopy (HSM) at a constant temperature of ca. 22 °C. Figure 4.10 shows a gradual colour change indicating the amount of iodine remaining in **1d** crystal. This shows the ability of **1d** MOFs to release iodine in the environment and can be monitored with the naked eye.

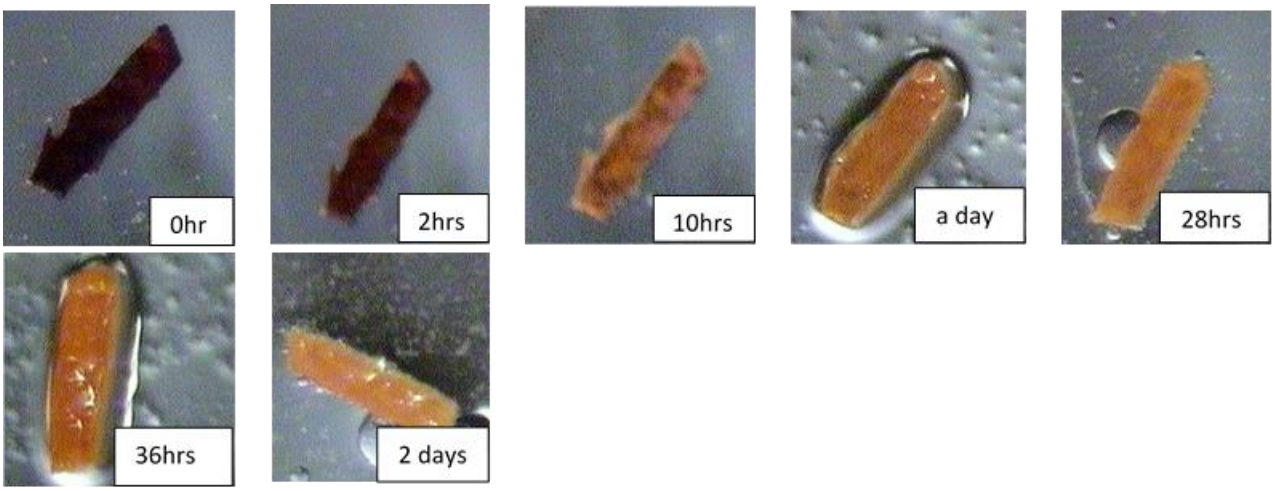

Figure 4.10: *Photographs showing colour change on the release of iodine from* ***1dI2*** *into methanol.*

TGA in Figure 4.11 shows different traces corresponding to a period of iodine absorption. The TGA traces allow us to conclude a period corresponding to complete sorption. Up to two weeks, the quantity of iodine absorbed in **1d** was 31%. Also, the quantity absorbed in eight days was close to this value. Thus, we concluded that 31% was the maximum giving a ratio of host:guest of 1:0.8 (**1d**:I_2). The temperature of desorption ranged between 80 and 220 ^oC. One can speculate that the broad temperature range of desorption could be due to interactions with the channel walls impeding the process of iodine leaving the channel.

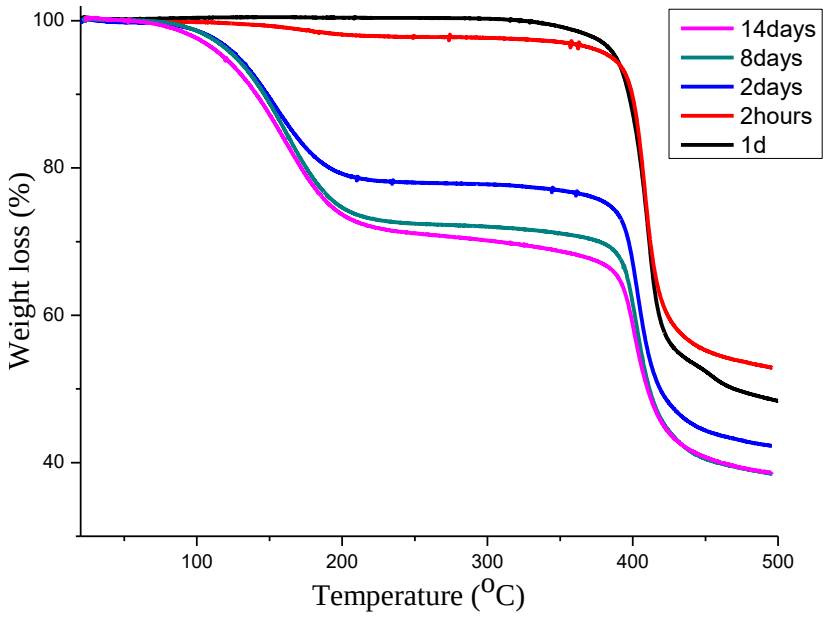

***Figure 4.11**: TG of iodine on sorption by **1d** at different time intervals.*

4.2.4.2. Solvatochromism in 1d on sorption of H_2O and NH_3

Their PXRD patterns (Figure 4.12) show that the sorption of H_2O and NH_3 by **1d** formed new phases (**1dw** and **1dNH$_3$**, respectively) with noticeable colour changes from red to khaki (Figure 4.13). Upon desorption, both **1dw** and **1dNH$_3$** resulted in purple powder phases, which are amorphous (**1dwTG** and **1dNH$_3$TG**). However, the crystallinity, as well as their khaki colours, were restored after reabsorption (**1dwTGw** and **1dNH$_3$TGNH$_3$**). Solvatochromism in MOFs has been reported to be the result of the supramolecular interactions such as hydrogen bonding and/or the coordination of the solvent molecules to the metal centres in the frameworks.[11,20,21] These interactions affect the energy associated with d-d transitions resulting in visible colour changes.[2,20]

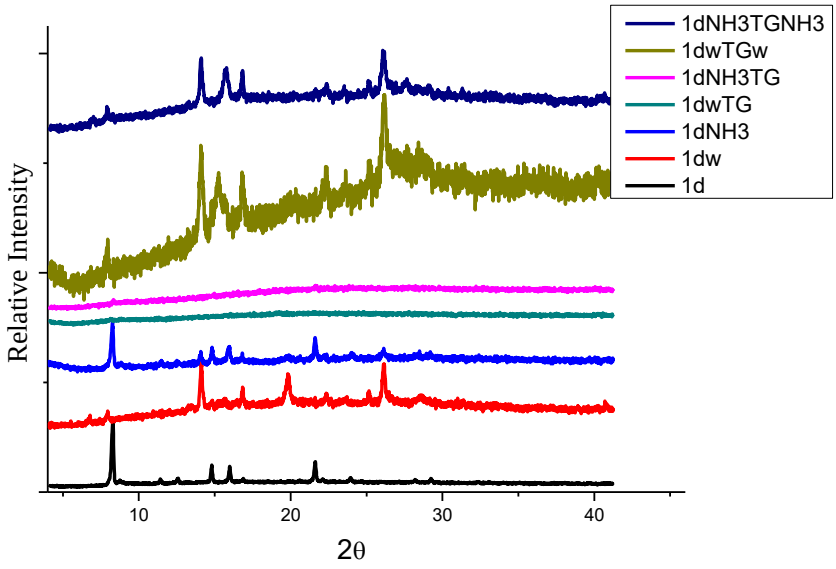

Figure 4.12: *PXRD patterns for reversible sorption for ammonia, and H_2O by* ***1d****.*

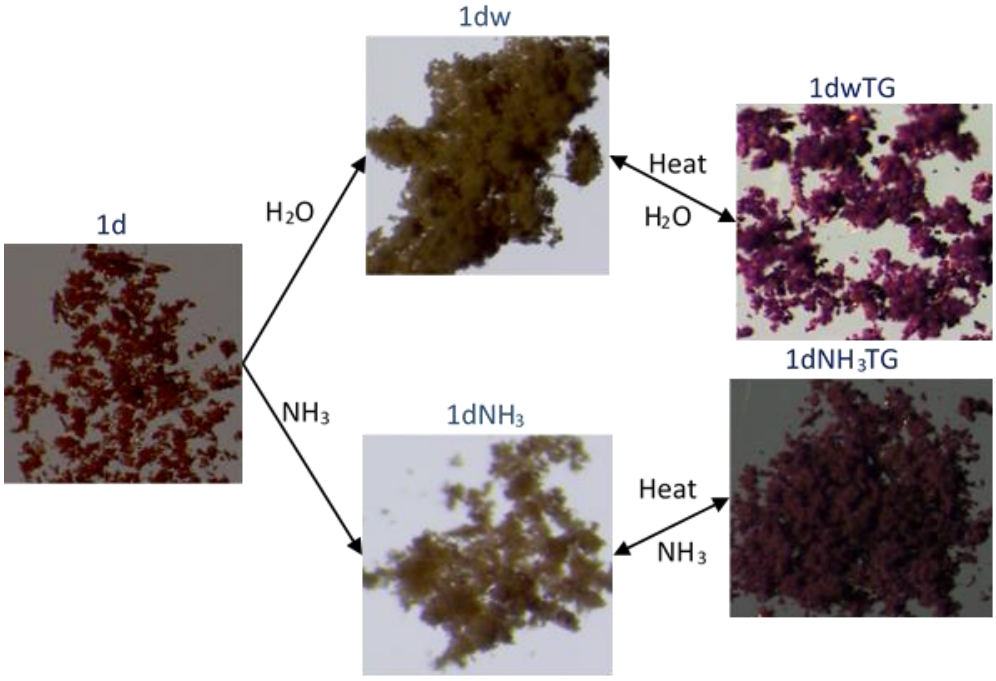

Figure 4.13: *reversible sorption of H_2O and NH_3 in* ***1d*** *associated with the respective colour change.*

4.2.5. Kinetics of guest desorption from 1, 3, 1d, and 3d

The kinetics of desorption of DMF (from **1** and **3**) or ammonia or water (from **1d** and **3d**) were studied using TGA. Both non-isothermal and isothermal methods can be used. While the isothermal methods are preferred for single processes and can give an indication of the mechanism of desorption, non-isothermal methods are of value where the desorption process is more complex or contains overlapping steps. The desorption of guest solvent, DMF from the synthesized compounds (**1** and **3**) and H_2O and NH_3 from activated ones (**1d** and **3d**) were investigated non-isothermally. On the other hand, desorption of some halogenated VOCs such as CH_2Cl_2, CH_2Br_2, and iodine (only from **1d**) was investigated isothermally. Their overall activation energies (Ea) of desorption were compared to those reported for similar systems.

4.2.5.1. Non-isothermal kinetics

TGA may be used to determine the activation energy (Ea) of the guest desorption process. We used the Ozawa model-free method[22] to study the removal of guests DMF, NH_3, and H_2O for both systems reported here. Samples of mass 1–2 mg were heated at different heating rates (5, 10, 20, and 30 $^oC\ min^{-1}$) in order to determine the activation energy associated with the removal of guest molecules from **1**, **3**, **1dw**, **3dw, 1dNH$_3$**, and **3dNH$_3$** (Figure 4.14).

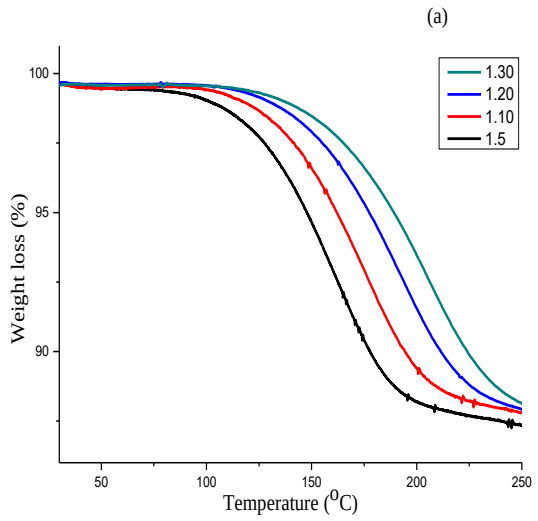
(a)
1.30
1.20
1.10
1.5
Weight loss (%)
Temperature (°C)

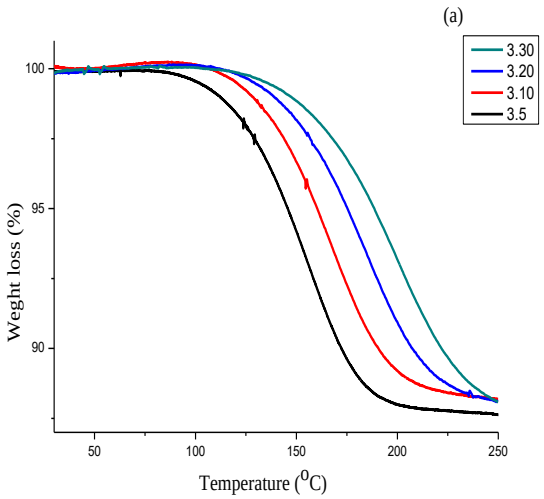
(a)
3.30
3.20
3.10
3.5
Weght loss (%)
Temperature (°C)

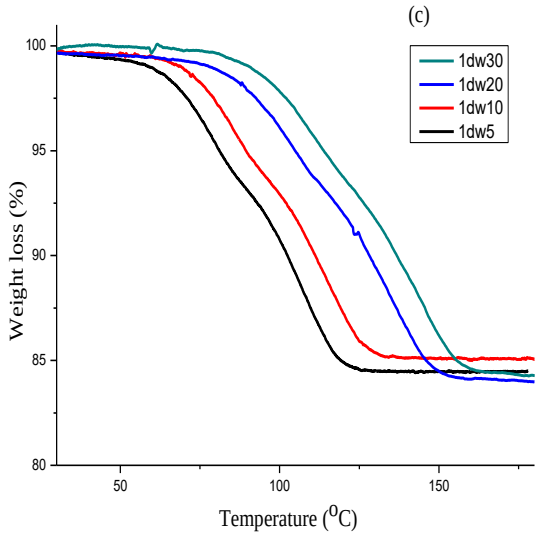
(c)
1dw30
1dw20
1dw10
1dw5
Weight loss (%)
Temperature (°C)

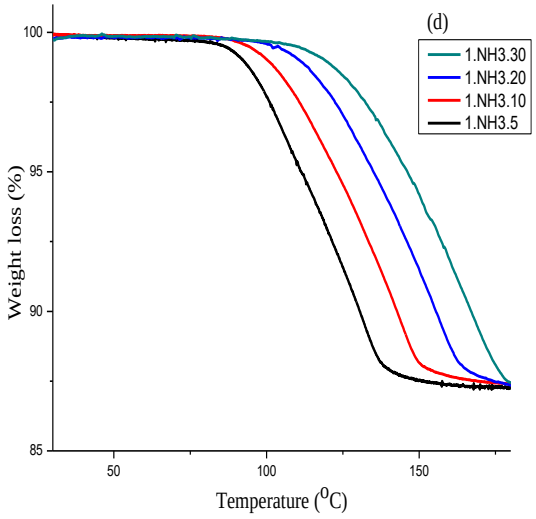
(d)
1.NH3.30
1.NH3.20
1.NH3.10
1.NH3.5
Weight loss (%)
Temperature (°C)

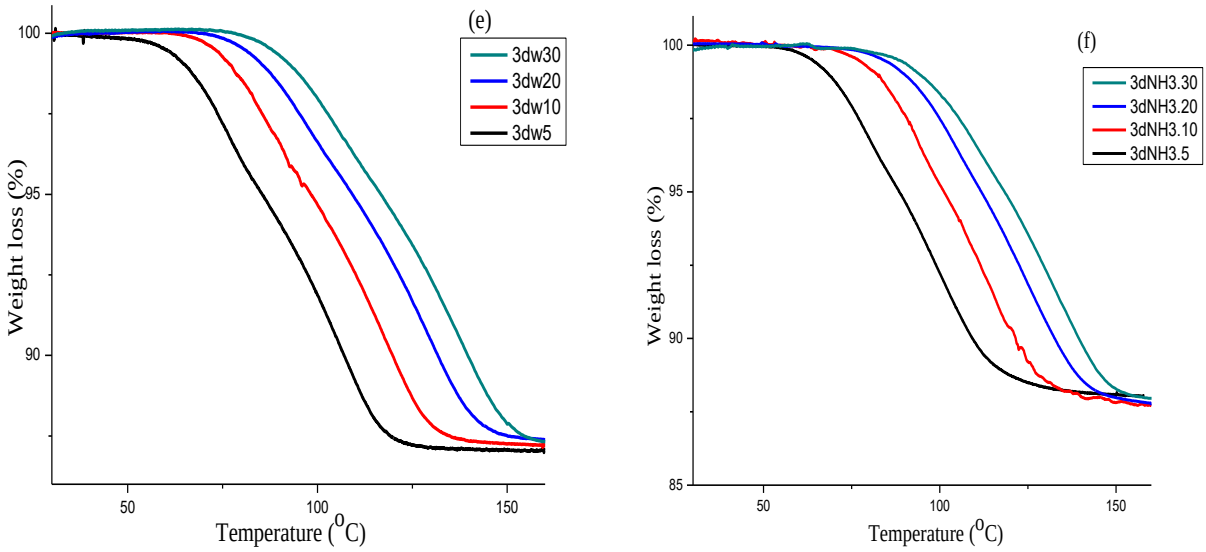

Figure 4.14: *TGA at different heating rates for (a) for removal of DMF from **1**, (b) for removal of DMF from **3**, (c) for removal of H_2O from **1dw**, (d) for removal of NH_3 from **1dHN$_3$**, (e) removal of H_2O from **3dw**, and (f) removal of NH_3 from **3dNH$_3$**.*

Percentage mass losses along with the corresponding temperature at each heating rate were used to determine the activation energy (Ea) according to the equation:

$$\log\beta\alpha = \log(A\alpha\, Ea\alpha/g(\alpha)R) - 2.315 - 0.457(Ea\alpha/RT\alpha) \qquad (2)$$

where βα is the heating rate, Aα is the frequency factor, Eaα is the activation energy, Tα is the temperature at each conversion level, and g(α) refers to the kinetic model. Figure 4.15 presents the plots of logβα versus reciprocal absolute temperature (in the form of 1000/T K^{-1}). Equating the slope to −0.457(Ea/RT) allows one to calculate the activation energies, which are given in Table 4.8.

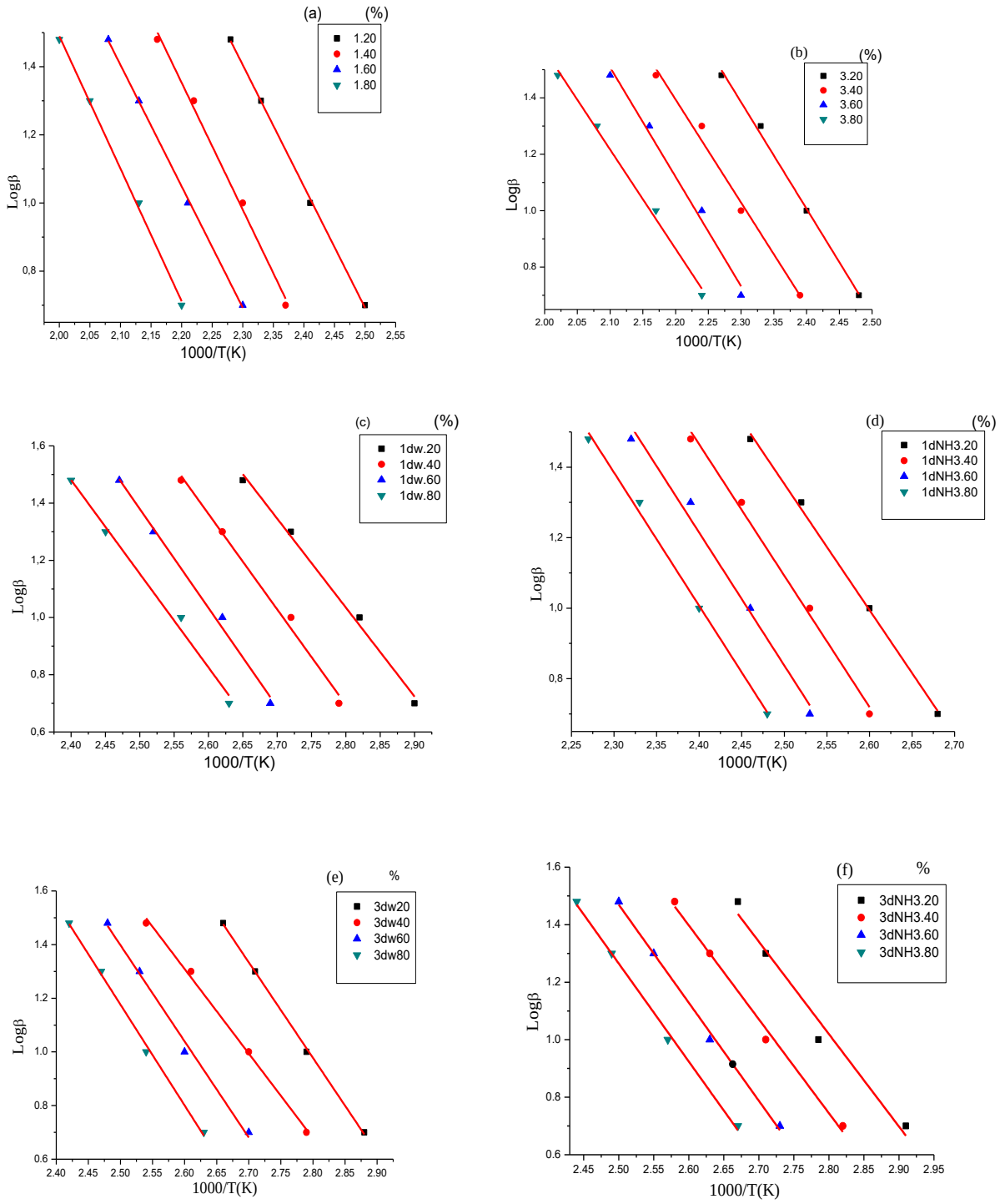

Figure 4.15: *Logarithm of heating rates versus reciprocal absolute temperature of (a)* ***1****, (b)* ***3****, (c)* ***1dw****, (d)* ***1dNH₃****, (e)* ***3dw****, and (f)* ***3dNH₃****.*

Table 4.8: *Activation energy associated with removal of guest molecules*

	E_a (kJ mol^{-1})					
Mass loss (%)	**DMF from 1d**	**DMF from 3d**	**H_2O from 1dW**	**H_2O from 3dW**	**NH_3 from 1dNH_3**	**NH_3 from 3dNH_3**
20	74.77	68.77	77.3	64.78	65. 10	58.46
40	75.31	66.50	72.59	57.35	67.8	59.39
60	72.77	70.57	75.24	65.23	68.61	62.01
80	77.30	64.08	74.75	68.38	68.77	62.01
Mean	**75.04±1.68**	**67.48±2.81**	**74.97±1.93**	**63.94±4.67**	**67.57±1.70**	**60.47±1.82**

The activation energies determined for desorption from **1d** are higher than the corresponding desorption from **3d**. This may be attributed to the difference in the metal centre as well as the solvent-accessible volume of the channels, viz. 549.0 $Å^3$ in **1d** and 571.4 $Å^3$ in **3d**, as the size of the cavities influences the supramolecular interactions possible between host and guest.[17,21] Activation energies associated with the desorption of DMF and H_2O are similar to one another but are higher than that of NH_3. Higher activation energies are generally associated with stronger host-guest interactions. The activation energies for desorption of DMF from **1d** and **3d** are comparable to those reported for the related MOF {[Co(34pba)$_2$]·DMF}n,[21] while the average activation energies for the desorption of H_2O for **1d** and **3d** are also comparable to those reported for [Co(34pba)$_2$] isomers and chromium(III) terephthalate (MIL-101).[20,23] There are no previous reports of desorption of ammonia from MOFs, so we compared our values to those reported for the desorption of NH_3 from Brønsted acid sites in zeolite ZSM-5 derivatives,[24] which were found to have activation energies between 50 and 60 kJ mol^{-1}. Activation energies determined in this study are of the same order of magnitude, suggesting that intermolecular interactions such as hydrogen bonding with the channel walls are of approximately the same strength as those in the zeolites.

4.2.5.2. Isothermal kinetics

The kinetic desorption from **1d** of several halogenated VOCs was performed using an isothermal method. In each case, the compound was held at a temperature a little below its desorption temperature for a period of time until complete desorption had occurred. The experiment was then repeated at a number of close temperatures. Each desorption curve was then fitted against a range of plausible desorption mechanisms,[25] and activation energy (E_a) was determined at each temperature. The results of the conversion vs time curves are shown in Figure 4.16, and the activation energies determined are given in Table 4.9. The kinetics of desorption for dichloromethane, iodine, and dibromomethane were all fitted to a 3D diffusion model. This means that the guest particles interact with the wall of adsorbent in a spherical zone. Recall that **1d** contains 1D channels. The E_a of desorption of dichloromethane and dibromomethane are almost the same while that for iodine is higher. This can be related to the higher temperature range as well as a higher temperature for the desorption of iodine. Similarly, this tendency was reported previously.[5]

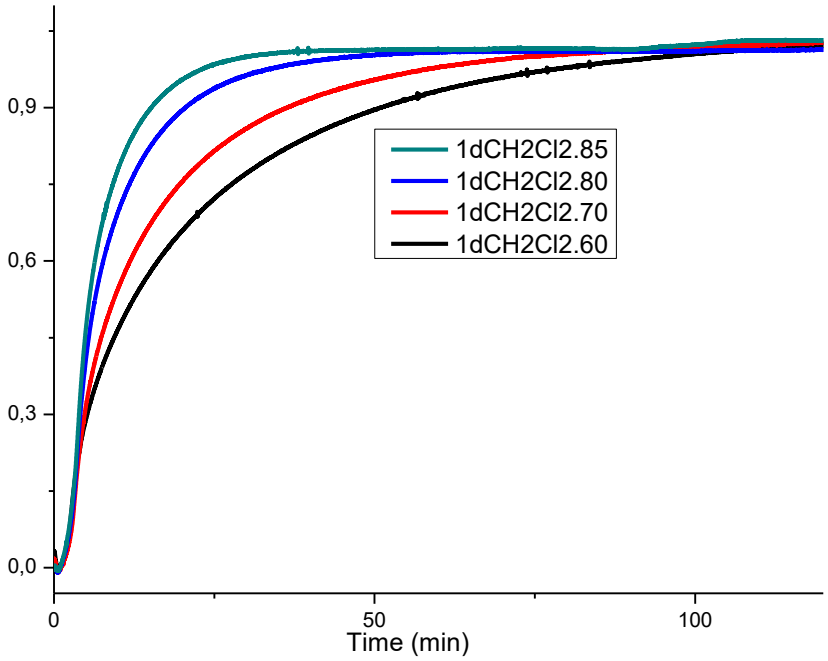
0,9
0,6
0,3
0,0
0
50
100
Time (min)
1dCH2Cl2.85
1dCH2Cl2.80
1dCH2Cl2.70
1dCH2Cl2.60

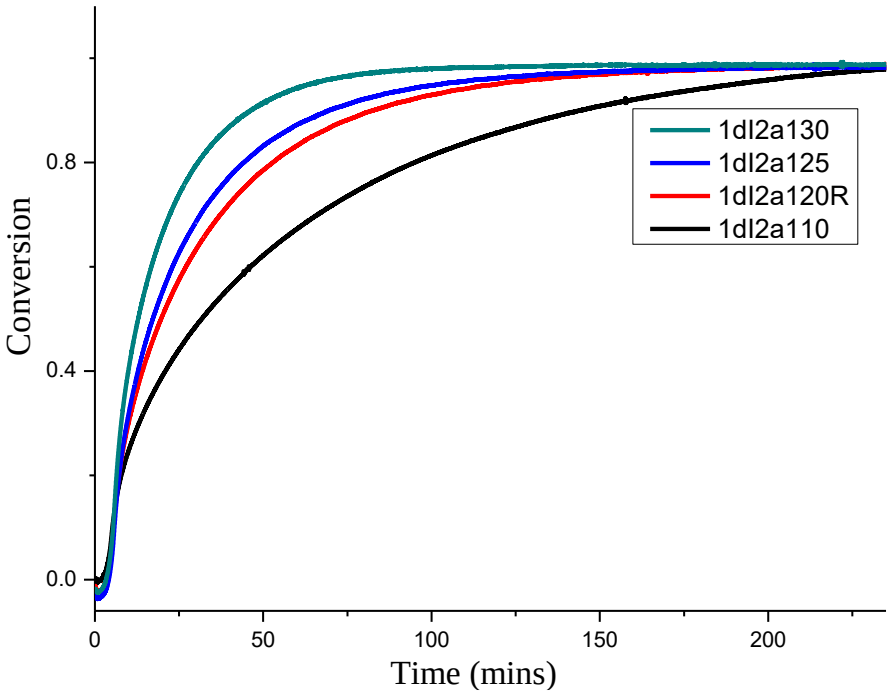
Conversion
0.8
0.4
0.0
0
50
100
150
200
Time (mins)
1dI2a130
1dI2a125
1dI2a120R
1dI2a110

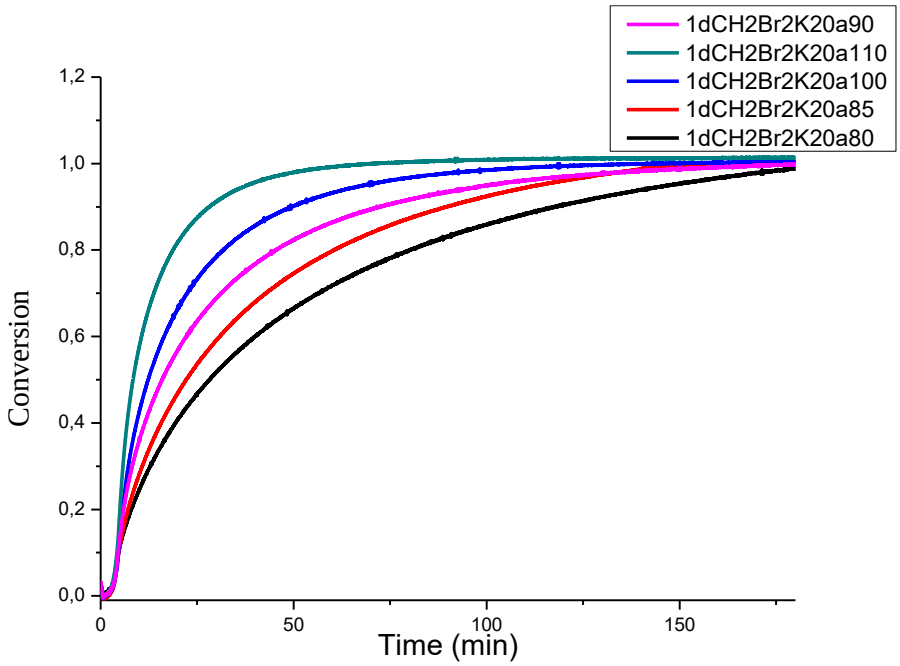

Figure 4.16: *Isothermal curves for desorption of CH_2Cl_2, I_2, and CH_2Br_2 performed at different temperatures.*

Table 4.9: *Activation energy on isothermal removal of CH_2Cl_2, I_2, and CH_2Br_2*

Compound	Ea (kJ/mol)	R^2 Coeff
1dCH_2Cl_2	69.50	0.963
1dCH_2Br_2	68.50	0.6649
1dI_2	76.90	0.898

4.3. SUMMARY

The use of **1d** and **3d** for the adsorption of halogenated and amines VOCs was appreciable. Single crystal X-ray diffraction showed supramolecular interactions of guest-host in the chlorinated samples. Other halogenated and amine VOCs led to crystals with poor quality for single crystal diffraction. It was observed that the halogenated VOCs have stronger interaction within the channels of the framework in the order of VOCs containing iodine > bromine > chlorine. PXRD studies showed a larger phase variation in amines than in halogenated VOCs. The reason for this

was drawn from the fact that amine VOCs showed even amorphous phases. Furthermore, the amines VOCs were characterized by the excess of the loading capacity and this was attributed to their stronger hydrogen bonding. In this regard, $BzNH_2$ was recorded with the highest as it has additional benzene ring stacking interactions. Thus, the nature or polarity of the VOCs plays a role in the interactions within the channels of the adsorbents. Selectivity for chlorinated VOCs from binary mixtures showed that guest solvent with higher vapour pressure was preferentially included. The recovery of **1d** and **3d** was achieved from the new phases, showing the robustness of the adsorbents.

1d showed the chromophoric properties depending on the nature of the guest molecules. To this end, the sorption of iodine in **1d** was characterized by the colour change relative to the amount of iodine in channels. Crystal structure analysis showed that iodine dimers in the channels have stabilizing interactions within the framework. The level of iodine in the adsorbent was also important as it affects structure as indicated by changes in the PXRD patterns. Furthermore, **1d** showed colour change from red to purple on the sorption for H_2O and amine. On the desorption, the purple colour turns to grey and this corresponds to a phase change. The colour changes were recyclable but do not return to **1d**.

The kinetic studies based on the non-isothermal desorption of different guest molecules such as DMF from **1** and **3**, H_2O and NH_3 from both **1d** and **3d** showed comparable activation energies to similar systems. Stronger interaction was recorded in **1d** adsorbent. Also, the isothermal kinetic desorption of I_2, CH_2Cl_2, and CH_2Br_2 from **1d** indicates that iodine requires more energy for the desorption in the range of the reported ones. Moreover, the two adsorbents showed appreciable adsorption for CO_2 and H_2. This study shows that, even though both adsorbents (**1d** and **3d**) showed similar trends, **1d** was showing higher adsorption capacity than **3d**. It was noted that there

is higher guest-host interaction in **1d** than in **3d** influenced by the nature of metal centre and smaller void volume.

4.4. REFERENCES

1. Mehlana, G., Bourne, S. A. & Ramon, G. A new class of thermo- and solvatochromic metal–organic frameworks based on 4-(pyridin-4-yl)benzoic acid. *Dalt. Trans.* **41**, 4224 (2012).

2. Hu, Z., C, Deibert, B. J. & Li, J. Luminescent metal–organic frameworks for chemical sensing and explosive detection. *Chem. Soc. Rev.* **43**, 5815–5840 (2014).

3. Mehlana, G., Bourne, S. A. & Ramon, G. The role of C–H···π interactions in modulating the breathing amplitude of a 2D square lattice net: alcohol sorption studies. *CrystEngComm* **16**, 8160 (2014).

4. Gao, Q., Xu, J., Cao, D., Chang, Z. & Bu, X. H. A Rigid Nested Metal–Organic Framework Featuring a Thermoresponsive Gating Effect Dominated by Counterions. *Angew. Chemie - Int. Ed.* **55**, 15027–15030 (2016).

5. Ndamyabera, C. A., Zacharias, S. C., Oliver, C. L. & Bourne, S. A. Solvatochromism and Selective Sorption of Volatile Organic Solvents in Pyridylbenzoate Metal-Organic Frameworks. *Chemistry (Easton).* **1**, 111–125 (2019).

6. Macrae, C. F., Bruno, I. J., Chisholm, J. A., Edgington, P. R., Mccabe, P., Pidcock, E., Rodriguez-monge, L., Taylor, R., Streek, J. V., Wood, P. A.. Mercury CSD 2.0 – new features for the visualization and investigation of crystal structures. *J. Appl. Crystallogr.* **41**, 466–470 (2008).

7. Davies, K., Bourne, S. A. & Oliver, C. L. Solvent- and Vapor-Mediated Solid-State Transformations in 1,3,5- Benzenetricarboxylate Metal−Organic Frameworks. *Cryst. Growth Des.* **12**, 1999–2003 (2012).

8. Zhou, H. L., Zhang, Y. B., Zhang, J. P. & Chen, X. M. Supramolecular-jack-like guest in ultramicroporous crystal for exceptional thermal expansion behaviour. *Nat. Commun.* **6**, 1–7 (2015).

9. Hwang, Y. K., Hong, D. Y. Chang, J.S., Jhung, S. H., Seo, Y. K., Kim, J., Vimont, A., Daturi, M., Serre, C., Férey, G. Amine grafting on coordinatively unsaturated metal centers of MOFs: Consequences for catalysis and metal encapsulation. *Angew. Chemie - Int. Ed.* **47**, 4144–4148 (2008).

10. Prodi, L., Bolletta, F., Montalti, M. & Zaccheroni, N. Luminescent chemosensors for transition metal ions. *Coord. Chem. Rev.* **205**, 59–83 (2000).

11. Britt, D., Tranchemontagne, D. & Yaghi, O. M. Metal-organic frameworks with high capacity and selectivity for harmful gases. *Proc. Natl. Acad. Sci.* **105**, 11623–11627 (2008).

12. Dybtsev, D. N., Chun, H. & Kim, K. Rigid and Flexible: A Highly Porous Metal–Organic Framework with Unusual Guest-Dependent Dynamic Behavior. *Angew. Chemie* **116**, 5143–5146 (2004).

13. Kim, H., Kim, S., Kim, J. & Ahn, W. Liquid phase adsorption of selected chloroaromatic compounds over metal organic frameworks. *Mater. Res. Bull.* **48**, 4499–4505 (2013).

14. Thommes, M., Kaneko, K., Neimark, A. V., Olivier, J. P., Rodriguez-Reinoso, F., Rouquerol, J., Sing, K. S. W. Physisorption of gases, with special reference to the evaluation of surface area and pore size distribution (IUPAC Technical Report). *Pure Appl. Chem.* **87**, 1051–1069 (2015).

15. Yang, Q., Lama, P., Sen, S., Lusi, M., Chen, K., Gao, W., Shivanna, M., Pham, T., Hosono, N., Kusaka, S., Iv, J. P., Ma, S., Space, B., Barbour, L. J., Kitagawa, S., Zaworotko, M. J.Reversible Switching between Highly Porous and Nonporous Phases of an Interpenetrated Diamondoid Coordination Network That Exhibits Gate-Opening at Methane Storage Pressures. *Angew. Chemie - Int. Ed.* 5684–5689 (2018).

16. Gcwensa, N., Chatterjee, N. & Oliver, C. L. Interchanged Hysteresis for Carbon Dioxide and Water Vapor Sorption in a Pair of Water-Stable, Breathing, Isoreticular, 2-Periodic, Zn(II)-Based Mixed-Ligand Metal-Organic Frameworks. *Inorg. Chem.* **58**, 2080–2088 (2019).

17. Khuong, T., Ramsahye, N. A., Trens, P., Tanchoux, N., Serre, C., Fajula, F., Férey, G. Microporous and Mesoporous Materials Adsorption of C5 – C9 hydrocarbons in microporous MOFs MIL-100 (Cr) and

MIL-101 (Cr): A manometric study. *Microporous Mesoporous Mater.* **134**, 134–140 (2010).

18. Chatterjee, N. & Oliver, C. L. A Dynamic, Breathing, Water-Stable, Partially Fluorinated, Two-Periodic, Mixed-Ligand Zn(II) Metal-Organic Framework Modulated by Solvent Exchange Showing a Large Change in Cavity Size: Gas and Vapor Sorption Studies. *Cryst. Growth Des.* **18**, 7570–7578 (2018).

19. Yin, Z., Wang, Q. X. & Zeng, M. H. Iodine release and recovery, influence of polyiodide anions on electrical conductivity and nonlinear optical activity in an interdigitated and interpenetrated bipillared-bilayer metal-organic framework. *J. Am. Chem. Soc.* **134**, 4857–4863 (2012).

20. Dzesse T, C. N., Nfor, E. N. & Bourne, S. A. Vapor Sorption and Solvatochromism in a Metal-Organic Framework of an Asymmetric Pyridylcarboxylate. *Cryst. Growth Des.* **18**, 416–423 (2018).

21. Mehlana, G., Bourne, S. A., Ramon, G. & Öhrström, L. Concomitant metal organic frameworks of cobalt(II) and 3-(4-pyridyl) benzoate: Optimized synthetic conditions of solvatochromic and thermochromic systems. *Cryst. Growth Des.* **13**, 633–644 (2013).

22. Ozawa, T. A New Method of Analyzing Thermogravimetric Data. *Bull. Chem. Soc. Jpn.* **38**, 1881–1886 (1965).

23. Xian, S., Yu, Y., Xiao, J., Zhang, Z., Xia, Q., Wang, H., Li, Z. Advances Competitive adsorption of water vapor with VOCs dichloroethane , ethyl acetate and benzene on. *RSC Adv.* **5**, 1827–1834 (2014).

24. Costa, C., Dzikh, I. P., Lopes, M. & Lemos, F. Activity–acidity relationship in zeolite ZSM-5. Application of Bronsted-type equations. *Mol. Catal. A* 193–201 (2000).

25. Khawam, A. & Flanagan, D. R. Solid-state kinetic models: Basics and mathematical fundamentals. *J. Phys. Chem. B* **110**, 17315–17328 (2006).

CHAPTER 5. REMOVAL OF INCLUDED WATER FROM *cis*-$[Co(en)_2Cl_2]Cl \cdot H_2O$ BY METHANOL

5.1. INTRODUCTION

In 2005, Saha and Bernal reported the interconversion of several hydrated forms in a cobalt(II) complex with triethylenediamine. Starting with [*cis*-α-(tri**en**)$CoCl_2$]Cl·$3H_2O$ (tri**en**: triethylenediamine) in which the water of hydration was stabilized in the channels through water-chloride interactions,[1] a series of different hydrated forms could be obtained by varying factors such as humidity and temperature. In this chapter, an investigation was carried out on the related compound *cis*-[$Co(en)_2Cl_2$]Cl·H_2O (where **en**: is ethylenediamine) (**Coen·H_2O**) to determine whether a similar process might occur. Furthermore, we investigated whether, in the presence of water, only the monohydrate or a range of hydrates can be formed, as well as the ability of the dried material to absorb a range of organic solvents. The activation energy associated with the removal of one water molecule was determined using a non-isothermal thermogravimetric method.[2]

The synthesis of **Coen·H_2O** was performed according to a previous report.[3] In a vial, 1 mL of 70% (0.10 mol/L) solution of **en** was added to a solution of 1.6 g of $CoCl_2·6H_2O$ in 12 mL of water. Oxygen was passed through the solution with stirring for 6 h and then the system was left open to the air for 1 h. 8 mL (0.8 mol/L conc.) HCl was added and the solution was then evaporated upon heating at 90 ^oC until 6 mL remained. The resulting green solution was left in a vented vial for three days to collect green crystals of *trans*-[$CoCl_2(en)_2$]Cl (previously reported, CSD refcode ETDCOC).[4] The crystals were washed with ethanol followed by ether and dried at 110 ^oC for 2 hrs. The solid was then dissolved in 6 mL of water and evaporated to 2 mL on heating in a water bath. Purple crystals of *cis*-[$Co(en)_2Cl_2$]Cl·H_2O (**Coen·H_2O**) were formed after 5 days. Crystals of **Coen·H_2O** were heated under vacuum at 120 ^oC for four hours. However, water guest molecules

could not be removed from the channels. Thus, we attempted to displace the water molecules by leaving crystals of **Coen·H_2O** in the environment of different solvent vapours.

5.2. CHARACTERIZATION AND SORPTION STUDY

5.2.1. Crystal structures and exposure to methanol vapour

A search of the Cambridge Structural Database (CSD)[5] found that the [$Co(en)_2Cl_2$] has been reported over 40 times, but only CENCOC[6] and CLECOC[7] correspond to *cis*-[$Co(en)_2Cl_2$]Cl·H_2O and are thus directly comparable to **Coen·H_2O**. In addition to those two structures, a sesquihydrate was reported by Bernal and Lalancette in 2020.[8] The isomer *trans*-[$Co(en)_2Cl_2$] has also been reported as the chloride (ETDCOC[4]) and the chloride monohydrate (ETDCOH[9]).

Coen·H_2O crystallises in the monoclinic system in space group $P2_1/n$. Cobalt centres are octahedrally coordinated by two **en** in a wing-like shape and two chloride ions (Figure 1a). Two nitrogen donor atoms from each **en** coordinate Co^{3+} centres. One wing-like (**en**) is almost in the right angle from the adjacent wing. Similarly, two chloride ligands make almost a right angle between themselves. The complexes contain chlorides as counter ions and water as guest molecules. **Coen·H_2O** is most similar to CLECOC but less similar to CENCOC. By comparing the packing diagrams in Figure 5.1 viewed onto the *a*-*c* plane, two adjacent complex units are oriented in the opposite direction for **Coen·H_2O** while they are oriented in the same direction for CLECOC. However, their unit cells are similar except the lengthening of the *c* axis. CENCOC has unit cell dimensions which are different from those in both CLECOC and **Coen·H_2O**, and the crystal structure has two independent structural complexes in its asymmetric unit.[6]

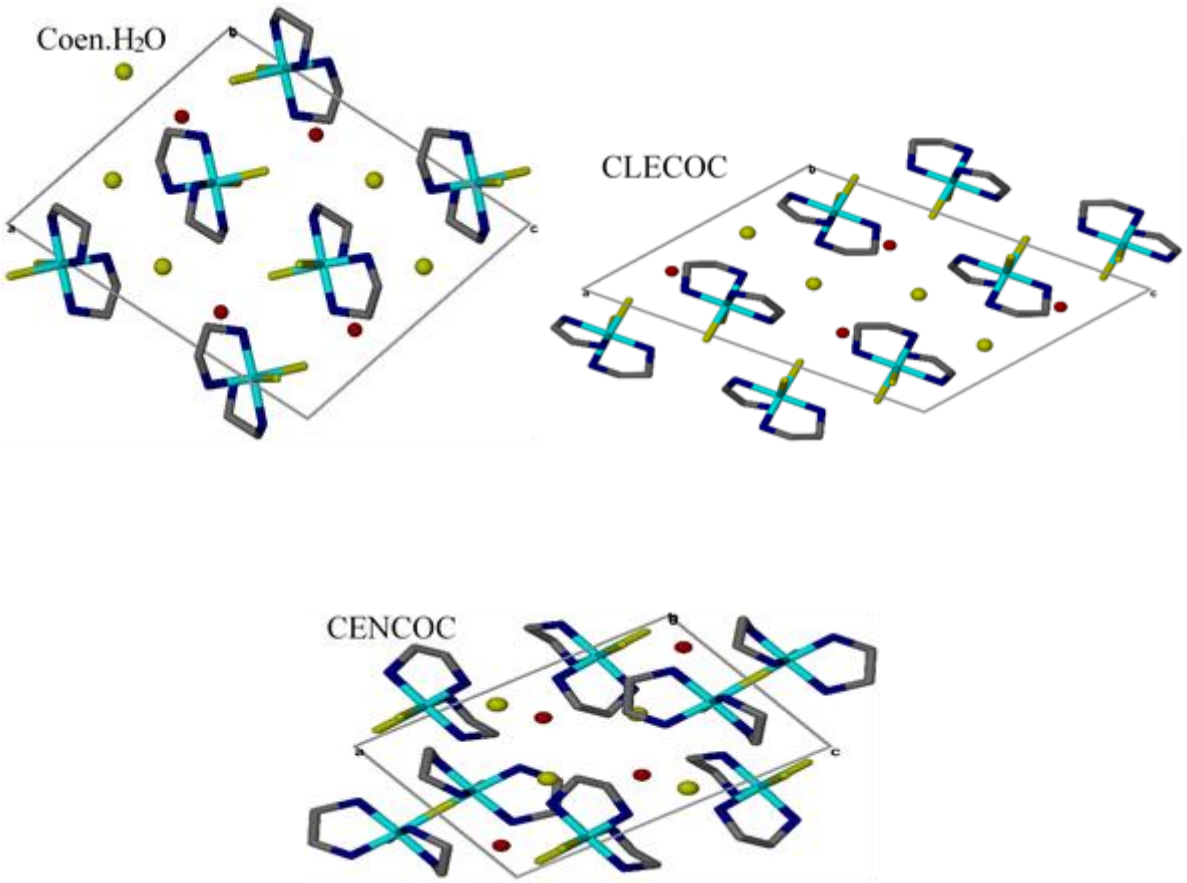

Figure 5.1: *Comparison of the packing of cis-$[Co(en)_2Cl_2]Cl{\cdot}H_2O$ structures as packed viewed onto the a-c plane.*

Coen·H_2O was then exposed to various organic solvent vapours for 1 to 5 days at 40 ^oC (Table 5.1). The effect of exposure was only observed in the experiment (Expt) 2, 3, and 11 and these were characterized by PXRD and TGA, while DFT calculations were used to attempt to rationalize the results.

Table 5.1: *Performed experiments of the exposure of* ***Coen·H₂O*** *to different solvent vapours*

Experiment (Expt)	Exposure to the vapours	Period	Results
1	$[Co(en)_2Cl_2]Cl·H_2O$	-	**Coen·H₂O**
2	Coen·H_2O in methanol	2 day	**Coen**
3	Coen in H_2O	1 day	**Coen·H₂O**
4	Coen·H_2O 10 mins after heating at 180 ^oC	10 mins in air	**Coen·H₂O**
5	Coen·H_2O in H_2O	1 day	**Coen·H₂O**
6	Coen·H_2O in ethanol	5 days	**Coen·H₂O**
7	Coen·H_2O in propanol	5 days	**Coen·H₂O**
8	Coen·H_2O in acetonitrile	5 days	**Coen·H₂O**
9	Coen·H_2O in toluene	5 days	**Coen·H₂O**
10	Coen·H_2O in benzonitrile	5 days	**Coen·H₂O**
11	Coen·H_2O in methylamine	1 day	**Coen·ma**
12	Coen.ma in H_2O	1 day	**Coen·ma**

Experiment 2 was the exposure of **Coen·H₂O** to methanol vapour (MeOH) to form a new crystal of **Coen**. The coordination in the latter crystal is similar to that of **Coen·H₂O**, Figure 2a and b. The crystal structure of **Coen** differs from **Coen·H₂O** in the absence of H_2O molecule in channels as characterized by SCXRD. They have the same crystal system as in **Coen·H₂O** (monoclinic in $P2_1/n$ space group). However, its unit cell is different from that of **Coen·H₂O** (Table 5.2). Selected bond lengths between nitrogen and cobalt centre were recorded in Table 5.3 and are in the expected range. Some differences in the two structures were observed as the higher bond length of Co1-N2B in **Coen** was 1.976(3) Å while the one of Co1-N2B in **Coen·H₂O** was 1.951(1) Å.

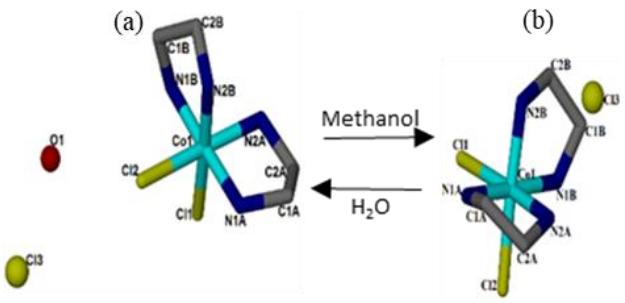

Figure 5.2: *(a) As made cis dichloro-bis(en)cobalt(III) chloride monohydrate (**Coen·H_2O**), and (b) its corresponding anhydrous form (**Coen**). Note that hydrogen atoms are omitted for clarity.*

Table 5.2: *Crystal data and refinement parameters*

Compound	ETDCOC	**Coen·H_2O**	**Coen**	CLECOC	CENCOC
Empirical formula	$[Co(C_2N_2H_8)_2Cl_2]Cl$	$[Co(C_2N_2H_4)_2Cl_2]Cl·H_2O$	$[Co(C_2N_2H_4)_2Cl_2]Cl$	$[Co(C_2N_2H_8)_2Cl_2]Cl·H_2O$	$[Co(C_2N_2H_8)_2Cl_2]Cl·H_2O$
Mass ($g.mol^{-1}$)	285.51	303.51	285.49	303.51	303.51
Crystal size (mm^3)		0.120 x 0.160 x 0.210	0.020 x 0.060 x 0.090		
Temperature/K	283-303	293(2)	293(2)	NA	NA
Crystal system	Monoclinic	Monoclinic	Monoclinic	Monoclinic	Monoclinic
Space group	$P2_1/a$	$P2_1/n$	$P2_1/n$	$P2_1/c$	$P2_1$
a/Å	9.490	11.9297(17)	7.3661(8)	12.000	12.070(8)
b/Å	8.960	6.7924(9)	7.7791(9)	6.870	11.520(7)
c/Å	6.260	14.3691(19)	19.604(2)	16.480	8.330(5)
B (º)	109.27	103.644(3)	95.012(2)	122	96.9(2)
$V/Å^3$	502.468	1131.5(3)	1119.1(4)	1152.168	1149.868
Z	4	4	4	4	4
$D_c/g\ cm^{-3}$		1.7814	1.6943		
$\mu(Mo{-}K\alpha)/mm^{-1}$		0.71073	0.71073		
F(000)		624	584		
range scanned, θ/°		2.001 - 33.662	2.819 - 28.336		
index ranges (h, k, l)		-17 - 17, -10 - 6, -20 – 21	-9 - 9, -10 – 10, -26 - 26		
no. reflections collected		18073	21806		
no. unique reflection		3975	2789		
no. reflections with I >2σ(I)		3355	2169		
data/parameters refine		121	109		
GooF		1.021	1.033		
final R indices		R1 = 0.0265	R1 = 0.0409		
(I >2σ(I))		WR2 = 0.0535	WR2 = 0.0981		
Final R indices (all data)		R1 = 0.0358	R1 = 0.0599		
		WR2 = 0.0572	WR2 = 0.1093		
min, max e density/e $Å^{-3}$		-0.724, 0.579	-1.021, 0.866		

Table 5.3: *Comparison between lengths in the coordination of nitrogen (from ethylenediamine) to cobalt for both* **Coen·H_2O** *and* ***Coen***

Coen·H_2O		**Coen**	
Coordination	Distance (Å)	Coordination	Distance (Å)
Co1-N1A	1.959(1)	Co1-N1A	1.949(3)
Co1-N2A	1.956(1)	Co1-N2A	1.965(3)
Co1-N1B	1.958(1)	Co1-N1B	1.967(3)
Co1-N2B	1.951(1)	Co1-N2B	1.976(3)

Figure 5.3 shows weak interactions between H_2O molecule with both chloride ion and a hydrogen atom from the **en** ligand. This shows that the presence of H_2O molecules in the channels of **Coen·H_2O** was stabilised by its supramolecular interactions with the chloride anions similarly as was observed in [cis-α-(triethylenetetramine)$CoCl_2$]Cl·3H_2O.[1] Selected torsion angles in CA-NA-Co-NB showed the differences in both structures (Table 5.4). Depending on the properties of the coordination complex, the removal of guest molecules from the channels can cause the change in crystal parameters[10,11] or even shrinking.[12]

Table 5.4*: Torsion angles in* ***Coen*** *and* ***Coen·H_2O***

Coordination Compound	**Coen·H_2O**	**Coen**
Angle (°)		
C1A-N1A-Co1-N2B	-85.4	-79.2
C2B-N2B-Co1-N1A	-162.0	-168.3
C2A-N2A-Co1-N1B	-157.0	-166.4
N2A-Co1-N1B-C1B	-101.9	-76.5

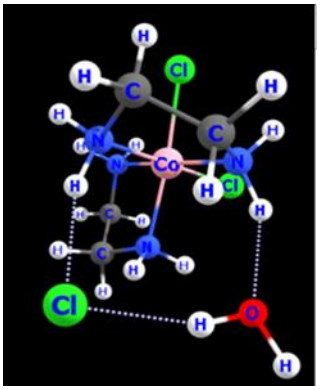

Figure 5.3: *Interactions involving H_2O with channels of cis-dichloro-bis(ethylenediamine)cobalt(III) chloride.*

DFT was used to understand the mechanism of the interaction between H_2O and methanol (MeOH) in the channels. The calculations showed that there is a possibility that three molecules of MeOH could exert hydrogen bonding with one H_2O molecule to form $H_2O{\cdot}3MeOH$ complex as shown by Figure 5.4. Literature on the similar complexations states that the structural formula depends on the ratios of both H_2O and MeOH in the media.[13,14]

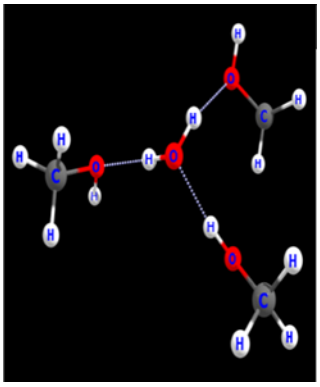

Figure 5.4: *Possible interactions between H_2O and methanol.*

Using Gaussian Density Functional Theory (DFT),[15] energies involving the interactions of guest molecules in the channel were determined. Total energies involved in the interaction between **H_2O-Coen·H_2O** channels (E_{INT} - Coen·H_2O) and energies between **H_2O-MeOH** (E_{INT} - MeOH) were different (Table 5.5). As explained in the experimental section, 6-311++G(d,p) provides more

accurate results, where E_{INT} - MeOH = -19.80 kcal mol^{-1} has more interaction energy than E_{INT}- Coen = -16.91 kcal mol^{-1}, thus suggesting that the interactions in **H_2O-MeOH** complex were stronger than those in **H_2O-Coen·H_2O** complex. It was assumed that the formed complex decomposed into CO_2 and H_2 gases which could easily be evacuated from the channels to form **Coen** leaving empty channels. This can be related to the previously reported reaction of H_2O and MeOH to produce CO_2 and H_2 upon heating under $Cu/ZnO/Al_2O_3$ catalyst.[16]

Table 5.5: *Comparison of interaction energies between H_2O and both **Coen·H_2O** channels and methanol*

Interaction	cc-pVDZ	6-311++G(d,p) (kcal mol^{-1})
E_{INT}-Coen	-17.47	-16.91
E_{INT}-MeOH	-19.30	-19.80

The Gaussian calculations also allowed the determination of lattice energy for both crystal structures as shown in Table 5.6. The calculated difference in lattice energies showed that **Coen·H_2O** has a more negative lattice energy (-158.702 kcal mol^{-1}) than **Coen** (-102.025 kcal mol^{-1}). These results are supporting the fact that **Coen** could easily adsorb H_2O even in a short period for a reversible sorption process forming **Coen·H_2O**. Obtaining the latter compound from the reversible reaction, it is safe to assume that the wings of the ligand are flexible to exhibit a dynamic motion in the presence of guest H_2O.[1] Thus, higher lattice energy in **Coen·H_2O** indicates a more stable phase compared to the one of **Coen**.

Table 5.6: *Difference lattice energy in both **Coen·H_2O** and **Coen***

Structure	Periodic energy (Hartrees)	Lattice energy (Hartrees)	difference in lattice energy (Hartrees)	difference in lattice energy (kcal mol^{-1})
Coen·H_2O	-12880.8	-12880.6	-0.25191	-158.702
Coen	-12575.2	-12575.0	-0.16195	-102.025

Figure 5.5 (a) shows the thermal behaviour of **Coen·H_2O** and its corresponding derivative phases from the effect of methanol and water reabsorption. The mass loss of 6.3% at 120 ^oC in **Coen·H_2O** corresponds to the removal of one H_2O molecule (calculated mass loss 6.0%). **Coen** did not show any mass loss and this confirms the absence of any guest molecule in the SCXRD structure. However, the mass losses in Expt 3 and Expt 4 were found to be 5.94%, closer to that in **Coen·H_2O.** Therefore, this mass loss confirmed the reversible uptake of H_2O by **Coen**.

Coen·H_2O and **Coen** (Figure 5.5 (b)) were also analyzed using DSC. The endothermic peak between 90 and 147 ^oC corresponds to the desorption of H_2O from **Coen·H_2O**. The DSC for **Coen** is featureless until the melt. Both **Coen·H_2O** and **Coen** show endothermic peaks at 245 and 252 °C respectively, which correspond to melting followed by decomposition.

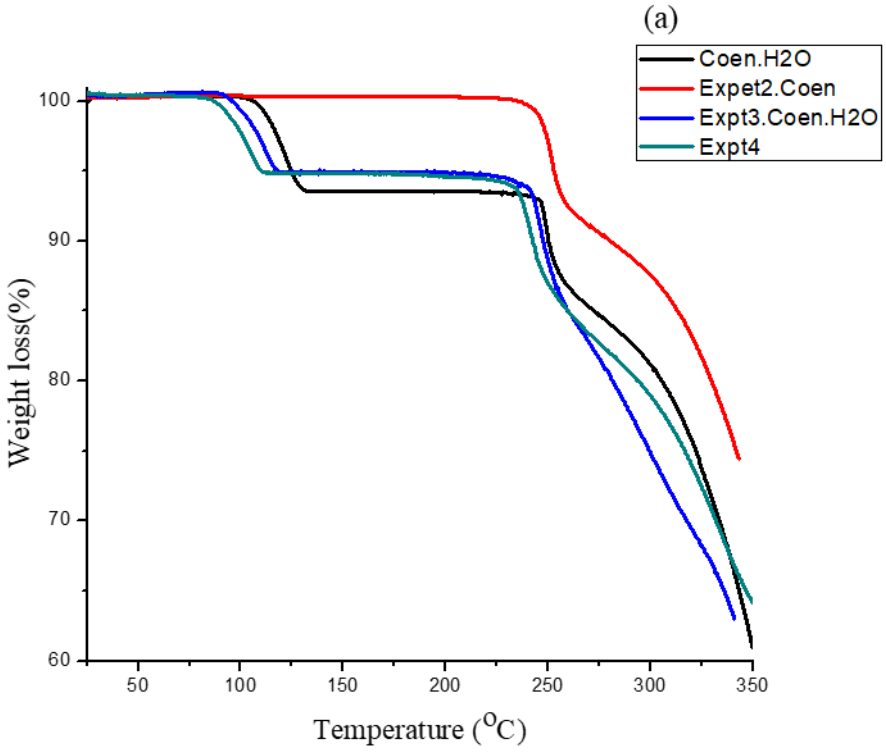

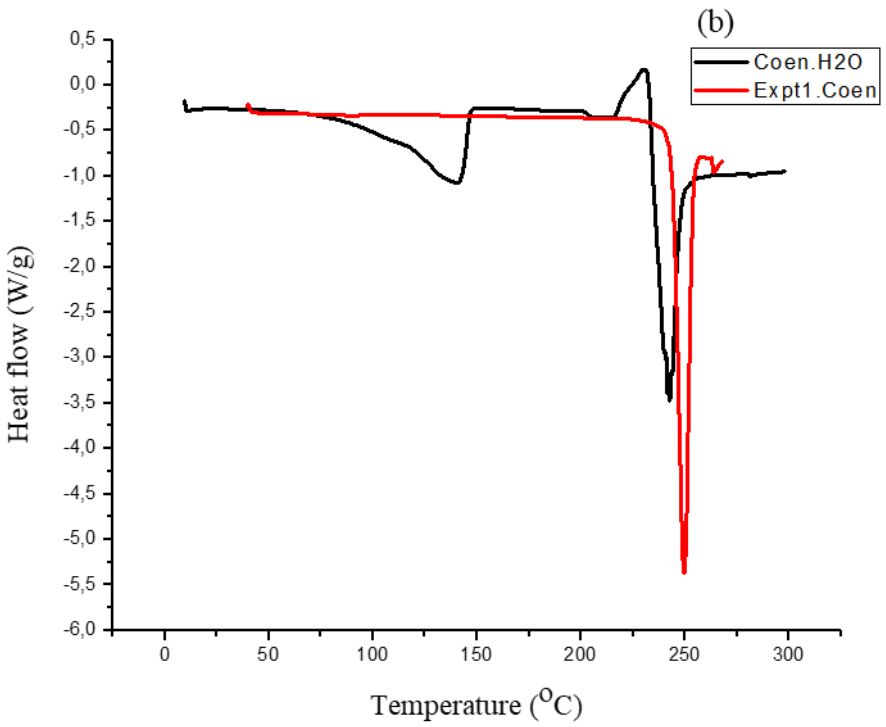

***Figure 5.5**: TGA (a) and DSC (b) curves of both **Coen·H₂O**, **Coen**, and derivative phases.*

PXRD patterns in Figure 5.6 shows that the transformation of **Coen·H₂O** to **Coen** is characterized by the disappearance of a peak at 8.8°, and the emergence of a new peak at 13.3°. This is attributed to the absence of H_2O in channels and the shortening in the unit cell *a* and *b* axes and the lengthening *c* axis. It might also be linked to some dissimilarities in torsion angles and related change of the parameters of the crystal structure as shown above. On the other hand, these peaks reappear in **expt3.Coen·H₂O** (after H_2O reabsorption) to show the recovery of the original phase, **Coen·H₂O**.

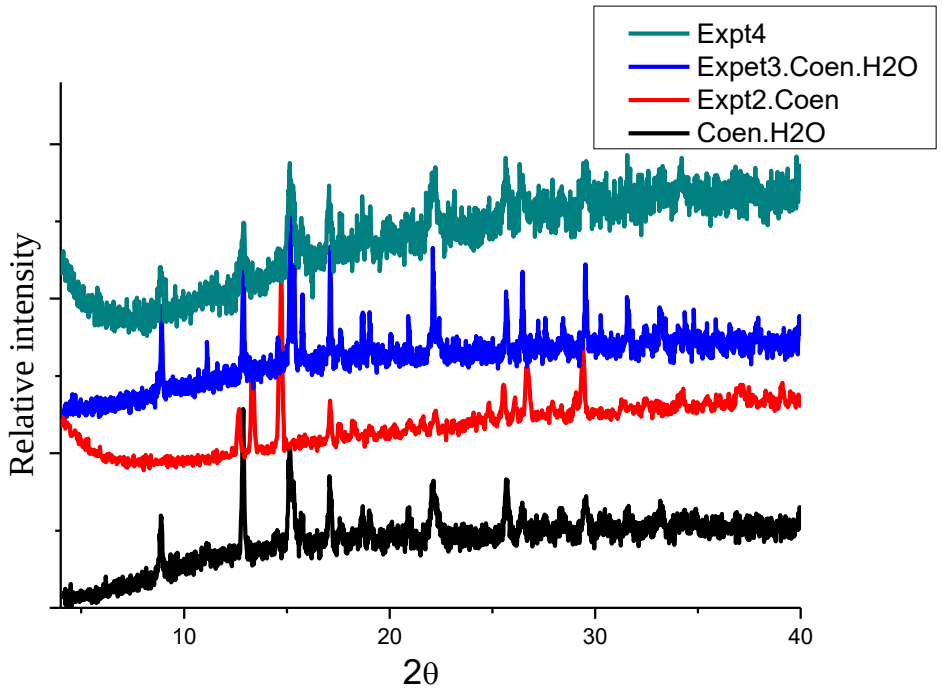

Figure 5.6: *Effect of methanol on* ***Coen·H₂O*** *and water reversible*

The effect of MeOH could be explained by its smaller kinetic diameter (Table 5.7) than other solvents which may make it easier to enter into the channels. Furthermore, it reacted with H_2O due to its higher polarity.[17] The size[18] and nature of the guest molecules[19,20] are reported among the factors that influence the sorption process.

Table 5.7: *Kinetic diameter of solvents which is among factors that govern their sorption*

Solvent	**Kinetic diameter (Å)**	**Ref**
Methanol	3.6	[21]
Ethanol	4.5	[21]
Propanol	4.7	[21]
Acetonitrile	4.3	[21]
Toluene	5.25	[22]
Benzonitrile	> 5.25	[21]

The kinetic diameter of benzonitrile might be higher than that of toluene.

5.2.2. Exposure of Coen·H_2O to other organic solvent vapours

Figure 5.7 shows that the weight loss in **Expt5** (5.9 %) is close to that of freshly made **Coen·H_2O**, thus confirming quick reabsorption of H_2O into **Coen**. For **Expt6**, **Expt7**, **Expt8**, **Expt9**, and **Expt10**, which correspond to exposure of **Coen·H_2O** to various solvent vapours, the mass loss (6.2 %) is similar to that in **Coen·H_2O**. The sample exposed to methylamine, **Expt11.Coen·ma**, showed a mass loss of 3.8 % while **Expt12.Coen·ma1** had a close mass loss of 3.2 %.

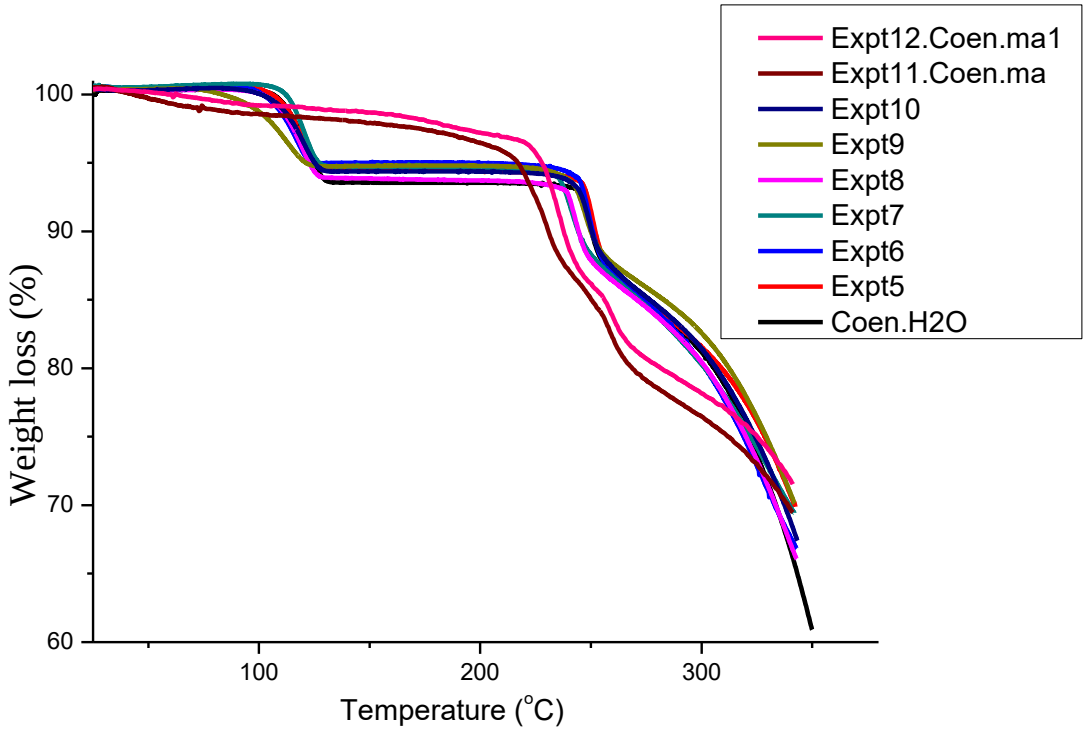

Figure 5.7: *TGA curves of* ***Coen·H_2O*** *and corresponding forms of* ***Expt5***, ***Expt6***, ***Expt7***, ***Expt8***, ***Expt9***, ***Expt11.Coen·ma***, *and* ***Expt12.Coen·ma1***.

Figure 5.8 illustrates PXRD patterns of **Coen·H_2O** and its exposure on water, ethanol, propanol, toluene, acetonitrile, and benzonitrile. As in TGA results, there is no observable change of patterns except in **Expt11.Coen·ma**. Thus, the absence of any effect of these solvents is confirmed. On the

other hand, **Expt11.Coen·ma** shows a new phase. Its exposure to water vapour does not show any PXRD change so the reversible change to **Coen·H_2O** does not occur.

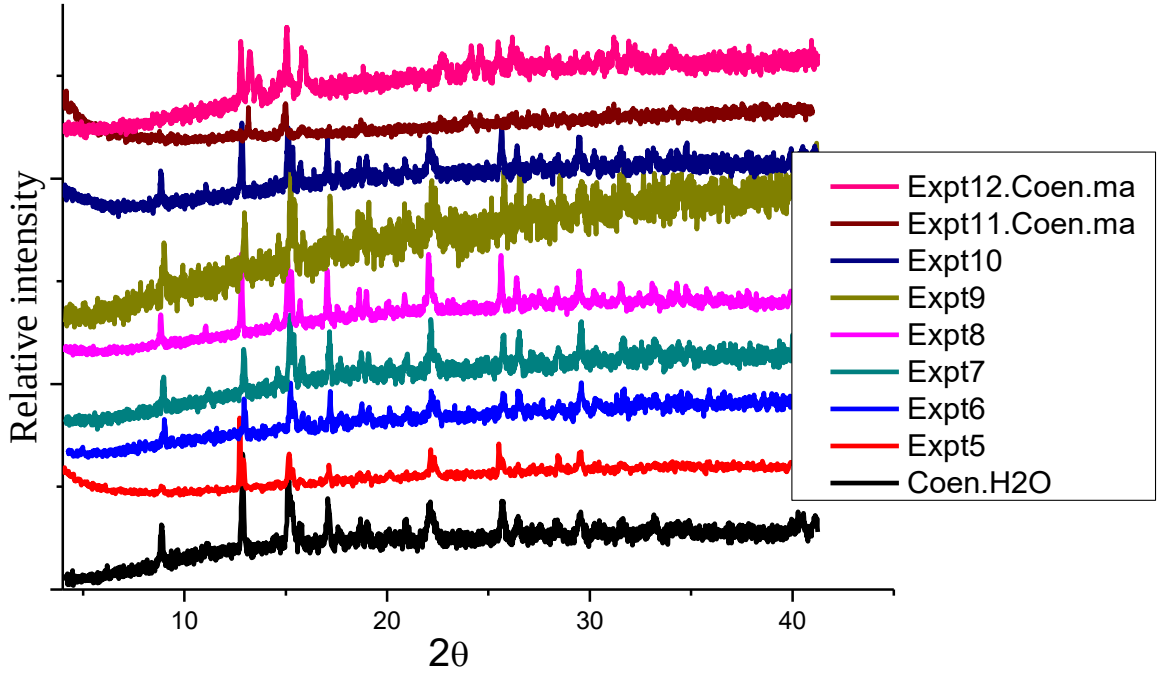

Figure 5.8: *PXRD patterns of* ***Coen·H_2O****, and its corresponding forms of* ***Expt5****,* ***Expt6****,* ***Expt7****,* ***Expt8****,* ***Expt9****,* ***Expt11.Coen·ma****, and* ***Expt12.Coen·ma1****.*

Solvents such as ammonia, methylamine, propylamine, and butylamine were reported to coordinate with **Coen·H_2O** by replacing coordinated chloride from cobalt centre.[23] In general, alkylamines are the simplest donors which offer the possibility to coordinate on metals and form complexes.[24] They have a strong nucleophilic attack which can allow them to replace some existing ligands.[25] Methylamine does so (**Expt11.Coen·ma**), to give unit cell parameters that match those of ZIXMAU, the methylamine adduct of **Coen**. To the best of our knowledge, this process of coordination did not occur for alcohol, acetonitrile, and toluene.

5.2.3. Kinetics of desorption of water from Coen·H_2O

The kinetics of the desorption of H_2O from **Coen·H_2O** was investigated following the model established by Ozawa to determine the activation energy (Ea) involved.[2] Using TGA, four different heating rates of 5, 10, 20, and 30 $^oC\ min^{-1}$ were used from room temperature to 180 ^oC as shown in Figure 5.9(a). Figure 5.9(b) illustrates the plotting of logarithm of heating rates versus reciprocal absolute temperature (in the form of $1000/T\ K^{-1}$) associated with the removal of H_2O molecule. The percentage weight loss along with the corresponding temperature for each heating rate allows one to determine the Ea using Equation 1:

$$\log\beta_\alpha = \log(A\alpha Ea\alpha/g(\alpha)R) - 2.315 - 0.457\ (Ea_\alpha/RT_\alpha) \qquad \textbf{Equation 1}$$

where β_α is the heating rate, $A\alpha$ is the frequency factor, $Ea\alpha$ is the activation energy, T_α is the temperature at each conversion level, and $g(\alpha)$ refers to the kinetic model. The thermogravimetric traces were converted to the extent of the reaction (α) versus temperature curves. The Ea was then determined by plotting $\log\beta_\alpha$ versus $1000/T_\alpha$. By equating the slopes of the curves to $0.457\frac{Ea}{8.314JK^{-1}mol^{-1}}$, the average of calculated Ea corresponded to 58.77 ± 0.64 kJ mol^{-1}.

This value corresponded to the necessary energy to break down the weak interactions which hold the water molecule in the channel. It was in the range of $59.1 - 68.6\ kJ\ mol^{-1}$ that had been reported for the dehydration of $\{[Co(34pba)_2]\}_n \cdot H_2O$ (34pba = 3-(4-pyridyl)benzoate).[26] Slight difference in the activation energies for both **Coen·H_2O** and $\{[Co(34pba)_2]\}_n \cdot H_2O$ could be attributed to the difference in supramolecular interactions between H_2O within the channels of specific compounds.[1,26]

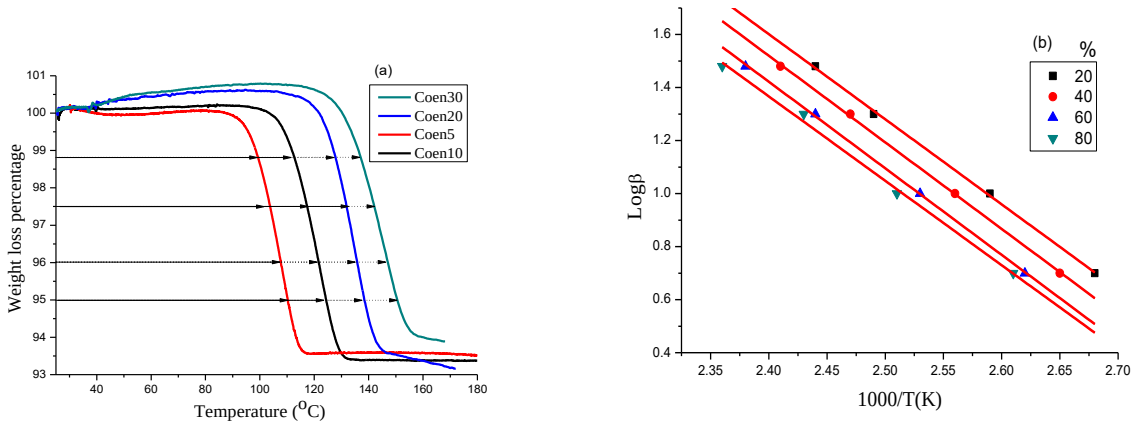

Figure 5.9: *(a) Desorption of H_2O molecules by* ***Coen·H₂O*** *at 5 K/min, 10 K/min, 20 K/min, and 30 K/min heating rates, (b) Plots of logarithm of heating rates versus reciprocal temperature in Kelvin for desorption of H_2O.*

5.3. SUMMARY

Monohydrate **Coen·H₂O** did not form any other hydrated forms in the presence of water vapour. Through supramolecular interactions, MeOH reacted with H_2O to result in empty channels of a new single crystal as **Coen**. The calculated lattice energy in **Coen·H₂O** (-158.702 kcal mol^{-1}) is more negative than that in **Coen** (-102.025 kcal mol^{-1}). Thus, **Coen** could be rehydrated and returned to the more stable **Coen·H₂O**. Kinetic studies associated with non-isothermal desorption of H_2O gave a value of 58.77 ± 0.64 $kJmol^{-1}$ for the activation energy. The remaining tested organic solvents neither displaced nor removed water from the channels. Therefore, the sensitivity of **Coen·H₂O** to MeOH could be due to factors such as higher polarity and lower kinetic diameter of MeOH. However, a similar structure, [cis-α-(triethylenetetramine)-$CoCl_2$]Cl could form a range of hydrated forms depending on the amount of water vapour environment. One may assume that the existence of an additional ethyl group changes can influence the formation of hydrated forms. **Experiment 12** shows that **Coen·ma** did not revert to **Coen·H₂O** when exposed to H_2O vapour as methylamine has strong coordination with the Co^{3+} centre.

5.4. REFERENCES

1. Saha, M. K. & Bernal, I. Environment-controlled switching between cyclic hexamer and helical conformations of a water chloride cluster : An old compound viewed in a new perspective. *Inorg. Chem. Commun.* **8**, 871–873 (2005).

2. Ozawa, T. A New Method of Analyzing Thermogravimetric Data. *Bull. Chem. Soc. Jpn.* **38**, 1881–1886 (1965).

3. Casadesus, M., Coogan, M. P., Davies, E. & Ooi, L. ling. Stereochemical studies of cobalt ethylenediamine complexes and their tetrathionate salts: Interactions between complex configuration and tetrathionate conformation. *Inorganica Chim. Acta* **361**, 63–78 (2008).

4. Becker, K. A., Grosse, G. & PLieth, K. Röntgenstrukturanalyse des trans-Dichlorodiäthylendiaminkobalt-III-chlorids. *Zeitschrift für Krist.* **384**, 375–384 (1959).

5. Groom, C. R., Bruno, I. J., Lightfoot, M. P. & Ward, S. C. The Cambridge Structural Database. *Acta Cryst* 171–179 (2016).

6. Matsumoto, K., Ooi, S. & Kuroya, H. The Crystal Structure of (+)589-Dichlorobis(ethylenediamine)cobalt(III) Chloride Monohydrate. *Bull. Chem. Soc. Jpn.* **43**, 3801–3804 (1970).

7. Hüllen, A., Plieth, K. & Ruban, G. Die Strukfur des 1,2-Dichloro-diäthylendiamin-kobalt(III)-chloridmonohydrats. *Naturwissenschaften* 618 (1965).

8. Bernal, I. & Lalancette, R. A. Serendipity: Werner′s argument that the ′two-only forms′ (green and violet) of [CoCl2(en)2]+ salts demanded his octahedral model was correct. True. *Acta Crystallogr. Sect. C Struct. Chem.* **76**, 298–301 (2020).

9. Nakahara, A., Saito, Y. & Kuroya, H. The Crystal Structure of Trans-dichloro-diethylenediamine-cobalt.(III). Chloride Hydrochloride Dihydrate, [Coen2Cl2]Cl.HCl.2H2O. *Bull. Chem. Soc. Jpn.* **25**, 331–336 (1952).

10. Grobler, I., Smith, V. J., Bhatt, P. M., Herbert, S. A. & Barbour, L. J. Tunable anisotropic thermal expansion of a porous zinc(II) metal-organic framework. *J. Am. Chem. Soc.* **135**, 6411–6414 (2013).

11. Valverde-Muñoz, F. J., Bartual-Murgui, C., Piñeiro-López, L., Muñoz, M. C. & Real, J. A. Influence of Host-Guest and Host-Host Interactions on the Spin-Crossover 3D Hofmann-type Clathrates {FeII(pina)[MI(CN)2]2}· xMeOH (MI = Ag, Au). *Inorg. Chem.* **58**, 10038–10046 (2019).

12. Biradha, K. & Fujita, M. A Springlike 3D-Coordination Network That Shrinks or Swells in a Crystal-to-Crystal Manner upon Guest Removal or Readsorption **. *Angew. Chemie Int. Ed.* **114**, 3392–3395 (2002).

13. Zhang, G. & Wu, C. Reentrant coil-to-globule-to-coil transition of a single linear homopolymer chain in a water/methanol mixture. *Phys. Rev. Lett.* **86**, 822–825 (2001).

14. Liu, M., Bian, F. & Sheng, F. FTIR study on molecular structure of poly(N-isopropylacrylamide) in mixed solvent of methanol and water. *Eur. Polym. J.* **41**, 283–291 (2005).

15. Ahmed, S. M., Kruger, H. G., Govender, T., Maguire, G. E. M., Sayed, Y., Ibrahim, M. A. A., Naicker, P., Soliman, M. E. S. Comparison of the Molecular Dynamics and Calculated Binding Free Energies for Nine FDA-Approved HIV-1 PR Drugs Against Subtype B and C-SA HIV PR. *Chem. Biol. Drug Des.* **81**, 208–218 (2013).

16. Jiang, C. J., Trimm, D. L. & Wainwright, M. S. Kinetic mechanism for the reaction between methanol and water over a Cu-ZnO-Al2O3 catalyst. *Appl. Catal. A Gen.* **97**, 145–158 (1993).

17. Rodriguez-Reinoso, F., Molina-Sabio, M. & Gonzalez, M. T. Effect of Oxygen Surface Groups on the Immersion Enthalpy of Activated Carbons in Liquids of Different Polarity. *Langmuir* **13**, 2354–2358

(1997).

18. Mehlana, G., Bourne, S. A. & Ramon, G. The role of C–H···π interactions in modulating the breathing amplitude of a 2D square lattice net: alcohol sorption studies. *CrystEngComm* **16**, 8160 (2014).

19. Tang, Y.-Y., Wang, C.-J., Chen, S. & Dai, H.-Y. A terbium(III) organic framework as a fluorescent probe for selectively sensing of organic small molecules and metal ions especially nitrobenzene and Fe3+. *J. Coord. Chem.* **70**, 3996–4007 (2017).

20. Janiak, A., Kwit, M. & Barbour, L. J. An unexpected relationship between solvent inclusion and gas sorption properties of chiral calixsalen solids*. *Supramol. Chem.* **30**, 479–487 (2018).

21. Sun, J.-K., Ji, M., Chen, C., Wang, W.-G., Wang, P., Chen, R. -P., Zhang, J. A charge-polarized porous metal–organic framework for gas chromatographic separation of alcohols from water. *Chem. Commun.* **49**, 1624 (2013).

22. Kwok, T. J., Jayasuriya, K., Damavarapu, R. & Brodman, B. W. Application of H-ZSM-5 Zeolite for Regioselective Mononitration of Toluene. *J. Org. Chem.* **59**, 4939–4942 (1994).

23. Bailar, J. C. & Clapp, L. B. The Preparation and Properties of Inorganic Coordination Compounds . I . The Action of Some Organic Amines upon Dichloro-diethylenediamine Cobaltic Chloride. *J. Am. Chem. Soc.* **67**, 171–175 (1945).

24. Prodi, L., Bolletta, F., Montalti, M. & Zaccheroni, N. Luminescent chemosensors for transition metal ions. *Coord. Chem. Rev.* **205**, 59–83 (2000).

25. Burfield, D. R., Smithers, R. H., Sui, A. & Tan, C. Desiccant Efficiency in Solvent and Reagent Drying. 5. Amines. *J. Org. Chem.* **46**, 629–631 (1981).

26. Dzesse T, C. N., Nfor, E. N. & Bourne, S. A. Vapor Sorption and Solvatochromism in a Metal-Organic Framework of an Asymmetric Pyridylcarboxylate. *Cryst. Growth Des.* **18**, 416–423 (2018).

CHAPTER 6. CONCLUSION AND FUTURE WORK

6.1. GENERAL SUMMARY

MOFs can be prepared using a wide range of synthetic methods and this is done by the variation of reaction conditions. Some MOFs present interesting properties to withstand high temperature and chemical alterations. They are characterized by pores structures and channels that facilitate various application. In this thesis, we have synthesized a series of MOFs using pyridylcarboxylate ligands and divalent metal centres. Mixed 44pba and 34pba ligands were used in connectivity with Co^{2+} and Zn^{2+} to form frameworks **1**, **2**, and **3**. The three MOFs were characterized as 3D structures. Using 34pba as a single ligand in connectivity with Cu^{2+} afforded **4** which is a 2D structure. On the other hand, the same 34pba afforded a 3D structural framework (**7)**. Functionalized ligands longer than 34pba and 44pba and were use to coordinate Cu^{2+} centre and formed two 1D structures, **5** and **6** which then form layers via hydrogen bonding. The sorption for a range of VOCs was investigated using the activated frameworks **1d**, **2d**, and **3d** from **1**, **2**, and **3**. Similarly, gas sorption for carbon dioxide and hydrogen was studied. The compound **4** was tested for solvent exchange with methanol. Crystal structure analysis of the synthesized compound was characterized using single crystal X-ray diffraction. Phase changes were analyzed using powder X-ray diffraction and infrared spectroscopy. Thermal analysis was used to characterize the behaviour of the compounds. Hot stage microscopy also assisted to monitor the colour change associated with VOCs sorption.

6.2. GENERAL CONCLUSION

Isomorphous MOFs **1** and **2** were solvothermally synthesized where the reaction conditions differ only in the use of dimethylformamide/ethanol and water/acetonitrile respectively. The guest molecule in **1** and **2** was DMF and acetone respectively. The presence of acetone in **2** was

unexpected. Conversion of acetonitrile to acetone is likely to proceed via hydrolysis to acetic acid followed by ketonization to form acetone. The dissimilarity of the crystal structures in the two MOFs was characterized as a hinge-like expansion or contraction due to the response on the solvent stimulus. The ligands in both frameworks respond to this stimulus by performing the torsion and rotation at different extent. The latter property is enabled by the single ligand between pyridyl and benzoic ring to result in flexible ligands. Isostructural MOF **3** was synthesized using the same reaction conditions as in **1** except Zn^{2+} metal salt was used rather than Co^{2+}. These three compounds contain 1D channels which can include guest solvents. An important property in solid adsorbent, the stability on the removal of guest molecules by heating under vacuum was characterized in **1d**, **2d**, and **3d**. The activation on heating under vacuum resulted in stable and retained structures **1d**, **2d**, and **3d** which is an important property for solid adsorbents.

Frameworks **4** and **7** were solvothermally synthesized through similar reaction conditions, except a slightly higher volume of HCl was used in the reaction mixture for **7**. Framework **4** has a square planar geometry coordinated through two oxygen and nitrogen atoms of the ligand. Heating under vacuum and soaking in methanol resulted in the removal of guest DMF with two different phases being formed. This was observed by comparing single crystal structures as the layers in the structures could contract and nest each other at different extent. Additionally, the ligands display different conformations. Compound **7** has square pyramidal geometry where chloride coordinate in addition to the coordination in **4**. The void volume in **7** was 5102 $Å^3$ corresponding to 46.9% of the unit cell contained disordered guest molecule which was refined using the SQUEEZE routine in PLATON. The channels run in all direction to form 3D channels. Unfortunately, there was not enough material of **7** for more analysis.

Functionalized single ligands 44paba and 34paba only differ by the position of the bent (-(pyridyn-4-ylmethyl)amino) branch allowed the preparation on slow evaporation of **5** and **6**. Framework **5** is formed by chains with Cu^{2+} centres coordinated in tetrahedral geometry. The chains are connected through hydrogen bonding to result in layers. There are hydrogen bondings that bridges DMF, H_2O guest molecules, and finally the framework. The compound is unstable and collapses on losing its guest molecules even at r.t. The collapse of the frameworks could be due to the breakage of hydrogen bonding. Framework **6** has a square pyramidal geometry due to the additional coordination of one water molecule on the metal centre. It is constructed by three different Cu^{2+} centres which form three different chains. Two chains are then connected by hydrogen bonding to form layers while the third chain forms its layer hosted in the middle of the two. The guest molecules can be removed at different temperatures on heating and result in a new phase.

The stable solid adsorbents **1d** and **3d** showed the sorption capacity for both halogenated and amine VOCs. Halogenated VOCs such as dichloromethane, chloroform, chlorobenzene, dibromomethane, bromoform, bromobenzene, diiodomethane, iodoform, and iodobenzene were characterized by different effects of interaction within the channels of the frameworks. Crystal structures of chlorinated VOCs showed C−H···π, C−H···C−H, and π···C−H interaction. Powder patterns indicated that halogenated VOCs containing iodine have more effect on the structure of the adsorbent followed by halogenated VOCs containing bromine and lastly chlorine. This shows that less polar and heavier have a stronger interaction with the channels. Higher sorption capacity for aliphatic halogenated VOCs was recorded from those with two halogen atoms, while, bromobenzene showed higher among aromatic halogenated VOCs. The test for the sorption selectivity showed that halogenated VOCs with a low boiling point were preferably adsorbed.

Amine VOCs showed different interaction effects within the adsorbent depending on the sorption capacity. The TGA sorption percentage of $BzNH_2$ in **1d** at 40% was still crystalline while that at 52% led to an amorphous phase. Their recorded loading capacities were even higher than the theoretical ones as they interact through a strong hydrogen bonding. For example, benzylamine showed a higher loading capacity with 575% in **1d** and 300% in **3d**. This is due to the presence of the aromatic ring as an additional feature for stacking interaction with the channels of the adsorbents. However, phenylethylamine showed a lower loading capacity with 57% in **1d** and 43% in **3d**. Thus, the loading capacity was influenced by the nature of the VOC and steric effect.

1d contains Co^{2+} as the metal centre and its sorption for some compounds led to the colour change. This chromophore was due to the interactions such as $I\cdots\pi$, $Co^{2+}\cdots O$, and $Co^{2+}\cdots N$ from iodine, H_2O and NH_3 respectively. The interactions cause the electron excitation associated with d-d transitions[1] and the tune the degree of charge delocalization[2] and result in visible colour changes. The reversible sorption for iodine was characterized by the colour change and the activated adsorbent could be recovered. The solvatochromism of **1d** for the adsorption of H_2O and NH_3 has changed from red to purple colour. Upon desorption, the red colour could not be recovered rather a grey clour of a new phase. The change from purple to grey colour was a reversible process.

Appreciable sorption for carbon dioxide and hydrogen was recorded at lower temperature 195 K and 77 K respectively. The sorption for carbon dioxide in **1d** was more than a double 114 cm^3 (STP) g^{-1} (2.35 molecules per ASU) compared to that of **3d** with 52 cm^3 (STP) g^{-1} with little hysteresis. The sorption for hydrogen was recorded only in **1d** as there might be less interaction in **3d**. These adsorbents are characterized by micropores with some mesopores features.

In the whole study, **1d** showed higher sorption capacity than **3d**. Kinetic studies for some solvents showed more activation energy in **1d** than in **3d**. For example, the activation for water desorption

was 74.97±1.93 and 63.94±4.67 respectively and the one for ammonia 67.57±1.70 and 60.47±1.82 respectively. In addition to the nature of a metal centre, **1d** has a cell the volume of 549.0 $Å^3$ which allow close contact and high sorption capacity than 3d with a cell volume of 571.4 $Å^3$ **1d**.

The activated frameworks, **1d** and **3d** can be used as solid adsorbents and they showed the important property of the selectivity on the removal of some VOCs. The desorption showed that they are robust and recyclable. An additional interesting property was the breathing mechanism observed on adsorption/desorption of benzylamine to recover **1d**. However, the same mechanism could not be observed with the sorption for H_2O and ammonia.

MOFs assembly offers a wide range of tunability to synthesize different frameworks. The variability of metal centres, functionalization of ligand, and the solvent mixture allow to achieve the diversity of MOFs. It was also noted that MOFs of the same topology (**1d** and **3d**) performed different sorption properties depending on the metal centre and cell volume. Therefore, a wide range of MOFs can be synthesized for a potential application. The comparison between **4** and **6** shows the functionalization of the linker, while the comparison between **5** and **6** shows the bent of the linker. This was expected to construct MOFs with functionalized and/or increased size of a stable framework.[3] However, it was not the case with these results.

This work also included the investigation of *cis*-dichlorobis(ethylenediamine) cobalt(III)chloride monohydrate on the interaction with some organic solvents. This was done in comparison with similar complex, a cationic and anhydrous structure, [cis-α-(triethylenetetramine)-$CoCl_2$]Cl that could form a range of hydration forms.[4] On the other hand, the compound did not show any effect with a range of organic solvents except for methanol. The effect of methanol resulted in emptying the channels of the compound. Yet, the nature and the size of the solvents were suggested as factors governing the interaction.

6.3. FUTURE WORK

The objectives of this study were successifully achieved through the approach used and created an ongoing work. The vapour pressure during selective adsorption of VOCs in MOFs were not compensated and only binary mixture was perfomed. Thus, the optimized sorption considering both factors are attractive. The synthesis of Cu-34pba compounds using HCl in mixture need to be optimized using other solvent mixtures or metal centres for a thorough investigation. The activated forms of MOF **4** should be tested for sorption of hydrogen carbon dioxide gas. Further attempts to produce MOFs using functionalized ligands (3-(pyridyn-4-ylmethyl)aminobenzoic acid and 4-(pyridyn-4-ylmethyl)aminobenzoic acid) i.e 34paba and 44paba will be carried out. Additionally, MOFs containing both (mixed i.e: 34paba and 44paba) ligands would be interesting to compare to **1** or **3**. Sorption properties for the resulting compounds could be performed.

6.4. REFERENCES

1. Kobayashi, A., Dosen, M., Chang, M. & Nakajima, K. Synthesis of Metal - Hydrazone Complexes and Vapochromic Behavior of Their Hydrogen-Bonded Proton-Transfer. *Am. Chem. Soc.* **132**, 15286–15298 (2010).

2. Wang, H., Vagin, S. I., Lane, S., Lin, W., Shyta, V., Heinz, W. R., Van D. C., Bergren, A. J., Gardner, K., Rieger, B., Meldrum, A. Metal-Organic Framework with Color-Switching and Strongly Polarized Emission. *Chem. Mater.* **31**, 5816–5823 (2019).

3. Britt, D., Tranchemontagne, D. & Yaghi, O. M. Metal-organic frameworks with high capacity and selectivity for harmful gases. *Proc. Natl. Acad. Sci.* **105**, 11623–11627 (2008).

4. Saha, M. K. & Bernal, I. Environment-controlled switching between cyclic hexamer and helical conformations of a water chloride cluster : An old compound viewed in a new perspective. *Inorg. Chem. Commun.* **8**, 871–873 (2005).

APPENDICES

These appendices provide some supplemental data divided into two parts. Figures and Tables are presented according to their respective chapters. Similarly, CIFCHECK crystallographic data are presented in their corresponding chapters. Crystallographic files are available on google drive at link.

1. FIGURES AND TABLES

1. Chapter 3

This chapter contains Figure S1.

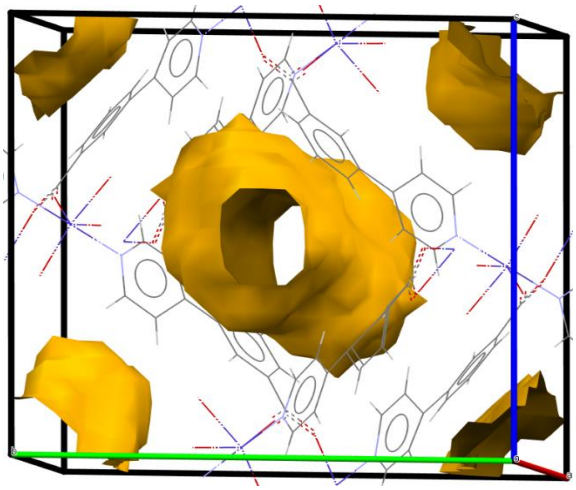

Figure S1: *Showing 1D channels viewed down the a-axis in* ***1d*** *or* ***3d****.*

2. Chapter 4

This chapter contains Table S1 and Figure S3-S5

Table S1: *boiling point of tested VOCs*

Guest molecules	Boiling point (^{o}C)
H_2O	100
NH_3	-33.34
$MeNH_2$	-6
$ProPNH_2$	47.8
$ButNH_2$	78
$BzNH_2$	185
$PhEtNH_2$	195
CH_2Cl_2	39.6
$CHCl_3$	61.2
CH_2Br_2	96.95
$CHBr_3$	149.1
CH_2I_2	181
CHI_3	218
ClBenz	132
BrBenz	156
IBenz	188

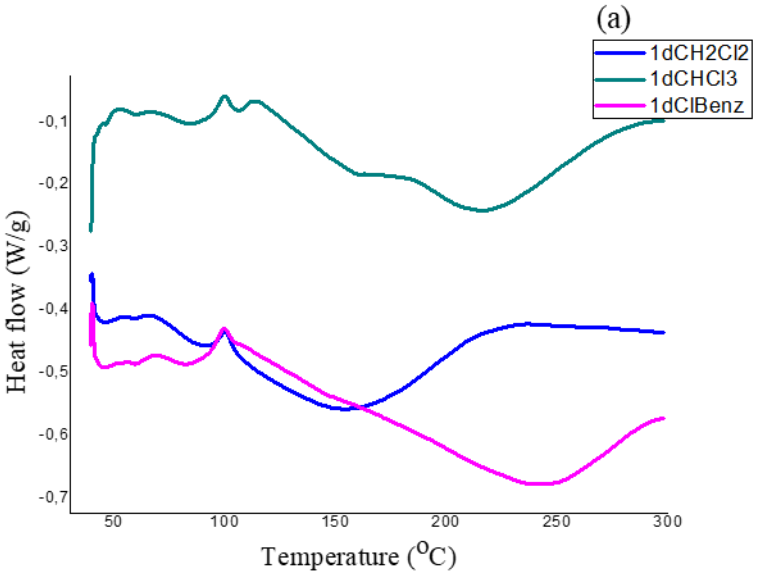

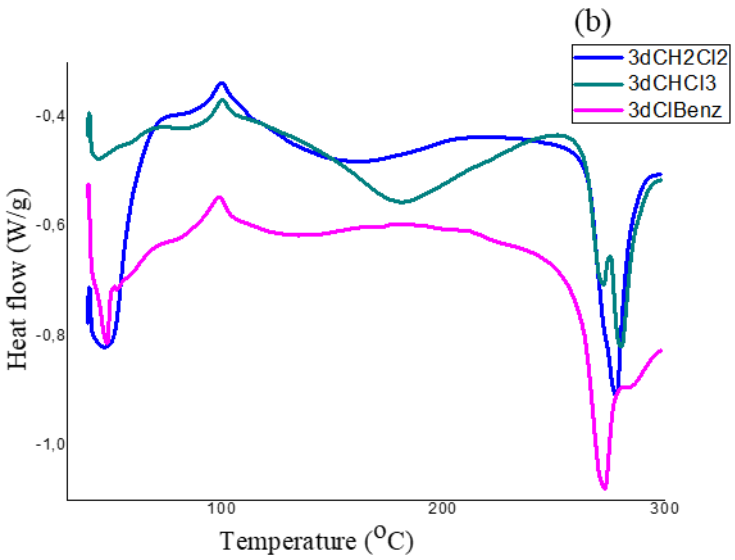

Figure S3: *DSC sorption behaviour for chlorinated VOCs in* ***1d*** *(top) and* ***3d*** *(bottom).*

Selectivity from 1d

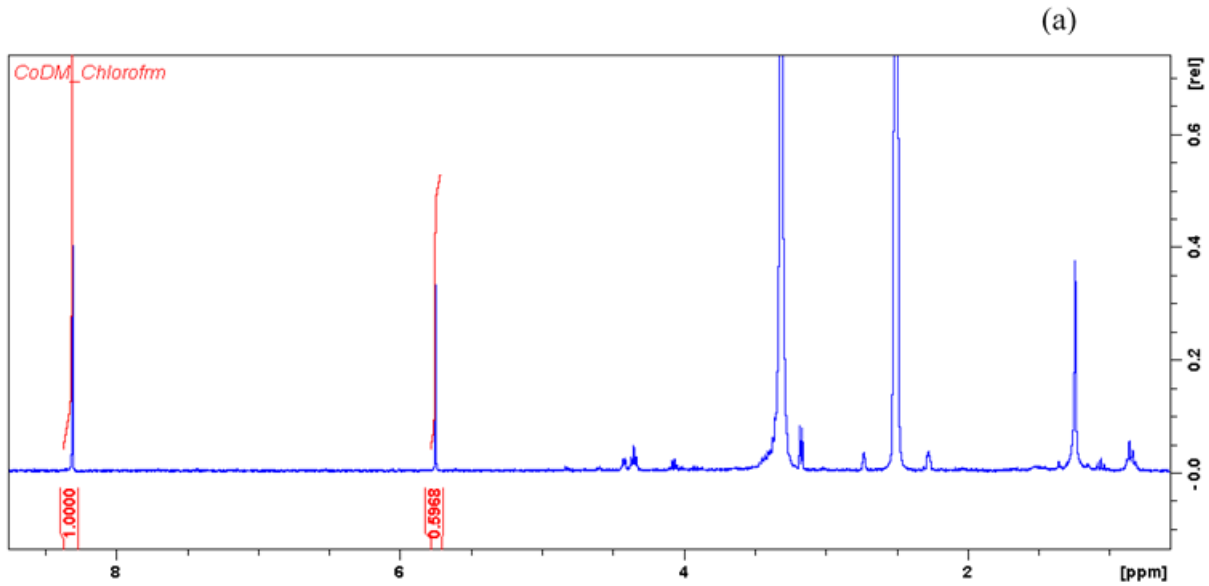

- *CH_2Cl_2:peak at 5.7 ppm: 0.6 dividing by 2 corresponds to 0.3*
- *Chloroform: peak at 8.1 ppm: 1 dividing by 3 corresponds to 0.3*

Molar ratio CH2CL2: Chloroform 1:1

(a)

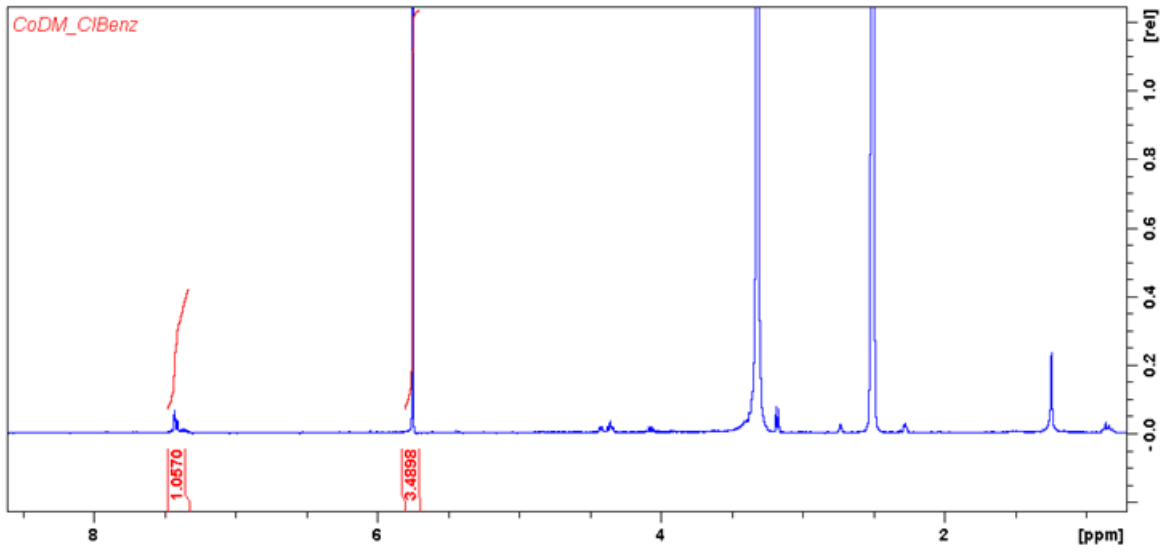

- *CH_2Cl_2: peak at 5.7 ppm: 3.4 dividing by 2 corresponds to 1.75*
- *ClBenzene: peak at 6.7 ppm: 1 dividing by 5 corresponds to 0.2*

Molar ratio CH2CL2:ClBenzene 8.3:1

(c)

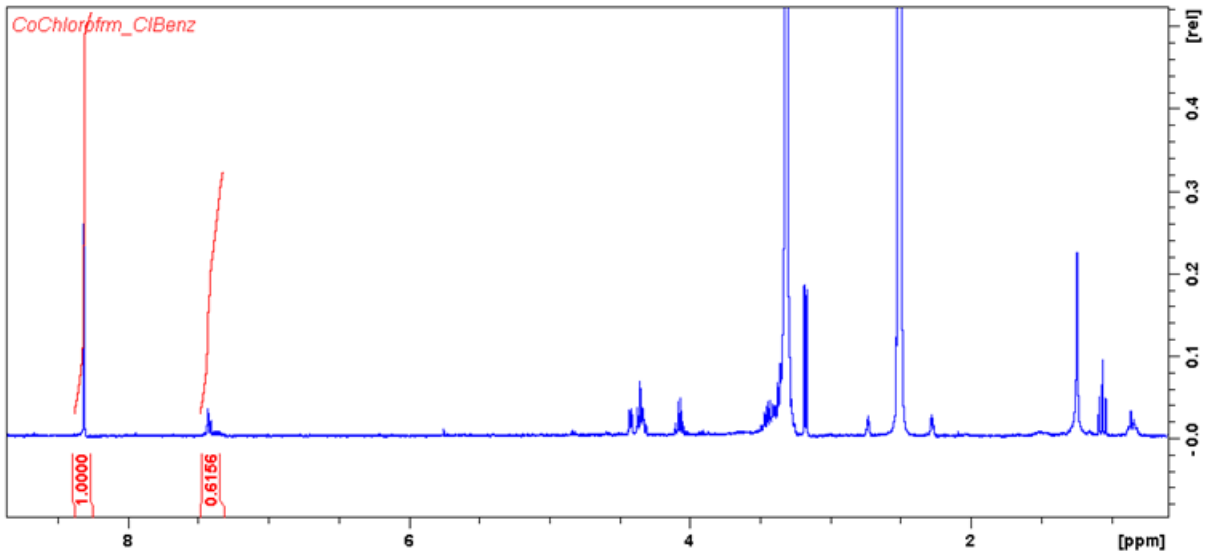

- *Chloroform: peak at 8.1 ppm: 1*
- *ClBenzene: peak at 6.7 ppm: 0.6 dividing by 5 corresponds to 0.12*

Molar ratio Chloroform: ClBenzene 10:1

Selectivity from 3d

(d)

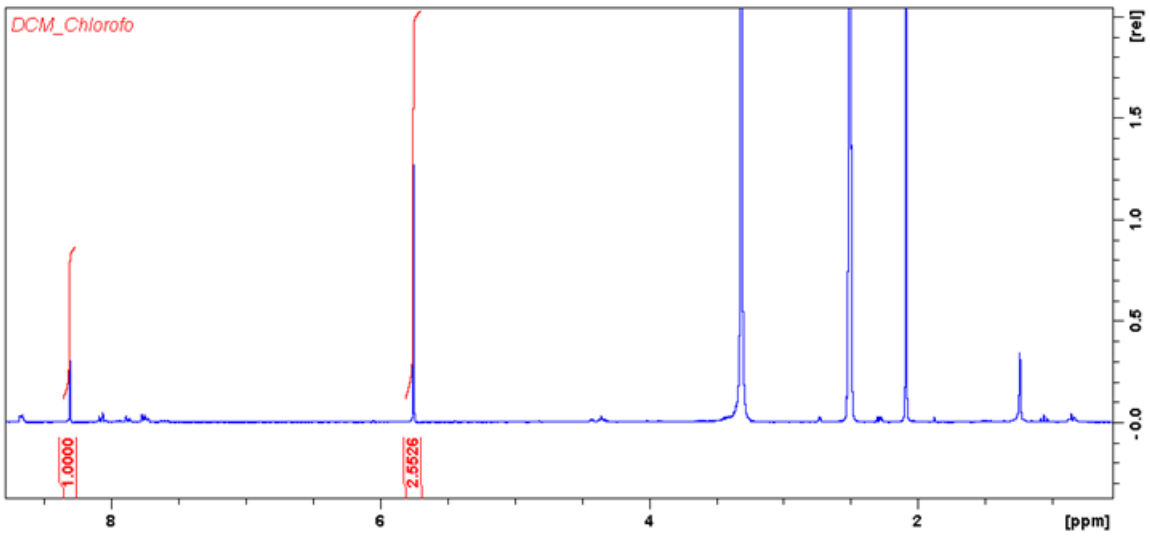

- *Chloroform: peak at 8.1 ppm: 1*
- *CH_2Cl_2: peak at 5.7 ppm: 2.55, dividing by 2 corresponds to 1.275*

Molar ratio: CH_2Cl_2_Chloroform: 1.3:1

(e)

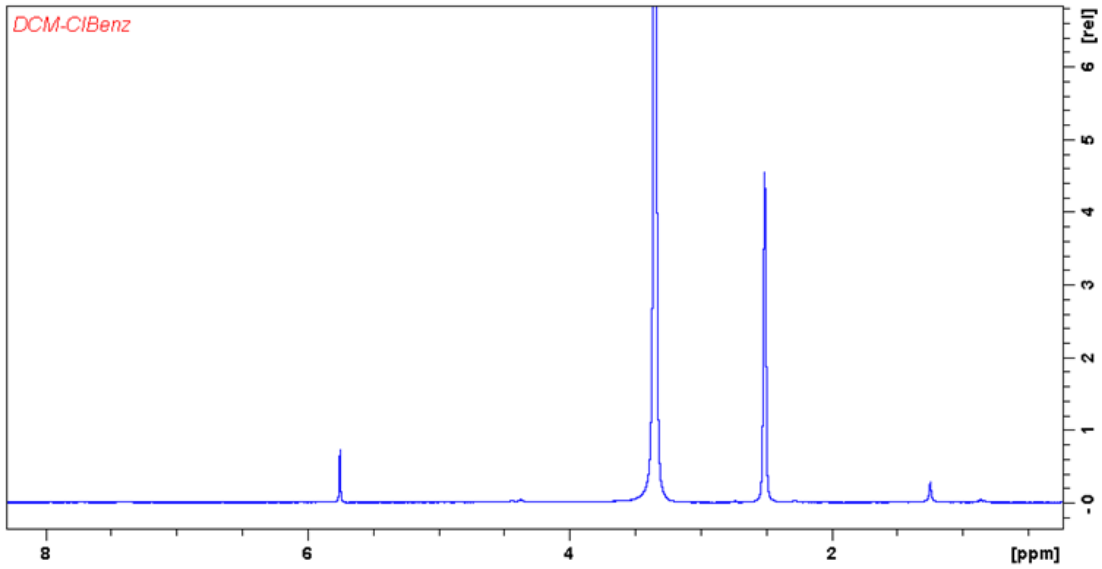

- *Only CH_2Cl_2: peak at 5.7 ppm: was sorbed.*

(f)

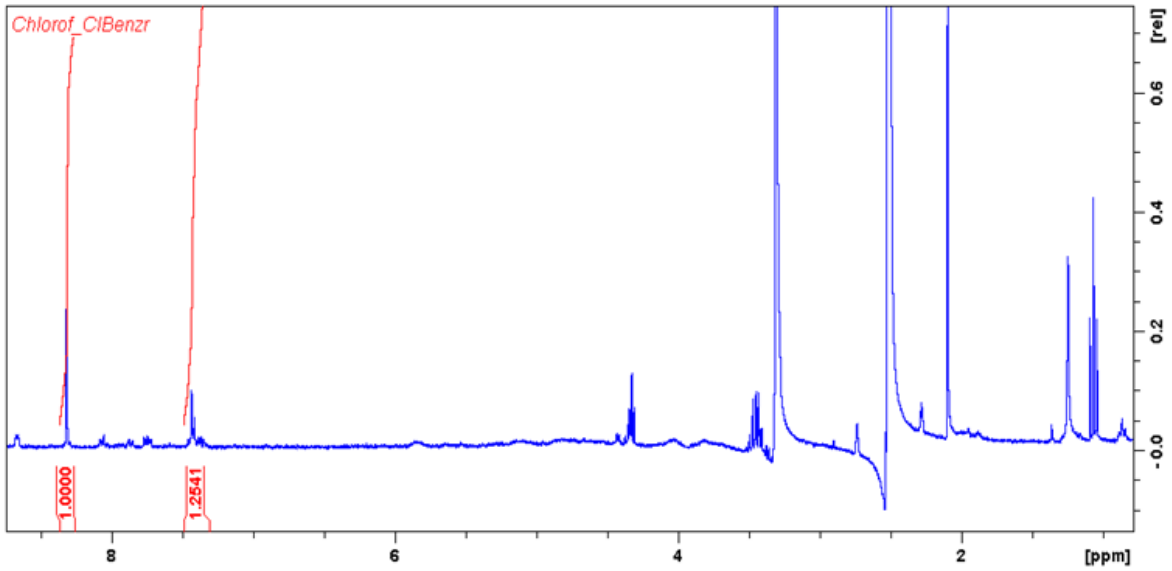

Chloroform: peak at 8.1 ppm: 1

ClBenzene: peak at 6.7 ppm: 1.25 dividing by 5 corresponds to 0.25

- *Molar ratio Chloroform: ClBenzene 1:0.3*

Figure S4: *(a, b, c, d, and e) NMR graphs showing relative selectivity of tested chlorinated VOCs in* ***1d*** *and* ***3d****.*

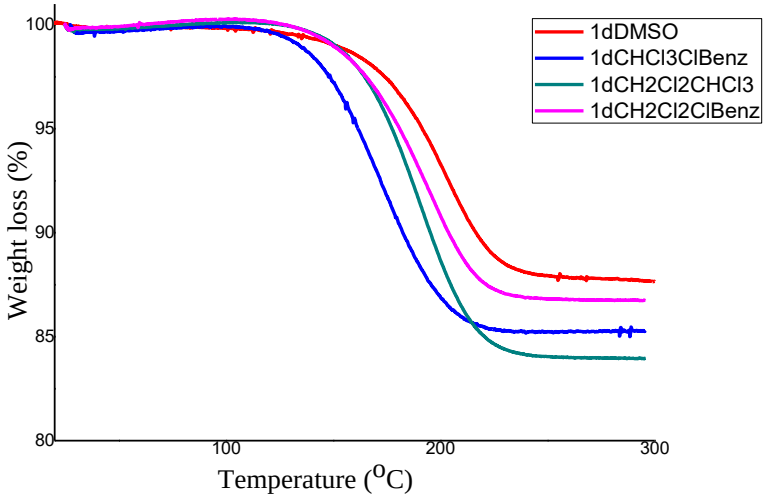

Figure S5: *TGA showing desorption of DMSO(deuterated) after exchang of chlorinated compounf for NMR analysis.*

2. CRYSTALLOGRAPHIC DATA: CIFCHECK reports

The data are from compound in chapter 3, 4, and 5.

1. Chapter 3

Compound 1

CIF Check

- **checkCIF/PLATON report**
- Structure factors have been supplied for datablock(s) C_1
- THIS REPORT IS FOR GUIDANCE ONLY. IF USED AS PART OF A REVIEW PROCEDURE
- FOR PUBLICATION, IT SHOULD NOT REPLACE THE EXPERTISE OF AN EXPERIENCED
- CRYSTALLOGRAPHIC REFEREE.
- No syntax errors found. CIF dictionary Interpreting this report
- **Datablock: C_1**
- Bond precision: C-C = 0.0041 A Wavelength=0.71073
- Cell: a=9.2030(18) b=17.823(4) c=14.718(3)
- alpha=90 beta=92.75(3) gamma=90
- Temperature: 293 K
- Calculated Reported
- Volume 2411.3(9) 2411.3(8)
- Space group P 21/c P 21/c
- Hall group -P 2ybc -P 2ybc
- Moiety formula
- C24 H16 Co N2 O4, C3 H7 N
- O
- ?
- Sum formula C27 H23 Co N3 O5 C27 H23 Co N3 O5
- Mr 528.41 528.41
- Dx,g cm-3 1.456 1.456
- Z 4 4
- Mu (mm-1) 0.756 0.756
- F000 1092.0 1092.0
- F000’ 1093.84
- h,k,lmax 12,23,19 12,23,19
- Nref 6022 5981
- Tmin,Tmax 0.920,0.941 0.920,0.941
- Tmin’ 0.920
- Correction method= # Reported T Limits: Tmin=0.920 Tmax=0.941
- AbsCorr = MULTI-SCAN

- Data completeness= 0.993 Theta(max)= 28.341
- R(reflections)= 0.0482(4089) wR2(reflections)= 0.1197(5981)
- S = 1.034 Npar= 327
- The following ALERTS were generated. Each ALERT has the format
- **test-name_ALERT_alert-type_alert-level.**
- Click on the hyperlinks for more details of the test.
- **Alert level C**
- PLAT213_ALERT_2_C Atom C6B has ADP max/min Ratio ..... 3.3 prolat
- PLAT213_ALERT_2_C Atom C7B has ADP max/min Ratio ..... 3.2 prolat
- PLAT220_ALERT_2_C NonSolvent Resd 1 C Ueq(max)/Ueq(min) Range 3.3 Ratio
- PLAT911_ALERT_3_C Missing FCF Refl Between Thmin & STh/L= 0.600 3 Report
- **Alert level G**
- PLAT004_ALERT_5_G Polymeric Structure Found with Maximum Dimension 3 Info
- PLAT066_ALERT_1_G Predicted and Reported Tmin&Tmax Range Identical ? Check
- PLAT199_ALERT_1_G Reported _cell_measurement_temperature ..... (K) 293 Check
- PLAT200_ALERT_1_G Reported _diffrn_ambient_temperature ..... (K) 293 Check
- PLAT794_ALERT_5_G Tentative Bond Valency for Co1 (II) . 1.95 Info
- PLAT883_ALERT_1_G No Info/Value for _atom_sites_solution_primary . Please Do !
- PLAT912_ALERT_4_G Missing # of FCF Reflections Above STh/L= 0.600 38 Note
- PLAT941_ALERT_3_G Average HKL Measurement Multiplicity ..... 3.8 Low
- PLAT978_ALERT_2_G Number C-C Bonds with Positive Residual Density. 7 Info
- 0 **ALERT level A** = Most likely a serious problem - resolve or explain
- 0 **ALERT level B** = A potentially serious problem, consider carefully
- 4 **ALERT level C** = Check. Ensure it is not caused by an omission or oversight
- 9 **ALERT level G** = General information/check it is not something unexpected
- 4 ALERT type 1 CIF construction/syntax error, inconsistent or missing data
- 4 ALERT type 2 Indicator that the structure model may be wrong or deficient
- 2 ALERT type 3 Indicator that the structure quality may be low
- 1 ALERT type 4 Improvement, methodology, query or suggestion
- 2 ALERT type 5 Informative message, check
- **Validation response form**
- Please find below a validation response form (VRF) that can be filled in and pasted into your CIF.
- # start Validation Reply Form
- _vrf_PLAT213_C_1
- ;
- PROBLEM: Atom C6B has ADP max/min Ratio ..... 3.3 prolat
- RESPONSE: ...
- ;
- _vrf_PLAT220_C_1
- ;
- PROBLEM: NonSolvent Resd 1 C Ueq(max)/Ueq(min) Range 3.3 Ratio
- RESPONSE: ...
- ;
- _vrf_PLAT911_C_1
- ;
- PROBLEM: Missing FCF Refl Between Thmin & STh/L= 0.600 3 Report
- RESPONSE: ...
- ;
- # end Validation Reply Form
- It is advisable to attempt to resolve as many as possible of the alerts in all categories. Often the

- minor alerts point to easily fixed oversights, errors and omissions in your CIF or refinement
- strategy, so attention to these fine details can be worthwhile. In order to resolve some of the more
- serious problems it may be necessary to carry out additional measurements or structure
- refinements. However, the purpose of your study may justify the reported deviations and the more
- serious of these should normally be commented upon in the discussion or experimental section of a
- paper or in the "special_details" fields of the CIF. checkCIF was carefully designed to identify
- outliers and unusual parameters, but every test has its limitations and alerts that are not important
- in a particular case may appear. Conversely, the absence of alerts does not guarantee there are no
- aspects of the results needing attention. It is up to the individual to critically assess their own
- results and, if necessary, seek expert advice.
- **Publication of your CIF in IUCr journals**
- A basic structural check has been run on your CIF. These basic checks will be run on all CIFs
- submitted for publication in IUCr journals (*Acta Crystallographica*, *Journal of Applied*
- *Crystallography*, *Journal of Synchrotron Radiation*); however, if you intend to submit to *Acta*
- *Crystallographica Section C* or *E* or *IUCrData*, you should make sure that full publication checks
- are run on the final version of your CIF prior to submission.
- **Publication of your CIF in other journals**
- Please refer to the *Notes for Authors* of the relevant journal for any special instructions relating to
- CIF submission.
- **PLATON version of 18/09/2020; check.def file version of 20/08/2020**
- **Datablock C_1** - ellipsoid plot

Compound 2

CIF Check

checkCIF/PLATON report

Structure factors have been supplied for datablock(s) C_2
THIS REPORT IS FOR GUIDANCE ONLY. IF USED AS PART OF A REVIEW PROCEDURE FOR PUBLICATION, IT SHOULD NOT REPLACE THE EXPERTISE OF AN EXPERIENCED CRYSTALLOGRAPHIC REFEREE.
No syntax errors found. CIF dictionary Interpreting this report

Datablock: C_2

```
Bond precision: C-C = 0.0056 A Wavelength=0.71073
Cell: a=10.068(4) b=15.632(5) c=15.399(5)
alpha=90 beta=98.588(7) gamma=90
```

Temperature: 293 K
Calculated Reported
Volume 2396.4(14) 2396.4(14)
Space group P 21/c P 21/c
Hall group -P 2ybc -P 2ybc
Moiety formula C24 H16 Co N2 O4, C3 H6 O ?
Sum formula C27 H22 Co N2 O5 C27 H22 Co N2 O5
Mr 513.40 513.39
Dx,g cm-3 1.423 1.423
Z 4 4
Mu (mm-1) 0.757 0.757
F000 1060.0 1060.0
F000' 1061.83
h,k,lmax 12,18,18 11,18,18
Nref 4262 4250
Tmin,Tmax 0.947,0.978 0.934,0.978
Tmin' 0.934
Correction method= # Reported T Limits: Tmin=0.934 Tmax=0.978
AbsCorr = MULTI-SCAN
Data completeness= 0.997 Theta(max)= 25.088
R(reflections)= 0.0493(2860) wR2(reflections)= 0.1239(4250)
S = 1.023 Npar= 318
The following ALERTS were generated. Each ALERT has the format
test-name_ALERT_alert-type_alert-level.
Click on the hyperlinks for more details of the test.

Alert level C

PLAT244_ALERT_4_C Low 'Solvent' Ueq as Compared to Neighbors of C1C Check
PLAT601_ALERT_2_C Unit Cell Contains Solvent Accessible VOIDS of . 37 Ang**3
PLAT911_ALERT_3_C Missing FCF Refl Between Thmin & STh/L= 0.597 12 Report

Alert level G

PLAT004_ALERT_5_G Polymeric Structure Found with Maximum Dimension 3 Info
PLAT066_ALERT_1_G Predicted and Reported Tmin&Tmax Range Identical ? Check
PLAT199_ALERT_1_G Reported _cell_measurement_temperature ..... (K) 293 Check
PLAT200_ALERT_1_G Reported _diffrn_ambient_temperature ..... (K) 293 Check
PLAT380_ALERT_4_G Incorrectly? Oriented X(sp2)-Methyl Moiety ..... C2C Check
PLAT794_ALERT_5_G Tentative Bond Valency for Co1 (II) . 1.98 Info
PLAT883_ALERT_1_G No Info/Value for _atom_sites_solution_primary . Please Do !
PLAT909_ALERT_3_G Percentage of I>2sig(I) Data at Theta(Max) Still 47% Note
PLAT941_ALERT_3_G Average HKL Measurement Multiplicity ..... 4.3 Low
PLAT978_ALERT_2_G Number C-C Bonds with Positive Residual Density. 0 Info
0 **ALERT level A** = Most likely a serious problem - resolve or explain
0 **ALERT level B** = A potentially serious problem, consider carefully
3 **ALERT level C** = Check. Ensure it is not caused by an omission or oversight
10 **ALERT level G** = General information/check it is not something unexpected
4 ALERT type 1 CIF construction/syntax error, inconsistent or missing data
2 ALERT type 2 Indicator that the structure model may be wrong or deficient
3 ALERT type 3 Indicator that the structure quality may be low
2 ALERT type 4 Improvement, methodology, query or suggestion
2 ALERT type 5 Informative message, check

Validation response form

Please find below a validation response form (VRF) that can be filled in and pasted into your CIF.

```
# start Validation Reply Form
_vrf_PLAT244_C_2
;
PROBLEM: Low 'Solvent' Ueq as Compared to Neighbors of C1C Check
RESPONSE: ...
;
```

```
_vrf_PLAT601_C_2
;
PROBLEM: Unit Cell Contains Solvent Accessible VOIDS of . 37 Ang**3
RESPONSE: ...
;
_vrf_PLAT911_C_2
;
PROBLEM: Missing FCF Refl Between Thmin & STh/L= 0.597 12 Report
RESPONSE: ...
;
# end Validation Reply Form
```

It is advisable to attempt to resolve as many as possible of the alerts in all categories. Often the minor alerts point to easily fixed oversights, errors and omissions in your CIF or refinement strategy, so attention to these fine details can be worthwhile. In order to resolve some of the more serious problems it may be necessary to carry out additional measurements or structure refinements. However, the purpose of your study may justify the reported deviations and the more serious of these should normally be commented upon in the discussion or experimental section of a paper or in the "special_details" fields of the CIF. checkCIF was carefully designed to identify outliers and unusual parameters, but every test has its limitations and alerts that are not important in a particular case may appear. Conversely, the absence of alerts does not guarantee there are no aspects of the results needing attention. It is up to the individual to critically assess their own results and, if necessary, seek expert advice.

Publication of your CIF in IUCr journals

A basic structural check has been run on your CIF. These basic checks will be run on all CIFs submitted for publication in IUCr journals (*Acta Crystallographica*, *Journal of Applied Crystallography*, *Journal of Synchrotron Radiation*); however, if you intend to submit to *Acta Crystallographica Section C* or *E* or *IUCrData*, you should make sure that full publication checks are run on the final version of your CIF prior to submission.

Publication of your CIF in other journals

Please refer to the *Notes for Authors* of the relevant journal for any special instructions relating to CIF submission.

PLATON version of 18/09/2020; check.def file version of 20/08/2020

Datablock C_2 - ellipsoid plot

Compound 3

CIF Check

checkCIF/PLATON report

Structure factors have been supplied for datablock(s) C_3

THIS REPORT IS FOR GUIDANCE ONLY. IF USED AS PART OF A REVIEW PROCEDURE FOR PUBLICATION, IT SHOULD NOT REPLACE THE EXPERTISE OF AN EXPERIENCED CRYSTALLOGRAPHIC REFEREE.

No syntax errors found. CIF dictionary Interpreting this report

Datablock: C_3

```
Bond precision: C-C = 0.0046 A Wavelength=0.71073
Cell: a=9.3389(15) b=17.677(3) c=14.735(3)
alpha=90 beta=93.189(5) gamma=90
Temperature: 293 K
Calculated Reported
```

Volume 2428.7(8) 2428.8(7)
Space group P 21/c P 21/c
Hall group -P 2ybc -P 2ybc
Moiety formula
C24 H16 N2 O4 Zn, C3 H7 N
O
?
Sum formula C27 H23 N3 O5 Zn C27 H23 N3 O5 Zn
Mr 534.87 534.85
Dx,g cm-3 1.463 1.463
Z 4 4
Mu (mm-1) 1.055 1.055
F000 1104.0 1104.0
F000' 1105.57
h,k,lmax 12,23,19 12,22,19
Nref 5607 5584
Tmin,Tmax 0.963,0.969 0.909,0.969
Tmin' 0.909
Correction method= # Reported T Limits: Tmin=0.909 Tmax=0.969
AbsCorr = MULTI-SCAN
Data completeness= 0.996 Theta(max)= 27.579
R(reflections)= 0.0468(3713) wR2(reflections)= 0.1108(5584)
S = 1.005 Npar= 327
The following ALERTS were generated. Each ALERT has the format
test-name_ALERT_alert-type_alert-level.
Click on the hyperlinks for more details of the test.

Alert level C

PLAT220_ALERT_2_C NonSolvent Resd 1 C Ueq(max)/Ueq(min) Range 3.5 Ratio
PLAT241_ALERT_2_C High 'MainMol' Ueq as Compared to Neighbors of C6A Check
PLAT241_ALERT_2_C High 'MainMol' Ueq as Compared to Neighbors of C7B Check
PLAT244_ALERT_4_C Low 'Solvent' Ueq as Compared to Neighbors of N2 Check

Alert level G

PLAT004_ALERT_5_G Polymeric Structure Found with Maximum Dimension 3 Info
PLAT066_ALERT_1_G Predicted and Reported Tmin&Tmax Range Identical ? Check
PLAT199_ALERT_1_G Reported _cell_measurement_temperature ..... (K) 293 Check
PLAT200_ALERT_1_G Reported _diffrn_ambient_temperature ..... (K) 293 Check
PLAT232_ALERT_2_G Hirshfeld Test Diff (M-X) Zn01 --O1B_b . 5.1 s.u.
PLAT720_ALERT_4_G Number of Unusual/Non-Standard Labels ..... 24 Note
PLAT794_ALERT_5_G Tentative Bond Valency for Zn01 (II) . 1.90 Info
PLAT883_ALERT_1_G No Info/Value for _atom_sites_solution_primary . Please Do !
PLAT912_ALERT_4_G Missing # of FCF Reflections Above STh/L= 0.600 23 Note
PLAT941_ALERT_3_G Average HKL Measurement Multiplicity ..... 3.9 Low
PLAT978_ALERT_2_G Number C-C Bonds with Positive Residual Density. 1 Info
0 **ALERT level A** = Most likely a serious problem - resolve or explain
0 **ALERT level B** = A potentially serious problem, consider carefully
4 **ALERT level C** = Check. Ensure it is not caused by an omission or oversight
11 **ALERT level G** = General information/check it is not something unexpected
4 ALERT type 1 CIF construction/syntax error, inconsistent or missing data
5 ALERT type 2 Indicator that the structure model may be wrong or deficient
1 ALERT type 3 Indicator that the structure quality may be low
3 ALERT type 4 Improvement, methodology, query or suggestion
2 ALERT type 5 Informative message, check

Validation response form

Please find below a validation response form (VRF) that can be filled in and pasted into your CIF.

start Validation Reply Form
_vrf_PLAT220_C_3
;

```
PROBLEM: NonSolvent Resd 1 C Ueq(max)/Ueq(min) Range 3.5 Ratio
RESPONSE: ...
;
_vrf_PLAT241_C_3
;
PROBLEM: High 'MainMol' Ueq as Compared to Neighbors of C6A Check
RESPONSE: ...
;
_vrf_PLAT244_C_3
;
PROBLEM: Low 'Solvent' Ueq as Compared to Neighbors of N2 Check
RESPONSE: ...
;
# end Validation Reply Form
```

It is advisable to attempt to resolve as many as possible of the alerts in all categories. Often the minor alerts point to easily fixed oversights, errors and omissions in your CIF or refinement strategy, so attention to these fine details can be worthwhile. In order to resolve some of the more serious problems it may be necessary to carry out additional measurements or structure refinements. However, the purpose of your study may justify the reported deviations and the more serious of these should normally be commented upon in the discussion or experimental section of a paper or in the "special_details" fields of the CIF. checkCIF was carefully designed to identify outliers and unusual parameters, but every test has its limitations and alerts that are not important in a particular case may appear. Conversely, the absence of alerts does not guarantee there are no aspects of the results needing attention. It is up to the individual to critically assess their own results and, if necessary, seek expert advice.

Publication of your CIF in IUCr journals

A basic structural check has been run on your CIF. These basic checks will be run on all CIFs submitted for publication in IUCr journals (*Acta Crystallographica*, *Journal of Applied Crystallography*, *Journal of Synchrotron Radiation*); however, if you intend to submit to *Acta Crystallographica Section C* or *E* or *IUCrData*, you should make sure that full publication checks are run on the final version of your CIF prior to submission.

Publication of your CIF in other journals

Please refer to the *Notes for Authors* of the relevant journal for any special instructions relating to CIF submission.

PLATON version of 18/09/2020; check.def file version of 20/08/2020

Datablock C_3 - ellipsoid plot

Compound 4

CIF Check

checkCIF/PLATON report

Structure factors have been supplied for datablock(s) C_4_a

THIS REPORT IS FOR GUIDANCE ONLY. IF USED AS PART OF A REVIEW PROCEDURE FOR PUBLICATION, IT SHOULD NOT REPLACE THE EXPERTISE OF AN EXPERIENCED CRYSTALLOGRAPHIC REFEREE.

No syntax errors found. CIF dictionary Interpreting this report

Datablock: C_4_a

```
Bond precision: C-C = 0.0040 A Wavelength=0.71073
Cell: a=23.443(3) b=5.5300(6) c=18.487(2)
alpha=90 beta=96.425(2) gamma=90
Temperature: 293 K
```

Calculated Reported
Volume 2381.6(5) 2381.6(5)
Space group C 2/c C 2/c
Hall group -C 2yc -C 2yc
Moiety formula
C24 H16 Cu N2 O4, C3 H9 N
O
?
Sum formula C27 H25 Cu N3 O5 C27 H27 Cu N3 O5
Mr 535.05 537.05
Dx,g cm-3 1.492 1.498
Z 4 4
Mu (mm-1) 0.962 0.962
F000 1108.0 1116.0
F000' 1109.71
h,k,lmax 30,7,23 30,7,23
Nref 2731 2720
Tmin,Tmax 0.822,0.972 0.817,0.972
Tmin' 0.817
Correction method= # Reported T Limits: Tmin=0.817 Tmax=0.972
AbsCorr = MULTI-SCAN
Data completeness= 0.996 Theta(max)= 27.473
R(reflections)= 0.0420(2169) wR2(reflections)= 0.1031(2720)
S = 1.120 Npar= 201
The following ALERTS were generated. Each ALERT has the format
test-name_ALERT_alert-type_alert-level.
Click on the hyperlinks for more details of the test.

Alert level A

PLAT310_ALERT_2_A H2B Deleted (Close to H7B) Dist ... 0.118 Ang.

Author Response: Deleted H2B is an error due to the hydrogen from disordered DMF

PLAT722_ALERT_1_A Angle Calc 54.00, Rep 50.8(6) Dev... 3.20 Degree
C3B -C2B -H7B 7.556 1.555 7.556 # 78 Check

Author Response: Error in the angle is due to the disordered carbon from DMF

PLAT722_ALERT_1_A Angle Calc 120.00, Rep 116.5(11) Dev... 3.50 Degree
N1B -C2B -H7B 1.555 1.555 7.556 # 79 Check

Author Response: Error in the angle is due to the disordered carbon from DMF

Alert level B

PLAT722_ALERT_1_B Angle Calc 102.00, Rep 105(4) Dev... 3.00 Degree
H3B -C2B -H7B 1.555 1.555 7.556 # 82 Check

Author Response: Error in the angle is due to the disordered carbon from DMF

Alert level C

PLAT041_ALERT_1_C Calc. and Reported SumFormula Strings Differ Please Check
PLAT043_ALERT_1_C Calculated and Reported Mol. Weight Differ by .. 2.00 Check
PLAT068_ALERT_1_C Reported F000 Differs from Calcd (or Missing)... Please Check
PLAT223_ALERT_4_C Solv./Anion Resd 2 H Ueq(max)/Ueq(min) Range 4.7 Ratio
PLAT250_ALERT_2_C Large U3/U1 Ratio for Average U(i,j) Tensor .... 2.2 Note
PLAT303_ALERT_2_C Full Occupancy Atom H9B with # Connections 1.50 Check
PLAT411_ALERT_2_C Short Inter H...H Contact H9B ..H9B . 2.11 Ang.
1/2-x,-1/2-y,1-z = 7_546 Check
PLAT711_ALERT_1_C BOND Unknown or Inconsistent Label ..... H2B Check
C2B H2B
PLAT712_ALERT_1_C ANGLE Unknown or Inconsistent Label ..... H2B Check
C3B C2B H2B
PLAT712_ALERT_1_C ANGLE Unknown or Inconsistent Label ..... H2B Check
N1B C2B H2B
PLAT712_ALERT_1_C ANGLE Unknown or Inconsistent Label ..... H2B Check

C1B C2B H2B
PLAT712_ALERT_1_C ANGLE Unknown or Inconsistent Label ..... H2B Check
H2B C2B H3B
PLAT712_ALERT_1_C ANGLE Unknown or Inconsistent Label ..... H2B Check
H2B C2B H9B
PLAT712_ALERT_1_C ANGLE Unknown or Inconsistent Label ..... H2B Check
H2B C2B H7B

Alert level G

PLAT004_ALERT_5_G Polymeric Structure Found with Maximum Dimension 2 Info
PLAT066_ALERT_1_G Predicted and Reported Tmin&Tmax Range Identical ? Check
PLAT083_ALERT_2_G SHELXL Second Parameter in WGHT Unusually Large 10.98 Why ?
PLAT199_ALERT_1_G Reported _cell_measurement_temperature ..... (K) 293 Check
PLAT200_ALERT_1_G Reported _diffrn_ambient_temperature ..... (K) 293 Check
PLAT300_ALERT_4_G Atom Site Occupancy of O1B Constrained at 0.5 Check
PLAT300_ALERT_4_G Atom Site Occupancy of C1B Constrained at 0.5 Check
PLAT300_ALERT_4_G Atom Site Occupancy of C2B Constrained at 0.5 Check
PLAT300_ALERT_4_G Atom Site Occupancy of C3B Constrained at 0.5 Check
PLAT300_ALERT_4_G Atom Site Occupancy of H5B Constrained at 0.5 Check
PLAT300_ALERT_4_G Atom Site Occupancy of H6B Constrained at 0.5 Check
PLAT300_ALERT_4_G Atom Site Occupancy of H7B Constrained at 0.5 Check
PLAT302_ALERT_4_G Anion/Solvent/Minor-Residue Disorder (Resd 2) 80% Note
PLAT412_ALERT_2_G Short Intra XH3 .. XHn H1B ..H5B . 1.30 Ang.
1/2-x,1/2-y,1-z = 7_556 Check
PLAT412_ALERT_2_G Short Intra XH3 .. XHn H1B ..H6B . 1.21 Ang.
1/2-x,1/2-y,1-z = 7_556 Check
PLAT412_ALERT_2_G Short Intra XH3 .. XHn H3B ..H7B . 1.66 Ang.
1/2-x,1/2-y,1-z = 7_556 Check
PLAT412_ALERT_2_G Short Intra XH3 .. XHn H7B ..H9B . 1.57 Ang.
1/2-x,1/2-y,1-z = 7_556 Check
PLAT720_ALERT_4_G Number of Unusual/Non-Standard Labels ..... 1 Note
PLAT721_ALERT_1_G Bond Calc 1.02000, Rep 0.96000 Dev... 0.06 Ang.
C3B -H7B 1.555 1.555 ..... # 32 Check
PLAT883_ALERT_1_G No Info/Value for _atom_sites_solution_primary . Please Do !
PLAT912_ALERT_4_G Missing # of FCF Reflections Above STh/L= 0.600 11 Note
PLAT978_ALERT_2_G Number C-C Bonds with Positive Residual Density. 7 Info
3 **ALERT level A** = Most likely a serious problem - resolve or explain
1 **ALERT level B** = A potentially serious problem, consider carefully
14 **ALERT level C** = Check. Ensure it is not caused by an omission or oversight
22 **ALERT level G** = General information/check it is not something unexpected
18 ALERT type 1 CIF construction/syntax error, inconsistent or missing data
10 ALERT type 2 Indicator that the structure model may be wrong or deficient
0 ALERT type 3 Indicator that the structure quality may be low
11 ALERT type 4 Improvement, methodology, query or suggestion
1 ALERT type 5 Informative message, check

It is advisable to attempt to resolve as many as possible of the alerts in all categories. Often the minor alerts point to easily fixed oversights, errors and omissions in your CIF or refinement strategy, so attention to these fine details can be worthwhile. In order to resolve some of the more serious problems it may be necessary to carry out additional measurements or structure refinements. However, the purpose of your study may justify the reported deviations and the more serious of these should normally be commented upon in the discussion or experimental section of a paper or in the "special_details" fields of the CIF. checkCIF was carefully designed to identify outliers and unusual parameters, but every test has its limitations and alerts that are not important in a particular case may appear. Conversely, the absence of alerts does not guarantee there are no aspects of the results needing attention. It is up to the individual to critically assess their own results and, if necessary, seek expert advice.

Publication of your CIF in IUCr journals

A basic structural check has been run on your CIF. These basic checks will be run on all CIFs submitted for publication in IUCr journals (*Acta Crystallographica*, *Journal of Applied Crystallography*, *Journal of Synchrotron Radiation*); however, if you intend to submit to *Acta*

Crystallographica Section C or *E* or *IUCrData*, you should make sure that full publication checks are run on the final version of your CIF prior to submission.

Publication of your CIF in other journals

Please refer to the *Notes for Authors* of the relevant journal for any special instructions relating to CIF submission.

Validation response form

Please find below a validation response form (VRF) that can be filled in and pasted into your CIF.

```
# start Validation Reply Form
_vrf_PLAT041_C_4_a
;
PROBLEM: Calc. and Reported SumFormula Strings Differ Please Check
RESPONSE: ...
;
_vrf_PLAT043_C_4_a
;
PROBLEM: Calculated and Reported Mol. Weight Differ by .. 2.00 Check
RESPONSE: ...
;
_vrf_PLAT068_C_4_a
;
PROBLEM: Reported F000 Differs from Calcd (or Missing)... Please Check
RESPONSE: ...
;
_vrf_PLAT223_C_4_a
;
PROBLEM: Solv./Anion Resd 2 H Ueq(max)/Ueq(min) Range 4.7 Ratio
RESPONSE: ...
;
_vrf_PLAT250_C_4_a
;
PROBLEM: Large U3/U1 Ratio for Average U(i,j) Tensor .... 2.2 Note
RESPONSE: ...
;
_vrf_PLAT303_C_4_a
;
PROBLEM: Full Occupancy Atom H9B with # Connections 1.50 Check
RESPONSE: ...
;
_vrf_PLAT411_C_4_a
;
PROBLEM: Short Inter H...H Contact H9B ..H9B . 2.11 Ang.
RESPONSE: ...
;
_vrf_PLAT711_C_4_a
;
PROBLEM: BOND Unknown or Inconsistent Label ..... H2B Check
RESPONSE: ...
;
_vrf_PLAT712_C_4_a
;
PROBLEM: ANGLE Unknown or Inconsistent Label ..... H2B Check
RESPONSE: ...
;
# end Validation Reply Form
```

PLATON version of 18/09/2020; check.def file version of 20/08/2020

Datablock C_4_a - ellipsoid plot

Compound 4d2

CIF Check

checkCIF/PLATON report

Structure factors have been supplied for datablock(s) C_4d2
THIS REPORT IS FOR GUIDANCE ONLY. IF USED AS PART OF A REVIEW PROCEDURE FOR PUBLICATION, IT SHOULD NOT REPLACE THE EXPERTISE OF AN EXPERIENCED CRYSTALLOGRAPHIC REFEREE.
No syntax errors found. CIF dictionary Interpreting this report

Datablock: C_4d2

Bond precision: C-C = 0.0034 A Wavelength=0.71073
Cell: a=20.2073(12) b=5.5595(3) c=18.4988(10)
alpha=90 beta=110.641(2) gamma=90
Temperature: 293 K
Calculated Reported
Volume 1944.80(19) 1944.80(19)
Space group C 2/c C 2/c
Hall group -C 2yc -C 2yc
Moiety formula C24 H16 Cu N2 O4 ?
Sum formula C24 H16 Cu N2 O4 C24 H16 Cu N2 O4
Mr 459.94 459.93
Dx,g cm-3 1.571 1.571
Z 4 4
Mu (mm-1) 1.159 1.159
F000 940.0 940.0
F000' 941.64
h,k,lmax 28,7,26 28,7,26
Nref 2968 2968
Tmin,Tmax 0.831,0.977 0.596,0.746
Tmin' 0.831
Correction method= # Reported T Limits: Tmin=0.596 Tmax=0.746
AbsCorr = MULTI-SCAN
Data completeness= 1.000 Theta(max)= 30.513
R(reflections)= 0.0469(2376) wR2(reflections)= 0.1010(2968)
S = 1.149 Npar= 142

The following ALERTS were generated. Each ALERT has the format
test-name_ALERT_alert-type_alert-level.
Click on the hyperlinks for more details of the test.

Alert level C

PLAT250_ALERT_2_C Large U3/U1 Ratio for Average U(i,j) Tensor .... 2.1 Note
PLAT906_ALERT_3_C Large K Value in the Analysis of Variance ..... 4.029 Check

Alert level G

PLAT004_ALERT_5_G Polymeric Structure Found with Maximum Dimension 2 Info
PLAT083_ALERT_2_G SHELXL Second Parameter in WGHT Unusually Large 8.49 Why ?
PLAT199_ALERT_1_G Reported _cell_measurement_temperature ..... (K) 293 Check
PLAT200_ALERT_1_G Reported _diffrn_ambient_temperature ..... (K) 293 Check
PLAT794_ALERT_5_G Tentative Bond Valency for Cu1 (II) . 2.05 Info
PLAT883_ALERT_1_G No Info/Value for _atom_sites_solution_primary . Please Do !
PLAT978_ALERT_2_G Number C-C Bonds with Positive Residual Density. 9 Info
0 **ALERT level A** = Most likely a serious problem - resolve or explain
0 **ALERT level B** = A potentially serious problem, consider carefully

```
2 ALERT level C = Check. Ensure it is not caused by an omission or oversight
7 ALERT level G = General information/check it is not something unexpected
3 ALERT type 1 CIF construction/syntax error, inconsistent or missing data
3 ALERT type 2 Indicator that the structure model may be wrong or deficient
1 ALERT type 3 Indicator that the structure quality may be low
0 ALERT type 4 Improvement, methodology, query or suggestion
2 ALERT type 5 Informative message, check
```

Validation response form

Please find below a validation response form (VRF) that can be filled in and pasted into your CIF.

```
# start Validation Reply Form
_vrf_PLAT250_C_4d2
;
PROBLEM: Large U3/U1 Ratio for Average U(i,j) Tensor .... 2.1 Note
RESPONSE: ...
;
_vrf_PLAT906_C_4d2
;
PROBLEM: Large K Value in the Analysis of Variance ...... 4.029 Check
RESPONSE: ...
;
# end Validation Reply Form
```

It is advisable to attempt to resolve as many as possible of the alerts in all categories. Often the minor alerts point to easily fixed oversights, errors and omissions in your CIF or refinement strategy, so attention to these fine details can be worthwhile. In order to resolve some of the more serious problems it may be necessary to carry out additional measurements or structure refinements. However, the purpose of your study may justify the reported deviations and the more serious of these should normally be commented upon in the discussion or experimental section of a paper or in the "special_details" fields of the CIF. checkCIF was carefully designed to identify outliers and unusual parameters, but every test has its limitations and alerts that are not important in a particular case may appear. Conversely, the absence of alerts does not guarantee there are no aspects of the results needing attention. It is up to the individual to critically assess their own results and, if necessary, seek expert advice.

Publication of your CIF in IUCr journals

A basic structural check has been run on your CIF. These basic checks will be run on all CIFs submitted for publication in IUCr journals (*Acta Crystallographica*, *Journal of Applied Crystallography*, *Journal of Synchrotron Radiation*); however, if you intend to submit to *Acta Crystallographica Section C* or *E* or *IUCrData*, you should make sure that full publication checks are run on the final version of your CIF prior to submission.

Publication of your CIF in other journals

Please refer to the *Notes for Authors* of the relevant journal for any special instructions relating to CIF submission.

PLATON version of 18/09/2020; check.def file version of 20/08/2020

Datablock C_4d2 - ellipsoid plot

Compound 5

CIF check

checkCIF/PLATON report

Structure factors have been supplied for datablock(s) C_5

THIS REPORT IS FOR GUIDANCE ONLY. IF USED AS PART OF A REVIEW PROCEDURE FOR PUBLICATION, IT SHOULD NOT REPLACE THE EXPERTISE OF AN EXPERIENCED CRYSTALLOGRAPHIC REFEREE.

No syntax errors found. CIF dictionary Interpreting this report

Datablock: C_5

Bond precision: C-C = 0.0028 A Wavelength=0.71073
Cell: a=7.9712(9) b=11.9326(14) c=17.924(2)
alpha=90 beta=96.718(3) gamma=90
Temperature: 293 K
Calculated Reported
Volume 1693.2(3) 1693.2(3)
Space group P 21/n P 21/n
Hall group -P 2yn -P 2yn
Moiety formula
C26 H26 Cu N4 O6, 2(C3 H7
N O)
?
Sum formula C32 H40 Cu N6 O8 C16 H20 Cu0.50 N3 O4
Mr 700.25 350.12
Dx,g cm-3 1.373 1.373
Z 2 4
Mu (mm-1) 0.703 0.703
F000 734.0 734.0
F000' 734.94
h,k,lmax 10,15,23 10,15,23
Nref 4255 4236
Tmin,Tmax 0.869,0.913 0.869,0.913
Tmin' 0.869
Correction method= # Reported T Limits: Tmin=0.869 Tmax=0.913
AbsCorr = MULTI-SCAN
Data completeness= 0.996 Theta(max)= 28.406
R(reflections)= 0.0381(3241) wR2(reflections)= 0.0953(4236)
S = 1.034 Npar= 294

The following ALERTS were generated. Each ALERT has the format
test-name_ALERT_alert-type_alert-level.
Click on the hyperlinks for more details of the test.

Alert level C

PLAT314_ALERT_2_C Small Angle for H2O: Metal-O1B -H1B . 84.87 Degree

Alert level G

PLAT004_ALERT_5_G Polymeric Structure Found with Maximum Dimension 1 Info
PLAT045_ALERT_1_G Calculated and Reported Z Differ by a Factor ... 0.50 Check
PLAT066_ALERT_1_G Predicted and Reported Tmin&Tmax Range Identical ? Check
PLAT164_ALERT_4_G Nr. of Refined C-H H-Atoms in Heavy-Atom Struct. 17 Note
PLAT199_ALERT_1_G Reported _cell_measurement_temperature ..... (K) 293 Check
PLAT200_ALERT_1_G Reported _diffrn_ambient_temperature ..... (K) 293 Check
PLAT380_ALERT_4_G Incorrectly? Oriented X(sp2)-Methyl Moiety ..... C2C Check
PLAT794_ALERT_5_G Tentative Bond Valency for Cu1 (II) . 2.09 Info
PLAT804_ALERT_5_G Number of ARU-Code Packing Problem(s) in PLATON 1 Info
PLAT883_ALERT_1_G No Info/Value for _atom_sites_solution_primary . Please Do !
PLAT912_ALERT_4_G Missing # of FCF Reflections Above STh/L= 0.600 19 Note
PLAT978_ALERT_2_G Number C-C Bonds with Positive Residual Density. 9 Info
0 **ALERT level A** = Most likely a serious problem - resolve or explain
0 **ALERT level B** = A potentially serious problem, consider carefully
1 **ALERT level C** = Check. Ensure it is not caused by an omission or oversight
12 **ALERT level G** = General information/check it is not something unexpected
5 ALERT type 1 CIF construction/syntax error, inconsistent or missing data
2 ALERT type 2 Indicator that the structure model may be wrong or deficient
0 ALERT type 3 Indicator that the structure quality may be low

```
3 ALERT type 4 Improvement, methodology, query or suggestion
3 ALERT type 5 Informative message, check
```

Validation response form

Please find below a validation response form (VRF) that can be filled in and pasted into your CIF.

```
# start Validation Reply Form
_vrf_PLAT314_C_5
;
PROBLEM: Small Angle for H2O: Metal-O1B -H1B . 84.87 Degree
RESPONSE: ...
;
# end Validation Reply Form
```

It is advisable to attempt to resolve as many as possible of the alerts in all categories. Often the minor alerts point to easily fixed oversights, errors and omissions in your CIF or refinement strategy, so attention to these fine details can be worthwhile. In order to resolve some of the more serious problems it may be necessary to carry out additional measurements or structure refinements. However, the purpose of your study may justify the reported deviations and the more serious of these should normally be commented upon in the discussion or experimental section of a paper or in the "special_details" fields of the CIF. checkCIF was carefully designed to identify outliers and unusual parameters, but every test has its limitations and alerts that are not important in a particular case may appear. Conversely, the absence of alerts does not guarantee there are no aspects of the results needing attention. It is up to the individual to critically assess their own results and, if necessary, seek expert advice.

Publication of your CIF in IUCr journals

A basic structural check has been run on your CIF. These basic checks will be run on all CIFs submitted for publication in IUCr journals (*Acta Crystallographica*, *Journal of Applied Crystallography*, *Journal of Synchrotron Radiation*); however, if you intend to submit to *Acta Crystallographica Section C* or *E* or *IUCrData*, you should make sure that full publication checks are run on the final version of your CIF prior to submission.

Publication of your CIF in other journals

Please refer to the *Notes for Authors* of the relevant journal for any special instructions relating to CIF submission.

PLATON version of 18/09/2020; check.def file version of 20/08/2020

Datablock C_5 - ellipsoid plot

Compound 6

CIF check

checkCIF/PLATON report

Structure factors have been supplied for datablock(s) C_6ab_a_a

THIS REPORT IS FOR GUIDANCE ONLY. IF USED AS PART OF A REVIEW PROCEDURE FOR PUBLICATION, IT SHOULD NOT REPLACE THE EXPERTISE OF AN EXPERIENCED CRYSTALLOGRAPHIC REFEREE.

No syntax errors found. CIF dictionary Interpreting this report

Datablock: C_6ab_a_a

```
Bond precision: C-C = 0.0038 A Wavelength=0.71073
Cell: a=10.3559(4) b=16.5278(8) c=21.954(1)
alpha=70.845(2) beta=78.490(1) gamma=73.568(1)
Temperature: 293 K
Calculated Reported
```

Volume 3380.9(3) 3380.9(3)
Space group P -1 P -1
Hall group -P 1 -P 1
Moiety formula
4(C26 H24 Cu N4 O5), C26
H22 Cu N4 O4, 2(C3.01
H7.04 N O), 2(C3
?
Sum formula
C142.03 H146.08 Cu5 N24
O28
C71.01 H73.04 Cu2.50 N12
O14
Mr 2955.00 1477.48
Dx,g cm-3 1.451 1.451
Z 1 2
Mu (mm-1) 0.858 0.858
F000 1535.3 1535.0
F000' 1537.44
h,k,lmax 13,22,29 13,22,29
Nref 16803 16767
Tmin,Tmax 0.857,0.910 0.850,0.910
Tmin' 0.850
Correction method= # Reported T Limits: Tmin=0.850 Tmax=0.910
AbsCorr = MULTI-SCAN
Data completeness= 0.998 Theta(max)= 28.301
R(reflections)= 0.0521(14524) wR2(reflections)= 0.1170(16767)
S = 1.083 Npar= 957

The following ALERTS were generated. Each ALERT has the format
test-name_ALERT_alert-type_alert-level.
Click on the hyperlinks for more details of the test.

Alert level B

PLAT097_ALERT_2_B Large Reported Max. (Positive) Residual Density 3.23 eA-3
PLAT971_ALERT_2_B Check Calcd Resid. Dens. 0.78A From Cu2 3.32 eA-3

Author Response: Residual density is close to copper atom and could be caused by inadequate adsorption collection

Alert level C

DIFMX02_ALERT_1_C The maximum difference density is > 0.1*ZMAX*0.75
The relevant atom site should be identified.

Author Response: Residual density is close to copper atom and could be caused by inadequate adsorption collection

PLAT094_ALERT_2_C Ratio of Maximum / Minimum Residual Density .... 2.01 Report
PLAT222_ALERT_3_C NonSolvent Resd 2 H Uiso(max)/Uiso(min) Range 5.8 Ratio
PLAT244_ALERT_4_C Low 'Solvent' Ueq as Compared to Neighbors of N1I Check
PLAT314_ALERT_2_C Small Angle for H2O: Metal-O1C -H2C . 89.02 Degree
PLAT314_ALERT_2_C Small Angle for H2O: Metal-O1E -H2E . 84.47 Degree
PLAT352_ALERT_3_C Short N-H (X0.87,N1.01A) N1G - H5G . 0.75 Ang.
PLAT355_ALERT_3_C Long O-H (X0.82,N0.98A) O1E - H1E . 1.01 Ang.
PLAT355_ALERT_3_C Long O-H (X0.82,N0.98A) O1E - H2E . 1.06 Ang.
PLAT369_ALERT_2_C Long C(sp2)-C(sp2) Bond C1D - C2D . 1.53 Ang.
PLAT420_ALERT_2_C D-H Without Acceptor N1A --H5A . Please Check
PLAT420_ALERT_2_C D-H Without Acceptor N1D --H5D . Please Check
PLAT420_ALERT_2_C D-H Without Acceptor N1G --H5G . Please Check
PLAT480_ALERT_4_C Long H...A H-Bond Reported H1G ..N1F . 2.70 Ang.
PLAT480_ALERT_4_C Long H...A H-Bond Reported H11D ..O1I . 2.61 Ang.

PLAT480_ALERT_4_C Long H...A H-Bond Reported H2G ..O2D . 2.61 Ang.
PLAT480_ALERT_4_C Long H...A H-Bond Reported H9D ..O1H . 2.61 Ang.
PLAT480_ALERT_4_C Long H...A H-Bond Reported H8D ..O1H . 2.61 Ang.
PLAT601_ALERT_2_C Unit Cell Contains Solvent Accessible VOIDS of . 66 Ang**3
PLAT906_ALERT_3_C Large K Value in the Analysis of Variance ..... 4.142 Check
PLAT910_ALERT_3_C Missing # of FCF Reflection(s) Below Theta(Min). 8 Note
PLAT911_ALERT_3_C Missing FCF Refl Between Thmin & STh/L= 0.600 3 Report
PLAT972_ALERT_2_C Check Calcd Resid. Dens. 0.64A From Cu2 -2.13 eA-3
PLAT975_ALERT_2_C Check Calcd Resid. Dens. 0.99A From O1D 1.38 eA-3
PLAT975_ALERT_2_C Check Calcd Resid. Dens. 0.95A From O1H 0.40 eA-3

Alert level G

PLAT004_ALERT_5_G Polymeric Structure Found with Maximum Dimension 1 Info
PLAT045_ALERT_1_G Calculated and Reported Z Differ by a Factor ... 0.50 Check
PLAT066_ALERT_1_G Predicted and Reported Tmin&Tmax Range Identical ? Check
PLAT068_ALERT_1_G Reported F000 Differs from Calcd (or Missing)... Please Check
PLAT083_ALERT_2_G SHELXL Second Parameter in WGHT Unusually Large 6.61 Why ?
PLAT164_ALERT_4_G Nr. of Refined C-H H-Atoms in Heavy-Atom Struct. 2 Note
PLAT199_ALERT_1_G Reported _cell_measurement_temperature ..... (K) 293 Check
PLAT200_ALERT_1_G Reported _diffrn_ambient_temperature ..... (K) 293 Check
PLAT302_ALERT_4_G Anion/Solvent/Minor-Residue Disorder (Resd 4) 20% Note
PLAT412_ALERT_2_G Short Intra XH3 .. XHn H6I' ..H4I . 2.04 Ang.
x,y,z = 1_555 Check
PLAT720_ALERT_4_G Number of Unusual/Non-Standard Labels ..... 4 Note
PLAT789_ALERT_4_G Atoms with Negative _atom_site_disorder_group # 4 Check
PLAT794_ALERT_5_G Tentative Bond Valency for Cu1 (II) . 2.08 Info
PLAT794_ALERT_5_G Tentative Bond Valency for Cu2 (II) . 2.08 Info
PLAT794_ALERT_5_G Tentative Bond Valency for Cu3 (II) . 2.28 Info
PLAT883_ALERT_1_G No Info/Value for _atom_sites_solution_primary . Please Do !
PLAT912_ALERT_4_G Missing # of FCF Reflections Above STh/L= 0.600 25 Note
PLAT913_ALERT_3_G Missing # of Very Strong Reflections in FCF .... 1 Note
PLAT978_ALERT_2_G Number C-C Bonds with Positive Residual Density. 13 Info
0 **ALERT level A** = Most likely a serious problem - resolve or explain
2 **ALERT level B** = A potentially serious problem, consider carefully
25 **ALERT level C** = Check. Ensure it is not caused by an omission or oversight
19 **ALERT level G** = General information/check it is not something unexpected
7 ALERT type 1 CIF construction/syntax error, inconsistent or missing data
16 ALERT type 2 Indicator that the structure model may be wrong or deficient
8 ALERT type 3 Indicator that the structure quality may be low
11 ALERT type 4 Improvement, methodology, query or suggestion
4 ALERT type 5 Informative message, check

Validation response form

Please find below a validation response form (VRF) that can be filled in and pasted into your CIF.

```
# start Validation Reply Form
_vrf_PLAT097_C_6ab_a_a
;
PROBLEM: Large Reported Max. (Positive) Residual Density 3.23 eA-3
RESPONSE: ...
;
_vrf_PLAT094_C_6ab_a_a
;
PROBLEM: Ratio of Maximum / Minimum Residual Density .... 2.01 Report
RESPONSE: ...
;
_vrf_PLAT222_C_6ab_a_a
;
PROBLEM: NonSolvent Resd 2 H Uiso(max)/Uiso(min) Range 5.8 Ratio
RESPONSE: ...
;
_vrf_PLAT244_C_6ab_a_a
;
PROBLEM: Low 'Solvent' Ueq as Compared to Neighbors of N1I Check
RESPONSE: ...
```

```
;
_vrf_PLAT314_C_6ab_a_a
;
PROBLEM: Small Angle for H2O: Metal-O1C -H2C . 89.02 Degree
RESPONSE: ...
;
_vrf_PLAT352_C_6ab_a_a
;
PROBLEM: Short N-H (X0.87,N1.01A) N1G - H5G . 0.75 Ang.
RESPONSE: ...
;
_vrf_PLAT355_C_6ab_a_a
;
PROBLEM: Long O-H (X0.82,N0.98A) O1E - H1E . 1.01 Ang.
RESPONSE: ...
;
_vrf_PLAT369_C_6ab_a_a
;
PROBLEM: Long C(sp2)-C(sp2) Bond C1D - C2D . 1.53 Ang.
RESPONSE: ...
;
_vrf_PLAT420_C_6ab_a_a
;
PROBLEM: D-H Without Acceptor N1A --H5A . Please Check
RESPONSE: ...
;
_vrf_PLAT480_C_6ab_a_a
;
PROBLEM: Long H...A H-Bond Reported H1G ..N1F . 2.70 Ang.
RESPONSE: ...
;
_vrf_PLAT601_C_6ab_a_a
;
PROBLEM: Unit Cell Contains Solvent Accessible VOIDS of . 66 Ang**3
RESPONSE: ...
;
_vrf_PLAT906_C_6ab_a_a
;
PROBLEM: Large K Value in the Analysis of Variance ..... 4.142 Check
RESPONSE: ...
;
_vrf_PLAT910_C_6ab_a_a
;
PROBLEM: Missing # of FCF Reflection(s) Below Theta(Min). 8 Note
RESPONSE: ...
;
_vrf_PLAT911_C_6ab_a_a
;
PROBLEM: Missing FCF Refl Between Thmin & STh/L= 0.600 3 Report
RESPONSE: ...
;
_vrf_PLAT972_C_6ab_a_a
;
PROBLEM: Check Calcd Resid. Dens. 0.64A From Cu2 -2.13 eA-3
RESPONSE: ...
;
_vrf_PLAT975_C_6ab_a_a
;
PROBLEM: Check Calcd Resid. Dens. 0.99A From O1D 1.38 eA-3
RESPONSE: ...
;
# end Validation Reply Form
```

It is advisable to attempt to resolve as many as possible of the alerts in all categories. Often the

minor alerts point to easily fixed oversights, errors and omissions in your CIF or refinement strategy, so attention to these fine details can be worthwhile. In order to resolve some of the more serious problems it may be necessary to carry out additional measurements or structure refinements. However, the purpose of your study may justify the reported deviations and the more serious of these should normally be commented upon in the discussion or experimental section of a paper or in the "special_details" fields of the CIF. checkCIF was carefully designed to identify outliers and unusual parameters, but every test has its limitations and alerts that are not important in a particular case may appear. Conversely, the absence of alerts does not guarantee there are no aspects of the results needing attention. It is up to the individual to critically assess their own results and, if necessary, seek expert advice.

Publication of your CIF in IUCr journals

A basic structural check has been run on your CIF. These basic checks will be run on all CIFs submitted for publication in IUCr journals (*Acta Crystallographica*, *Journal of Applied Crystallography*, *Journal of Synchrotron Radiation*); however, if you intend to submit to *Acta Crystallographica Section C* or *E* or *IUCrData*, you should make sure that full publication checks are run on the final version of your CIF prior to submission.

Publication of your CIF in other journals

Please refer to the *Notes for Authors* of the relevant journal for any special instructions relating to CIF submission.

PLATON version of 18/09/2020; check.def file version of 20/08/2020

Datablock C_6ab_a_a - ellipsoid plot

Compound 7

CIF check

checkCIF/PLATON report

Structure factors have been supplied for datablock(s) C_7_a

THIS REPORT IS FOR GUIDANCE ONLY. IF USED AS PART OF A REVIEW PROCEDURE FOR PUBLICATION, IT SHOULD NOT REPLACE THE EXPERTISE OF AN EXPERIENCED CRYSTALLOGRAPHIC REFEREE.

No syntax errors found. CIF dictionary Interpreting this report

Datablock: C_7_a

```
Bond precision: C-C = 0.0046 A Wavelength=0.71073
Cell: a=17.7559(10) b=17.7559(10) c=18.689(2)
alpha=90 beta=90 gamma=120
Temperature: 293 K
Calculated Reported
Volume 5102.7(8) 5102.8(8)
Space group P -3 1 c P -3 1 c
Hall group -P 3 2c -P 3 2c
Moiety formula
3(C24 H16 Cl Cu N2 O4), Cl
[+ solvent]
?
Sum formula
C72 H48 Cl4 Cu3 N6 O12 [+
solvent]
C24 H16 Cl1.33 Cu N2 O4
```

Mr 1521.61 507.19
Dx,g cm-3 0.990 0.990
Z 2 6
Mu (mm-1) 0.769 0.769
F000 1546.0 1546.0
F000' 1549.66
h,k,lmax 22,22,23 22,22,23
Nref 3493 3495
Tmin,Tmax 0.794,0.857 0.794,0.857
Tmin' 0.794
Correction method= # Reported T Limits: Tmin=0.794 Tmax=0.857
AbsCorr = MULTI-SCAN
Data completeness= 1.001 Theta(max)= 26.367
R(reflections)= 0.0468(2500) wR2(reflections)= 0.1418(3495)
S = 1.070 Npar= 148
The following ALERTS were generated. Each ALERT has the format
test-name_ALERT_alert-type_alert-level.
Click on the hyperlinks for more details of the test.

Alert level A

PLAT431_ALERT_2_A Short Inter HL..A Contact Cl2 ..O2 . 2.29 Ang.
2-y,2-x,-1/2-z = 4_774 Check

Author Response: O2 is a free carboxylate oxygen which forms a non-covalent interaction

PLAT431_ALERT_2_A Short Inter HL..A Contact Cl2 ..O2 . 2.29 Ang.
2-x+y,y,-1/2-z = 5_754 Check

Author Response: O2 is a free carboxylate oxygen which forms a non-covalent interaction

PLAT431_ALERT_2_A Short Inter HL..A Contact Cl2 ..O2 . 2.29 Ang.
2-y,x-y,z = 2_755 Check

Author Response: O2 is a free carboxylate oxygen which forms a non-covalent interaction

PLAT431_ALERT_2_A Short Inter HL..A Contact Cl2 ..O2 . 2.29 Ang.
x,y,z = 1_555 Check

Author Response: O2 is a free carboxylate oxygen which forms a non-covalent interaction

PLAT431_ALERT_2_A Short Inter HL..A Contact Cl2 ..O2 . 2.29 Ang.
x,x-y,-1/2-z = 6_554 Check

Author Response: O2 is a free carboxylate oxygen which forms a non-covalent interaction

PLAT431_ALERT_2_A Short Inter HL..A Contact Cl2 ..O2 . 2.29 Ang.
2-x+y,2-x,z = 3_775 Check

Author Response: O2 is a free carboxylate oxygen which forms a non-covalent interaction

Alert level C

PLAT213_ALERT_2_C Atom C3 has ADP max/min Ratio ..... 3.5 prolat
PLAT220_ALERT_2_C NonSolvent Resd 1 C Ueq(max)/Ueq(min) Range 3.1 Ratio
PLAT241_ALERT_2_C High 'MainMol' Ueq as Compared to Neighbors of C3 Check
PLAT242_ALERT_2_C Low 'MainMol' Ueq as Compared to Neighbors of Cu1 Check
PLAT242_ALERT_2_C Low 'MainMol' Ueq as Compared to Neighbors of C4 Check
PLAT250_ALERT_2_C Large U3/U1 Ratio for Average U(i,j) Tensor .... 2.9 Note
PLAT905_ALERT_3_C Negative K value in the Analysis of Variance ... -1.134 Report
PLAT923_ALERT_1_C S Values in the CIF and FCF Differ by ..... 0.011 Check
PLAT934_ALERT_3_C Number of (Iobs-Icalc)/Sigma(W) > 10 Outliers .. 1 Check

Alert level G

PLAT004_ALERT_5_G Polymeric Structure Found with Maximum Dimension 1 Info
PLAT045_ALERT_1_G Calculated and Reported Z Differ by a Factor ... 0.33 Check

```
PLAT066_ALERT_1_G Predicted and Reported Tmin&Tmax Range Identical ? Check
PLAT199_ALERT_1_G Reported _cell_measurement_temperature ..... (K) 293 Check
PLAT200_ALERT_1_G Reported _diffrn_ambient_temperature ..... (K) 293 Check
PLAT232_ALERT_2_G Hirshfeld Test Diff (M-X) Cu1 --Cl1 . 25.3 s.u.
PLAT606_ALERT_4_G Solvent Accessible VOID(S) in Structure ........ ! Info
PLAT794_ALERT_5_G Tentative Bond Valency for Cu1 (II) . 1.97 Info
PLAT802_ALERT_4_G CIF Input Record(s) with more than 80 Characters 1 Info
PLAT869_ALERT_4_G ALERTS Related to the Use of SQUEEZE Suppressed ! Info
PLAT883_ALERT_1_G No Info/Value for _atom_sites_solution_primary . Please Do !
PLAT910_ALERT_3_G Missing # of FCF Reflection(s) Below Theta(Min). 1 Note
PLAT933_ALERT_2_G Number of OMIT Records in Embedded .res File ... 1 Note
PLAT965_ALERT_2_G The SHELXL WEIGHT Optimisation has not Converged Please Check
PLAT978_ALERT_2_G Number C-C Bonds with Positive Residual Density. 5 Info
6 ALERT level A = Most likely a serious problem - resolve or explain
0 ALERT level B = A potentially serious problem, consider carefully
9 ALERT level C = Check. Ensure it is not caused by an omission or oversight
15 ALERT level G = General information/check it is not something unexpected
6 ALERT type 1 CIF construction/syntax error, inconsistent or missing data
16 ALERT type 2 Indicator that the structure model may be wrong or deficient
3 ALERT type 3 Indicator that the structure quality may be low
3 ALERT type 4 Improvement, methodology, query or suggestion
2 ALERT type 5 Informative message, check
```

It is advisable to attempt to resolve as many as possible of the alerts in all categories. Often the minor alerts point to easily fixed oversights, errors and omissions in your CIF or refinement strategy, so attention to these fine details can be worthwhile. In order to resolve some of the more serious problems it may be necessary to carry out additional measurements or structure refinements. However, the purpose of your study may justify the reported deviations and the more serious of these should normally be commented upon in the discussion or experimental section of a paper or in the "special_details" fields of the CIF. checkCIF was carefully designed to identify outliers and unusual parameters, but every test has its limitations and alerts that are not important in a particular case may appear. Conversely, the absence of alerts does not guarantee there are no aspects of the results needing attention. It is up to the individual to critically assess their own results and, if necessary, seek expert advice.

Publication of your CIF in IUCr journals

A basic structural check has been run on your CIF. These basic checks will be run on all CIFs submitted for publication in IUCr journals (*Acta Crystallographica*, *Journal of Applied Crystallography*, *Journal of Synchrotron Radiation*); however, if you intend to submit to *Acta Crystallographica Section C* or *E* or *IUCrData*, you should make sure that full publication checks are run on the final version of your CIF prior to submission.

Publication of your CIF in other journals

Please refer to the *Notes for Authors* of the relevant journal for any special instructions relating to CIF submission.

Validation response form

Please find below a validation response form (VRF) that can be filled in and pasted into your CIF.

```
# start Validation Reply Form
_vrf_PLAT213_C_7_a
;
PROBLEM: Atom C3 has ADP max/min Ratio ..... 3.5 prolat
RESPONSE: ...
;
_vrf_PLAT220_C_7_a
;
PROBLEM: NonSolvent Resd 1 C Ueq(max)/Ueq(min) Range 3.1 Ratio
RESPONSE: ...
;
_vrf_PLAT241_C_7_a
;
PROBLEM: High 'MainMol' Ueq as Compared to Neighbors of C3 Check
```

```
RESPONSE: ...
;
_vrf_PLAT242_C_7_a
;
PROBLEM: Low 'MainMol' Ueq as Compared to Neighbors of Cu1 Check
RESPONSE: ...
;
_vrf_PLAT250_C_7_a
;
PROBLEM: Large U3/U1 Ratio for Average U(i,j) Tensor .... 2.9 Note
RESPONSE: ...
;
_vrf_PLAT905_C_7_a
;
PROBLEM: Negative K value in the Analysis of Variance ... -1.134 Report
RESPONSE: ...
;
_vrf_PLAT923_C_7_a
;
PROBLEM: S Values in the CIF and FCF Differ by ....... 0.011 Check
RESPONSE: ...
;
_vrf_PLAT934_C_7_a
;
PROBLEM: Number of (Iobs-Icalc)/Sigma(W) > 10 Outliers .. 1 Check
RESPONSE: ...
;
# end Validation Reply Form
```

PLATON version of 18/09/2020; check.def file version of 20/08/2020

Datablock C_7_a - ellipsoid plot

1. Chapter 4

Compound 1d

CIF Check

checkCIF/PLATON report

Structure factors have been supplied for datablock(s)
C__Users_Adrien_Desktop_1D_COR~1_NEWFOL~1_1d_a
THIS REPORT IS FOR GUIDANCE ONLY. IF USED AS PART OF A REVIEW PROCEDURE FOR PUBLICATION, IT SHOULD NOT REPLACE THE EXPERTISE OF AN EXPERIENCED CRYSTALLOGRAPHIC REFEREE.
No syntax errors found. CIF dictionary Interpreting this report

Datablock: C__Users_Adrien_Desktop_1D_COR~1_NEWFOL~1_1d_a

```
Bond precision: C-C = 0.0067 A Wavelength=0.71073
Cell: a=10.3931(14) b=16.027(2) c=14.996(2)
alpha=90 beta=98.243(2) gamma=90
Temperature: 293 K
Calculated Reported
Volume 2472.1(6) 2472.2(6)
Space group P 21/c P 21/c
Hall group -P 2ybc -P 2ybc
```

Moiety formula C24 H16 Co N2 O4 ?
Sum formula C24 H16 Co N2 O4 C24 H16 Co N2 O4
Mr 455.32 455.32
Dx,g cm-3 1.223 1.223
Z 4 4
Mu (mm-1) 0.722 0.722
F000 932.0 932.0
F000' 933.77
h,k,lmax 13,21,19 13,20,19
Nref 5938 5859
Tmin,Tmax 0.925,0.944 0.904,0.944
Tmin' 0.904
Correction method= # Reported T Limits: Tmin=0.904 Tmax=0.944
AbsCorr = MULTI-SCAN
Data completeness= 0.987 Theta(max)= 27.963
R(reflections)= 0.0639(3863) wR2(reflections)= 0.1687(5859)
S = 1.044 Npar= 336

The following ALERTS were generated. Each ALERT has the format
test-name_ALERT_alert-type_alert-level.
Click on the hyperlinks for more details of the test.

Alert level A

PLAT601_ALERT_2_A Unit Cell Contains Solvent Accessible VOIDS of . 260 Ang**3

Author Response: This is due to the evacuated guest molecules.

Alert level C

PLAT213_ALERT_2_C Atom C3 has ADP max/min Ratio ..... 3.4 prolat
PLAT213_ALERT_2_C Atom C6B has ADP max/min Ratio ..... 4.0 prolat
PLAT213_ALERT_2_C Atom C7B has ADP max/min Ratio ..... 3.5 prolat
PLAT220_ALERT_2_C NonSolvent Resd 1 C Ueq(max)/Ueq(min) Range 4.1 Ratio
PLAT241_ALERT_2_C High 'MainMol' Ueq as Compared to Neighbors of C6A Check
PLAT241_ALERT_2_C High 'MainMol' Ueq as Compared to Neighbors of C9A Check
PLAT241_ALERT_2_C High 'MainMol' Ueq as Compared to Neighbors of C10A Check
PLAT242_ALERT_2_C Low 'MainMol' Ueq as Compared to Neighbors of N1A Check
PLAT242_ALERT_2_C Low 'MainMol' Ueq as Compared to Neighbors of C8A Check
PLAT341_ALERT_3_C Low Bond Precision on C-C Bonds ..... 0.00675 Ang.
PLAT906_ALERT_3_C Large K Value in the Analysis of Variance ..... 3.168 Check
PLAT911_ALERT_3_C Missing FCF Refl Between Thmin & STh/L= 0.600 42 Report

Alert level G

PLAT002_ALERT_2_G Number of Distance or Angle Restraints on AtSite 3 Note
PLAT004_ALERT_5_G Polymeric Structure Found with Maximum Dimension 3 Info
PLAT066_ALERT_1_G Predicted and Reported Tmin&Tmax Range Identical ? Check
PLAT083_ALERT_2_G SHELXL Second Parameter in WGHT Unusually Large 5.05 Why ?
PLAT172_ALERT_4_G The CIF-Embedded .res File Contains DFIX Records 2 Report
PLAT199_ALERT_1_G Reported _cell_measurement_temperature ..... (K) 293 Check
PLAT200_ALERT_1_G Reported _diffrn_ambient_temperature ..... (K) 293 Check
PLAT301_ALERT_3_G Main Residue Disorder .....(Resd 1) 19% Note
PLAT367_ALERT_2_G Long? C(sp?)-C(sp?) Bond C1B - C2B . 1.51 Ang.
PLAT367_ALERT_2_G Long? C(sp?)-C(sp?) Bond C4A - C8A . 1.50 Ang.
PLAT410_ALERT_2_G Short Intra H...H Contact H2B ..H5B . 2.00 Ang.
x,y,z = 1_555 Check
PLAT720_ALERT_4_G Number of Unusual/Non-Standard Labels ..... 5 Note
PLAT860_ALERT_3_G Number of Least-Squares Restraints ..... 2 Note
PLAT883_ALERT_1_G No Info/Value for _atom_sites_solution_primary . Please Do !
PLAT910_ALERT_3_G Missing # of FCF Reflection(s) Below Theta(Min). 4 Note
PLAT912_ALERT_4_G Missing # of FCF Reflections Above STh/L= 0.600 28 Note
PLAT933_ALERT_2_G Number of OMIT Records in Embedded .res File ... 37 Note
PLAT941_ALERT_3_G Average HKL Measurement Multiplicity ..... 3.9 Low
PLAT965_ALERT_2_G The SHELXL WEIGHT Optimisation has not Converged Please Check
PLAT978_ALERT_2_G Number C-C Bonds with Positive Residual Density. 1 Info

1 **ALERT level A** = Most likely a serious problem - resolve or explain
0 **ALERT level B** = A potentially serious problem, consider carefully
12 **ALERT level C** = Check. Ensure it is not caused by an omission or oversight
20 **ALERT level G** = General information/check it is not something unexpected
4 ALERT type 1 CIF construction/syntax error, inconsistent or missing data
18 ALERT type 2 Indicator that the structure model may be wrong or deficient
7 ALERT type 3 Indicator that the structure quality may be low
3 ALERT type 4 Improvement, methodology, query or suggestion
1 ALERT type 5 Informative message, check

It is advisable to attempt to resolve as many as possible of the alerts in all categories. Often the minor alerts point to easily fixed oversights, errors and omissions in your CIF or refinement strategy, so attention to these fine details can be worthwhile. In order to resolve some of the more serious problems it may be necessary to carry out additional measurements or structure refinements. However, the purpose of your study may justify the reported deviations and the more serious of these should normally be commented upon in the discussion or experimental section of a paper or in the "special_details" fields of the CIF. checkCIF was carefully designed to identify outliers and unusual parameters, but every test has its limitations and alerts that are not important in a particular case may appear. Conversely, the absence of alerts does not guarantee there are no aspects of the results needing attention. It is up to the individual to critically assess their own results and, if necessary, seek expert advice.

Publication of your CIF in IUCr journals

A basic structural check has been run on your CIF. These basic checks will be run on all CIFs submitted for publication in IUCr journals (*Acta Crystallographica*, *Journal of Applied Crystallography*, *Journal of Synchrotron Radiation*); however, if you intend to submit to *Acta Crystallographica Section C* or *E* or *IUCrData*, you should make sure that full publication checks are run on the final version of your CIF prior to submission.

Publication of your CIF in other journals

Please refer to the *Notes for Authors* of the relevant journal for any special instructions relating to CIF submission.

Validation response form

Please find below a validation response form (VRF) that can be filled in and pasted into your CIF.

```
# start Validation Reply Form
_vrf_PLAT213_C__Users_Adrien_Desktop_1D_COR~1_NEWFOL~1_1d_a
;
PROBLEM: Atom C3 has ADP max/min Ratio ..... 3.4 prolat
RESPONSE: ...
;
_vrf_PLAT220_C__Users_Adrien_Desktop_1D_COR~1_NEWFOL~1_1d_a
;
PROBLEM: NonSolvent Resd 1 C Ueq(max)/Ueq(min) Range 4.1 Ratio
RESPONSE: ...
;
_vrf_PLAT241_C__Users_Adrien_Desktop_1D_COR~1_NEWFOL~1_1d_a
;
PROBLEM: High 'MainMol' Ueq as Compared to Neighbors of C6A Check
RESPONSE: ...
;
_vrf_PLAT242_C__Users_Adrien_Desktop_1D_COR~1_NEWFOL~1_1d_a
;
PROBLEM: Low 'MainMol' Ueq as Compared to Neighbors of N1A Check
RESPONSE: ...
;
_vrf_PLAT341_C__Users_Adrien_Desktop_1D_COR~1_NEWFOL~1_1d_a
;
PROBLEM: Low Bond Precision on C-C Bonds ............... 0.00675 Ang.
RESPONSE: ...
;
_vrf_PLAT906_C__Users_Adrien_Desktop_1D_COR~1_NEWFOL~1_1d_a
```

;
PROBLEM: Large K Value in the Analysis of Variance ..... 3.168 Check
RESPONSE: ...
;
_vrf_PLAT911_C__Users_Adrien_Desktop_1D_COR~1_NEWFOL~1_1d_a
;
PROBLEM: Missing FCF Refl Between Thmin & STh/L= 0.600 42 Report
RESPONSE: ...
;
end Validation Reply Form

PLATON version of 18/09/2020; check.def file version of 20/08/2020

Datablock C__Users_Adrien_Desktop_1D_COR~1_NEWFOL~1_1d_a - ellipsoid plot

Compound 1dCH$_2$Cl$_2$

CIF Check

checkCIF/PLATON report

Structure factors have been supplied for datablock(s) C_1dCH2Cl2

THIS REPORT IS FOR GUIDANCE ONLY. IF USED AS PART OF A REVIEW PROCEDURE FOR PUBLICATION, IT SHOULD NOT REPLACE THE EXPERTISE OF AN EXPERIENCED CRYSTALLOGRAPHIC REFEREE.

No syntax errors found. CIF dictionary Interpreting this report

Datablock: C_1dCH2Cl2

Bond precision: C-C = 0.0037 A Wavelength=0.71073
Cell: a=10.5973(11) b=15.3082(15) c=14.8848(15)
alpha=90 beta=99.964(2) gamma=90
Temperature: 293 K
Calculated Reported
Volume 2378.3(4) 2378.3(4)
Space group P 21/c P 21/c
Hall group -P 2ybc -P 2ybc
Moiety formula C24 H16 Co N2 O4, C H2 Cl2 ?
Sum formula C25 H18 Cl2 Co N2 O4 C25 H18 Cl2 Co N2 O4
Mr 540.24 540.24
Dx,g cm-3 1.509 1.509
Z 4 4
Mu (mm-1) 0.981 0.981
F000 1100.0 1100.0
F000' 1102.97
h,k,lmax 14,20,19 14,20,19
Nref 5822 5821
Tmin,Tmax 0.790,0.851 0.715,0.851
Tmin' 0.715
Correction method= # Reported T Limits: Tmin=0.715 Tmax=0.851
AbsCorr = MULTI-SCAN
Data completeness= 1.000 Theta(max)= 28.141
R(reflections)= 0.0454(4338) wR2(reflections)= 0.1092(5821)
S = 1.015 Npar= 335
The following ALERTS were generated. Each ALERT has the format

test-name_ALERT_alert-type_alert-level.
Click on the hyperlinks for more details of the test.

Alert level C

PLAT260_ALERT_2_C Large Average Ueq of Residue Including Cl3 0.125 Check
PLAT260_ALERT_2_C Large Average Ueq of Residue Including Cl1 0.158 Check

Alert level G

PLAT004_ALERT_5_G Polymeric Structure Found with Maximum Dimension 3 Info
PLAT066_ALERT_1_G Predicted and Reported Tmin&Tmax Range Identical ? Check
PLAT199_ALERT_1_G Reported _cell_measurement_temperature ..... (K) 293 Check
PLAT200_ALERT_1_G Reported _diffrn_ambient_temperature ..... (K) 293 Check
PLAT232_ALERT_2_G Hirshfeld Test Diff (M-X) Co01 --O005_b . 6.0 s.u.
PLAT302_ALERT_4_G Anion/Solvent/Minor-Residue Disorder (Resd 2) 100% Note
PLAT302_ALERT_4_G Anion/Solvent/Minor-Residue Disorder (Resd 3) 100% Note
PLAT720_ALERT_4_G Number of Unusual/Non-Standard Labels ..... 47 Note
PLAT794_ALERT_5_G Tentative Bond Valency for Co01 (II) . 1.95 Info
PLAT883_ALERT_1_G No Info/Value for _atom_sites_solution_primary . Please Do !
PLAT912_ALERT_4_G Missing # of FCF Reflections Above STh/L= 0.600 1 Note
PLAT978_ALERT_2_G Number C-C Bonds with Positive Residual Density. 9 Info
0 **ALERT level A** = Most likely a serious problem - resolve or explain
0 **ALERT level B** = A potentially serious problem, consider carefully
2 **ALERT level C** = Check. Ensure it is not caused by an omission or oversight
12 **ALERT level G** = General information/check it is not something unexpected
4 ALERT type 1 CIF construction/syntax error, inconsistent or missing data
4 ALERT type 2 Indicator that the structure model may be wrong or deficient
0 ALERT type 3 Indicator that the structure quality may be low
4 ALERT type 4 Improvement, methodology, query or suggestion
2 ALERT type 5 Informative message, check

Validation response form

Please find below a validation response form (VRF) that can be filled in and pasted into your CIF.

```
# start Validation Reply Form
_vrf_PLAT260_C_1dCH2Cl2
;
PROBLEM: Large Average Ueq of Residue Including Cl3 0.125 Check
RESPONSE: ...
;
# end Validation Reply Form
```

It is advisable to attempt to resolve as many as possible of the alerts in all categories. Often the minor alerts point to easily fixed oversights, errors and omissions in your CIF or refinement strategy, so attention to these fine details can be worthwhile. In order to resolve some of the more serious problems it may be necessary to carry out additional measurements or structure refinements. However, the purpose of your study may justify the reported deviations and the more serious of these should normally be commented upon in the discussion or experimental section of a paper or in the "special_details" fields of the CIF. checkCIF was carefully designed to identify outliers and unusual parameters, but every test has its limitations and alerts that are not important in a particular case may appear. Conversely, the absence of alerts does not guarantee there are no aspects of the results needing attention. It is up to the individual to critically assess their own results and, if necessary, seek expert advice.

Publication of your CIF in IUCr journals

A basic structural check has been run on your CIF. These basic checks will be run on all CIFs submitted for publication in IUCr journals (*Acta Crystallographica*, *Journal of Applied Crystallography*, *Journal of Synchrotron Radiation*); however, if you intend to submit to *Acta Crystallographica Section C* or *E* or *IUCrData*, you should make sure that full publication checks are run on the final version of your CIF prior to submission.

Publication of your CIF in other journals

Please refer to the *Notes for Authors* of the relevant journal for any special instructions relating to CIF submission.

PLATON version of 18/09/2020; check.def file version of 20/08/2020

Compound 1dCHCl$_3$

CIF Check

checkCIF/PLATON report

Structure factors have been supplied for datablock(s) C_1dCHCl3
THIS REPORT IS FOR GUIDANCE ONLY. IF USED AS PART OF A REVIEW PROCEDURE FOR PUBLICATION, IT SHOULD NOT REPLACE THE EXPERTISE OF AN EXPERIENCED CRYSTALLOGRAPHIC REFEREE.
No syntax errors found. CIF dictionary Interpreting this report

Datablock: C_1dCHCl3

```
Bond precision: C-C = 0.0040 A Wavelength=0.71073
Cell: a=10.0048(16) b=16.371(3) c=15.036(3)
alpha=90 beta=97.402(3) gamma=90
Temperature: 293 K
Calculated Reported
Volume 2442.2(8) 2442.3(7)
Space group P 21/c P 21/c
Hall group -P 2ybc -P 2ybc
Moiety formula
C24 H16 Co N2 O4, C H0.84
Cl3
?
Sum formula C25 H16.84 Cl3 Co N2 O4 C25 H16.83 Cl3 Co N2 O4
Mr 574.52 574.52
Dx,g cm-3 1.563 1.562
Z 4 4
Mu (mm-1) 1.066 1.066
F000 1163.4 1163.0
F000' 1166.93
h,k,lmax 13,21,20 13,21,20
Nref 6087 6062
Tmin,Tmax 0.761,0.888 0.707,0.888
Tmin' 0.707
Correction method= # Reported T Limits: Tmin=0.707 Tmax=0.888
AbsCorr = MULTI-SCAN
Data completeness= 0.996 Theta(max)= 28.310
R(reflections)= 0.0479( 4504) wR2(reflections)= 0.1293( 6062)
S = 1.019 Npar= 326
```

The following ALERTS were generated. Each ALERT has the format **test-name_ALERT_alert-type_alert-level.**
Click on the hyperlinks for more details of the test.

Alert level C

PLAT041_ALERT_1_C Calc. and Reported SumFormula Strings Differ Please Check
PLAT244_ALERT_4_C Low 'Solvent' Ueq as Compared to Neighbors of C00Z Check
PLAT260_ALERT_2_C Large Average Ueq of Residue Including Cl1 0.131 Check
PLAT977_ALERT_2_C Check Negative Difference Density on H00B -0.34 eA-3

Alert level G

FORMU01_ALERT_2_G There is a discrepancy between the atom counts in the

```
_chemical_formula_sum and the formula from the _atom_site* data.
Atom count from _chemical_formula_sum:C25 H16.83 Cl3 Co1 N2 O4
Atom count from the _atom_site data: C25 H16.84 Cl3 Co1 N2 O4
PLAT004_ALERT_5_G Polymeric Structure Found with Maximum Dimension 3 Info
PLAT066_ALERT_1_G Predicted and Reported Tmin&Tmax Range Identical ? Check
PLAT068_ALERT_1_G Reported F000 Differs from Calcd (or Missing)... Please Check
PLAT199_ALERT_1_G Reported _cell_measurement_temperature ..... (K) 293 Check
PLAT200_ALERT_1_G Reported _diffrn_ambient_temperature ..... (K) 293 Check
PLAT232_ALERT_2_G Hirshfeld Test Diff (M-X) Co01 --O006_b . 6.1 s.u.
PLAT302_ALERT_4_G Anion/Solvent/Minor-Residue Disorder (Resd 2 ) 25% Note
PLAT720_ALERT_4_G Number of Unusual/Non-Standard Labels .......... 50 Note
PLAT779_ALERT_4_G Suspect or Irrelevant (Bond) Angle(s) in CIF . # 110 Check
CL4 -C00Z -CL3 1.555 1.555 1.555 13.40 Deg.
PLAT794_ALERT_5_G Tentative Bond Valency for Co01 (II) . 1.92 Info
PLAT883_ALERT_1_G No Info/Value for _atom_sites_solution_primary . Please Do !
PLAT912_ALERT_4_G Missing # of FCF Reflections Above STh/L= 0.600 25 Note
PLAT978_ALERT_2_G Number C-C Bonds with Positive Residual Density. 13 Info
0 ALERT level A = Most likely a serious problem - resolve or explain
0 ALERT level B = A potentially serious problem, consider carefully
4 ALERT level C = Check. Ensure it is not caused by an omission or oversight
14 ALERT level G = General information/check it is not something unexpected
6 ALERT type 1 CIF construction/syntax error, inconsistent or missing data
5 ALERT type 2 Indicator that the structure model may be wrong or deficient
0 ALERT type 3 Indicator that the structure quality may be low
5 ALERT type 4 Improvement, methodology, query or suggestion
2 ALERT type 5 Informative message, check
```

Validation response form

Please find below a validation response form (VRF) that can be filled in and pasted into your CIF.

```
# start Validation Reply Form
_vrf_PLAT041_C_1dCHCl3
;
PROBLEM: Calc. and Reported SumFormula Strings Differ Please Check
RESPONSE: ...
;
_vrf_PLAT244_C_1dCHCl3
;
PROBLEM: Low 'Solvent' Ueq as Compared to Neighbors of C00Z Check
RESPONSE: ...
;
_vrf_PLAT260_C_1dCHCl3
;
PROBLEM: Large Average Ueq of Residue Including Cl1 0.131 Check
RESPONSE: ...
;
_vrf_PLAT977_C_1dCHCl3
;
PROBLEM: Check Negative Difference Density on H00B -0.34 eA-3
RESPONSE: ...
;
# end Validation Reply Form
```

It is advisable to attempt to resolve as many as possible of the alerts in all categories. Often the minor alerts point to easily fixed oversights, errors and omissions in your CIF or refinement strategy, so attention to these fine details can be worthwhile. In order to resolve some of the more serious problems it may be necessary to carry out additional measurements or structure refinements. However, the purpose of your study may justify the reported deviations and the more serious of these should normally be commented upon in the discussion or experimental section of a paper or in the "special_details" fields of the CIF. checkCIF was carefully designed to identify outliers and unusual parameters, but every test has its limitations and alerts that are not important in a particular case may appear. Conversely, the absence of alerts does not guarantee there are no aspects of the results needing attention. It is up to the individual to critically assess their own

results and, if necessary, seek expert advice.

Publication of your CIF in IUCr journals

A basic structural check has been run on your CIF. These basic checks will be run on all CIFs submitted for publication in IUCr journals (*Acta Crystallographica*, *Journal of Applied Crystallography*, *Journal of Synchrotron Radiation*); however, if you intend to submit to *Acta Crystallographica Section C* or *E* or *IUCrData*, you should make sure that full publication checks are run on the final version of your CIF prior to submission.

Publication of your CIF in other journals

Please refer to the *Notes for Authors* of the relevant journal for any special instructions relating to CIF submission.

PLATON version of 18/09/2020; check.def file version of 20/08/2020

Datablock C_1dCHCl3 - ellipsoid plot

Compound 1dClBenz

CIF Check

checkCIF/PLATON report

Structure factors have been supplied for datablock(s) C_1dClBenz

THIS REPORT IS FOR GUIDANCE ONLY. IF USED AS PART OF A REVIEW PROCEDURE FOR PUBLICATION, IT SHOULD NOT REPLACE THE EXPERTISE OF AN EXPERIENCED CRYSTALLOGRAPHIC REFEREE.

No syntax errors found. CIF dictionary Interpreting this report

Datablock: C_1dClBenz

```
Bond precision: C-C = 0.0055 A Wavelength=0.71073
Cell: a=10.2944(16) b=16.272(3) c=15.248(3)
alpha=90 beta=95.232(4) gamma=90
Temperature: 293 K
Calculated Reported
Volume 2543.6(8) 2543.6(7)
Space group P 21/c P 21/c
Hall group -P 2ybc -P 2ybc
Moiety formula C24 H16 Co N2 O4, C6 H5 Cl ?
Sum formula C30 H21 Cl Co N2 O4 C30 H21 Cl Co N2 O4
Mr 567.87 567.87
Dx,g cm-3 1.483 1.483
Z 4 4
Mu (mm-1) 0.820 0.820
F000 1164.0 1164.0
F000' 1166.42
h,k,lmax 13,21,20 13,21,20
Nref 6303 6296
Tmin,Tmax 0.880,0.921 0.849,0.921
Tmin' 0.849
Correction method= # Reported T Limits: Tmin=0.849 Tmax=0.921
AbsCorr = MULTI-SCAN
Data completeness= 0.999 Theta(max)= 28.263
R(reflections)= 0.0550( 4493) wR2(reflections)= 0.1571( 6296)
S = 1.038 Npar= 343
The following ALERTS were generated. Each ALERT has the format
```

test-name_ALERT_alert-type_alert-level.
Click on the hyperlinks for more details of the test.

Alert level C

PLAT243_ALERT_4_C High 'Solvent' Ueq as Compared to Neighbors of C012 Check
PLAT244_ALERT_4_C Low 'Solvent' Ueq as Compared to Neighbors of C00Z Check
PLAT250_ALERT_2_C Large U3/U1 Ratio for Average U(i,j) Tensor .... 2.1 Note
PLAT480_ALERT_4_C Long H...A H-Bond Reported H00G ..CL00 . 2.97 Ang.
PLAT480_ALERT_4_C Long H...A H-Bond Reported H00O ..CL00 . 2.92 Ang.

Alert level G

PLAT004_ALERT_5_G Polymeric Structure Found with Maximum Dimension 3 Info
PLAT066_ALERT_1_G Predicted and Reported Tmin&Tmax Range Identical ? Check
PLAT199_ALERT_1_G Reported _cell_measurement_temperature ..... (K) 293 Check
PLAT200_ALERT_1_G Reported _diffrn_ambient_temperature ..... (K) 293 Check
PLAT231_ALERT_4_G Hirshfeld Test (Solvent) C00X --C00Y . 6.3 s.u.
PLAT231_ALERT_4_G Hirshfeld Test (Solvent) C00X --C011 . 8.0 s.u.
PLAT231_ALERT_4_G Hirshfeld Test (Solvent) C00Z --C010 . 5.2 s.u.
PLAT232_ALERT_2_G Hirshfeld Test Diff (M-X) Co01 --O006 . 6.1 s.u.
PLAT720_ALERT_4_G Number of Unusual/Non-Standard Labels ..... 59 Note
PLAT794_ALERT_5_G Tentative Bond Valency for Co01 (II) . 1.92 Info
PLAT883_ALERT_1_G No Info/Value for _atom_sites_solution_primary . Please Do !
PLAT912_ALERT_4_G Missing # of FCF Reflections Above STh/L= 0.600 8 Note
PLAT978_ALERT_2_G Number C-C Bonds with Positive Residual Density. 6 Info
0 **ALERT level A** = Most likely a serious problem - resolve or explain
0 **ALERT level B** = A potentially serious problem, consider carefully
5 **ALERT level C** = Check. Ensure it is not caused by an omission or oversight
13 **ALERT level G** = General information/check it is not something unexpected
4 ALERT type 1 CIF construction/syntax error, inconsistent or missing data
3 ALERT type 2 Indicator that the structure model may be wrong or deficient
0 ALERT type 3 Indicator that the structure quality may be low
9 ALERT type 4 Improvement, methodology, query or suggestion
2 ALERT type 5 Informative message, check

Validation response form

Please find below a validation response form (VRF) that can be filled in and pasted into your CIF.

```
# start Validation Reply Form
_vrf_PLAT243_C_1dClBenz
;
PROBLEM: High 'Solvent' Ueq as Compared to Neighbors of C012 Check
RESPONSE: ...
;
_vrf_PLAT244_C_1dClBenz
;
PROBLEM: Low 'Solvent' Ueq as Compared to Neighbors of C00Z Check
RESPONSE: ...
;
_vrf_PLAT250_C_1dClBenz
;
PROBLEM: Large U3/U1 Ratio for Average U(i,j) Tensor .... 2.1 Note
RESPONSE: ...
;
_vrf_PLAT480_C_1dClBenz
;
PROBLEM: Long H...A H-Bond Reported H00G ..CL00 . 2.97 Ang.
RESPONSE: ...
;
# end Validation Reply Form
```

It is advisable to attempt to resolve as many as possible of the alerts in all categories. Often the minor alerts point to easily fixed oversights, errors and omissions in your CIF or refinement strategy, so attention to these fine details can be worthwhile. In order to resolve some of the more serious problems it may be necessary to carry out additional measurements or structure refinements. However, the purpose of your study may justify the reported deviations and the more serious of these should normally be commented upon in the discussion or experimental section of a

paper or in the "special_details" fields of the CIF. checkCIF was carefully designed to identify outliers and unusual parameters, but every test has its limitations and alerts that are not important in a particular case may appear. Conversely, the absence of alerts does not guarantee there are no aspects of the results needing attention. It is up to the individual to critically assess their own results and, if necessary, seek expert advice.

Publication of your CIF in IUCr journals

A basic structural check has been run on your CIF. These basic checks will be run on all CIFs submitted for publication in IUCr journals (*Acta Crystallographica*, *Journal of Applied Crystallography*, *Journal of Synchrotron Radiation*); however, if you intend to submit to *Acta Crystallographica Section C* or *E* or *IUCrData*, you should make sure that full publication checks are run on the final version of your CIF prior to submission.

Publication of your CIF in other journals

Please refer to the *Notes for Authors* of the relevant journal for any special instructions relating to CIF submission.

PLATON version of 18/09/2020; check.def file version of 20/08/2020

Datablock C_1dClBenz - ellipsoid plot

Compound 1dI₂

CIF Check

checkCIF/PLATON report

Structure factors have been supplied for datablock(s) C_di2_a

THIS REPORT IS FOR GUIDANCE ONLY. IF USED AS PART OF A REVIEW PROCEDURE FOR PUBLICATION, IT SHOULD NOT REPLACE THE EXPERTISE OF AN EXPERIENCED CRYSTALLOGRAPHIC REFEREE.

No syntax errors found. CIF dictionary Interpreting this report

Datablock: C_di2_a

```
Bond precision: C-C = 0.0099 A Wavelength=0.71073
Cell: a=10.114(3) b=16.501(4) c=14.700(4)
alpha=90 beta=97.159(4) gamma=90
Temperature: 293 K
Calculated Reported
Volume 2434.2(11) 2434.3(11)
Space group P 21/c P 21/c
Hall group -P 2ybc -P 2ybc
Moiety formula
C24 H16 Co N2 O4,
2.2(I0.20), I0.20
?
Sum formula C24 H16 Co I1.60 N2 O4 C24 H16 Co I1.60 N2 O4
Mr 658.36 658.36
Dx,g cm-3 1.796 1.796
Z 4 4
Mu (mm-1) 2.766 2.766
F000 1271.2 1271.0
F000' 1270.02
h,k,lmax 12,20,18 12,20,18
Nref 5013 4970
Tmin,Tmax 0.633,0.712 0.478,0.633
```

Tmin' 0.576
Correction method= # Reported T Limits: Tmin=0.478 Tmax=0.633
AbsCorr = MULTI-SCAN
Data completeness= 0.991 Theta(max)= 26.425
R(reflections)= 0.0685(3691) wR2(reflections)= 0.1903(4970)
S = 1.089 Npar= 334
The following ALERTS were generated. Each ALERT has the format
test-name_ALERT_alert-type_alert-level.
Click on the hyperlinks for more details of the test.

Alert level C

PLAT077_ALERT_4_C Unitcell Contains Non-integer Number of Atoms .. Please Check
PLAT094_ALERT_2_C Ratio of Maximum / Minimum Residual Density .... 3.48 Report
PLAT213_ALERT_2_C Atom C6B has ADP max/min Ratio ..... 3.2 prolat
PLAT213_ALERT_2_C Atom C7B has ADP max/min Ratio ..... 3.2 prolat
PLAT220_ALERT_2_C NonSolvent Resd 1 C Ueq(max)/Ueq(min) Range 4.9 Ratio
PLAT241_ALERT_2_C High 'MainMol' Ueq as Compared to Neighbors of C6B Check
PLAT241_ALERT_2_C High 'MainMol' Ueq as Compared to Neighbors of C7B Check
PLAT242_ALERT_2_C Low 'MainMol' Ueq as Compared to Neighbors of C2B Check
PLAT242_ALERT_2_C Low 'MainMol' Ueq as Compared to Neighbors of C5B Check
PLAT260_ALERT_2_C Large Average Ueq of Residue Including I3 0.129 Check
PLAT260_ALERT_2_C Large Average Ueq of Residue Including I5 0.163 Check
PLAT334_ALERT_2_C Small Aver. Benzene C-C Dist C2B -C7B 1.37 Ang.
PLAT342_ALERT_3_C Low Bond Precision on C-C Bonds ..... 0.00992 Ang.
PLAT906_ALERT_3_C Large K Value in the Analysis of Variance ..... 3.853 Check
PLAT911_ALERT_3_C Missing FCF Refl Between Thmin & STh/L= 0.600 25 Report
PLAT934_ALERT_3_C Number of (Iobs-Icalc)/Sigma(W) > 10 Outliers .. 1 Check
PLAT971_ALERT_2_C Check Calcd Resid. Dens. 1.47A From I5 2.09 eA-3
PLAT977_ALERT_2_C Check Negative Difference Density on H6B -0.34 eA-3

Alert level G

PLAT002_ALERT_2_G Number of Distance or Angle Restraints on AtSite 6 Note
PLAT004_ALERT_5_G Polymeric Structure Found with Maximum Dimension 3 Info
PLAT068_ALERT_1_G Reported F000 Differs from Calcd (or Missing)... Please Check
PLAT083_ALERT_2_G SHELXL Second Parameter in WGHT Unusually Large 19.04 Why ?
PLAT172_ALERT_4_G The CIF-Embedded .res File Contains DFIX Records 3 Report
PLAT199_ALERT_1_G Reported _cell_measurement_temperature ..... (K) 293 Check
PLAT200_ALERT_1_G Reported _diffrn_ambient_temperature ..... (K) 293 Check
PLAT300_ALERT_4_G Atom Site Occupancy of I1 Constrained at 0.3 Check
PLAT300_ALERT_4_G Atom Site Occupancy of I2 Constrained at 0.3 Check
PLAT300_ALERT_4_G Atom Site Occupancy of I3 Constrained at 0.3 Check
PLAT300_ALERT_4_G Atom Site Occupancy of I4 Constrained at 0.3 Check
PLAT300_ALERT_4_G Atom Site Occupancy of I5 Constrained at 0.2 Check
PLAT300_ALERT_4_G Atom Site Occupancy of I6 Constrained at 0.2 Check
PLAT302_ALERT_4_G Anion/Solvent/Minor-Residue Disorder (Resd 2) 100% Note
PLAT302_ALERT_4_G Anion/Solvent/Minor-Residue Disorder (Resd 3) 100% Note
PLAT302_ALERT_4_G Anion/Solvent/Minor-Residue Disorder (Resd 4) 100% Note
PLAT302_ALERT_4_G Anion/Solvent/Minor-Residue Disorder (Resd 5) 100% Note
PLAT302_ALERT_4_G Anion/Solvent/Minor-Residue Disorder (Resd 6) 100% Note
PLAT302_ALERT_4_G Anion/Solvent/Minor-Residue Disorder (Resd 7) 100% Note
PLAT432_ALERT_2_G Short Inter X...Y Contact I4 ..C5A 3.46 Ang.
x,y,z = 1_555 Check
PLAT764_ALERT_4_G Overcomplete CIF Bond List Detected (Rep/Expd) . 1.11 Ratio
PLAT794_ALERT_5_G Tentative Bond Valency for Co1 (II) . 2.00 Info
PLAT860_ALERT_3_G Number of Least-Squares Restraints ..... 3 Note
PLAT883_ALERT_1_G No Info/Value for _atom_sites_solution_primary . Please Do !
PLAT910_ALERT_3_G Missing # of FCF Reflection(s) Below Theta(Min). 1 Note
PLAT912_ALERT_4_G Missing # of FCF Reflections Above STh/L= 0.600 17 Note
PLAT933_ALERT_2_G Number of OMIT Records in Embedded .res File ... 15 Note
PLAT941_ALERT_3_G Average HKL Measurement Multiplicity ..... 3.7 Low
PLAT965_ALERT_2_G The SHELXL WEIGHT Optimisation has not Converged Please Check
PLAT978_ALERT_2_G Number C-C Bonds with Positive Residual Density. 1 Info
0 **ALERT level A** = Most likely a serious problem - resolve or explain

0 **ALERT level B** = A potentially serious problem, consider carefully
18 **ALERT level C** = Check. Ensure it is not caused by an omission or oversight
30 **ALERT level G** = General information/check it is not something unexpected
4 ALERT type 1 CIF construction/syntax error, inconsistent or missing data
19 ALERT type 2 Indicator that the structure model may be wrong or deficient
7 ALERT type 3 Indicator that the structure quality may be low
16 ALERT type 4 Improvement, methodology, query or suggestion
2 ALERT type 5 Informative message, check

Validation response form

Please find below a validation response form (VRF) that can be filled in and pasted into your CIF.

```
# start Validation Reply Form
_vrf_PLAT077_C_di2_a
;
PROBLEM: Unitcell Contains Non-integer Number of Atoms .. Please Check
RESPONSE: ...
;
_vrf_PLAT094_C_di2_a
;
PROBLEM: Ratio of Maximum / Minimum Residual Density .... 3.48 Report
RESPONSE: ...
;
_vrf_PLAT213_C_di2_a
;
PROBLEM: Atom C6B has ADP max/min Ratio ..... 3.2 prolat
RESPONSE: ...
;
_vrf_PLAT220_C_di2_a
;
PROBLEM: NonSolvent Resd 1 C Ueq(max)/Ueq(min) Range 4.9 Ratio
RESPONSE: ...
;
_vrf_PLAT241_C_di2_a
;
PROBLEM: High 'MainMol' Ueq as Compared to Neighbors of C6B Check
RESPONSE: ...
;
_vrf_PLAT242_C_di2_a
;
PROBLEM: Low 'MainMol' Ueq as Compared to Neighbors of C2B Check
RESPONSE: ...
;
_vrf_PLAT260_C_di2_a
;
PROBLEM: Large Average Ueq of Residue Including I3 0.129 Check
RESPONSE: ...
;
_vrf_PLAT334_C_di2_a
;
PROBLEM: Small Aver. Benzene C-C Dist C2B -C7B 1.37 Ang.
RESPONSE: ...
;
_vrf_PLAT342_C_di2_a
;
PROBLEM: Low Bond Precision on C-C Bonds ............... 0.00992 Ang.
RESPONSE: ...
;
_vrf_PLAT906_C_di2_a
;
PROBLEM: Large K Value in the Analysis of Variance ...... 3.853 Check
RESPONSE: ...
;
_vrf_PLAT911_C_di2_a
;
```

```
PROBLEM: Missing FCF Refl Between Thmin & STh/L= 0.600 25 Report
RESPONSE: ...
;
_vrf_PLAT934_C_di2_a
;
PROBLEM: Number of (Iobs-Icalc)/Sigma(W) > 10 Outliers .. 1 Check
RESPONSE: ...
;
_vrf_PLAT971_C_di2_a
;
PROBLEM: Check Calcd Resid. Dens. 1.47A From I5 2.09 eA-3
RESPONSE: ...
;
_vrf_PLAT977_C_di2_a
;
PROBLEM: Check Negative Difference Density on H6B -0.34 eA-3
RESPONSE: ...
;
# end Validation Reply Form
```

It is advisable to attempt to resolve as many as possible of the alerts in all categories. Often the minor alerts point to easily fixed oversights, errors and omissions in your CIF or refinement strategy, so attention to these fine details can be worthwhile. In order to resolve some of the more serious problems it may be necessary to carry out additional measurements or structure refinements. However, the purpose of your study may justify the reported deviations and the more serious of these should normally be commented upon in the discussion or experimental section of a paper or in the "special_details" fields of the CIF. checkCIF was carefully designed to identify outliers and unusual parameters, but every test has its limitations and alerts that are not important in a particular case may appear. Conversely, the absence of alerts does not guarantee there are no aspects of the results needing attention. It is up to the individual to critically assess their own results and, if necessary, seek expert advice.

Publication of your CIF in IUCr journals

A basic structural check has been run on your CIF. These basic checks will be run on all CIFs submitted for publication in IUCr journals (*Acta Crystallographica*, *Journal of Applied Crystallography*, *Journal of Synchrotron Radiation*); however, if you intend to submit to *Acta Crystallographica Section C* or *E* or *IUCrData*, you should make sure that full publication checks are run on the final version of your CIF prior to submission.

Publication of your CIF in other journals

Please refer to the *Notes for Authors* of the relevant journal for any special instructions relating to CIF submission.

PLATON version of 18/09/2020; check.def file version of 20/08/2020

Datablock C_di2_a - ellipsoid plot

Compound 1dI$_2$d

CIF Check

checkCIF/PLATON report

Structure factors have been supplied for datablock(s) C_1dI2d

THIS REPORT IS FOR GUIDANCE ONLY. IF USED AS PART OF A REVIEW PROCEDURE FOR PUBLICATION, IT SHOULD NOT REPLACE THE EXPERTISE OF AN EXPERIENCED CRYSTALLOGRAPHIC REFEREE.

No syntax errors found. CIF dictionary Interpreting this report

Datablock: C_1dI2d

Bond precision: C-C = 0.0049 A Wavelength=0.71073
Cell: a=10.4014(11) b=16.1330(17) c=14.6878(15)
alpha=90 beta=98.482(2) gamma=90
Temperature: 293 K
Calculated Reported
Volume 2437.7(4) 2437.7(4)
Space group P 21/c P 21/c
Hall group -P 2ybc -P 2ybc
Moiety formula C24 H16 Co N2 O4 ?
Sum formula C24 H16 Co N2 O4 C24 H16 Co N2 O4
Mr 455.32 455.32
Dx,g cm-3 1.241 1.241
Z 4 4
Mu (mm-1) 0.733 0.733
F000 932.0 932.0
F000' 933.77
h,k,lmax 12,19,17 12,19,17
Nref 4312 4301
Tmin,Tmax 0.900,0.943 0.876,0.943
Tmin' 0.876
Correction method= # Reported T Limits: Tmin=0.876 Tmax=0.943
AbsCorr = MULTI-SCAN
Data completeness= 0.997 Theta(max)= 25.043
R(reflections)= 0.0430(3067) wR2(reflections)= 0.1071(4301)
S = 1.031 Npar= 358

The following ALERTS were generated. Each ALERT has the format
test-name_ALERT_alert-type_alert-level.
Click on the hyperlinks for more details of the test.

Alert level A

PLAT601_ALERT_2_A Unit Cell Contains Solvent Accessible VOIDS of . 238 Ang**3

Author Response: This is due to the evacuated guest molecules.

Alert level C

PLAT018_ALERT_1_C _diffrn_measured_fraction_theta_max .NE. *_full ! Check
PLAT213_ALERT_2_C Atom C91 has ADP max/min Ratio ..... 3.8 oblate
PLAT220_ALERT_2_C NonSolvent Resd 1 C Ueq(max)/Ueq(min) Range 3.4 Ratio
PLAT234_ALERT_4_C Large Hirshfeld Difference C8A --C121 . 0.19 Ang.
PLAT241_ALERT_2_C High 'MainMol' Ueq as Compared to Neighbors of C6A Check
PLAT480_ALERT_4_C Long H...A H-Bond Reported H6 ..O2A . 2.61 Ang.
PLAT911_ALERT_3_C Missing FCF Refl Between Thmin & STh/L= 0.596 11 Report

Alert level G

PLAT004_ALERT_5_G Polymeric Structure Found with Maximum Dimension 3 Info
PLAT066_ALERT_1_G Predicted and Reported Tmin&Tmax Range Identical ? Check
PLAT093_ALERT_1_G No s.u.'s on H-positions, Refinement Reported as mixed Check
PLAT199_ALERT_1_G Reported _cell_measurement_temperature ..... (K) 293 Check
PLAT200_ALERT_1_G Reported _diffrn_ambient_temperature ..... (K) 293 Check
PLAT301_ALERT_3_G Main Residue Disorder .....(Resd 1) 26% Note
PLAT410_ALERT_2_G Short Intra H...H Contact H2 ..H4B . 2.05 Ang.
x,y,z = 1_555 Check
PLAT410_ALERT_2_G Short Intra H...H Contact H2 ..H41 . 2.12 Ang.
x,y,z = 1_555 Check
PLAT410_ALERT_2_G Short Intra H...H Contact H26 ..H121 . 2.11 Ang.
x,y,z = 1_555 Check
PLAT726_ALERT_2_G H...A Calc 2.37000, Rep 2.38000 Dev... 0.01 Ang.
H2 -O1B 1.555 4.556 ..... # 56 Check
PLAT764_ALERT_4_G Overcomplete CIF Bond List Detected (Rep/Expd) . 1.12 Ratio
PLAT811_ALERT_5_G No ADDSYM Analysis: Too Many Excluded Atoms .... ! Info
PLAT883_ALERT_1_G No Info/Value for _atom_sites_solution_primary . Please Do !

```
PLAT909_ALERT_3_G Percentage of I>2sig(I) Data at Theta(Max) Still 48% Note
PLAT933_ALERT_2_G Number of OMIT Records in Embedded .res File ... 7 Note
PLAT941_ALERT_3_G Average HKL Measurement Multiplicity ..... 3.2 Low
PLAT978_ALERT_2_G Number C-C Bonds with Positive Residual Density. 3 Info
1 ALERT level A = Most likely a serious problem - resolve or explain
0 ALERT level B = A potentially serious problem, consider carefully
7 ALERT level C = Check. Ensure it is not caused by an omission or oversight
17 ALERT level G = General information/check it is not something unexpected
6 ALERT type 1 CIF construction/syntax error, inconsistent or missing data
10 ALERT type 2 Indicator that the structure model may be wrong or deficient
4 ALERT type 3 Indicator that the structure quality may be low
3 ALERT type 4 Improvement, methodology, query or suggestion
2 ALERT type 5 Informative message, check
```

It is advisable to attempt to resolve as many as possible of the alerts in all categories. Often the minor alerts point to easily fixed oversights, errors and omissions in your CIF or refinement strategy, so attention to these fine details can be worthwhile. In order to resolve some of the more serious problems it may be necessary to carry out additional measurements or structure refinements. However, the purpose of your study may justify the reported deviations and the more serious of these should normally be commented upon in the discussion or experimental section of a paper or in the "special_details" fields of the CIF. checkCIF was carefully designed to identify outliers and unusual parameters, but every test has its limitations and alerts that are not important in a particular case may appear. Conversely, the absence of alerts does not guarantee there are no aspects of the results needing attention. It is up to the individual to critically assess their own results and, if necessary, seek expert advice.

Publication of your CIF in IUCr journals

A basic structural check has been run on your CIF. These basic checks will be run on all CIFs submitted for publication in IUCr journals (*Acta Crystallographica*, *Journal of Applied Crystallography*, *Journal of Synchrotron Radiation*); however, if you intend to submit to *Acta Crystallographica Section C* or *E* or *IUCrData*, you should make sure that full publication checks are run on the final version of your CIF prior to submission.

Publication of your CIF in other journals

Please refer to the *Notes for Authors* of the relevant journal for any special instructions relating to CIF submission.

Validation response form

Please find below a validation response form (VRF) that can be filled in and pasted into your CIF.

```
# start Validation Reply Form
_vrf_PLAT018_C_1dI2d
;
PROBLEM: _diffrn_measured_fraction_theta_max .NE. *_full ! Check
RESPONSE: ...
;
_vrf_PLAT213_C_1dI2d
;
PROBLEM: Atom C91 has ADP max/min Ratio ..... 3.8 oblate
RESPONSE: ...
;
_vrf_PLAT220_C_1dI2d
;
PROBLEM: NonSolvent Resd 1 C Ueq(max)/Ueq(min) Range 3.4 Ratio
RESPONSE: ...
;
_vrf_PLAT234_C_1dI2d
;
PROBLEM: Large Hirshfeld Difference C8A --C121 . 0.19 Ang.
RESPONSE: ...
;
_vrf_PLAT241_C_1dI2d
;
```

```
PROBLEM: High 'MainMol' Ueq as Compared to Neighbors of C6A Check
RESPONSE: ...
;
_vrf_PLAT480_C_1dI2d
;
PROBLEM: Long H...A H-Bond Reported H6 ..O2A . 2.61 Ang.
RESPONSE: ...
;
_vrf_PLAT911_C_1dI2d
;
PROBLEM: Missing FCF Refl Between Thmin & STh/L= 0.596 11 Report
RESPONSE: ...
;
# end Validation Reply Form
```

PLATON version of 18/09/2020; check.def file version of 20/08/2020

Datablock C_1dI2d - ellipsoid plot

Chapter 5

Compound Coen·H_2O

CIF Check

checkCIF/PLATON report

Structure factors have been supplied for datablock(s) C_Coen.H2O

THIS REPORT IS FOR GUIDANCE ONLY. IF USED AS PART OF A REVIEW PROCEDURE FOR PUBLICATION, IT SHOULD NOT REPLACE THE EXPERTISE OF AN EXPERIENCED CRYSTALLOGRAPHIC REFEREE.

No syntax errors found. CIF dictionary Interpreting this report

Datablock: C_Coen.H2O

```
Bond precision: C-C = 0.0020 A Wavelength=0.71073
Cell: a=11.9297(17) b=6.7924(9) c=14.3691(19)
alpha=90 beta=103.644(3) gamma=90
Temperature: 293 K
Calculated Reported
Volume 1131.5(3) 1131.5(3)
Space group P 21/n P 21/n
Hall group -P 2yn -P 2yn
Moiety formula C4 H16 Cl2 Co N4, Cl, H2 O ?
Sum formula C4 H18 Cl3 Co N4 O C4 H18 Cl3 Co N4 O
Mr 303.50 303.50
Dx,g cm-3 1.782 1.782
Z 4 4
Mu (mm-1) 2.196 2.196
F000 624.0 624.0
F000' 627.26
h,k,lmax 18,10,22 17,10,21
Nref 4507 3975
Tmin,Tmax 0.663,0.768 0.624,0.768
```

Tmin' 0.624
Correction method= # Reported T Limits: Tmin=0.624 Tmax=0.768
AbsCorr = MULTI-SCAN
Data completeness= 0.882 Theta(max)= 33.662
R(reflections)= 0.0265(3355) wR2(reflections)= 0.0572(3975)
S = 1.021 Npar= 121
The following ALERTS were generated. Each ALERT has the format
test-name_ALERT_alert-type_alert-level.
Click on the hyperlinks for more details of the test.

Alert level C

PLAT480_ALERT_4_C Long H...A H-Bond Reported H4B ..CL3B . 2.96 Ang.
PLAT480_ALERT_4_C Long H...A H-Bond Reported H3B ..CL3B . 2.88 Ang.

Alert level G

PLAT007_ALERT_5_G Number of Unrefined Donor-H Atoms ..... 10 Report
PLAT066_ALERT_1_G Predicted and Reported Tmin&Tmax Range Identical ? Check
PLAT199_ALERT_1_G Reported _cell_measurement_temperature ..... (K) 293 Check
PLAT200_ALERT_1_G Reported _diffrn_ambient_temperature ..... (K) 293 Check
PLAT232_ALERT_2_G Hirshfeld Test Diff (M-X) Co1 --Cl1B . 6.4 s.u.
PLAT232_ALERT_2_G Hirshfeld Test Diff (M-X) Co1 --Cl2B . 5.8 s.u.
PLAT790_ALERT_4_G Centre of Gravity not Within Unit Cell: Resd. # 2 Note
Cl
PLAT794_ALERT_5_G Tentative Bond Valency for Co1 (III) . 3.41 Info
PLAT883_ALERT_1_G No Info/Value for _atom_sites_solution_primary . Please Do !
PLAT912_ALERT_4_G Missing # of FCF Reflections Above STh/L= 0.600 499 Note
PLAT941_ALERT_3_G Average HKL Measurement Multiplicity ..... 4.5 Low
PLAT978_ALERT_2_G Number C-C Bonds with Positive Residual Density. 2 Info
0 **ALERT level A** = Most likely a serious problem - resolve or explain
0 **ALERT level B** = A potentially serious problem, consider carefully
2 **ALERT level C** = Check. Ensure it is not caused by an omission or oversight
12 **ALERT level G** = General information/check it is not something unexpected
4 ALERT type 1 CIF construction/syntax error, inconsistent or missing data
3 ALERT type 2 Indicator that the structure model may be wrong or deficient
1 ALERT type 3 Indicator that the structure quality may be low
4 ALERT type 4 Improvement, methodology, query or suggestion
2 ALERT type 5 Informative message, check

Validation response form

Please find below a validation response form (VRF) that can be filled in and pasted into your CIF.

```
# start Validation Reply Form
_vrf_PLAT480_C_Coen.H2O
;
PROBLEM: Long H...A H-Bond Reported H4B ..CL3B . 2.96 Ang.
RESPONSE: ...
;
# end Validation Reply Form
```

It is advisable to attempt to resolve as many as possible of the alerts in all categories. Often the minor alerts point to easily fixed oversights, errors and omissions in your CIF or refinement strategy, so attention to these fine details can be worthwhile. In order to resolve some of the more serious problems it may be necessary to carry out additional measurements or structure refinements. However, the purpose of your study may justify the reported deviations and the more serious of these should normally be commented upon in the discussion or experimental section of a paper or in the "special_details" fields of the CIF. checkCIF was carefully designed to identify outliers and unusual parameters, but every test has its limitations and alerts that are not important in a particular case may appear. Conversely, the absence of alerts does not guarantee there are no aspects of the results needing attention. It is up to the individual to critically assess their own results and, if necessary, seek expert advice.

Publication of your CIF in IUCr journals

A basic structural check has been run on your CIF. These basic checks will be run on all CIFs

submitted for publication in IUCr journals (*Acta Crystallographica*, *Journal of Applied Crystallography*, *Journal of Synchrotron Radiation*); however, if you intend to submit to *Acta Crystallographica Section C* or *E* or *IUCrData*, you should make sure that full publication checks are run on the final version of your CIF prior to submission.

Publication of your CIF in other journals

Please refer to the *Notes for Authors* of the relevant journal for any special instructions relating to CIF submission.

PLATON version of 18/09/2020; check.def file version of 20/08/2020

Datablock C_Coen.H2O - ellipsoid plot

Compound Coen

CIF Check

checkCIF/PLATON report

Structure factors have been supplied for datablock(s) C_coen_a

THIS REPORT IS FOR GUIDANCE ONLY. IF USED AS PART OF A REVIEW PROCEDURE FOR PUBLICATION, IT SHOULD NOT REPLACE THE EXPERTISE OF AN EXPERIENCED CRYSTALLOGRAPHIC REFEREE.

No syntax errors found. CIF dictionary Interpreting this report

Datablock: C_coen_a

```
Bond precision: C-C = 0.0050 A Wavelength=0.71073
Cell: a=7.3661(8) b=7.7791(9) c=19.604(2)
alpha=90 beta=95.012(2) gamma=90
Temperature: 293 K
Calculated Reported
Volume 1119.1(2) 1119.1(2)
Space group P 21/n P 21/n
Hall group -P 2yn -P 2yn
Moiety formula C4 H16 Cl2 Co N4, Cl ?
Sum formula C4 H16 Cl3 Co N4 C4 H16 Cl3 Co N4
Mr 285.49 285.49
Dx,g cm-3 1.694 1.694
Z 4 4
Mu (mm-1) 2.208 2.208
F000 584.0 584.0
F000' 587.22
h,k,lmax 9,10,26 9,10,26
Nref 2799 2795
Tmin,Tmax 0.853,0.957 0.820,0.957
Tmin' 0.820
Correction method= # Reported T Limits: Tmin=0.820 Tmax=0.957
AbsCorr = MULTI-SCAN
Data completeness= 0.999 Theta(max)= 28.336
R(reflections)= 0.0409( 2174) wR2(reflections)= 0.1093( 2795)
S = 1.043 Npar= 109
```

The following ALERTS were generated. Each ALERT has the format **test-name_ALERT_alert-type_alert-level**.

Click on the hyperlinks for more details of the test.

Alert level C

PLAT975_ALERT_2_C Check Calcd Resid. Dens. 1.08A From N006 0.80 eA-3
PLAT975_ALERT_2_C Check Calcd Resid. Dens. 0.98A From N005 0.76 eA-3
PLAT975_ALERT_2_C Check Calcd Resid. Dens. 1.01A From N007 0.68 eA-3
PLAT975_ALERT_2_C Check Calcd Resid. Dens. 1.07A From N008 0.59 eA-3
PLAT975_ALERT_2_C Check Calcd Resid. Dens. 1.01A From N005 0.46 eA-3
PLAT976_ALERT_2_C Check Calcd Resid. Dens. 0.88A From N005 -0.54 eA-3
PLAT976_ALERT_2_C Check Calcd Resid. Dens. 0.89A From N006 -0.42 eA-3
PLAT977_ALERT_2_C Check Negative Difference Density on H00A -0.58 eA-3
PLAT977_ALERT_2_C Check Negative Difference Density on H00C -0.80 eA-3
PLAT977_ALERT_2_C Check Negative Difference Density on H00E -0.54 eA-3
PLAT977_ALERT_2_C Check Negative Difference Density on H00G -0.85 eA-3

Alert level G

PLAT007_ALERT_5_G Number of Unrefined Donor-H Atoms ..... 8 Report
PLAT066_ALERT_1_G Predicted and Reported Tmin&Tmax Range Identical ? Check
PLAT199_ALERT_1_G Reported _cell_measurement_temperature ..... (K) 293 Check
PLAT200_ALERT_1_G Reported _diffrn_ambient_temperature ..... (K) 293 Check
PLAT303_ALERT_2_G Full Occupancy Atom H00A with # Connections 2.00 Check
PLAT303_ALERT_2_G Full Occupancy Atom H00C with # Connections 2.00 Check
PLAT303_ALERT_2_G Full Occupancy Atom H00E with # Connections 2.00 Check
PLAT303_ALERT_2_G Full Occupancy Atom H00G with # Connections 2.00 Check
PLAT720_ALERT_4_G Number of Unusual/Non-Standard Labels ..... 28 Note
PLAT764_ALERT_4_G Overcomplete CIF Bond List Detected (Rep/Expd) . 1.50 Ratio
PLAT779_ALERT_4_G Suspect or Irrelevant (Bond) Angle(s) in CIF . # 18 Check
CO01 -N005 -H00A 1.555 1.555 1.555 39.10 Deg.
PLAT779_ALERT_4_G Suspect or Irrelevant (Bond) Angle(s) in CIF . # 24 Check
CO01 -N006 -H00C 1.555 1.555 1.555 37.80 Deg.
PLAT779_ALERT_4_G Suspect or Irrelevant (Bond) Angle(s) in CIF . # 30 Check
CO01 -N007 -H00E 1.555 1.555 1.555 38.20 Deg.
PLAT779_ALERT_4_G Suspect or Irrelevant (Bond) Angle(s) in CIF . # 36 Check
CO01 -N008 -H00G 1.555 1.555 1.555 35.70 Deg.
PLAT794_ALERT_5_G Tentative Bond Valency for Co01 (III) . 3.36 Info
PLAT883_ALERT_1_G No Info/Value for _atom_sites_solution_primary . Please Do !
PLAT912_ALERT_4_G Missing # of FCF Reflections Above STh/L= 0.600 4 Note
PLAT978_ALERT_2_G Number C-C Bonds with Positive Residual Density. 2 Info
0 **ALERT level A** = Most likely a serious problem - resolve or explain
0 **ALERT level B** = A potentially serious problem, consider carefully
11 **ALERT level C** = Check. Ensure it is not caused by an omission or oversight
18 **ALERT level G** = General information/check it is not something unexpected
4 ALERT type 1 CIF construction/syntax error, inconsistent or missing data
16 ALERT type 2 Indicator that the structure model may be wrong or deficient
0 ALERT type 3 Indicator that the structure quality may be low
7 ALERT type 4 Improvement, methodology, query or suggestion
2 ALERT type 5 Informative message, check

Validation response form

Please find below a validation response form (VRF) that can be filled in and pasted into your CIF.

```
# start Validation Reply Form
_vrf_PLAT975_C_coen_a
;
PROBLEM: Check Calcd Resid. Dens. 1.08A From N006 0.80 eA-3
RESPONSE: ...
;
_vrf_PLAT976_C_coen_a
;
PROBLEM: Check Calcd Resid. Dens. 0.88A From N005 -0.54 eA-3
RESPONSE: ...
;
_vrf_PLAT977_C_coen_a
;
PROBLEM: Check Negative Difference Density on H00A -0.58 eA-3
RESPONSE: ...
```

;
end Validation Reply Form

It is advisable to attempt to resolve as many as possible of the alerts in all categories. Often the minor alerts point to easily fixed oversights, errors and omissions in your CIF or refinement strategy, so attention to these fine details can be worthwhile. In order to resolve some of the more serious problems it may be necessary to carry out additional measurements or structure refinements. However, the purpose of your study may justify the reported deviations and the more serious of these should normally be commented upon in the discussion or experimental section of a paper or in the "special_details" fields of the CIF. checkCIF was carefully designed to identify outliers and unusual parameters, but every test has its limitations and alerts that are not important in a particular case may appear. Conversely, the absence of alerts does not guarantee there are no aspects of the results needing attention. It is up to the individual to critically assess their own results and, if necessary, seek expert advice.

Publication of your CIF in IUCr journals

A basic structural check has been run on your CIF. These basic checks will be run on all CIFs submitted for publication in IUCr journals (*Acta Crystallographica*, *Journal of Applied Crystallography*, *Journal of Synchrotron Radiation*); however, if you intend to submit to *Acta Crystallographica Section C* or *E* or *IUCrData*, you should make sure that full publication checks are run on the final version of your CIF prior to submission.

Publication of your CIF in other journals

Please refer to the *Notes for Authors* of the relevant journal for any special instructions relating to CIF submission.

PLATON version of 18/09/2020; check.def file version of 20/08/2020

Datablock C_coen_a - ellipsoid plot